

**Controlling and exploiting the caesium effect in palladium  
catalysed coupling reactions**

Thomas J. Dent

Submitted in accordance with the requirements for the degree  
of

Doctor of Philosophy

The University of Leeds

School of Chemistry

May 2019

The candidate confirms that the work submitted is his own and that appropriate credit has been given where reference has been made to the work of others.

This copy has been supplied on the understanding that it is copyright material and that no quotation from the report may be published without proper acknowledgement

The right of Thomas Dent to be identified as Author of this work has been asserted by him in accordance with the Copyright, Designs and Patents Act 1988.

© 2019 The University of Leeds and Thomas J. Dent

## Acknowledgements

This project could not have been completed without the help of several individuals who've helped guide the project into the finished article. First and foremost I'd like to thank Dr. Bao Nguyen his support, useful discussions and the ability to sift through hundreds of experiments of kinetic data to put together a coherent figure. My writing has come a long way from my transfer report, so all the comments and suggestions seem to have mostly not been in vain.

To Paddy, the discussions relating to the NMR studies and anything vaguely inorganic were incredibly useful, and provided me with data that supported our hypothesis with more direct evidence than just the reaction monitoring experiments.

Rob, I really enjoyed my time at AZ and your support during my time there was incredibly useful so I could maximise my short secondment when I was getting more results than I knew what to do with. The warm welcome I got from you and all of CPUT made my decision to move into industry after my PhD an easy one. Jan and Matt, I'm glad you gave me the opportunity to run my base on the AZ3293 product. I wasn't expecting to go into my first pharmaceutically active project at multi-gram scale but the reaction worked well, and gave an interesting result.

To Mike, Simon and more recently Mark: I know nobody ever uses  $^{133}\text{Cs}$  NMR except me so thank you for taking a significant proportion of time to set up the machines to run my weird nucleus. Without you all we wouldn't have been able to disprove the 'Occam's razor' hypothesis dating back to the 80's.

I have to say to Mary thank you for putting up with me, and my product that just wanted to crash out after sampling and filtration. Thankfully it's been about 2 years since I've managed to block a GC column now!

Rosie, somehow you've managed to proofread and punctuation check this entire document, I'm honestly not sure how you can read Czeum over 600 times but somehow you managed.

To Sam, Joe and Rosie, our Friday afternoons playing curve based multiplayer games will be missed, along with the wholesome meatball moment of the week. Thanks for keeping me mostly sane, even if the nitrogen never ever gets taken out.

Abbie, thanks for being there and giving me the optimistic motivation I needed when the experiments weren't working. You still do the best breakfast cake!

## Abstract

Caesium bases are routinely used in several industrially relevant palladium-catalysed coupling reactions such as Suzuki-Miyaura and Buchwald-Hartwig amination, and regularly excel as the optimal base in published work. The mechanism by which caesium bases can improve yields and rates is not well understood, and this so called 'caesium effect' has anecdotally been attributed to factors such as increased solubility or the polarizability of the cation.

In this project, non-commercial caesium species have been synthesised and utilised in reaction monitoring studies to probe in which palladium-catalysed coupling reactions the 'caesium effect' was present. Increased knowledge of the mechanism and magnitude of the effect will allow for better optimisation of these industrially relevant reaction classes.

Evidence is provided against the theory that solubility is the prevailing reason for increased reaction rate using caesium bases, and that a direct interaction of the caesium cation with the palladium catalyst is more likely, reducing the activation energy barrier of the rate limiting step resulting in higher rates in Buchwald-Hartwig amination and Suzuki cross couplings.

$^{133}\text{Cs}$  and  $^{31}\text{P}$  NMR monitoring experiments along with X-Ray diffraction techniques on palladium species provide evidence towards a potential Pd-Cs bimetallic intermediate in these reactions, corroborating previous DFT results in the literature which propose Pd-Cs intermediate and Cs stabilised transition states.

The utility of caesium phosphate monohydrate in Suzuki-Miyaura cross coupling reactions involving boronic acids liable to protodeboronation under reaction conditions is discussed, with the base proposed to be a viable alternative to existing methodologies of boronic acid protection and precatalyst activation. The use of caesium phosphate in base screens for these reactions provides a facile pathway for increased yields and negates the need for expensive catalyst or additional synthetic steps, which can be prohibitively expensive at process scale.

**Table of contents**

<b>Abstract</b>	<b>iii</b>
<b>Table of contents</b>	<b>iv</b>
<b>List of Figures</b>	<b>viii</b>
<b>List of Schemes</b>	<b>xiv</b>
<b>List of Tables</b>	<b>xvii</b>
<b>List of Abbreviations</b>	<b>xviii</b>
<b>Chapter 1: Introduction</b>	<b>1</b>
<b>1.1 Effect of Caesium Base in Organic Reactions</b>	<b>2</b>
<b>1.1.1 Macrocyclic ring formation</b>	<b>2</b>
<b>1.1.2 Alkylation and Alkynylation reactions</b>	<b>4</b>
<b>1.2 Role of base in palladium catalysed coupling reactions</b>	<b>7</b>
<b>1.2.1 Heck Coupling reaction</b>	<b>7</b>
<b>1.2.2 Sonogashira coupling</b>	<b>10</b>
<b>1.2.3 Buchwald-Hartwig amination</b>	<b>12</b>
<b>1.2.4 Pd catalysed C-H activation</b>	<b>15</b>
<b>1.2.5 Suzuki coupling</b>	<b>19</b>
<b>1.2.6 Protodeboronation reactions in Suzuki coupling</b>	<b>23</b>
<b>1.3 Evidence of direct Cs involvement in catalysis</b>	<b>26</b>
<b>1.3.1 Synthetic incorporation of caesium base in catalysis</b>	<b>26</b>
<b>1.3.2 DFT calculations of caesium containing intermediates</b>	<b>29</b>
<b>1.4 Summary</b>	<b>31</b>
<b>1.5 References</b>	<b>32</b>
<b>Chapter 2: Synthesis and reactivity of non-commercial caesium species</b>	<b>38</b>
<b>2.1 Synthesis of caesium phosphate monohydrate</b>	<b>38</b>
<b>2.2 Analysis and characterisation of caesium phosphate monohydrate</b>	<b>39</b>

2.2.1 Investigation of caesium phosphate monohydrate solubility in organic solvents	41
2.3 Assessment of base mediated palladium catalysed coupling reactions for base screen	46
2.3.1 Heck coupling reaction	48
2.3.2 C-H Arylation reaction	50
2.3.3 Sonogashira cross coupling	53
2.3.4 Buchwald-Hartwig amination	58
2.3.5 Suzuki-Miyaura cross-coupling	60
2.4 Synthesis and characterization of caesium tetrafluoroborate monohydrate	63
2.4.1 Utilization of caesium tetrafluoroborate in Buchwald-Hartwig amination reactions	64
2.5 Synthesis of tetrabutyl ammonium phosphate	67
2.6 Conclusions & Future work	69
2.7 Experimental details	71
2.8 References	80
<b>Chapter 3: Investigation into the effectiveness of caesium bases in Buchwald-Hartwig amination reactions</b>	<b>83</b>
3.1 Investigation into the rate determining step of Buchwald-Hartwig amination reactions and the influence of base	84
3.1.1 Reactions with aryl iodides	85
3.1.2 Reactions using aryl bromides and chlorides	89
3.2 Use of KOtBu in Buchwald-Hartwig amination reaction	94
3.3 Increasing solubility of bases via crown ether complexation	97
3.4 Elucidating rate limiting step of Buchwald-Hartwig amination reactions by changing concentration of limiting reagents	99
3.5 Effects of coordinating solvent on amination reaction rates and yields	104
3.6 Investigation into catalyst stability due to water content of Cs <sub>3</sub> PO <sub>4</sub> ·H <sub>2</sub> O	107

3.6.1 Water spiking experiments using non hygroscopic base	108
3.6.2 Use of molecular sieves to reduce [H <sub>2</sub> O] in reaction	112
3.7 NMR studies	113
3.8 Conclusions & future work	121
3.9 Experimental procedures	123
3.10 References	127
<b>Appendix: XRD data</b>	<b>130</b>
<b>Chapter 4: Investigation into the effectiveness of caesium bases in Suzuki-Miyaura cross coupling reactions</b>	<b>132</b>
4.1 Investigation into the transmetallation step of Suzuki-Miyaura coupling reactions and influence of base on reaction performance	134
4.1.1 Reactions with 4-iodoanisole	134
4.1.2 Reactions using 4-bromoanisole	136
4.1.3 NMR monitoring experiments	140
4.1.4 Investigation into phase separation of dual solvent Suzuki-Miyaura cross couplings	144
4.1.5 Crown ether complexation of alkali metal cations	145
4.2 Troublesome heteroaromatic boronic acids in Suzuki reactions	147
4.2.1 Initial screening reaction	150
4.2.2 Choice of substrates to probe scope of caesium phosphate monohydrate acceleration	152
4.2.3 Validation of boronic acid half-life	160
4.2.4 Classification of boronic acids	161
4.2.5 Boronic acid selection for screening	163
4.2.6 Class 1 boronic acids	167
4.2.7 Class 2 boronic acids	168
4.2.8 Class 3 boronic acids	171

<b>4.2.9</b> Cation influence on protodeboronation reactions	174
<b>4.2.10</b> Lower temperature runs	178
<b>4.2.11</b> Chloride investigation	180
<b>4.2.12</b> Reaction Scale-up	181
<b>4.2.13</b> Investigation into increased solubility imparted by crown ethers	183
<b>4.2.14</b> Improvement of API procedure	185
<b>4.3</b> Conclusions & future work	187
<b>5.4</b> Experimental procedures	191
<b>5.5</b> References	206

## List of Figures

### Chapter 1

Figure 1: Caesium steric bulk hindering dialkylation .....	5
Figure 2: Caesium hydroxide accelerated <i>P</i> -alkylation forming benzylidiphenylphosphine .....	6
Figure 3: Conditions illustrating Cs effect in tandem Heck-C-H trifluoroethylation .....	10
Figure 4: Optimisation of caesium carbonate mediated Sonogashira coupling to form 1,4-diynes .....	11
Figure 5: Copper-free Sonogashira mechanism with base-mediated step highlighted	12
Figure 6: Illustration of caesium outperforming conventional <i>tert</i> -butoxide bases in B- H amination reaction.....	15
Figure 7: Base assisted C-H activation mechanism using carbonate anion .....	16
Figure 8: Observed Cs effect in C-H activation of benzoic acid with 4-iodoanisole .....	18
Figure 9: Proposed Cs containing catalytic intermediate facilitating quantitative conversion of coupling product when run stoichiometrically .....	18
Figure 10: Caesium effect in Suzuki-Miyaura cross coupling reactions using palladacycle catalyst.....	22
Figure 11: Evidence of Cs effect in Suzuki-Miyaura cross coupling reactions using troublesome boronic acid .....	23
Figure 12: Caesium mediated C-H carboxylation reaction indicating isolated Pd-Cs species in red and CO <sub>2</sub> in blue.....	29

### Chapter 2

Figure 13: Titration of caesium phosphate species and comparison with tripotassium phosphate.....	40
Figure 14: Coaxial insert NMR tube for solubility measurements.....	42
Figure 15: Representation of base effect in C-H activation reactions using carbonate anion.....	52
Figure 16: Kinetic plot of C-H activation base screen using bromobenzene .....	52
Figure 17: Cu assisted (blue) and palladium only (red) Sonogashira mechanistic proposals .....	54
Figure 18: Kinetic profiles of Sonogashira base screen.....	56

Figure 19 Sonogashira coupling product, and Glaser-Hay homocoupling product (not observed).....	57
Figure 20: Sonogashira water spike at t = 30 min using potassium carbonate base....	57
Figure 21: Evidence of Pd-Cs catalytic species in C-H carboxylation reactions .....	63
Figure 22 Proposed changes of mechanistic pathways based on [anion] and [cation].....	65
Figure 23: Kinetic plot of amination reaction showing slowdown on addition of CsBF <sub>4</sub> spiking agent (present in reaction at t = 0) .....	66

### Chapter 3

Figure 24: Possible mechanistic pathways in Buchwald-Hartwig amination.....	83
Figure 25: Conditions for amination reaction base screen .....	84
Figure 26: Base screen comparison of B-H amination with aryl iodide .....	85
Figure 27: Comparison between internal and external proton abstraction rate limiting steps .....	86
Figure 28: External proton abstraction step illustrating caesium destabilisation of Pd-I bond .....	88
Figure 29: Illustration of how low solubility bases can be drawn into solution via precipitation of base by-products.....	89
Figure 30: Buchwald-Hartwig Amination reaction with bromide leaving group base screen .....	90
Figure 31: Internal rate limiting proton abstraction step which does not involve base cation.....	90
Figure 32: Rate limiting external proton abstraction step illustrating similar Cs and K destabilisation of the Pd-Br bond .....	91
Figure 33: Relative interactions of carbonate and phosphate anions in rate limiting proton abstraction steps based on change in mechanistic pathway .....	93
Figure 34: Potassium <i>tert</i> -butoxide in Buchwald-Hartwig amination .....	94
Figure 35: Representation of overarylation of anilines using KO <sup>t</sup> Bu.....	96
Figure 36: Representation of crown ether complexation of sodium and potassium cations .....	97
Figure 37: Increase in performance using crown ethers in amination reaction with iodide leaving group (Figure 25) .....	98

Figure 38: External proton abstraction step showing multiple components present in rate limiting step .....	99
Figure 39: EasySampler setup showing sampling arm, vials and inerted flask.....	100
Figure 40: Rate determination experiments found from changing reagent concentrations .....	101
Figure 41: Proposed Buchwald-Hartwig mechanism indicating unlikely rate determining steps in red and viable rate determining steps in blue.....	102
Figure 42: Change in reaction performance of iodide leaving group amination reaction relative to solvent polarity .....	105
Figure 43: Change in reaction performance of bromide leaving group amination reaction relative to solvent polarity.....	106
Figure 44: Figure showing plausible method of action enabling DMF solvent to increase [monomer], along with caesium cation reducing decomposition rate.....	107
Figure 45: Buchwald-Hartwig amination reaction robust to 100 mol% water addition .....	108
Figure 46: Caesium carbonate spiking reaction in bromide leaving group with water spike shown in red at 30 minutes .....	109
Figure 47: Proposed palladium 'resurrection' reaction via aryl halide reduction .....	110
Figure 48: Resurrection of oxidised palladium by aniline addition showing water spike (red) and aniline spike (blue) .....	111
Figure 49: Plausible mechanism for palladium resurrection by aniline.....	112
Figure 50: Bromoanisole reaction using molecular sieves, showing decreased performance on addition of drying agent.....	113
Figure 51: $^{133}\text{Cs}$ NMR showing the difference between Cs salt and Cs species in reaction .....	116
Figure 52: $^{31}\text{P}$ NMR spectra of assumed <i>trans</i> P-Pd-P species TD-136 A (green) and TD-136 B (red), with unknown (blue) .....	116
Figure 53: X-Ray diffraction structure (top) and representation (bottom) of TD-136 A (PdSPhosdba) .....	117
Figure 54: X-Ray diffraction structure (top) and representation (bottom) of TD-136 B .....	118
Figure 55: Expected oxidative addition product and dimer relationship .....	119

Figure 56 Proposed homocoupling pathway to form dimerised catalyst TD-136 B species (Figure 53).....	120
<b>Chapter 4</b>	
Figure 57: Overall Suzuki-Miyaura cross coupling mechanism highlighting less well understood transmetallation step .....	132
Figure 58: Proposed transmetallation pathways of Suzuki-Miyaura cross coupling.....	133
Figure 59: Base effect of Suzuki-Miyaura coupling reaction using iodide leaving group .....	134
Figure 60: Standard Suzuki reaction screen with 4-bromoanisole substrate.....	137
Figure 61: Figure detailing transmetallation pathway interconversion based on base anion using bromide leaving group.....	138
Figure 62: Proposed competition between phosphate anion and hydroxide slowing formation of oxo-Pd species .....	139
Figure 63: Proposed formation of active Pd-OB(OH) <sub>2</sub> R species in Aryl bromide Suzuki reaction involving caesium phosphate by <sup>31</sup> P NMR.....	139
Figure 64: Observable Cs-P intermediates in <sup>31</sup> P (left) and <sup>133</sup> Cs (right) NMR.....	142
Figure 65: Suzuki iodide coupling rates when using 18-crown-6 additive.....	146
Figure 66: AmigoChem runs of 3-pyridyl boronic acid.....	155
Figure 67: AmigoChem runs of 2-thiophene boronic acid .....	156
Figure 68: AmigoChem runs of NBoc-2pyrrole boronic acid .....	157
Figure 69: AmigoChem runs of N-Boc-2indole boronic acid.....	158
Figure 70: Comparison between GLJ (top) and BNN protodeboronation (bottom) reaction conditions.....	160
Figure 71 Representative protodeboronation rates for Class 1-3 boronic acids.....	162
Figure 72: Illustration of catalytically active Pd-Cs species in literature (left), and proposed Pd-Cs species observable in <sup>31</sup> P NMR (right), (Scheme 42) .....	165
Figure 73: Example of possible Cs-B species reducing protodeboronation rate in troublesome Suzuki cross coupling reactions.....	166
Figure 74: Base screen of class 1 3-pyridyl boronic acid using homologated conditions .....	167
Figure 75: Base screen of class 1 3-thiophene boronic acid using homologated conditions.....	167

Figure 76: Base screen of class 2 N-Methyl pyrazole 2-boronic acid using homologated conditions.....	168
Figure 77: Base screen of class 2 2-thiophene boronic acid using homologated conditions.....	169
Figure 78: Base screen of class 2, 2,4,5-trifluorophenyl boronic acid using homologated conditions .....	169
Figure 79: Base screen of class 2 N-Boc indole 2-boronic acid using homologated conditions.....	170
Figure 80: Base screen of class 3 2,5-dimethyl isoxazole boronic acid using homologated conditions .....	171
Figure 81: Base screen of class 3 NBoc-2-pyrrole boronic acid using homologated conditions.....	171
Figure 82: Base screen of class 3 2,3,5-trifluorophenyl boronic acid using homologated conditions.....	172
Figure 83: Base screen of class 3 2,6-difluorophenyl boronic acid using homologated conditions.....	172
Figure 84: Base screen of class 3 2,4,6-trifluorophenyl boronic acid using homologated conditions.....	173
Figure 85: Cation influence of protodeboronation rate on class 2 N-methyl pyrazole boronic acid.....	176
Figure 86: Cation influence of protodeboronation rate on class 2 2-thiophene boronic acid .....	176
Figure 87: Cation influence of protodeboronation rate on class 3 3,5-dimethyl isoxazole boronic acid .....	177
Figure 88: Lower temperature base screen of class 2 N-methyl pyrazole boronic acid .....	178
Figure 89: Lower temperature base screen of class 3 2,3,5trifluorophenyl boronic acid .....	178
Figure 90: Lower temperature base screen of class 3 2,6-difluorophenyl boronic acid .....	179
Figure 91: 3,5-dimethylisoxazole boronic acid chloride experiments using phosphate bases.....	180

Figure 92: Effect of scale-up on mass transfer of Suzuki reactions from 1.0 mmol to 4.0 mmol .....	182
Figure 93: Effect of crown ether complexation on coupling reaction of 3,5-dimethyl isoxazole boronic acid using standard conditions .....	184
Figure 94: AZD3293 final step reaction screening existing procedure and kinetics using $K_3PO_4$ base .....	185
Figure 95: Caesium phosphate monohydrate effect on induction period of AZD3293 .....	186

## List of Schemes

### Chapter 1

Scheme 1: Base effect in optically active phosphine boranes .....	1
Scheme 2: Investigation into caesium effect in formation of cyclic lactones.....	3
Scheme 3: Possible mechanism of macrocyclic ring formation on caesium cation surface .....	3
Scheme 4: Investigation into alkylation of primary amines with Group I bases .....	5
Scheme 5: Caesium hydroxide-facilitated monoalkylation of benzylamine in ionic liquids .....	6
Scheme 6: Heck reaction cycle with different elimination pathways.....	8
Scheme 7: Base effect on $\beta$ -elimination products in Heck reactions .....	9
Scheme 8: Role of the base in traditional tandem Pd, Cu Sonogashira couplings .....	11
Scheme 9: Competing Buchwald-Hartwig amination reaction cycles .....	13
Scheme 10: Pd catalysed C-H activation reaction with caesium fluoride.....	17
Scheme 11: Caesium-stabilised transition state for reductive elimination of C-H activation product .....	17
Scheme 12: Competing base activation pathways of boronic acid in Suzuki Couplings, showing hydroxide formation step .....	19
Scheme 13: Synthesis of Buchwald XPhos precatalyst .....	25
Scheme 14 General scheme for protected boronic acid coupling.....	25
Scheme 15: Representation of caesium effect in arylation of phenols.....	27
Scheme 16: Synthesis of Cu-I-Cs species.....	28
Scheme 17: 'caesium effect' exerted by Pd-Cs intermediate in C-H carboxylation reaction .....	28
Scheme 18: Proposed catalytic cycle for carboxylation of phenylacetylene.....	30
Scheme 19: Direct Cs <sup>+</sup> involvement in the rate determining nickelation step .....	31

### Chapter 2

Scheme 20: Literature synthesis of caesium phosphate .....	38
Scheme 21: Comparison of literature and BNN caesium phosphate drying methods .	39
Scheme 22: Carrow group diazonium Suzuki coupling of sensitive boronic acids .....	46
Scheme 23: Heck reaction key step in synthesis of Naproxen .....	47

Scheme 24: Heck cross coupling reaction chosen for base screen.....	48
Scheme 25: Investigation into base effect in palladium catalysed C-H arylation.....	50
Scheme 26: Facile synthesis of imidazopyridine starting material for C-H activation reaction .....	50
Scheme 27: Sonogashira coupling reaction selected for base screen.....	55
Scheme 28 Buchwald-Hartwig amination reaction chosen for base screen .....	59
Scheme 29: Suzuki-Miyaura cross coupling selected for initial base screen.....	62
Scheme 30: synthesis of caesium tetrafluoroborate monohydrate .....	63
Scheme 31: Synthesis of more soluble organobase TBAP .....	67
Scheme 32: Initial test of TBAP reaction performance .....	68
<b>Chapter 3</b>	
Scheme 33: Side product formation in Buchwald-Hartwig amination .....	95
Scheme 34: Standard conditions for EasySampler reactions forming 4-tolyl- <i>p</i> -anisidine .....	101
Scheme 35: Literature proposed mechanism for caesium cation stabilisation of Pd(0) formation influencing induction period observed in DFT calculations.....	104
Scheme 36: Investigation into reaction performance using DMF solvent.....	105
Scheme 37: General scheme of NMR measurements to follow caesium catalytic involvement.....	115
<b>Chapter 4</b>	
Scheme 38: Reaction scheme of initial base effect test of Suzuki coupling .....	134
Scheme 39: M-X species where caesium cation accelerates formation of oxo-palladium rate determining step .....	135
Scheme 40: Standard Suzuki reaction conditions with bromide leaving group .....	136
Scheme 41: Conditions for NMR monitoring reaction mimicking standard Suzuki conditions.....	141
Scheme 42: Proposed Pd-Cs species visible by heteronuclear NMR.....	143
Scheme 43: Proposed Pd-Cs species allowing for catalyst decomposition .....	143
Scheme 44: Heteroaromatic Suzuki key step in Synthesis of Zytiga.....	148
Scheme 45: General scheme of protodeboronation reactions of heteroaromatic and fluorinated boronic acids .....	149

Scheme 46: Scheme showing how boronic acid protecting groups enhance reaction rates.....	149
Scheme 47: Adaptation of literature procedures to investigate caesium phosphate monohydrate in heteroaromatic Suzuki reactions .....	151
Scheme 48: Standard Suzuki conditions selected for catalyst screening of troublesome boronic acids .....	159
Scheme 49: Conditions to assess extent of cation influence on protodeboronation rate .....	175

## List of Tables

### Chapter 1

Table 1: Evidence of increased solubility of group I carbonates in dipolar aprotic solvents .....	4
---	---

### Chapter 2

Table 2: Cs <sub>3</sub> PO <sub>4</sub> .H <sub>2</sub> O solubility in reaction solvents .....	43
Table 3: K <sub>3</sub> PO <sub>4</sub> solubility in organic reaction solvents by NMR.....	43
Table 4: NMR VT solubility of phosphate bases using coaxial insert method .....	44
Table 5: Reactions for caesium phosphate monohydrate base screening .....	47
Table 6: Overnight conversion (GC) of Heck reaction.....	49
Table 7: Base screen of C-H arylation reaction using chloride leaving group with alkali metal carbonate and phosphate bases.....	51
Table 8: Results of initial Sonogashira base screen experiments .....	55
Table 9: Base screen for initial Buchwald-Hartwig amination reaction.....	59
Table 10: Observable caesium base cation effect in Suzuki cross coupling .....	62
Table 11: Effect of CsBF <sub>4</sub> spiking agent on Buchwald-Hartwig amination reaction .....	64
Table 12: Conversion figures using TBAP organic base.....	68

### Chapter 3

Table 13: Buchwald-Hartwig amination (Figure 25) reaction with chloride leaving group .....	92
Table 14: Side product in amination reaction with KOtBu based on leaving group.....	96

### Chapter 4

Table 15: Base performance under 3-pyridine Suzuki conditions .....	151
Table 16: Initial choices of literature reactions to conduct base screen .....	154
Table 17: Validation of $t_{1/2}$ using coupling reaction conditions.....	161
Table 18: Unstable boronic acids chosen for kinetic run to probe base effect .....	164

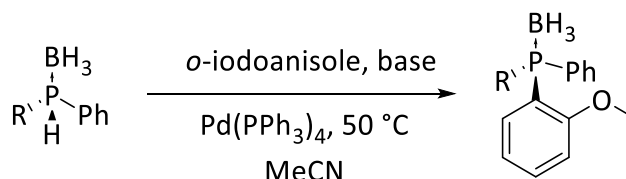
**List of Abbreviations**

AAS	Atomic Absorption Spectroscopy
BINAP	(2,2'-bis(diphenylphosphino)-1,1'-binaphthyl)
[bmim][PF <sub>6</sub> ]	1-Butyl-3-methylimidazolium hexafluorophosphate
Boc	<i>tert</i> -Butyloxycarbonyl
COSY	Correlation Spectroscopy
DABO	Diethanolamine complexed boronic acid
Dbp	Dibenzylideneacetone
DCM	Dichloromethane
DEPT	Distortionless enhancement by polarization transfer
DFT	Density Functional Theory
DIPEA	N,N-Diisopropylethylamine
DMAc	Dimethylacetamide
DMF	Dimethylformamide
DMSO	Dimethyl sulfoxide
GC	Gas Chromatography
HFIP	Hexafluoroisopropanol
HMBC	Heteronuclear Multiple-Bond Correlation
HPLC	High Performance Liquid Chromatography
HRMS	High resolution Mass spectrometry
LDA	Lithium diisopropylamide
MIDA	<i>N</i> -methyliminodiacetic acid
MS	Molecular sieves
NMR	Nuclear Magnetic Resonance

Ox. Add.	Oxidative Addition
<i>O</i> -tol	<i>ortho</i> -tolyl
Piv	Pivalate
Red Elim	Reductive Elimination
(S)-QUINAP	(S)-1-(2-Diphenylphosphino-1-naphthyl)isoquinoline
(S)-NMDPP	(S)-(+)-Neomenthyl-diphenylphosphine
TBAP	Tetrabutylammonium Phosphate
TFA	Trifluoroacetate
THF	Tetrahydrofuran
TON	Turnover Number
XRD	X-Ray Diffraction

## Chapter 1: Introduction

The correct choice of base in a reaction system can have a large effect on product selectivity and yield, as well as reaction rate.<sup>1</sup> For example, in the formation of optically active phosphine boranes by Imamoto *et al.*, the simple change of base from potassium carbonate to caesium fluoride can provide higher yields and selectivity with a shorter reaction time, illustrating the multifaceted potential of caesium bases.



**Scheme 1:** Base effect in optically active phosphine boranes<sup>1</sup>

Base	Reaction time (h)	Yield (%)	ee (%)
K <sub>2</sub> CO <sub>3</sub>	6	77	96
CsF	4	89	98

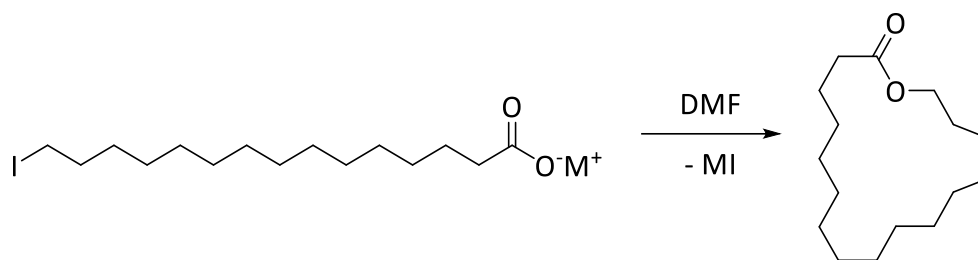
In many reaction systems, base screenings are conducted to find the ideal base for the reaction based on pK<sub>a</sub>, steric bulk, and substrate interactions.<sup>2</sup> Several studies in organic chemistry have shown that caesium bases are able to give increased selectivity and milder conditions for identical reactions compared to other group I carbonate and fluoride bases.<sup>3</sup> The effectiveness of the caesium bases is thought to arise from the solubility of the Cs<sup>+</sup> cation, which is up to 50 times more soluble than Na<sup>+</sup> equivalents in dipolar aprotic solvents such as DMF and DMSO. This renders the anion highly reactive and effectively free in solution,<sup>4</sup> thereby increasing the reactivity of the base and enabling caesium bases to have improved performance in reactions.<sup>5</sup> This may go some way to explain the extent of increased kinetic performance over other group I bases, but does little to explain why one pathway would be favoured in the case of better product selectivity. It can therefore be deduced that this is not a purely kinetic factor and can be affected by equilibria, steric and thermodynamic effects to give different products,<sup>6-8</sup> as well as direct interaction of the base with the reaction mechanism.<sup>9,10</sup>

The improved performance of caesium bases in organic and organometallic reactions over other alkali metal bases is referred to as the 'caesium effect'.<sup>4</sup> Many reactions have been shown to have improved performance when using caesium bases, and as such have become extremely useful bases in research environments.

## **1.1 Effect of Caesium Base in Organic Reactions**

### **1.1.1 Macrocyclic ring formation**

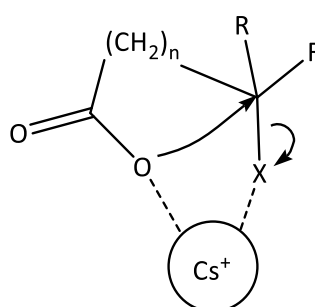
Macrocyclic lactones are a pharmaceutically useful class of compounds with antiparasitic and insecticidal properties.<sup>11</sup> While the drug Avermectin is biosynthesized by bacteria,<sup>12</sup> analogues and other macrocyclic lactones must be synthesized chemically, thus the mechanism of the chemical synthesis is scientifically useful to discover. Kellogg and co-workers investigated the effect of base cation in the ring closing reaction of macrocyclic lactones and found that incorporation of caesium carbonate base gave an increase in yield of up to 70% over potassium carbonate.<sup>13</sup> The hypothesised reasoning behind this 'caesium effect' was one of polarizability, therefore in addition to group I carbonates, thallium carbonate was investigated as a pseudo group I carbonate.<sup>14</sup> While caesium has the highest ionic radius and lowest electronegativity of all elements, it is second only to thallium in polarizability.<sup>15</sup> The results of the base screening within this study are reported in Scheme 2. If the 'caesium effect' was only related to polarizability, it would be expected that thallium would have an even larger effect and would produce higher yields than even caesium bases. However, while thallium carbonate performed well, it was inferior to the caesium equivalent and therefore we would conclude that any effect on reaction performance is not solely dictated by polarizability, and that other factors must play a part.



**Scheme 2:** Investigation into caesium effect in formation of cyclic lactones<sup>13</sup>

M <sup>+</sup>	Li	Na	K	Rb	Cs	Tl
Ionic radius (Å)	0.9	1.16	1.52	1.66	1.81	1.64
Yield %	0	54	67	68	80	64

The favourability of caesium salts towards intramolecular ring formation and polymerization such as in the caesium-mediated polymerization of propylene oxide<sup>16</sup> has led researchers to believe that the final ring closure step in these reactions actually occurs on the surface of the Cs<sup>+</sup> cation, as the ionic radius is such that it provides a pre-orientation of reactants so that intramolecular ring formation may occur. These “triple ions” involving O<sup>-</sup>, X<sup>-</sup> and Cs<sup>+</sup>, have been proposed to be the reason behind increased rates of polymerisation in a conductivity study discussing the base catalysed formation of polystyrene in THF.<sup>17</sup>



**Scheme 3:** Possible mechanism of macrocyclic ring formation on caesium cation surface<sup>17</sup>

While this “triple ion” mechanism and pre-orientation of reactants may increase the rate of reaction in these specific cyclization reactions, the general mechanism may also be present in other more complex or catalytic reactions, providing a method of action of the caesium effect unrelated to solubility or polarizability. No caesium-containing

intermediates have been isolated and analysed chemically, and though computational evidence points towards the caesium taking an active role to increase reaction performance in certain classes of reaction,<sup>18, 19</sup> the mechanistic reasoning behind this increase is unlikely to be the same for all reactions where the 'caesium effect' is present.

In all of these systems, a polar aprotic solvent such as DMF is required to allow caesium bases to facilitate higher reaction yields than competing alkali metal bases. While this may be due to increased solubility of caesium bases in dipolar aprotic solvents, another possibility may be due to the coordinating effect of dipolar aprotic solvents, which are able to preorganise the reactants into a favourable orientation for successful collision.<sup>20</sup>

**Table 1:** Evidence of increased solubility of group I carbonates in dipolar aprotic solvents<sup>20</sup>

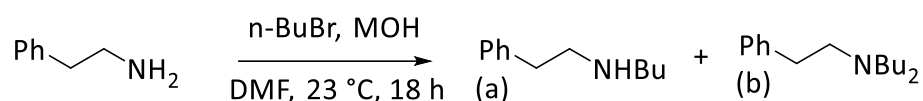
Solubility of M <sub>2</sub> CO <sub>3</sub> in dipolar aprotics (g/L)			
Solvent	Na	K	Cs
DMF	3.8	7.5	119.5
DMSO	14.3	47.0	362.5

While the solubility of caesium bases relative to other alkali metal bases has been studied in dipolar aprotic and aqueous solvents, the difference in solubility of alkali metal bases in other common reaction solvents including non-polar solvents has not been investigated. Although authors have suggested that increased solubility will allow the anion to be more free and reactive in solution, thereby increasing performance of caesium bases,<sup>21</sup> other properties may also be relevant such as the coordinating power and affinity towards a catalyst of any particular solvent field. In addition, dipolar aprotics tend to coordinate better to the caesium cation due to their intrinsic net nucleophilicity.<sup>22</sup>

### **1.1.2. Alkylation and Alkynylation reactions**

Caesium salts also find use as an effective bases in alkylation reactions of primary amines. The caesium base in these reactions both suppresses over-alkylation to the

tertiary amine as well as providing the secondary amine in high yield. The ratio of secondary amine to tertiary amine allows us to see how favourable the second addition step is, as a reaction with low conversion from starting material retains the reactants for reuse, for example in a flow rig, whereas any conversion to the tertiary by-product would result in loss of valuable chemicals.<sup>23</sup> The high performance of caesium hydroxide over other alkali metal hydroxides is useful to synthetic chemists looking for a single step monoalkylation of primary amines. Results of this reaction reported by Salvatore can be seen in Scheme 4.



**Scheme 4:** Investigation into alkylation of primary amines with Group I bases<sup>23</sup>

M	Yield a (%)	Yield b (%)	Ratio a/b
Li	62	21	3/1
Na	51	26	2/1
K	55	29	2/1
Rb	65	24	3/1
Cs	89	10	9/1

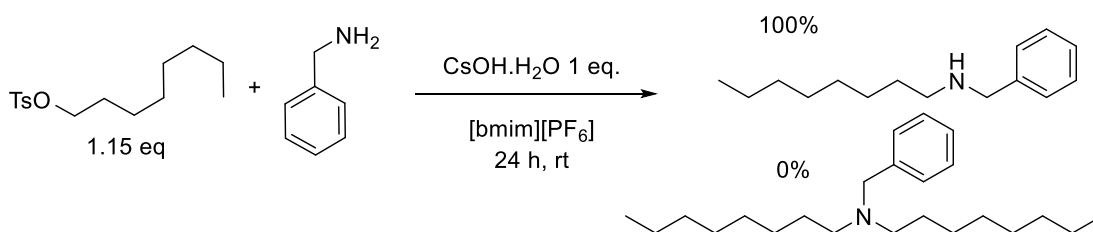
The rationale proposed linking the ratio between the primary and secondary amine formation was proposed by Jung *et al.* who stated that the large caesium atom bonded to the secondary amine prevented further alkylation due to steric hindrance of the dialkyl quaternary ammonium caesium salt (Figure 1) preventing close approach of the hydroxide anion. Other group I hydroxides are not sufficiently large to cause steric hindrance and as such are not as effective at inhibiting over alkylations to the tertiary by-product.<sup>23</sup>



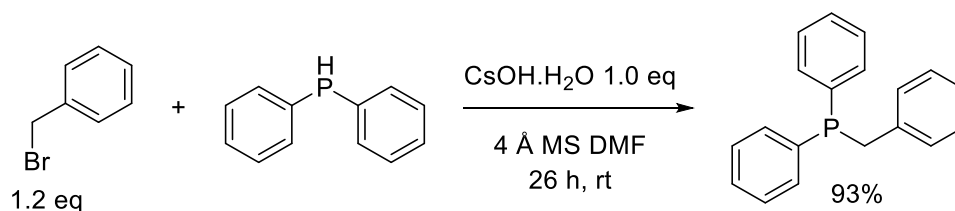
**Figure 1:** Caesium steric bulk hindering dialkylation<sup>23</sup>

Despite alkylation mechanisms being relatively simple, the confirmation of the steric bulk imparted by the caesium cation shows that it can be applied to other reactions involving nucleophilic addition to a deprotonated substrate, which occur in many catalysed coupling reactions which require base.

These alkylation reactions have been expanded to include diverse functionalities, including  $\beta$ -amino esters,<sup>24</sup> as well as chiral amines,<sup>25</sup> direct *P*-alkylation for phosphine synthesis,<sup>26</sup> and *O*-alkylation to efficiently perform ether syntheses.<sup>27</sup>



**Scheme 5:** Caesium hydroxide-facilitated monoalkylation of benzylamine in ionic liquids<sup>24</sup>



Entry	Base	Yield (%)
1	LiOH	3
2	NaOH	31
3	KOH	35
4	RbOH	41
5	CsOH.H <sub>2</sub> O	93

**Figure 2:** Caesium hydroxide accelerated *P*-alkylation forming benzyldiphenylphosphine<sup>26</sup>

While caesium hydroxide is especially useful in these monoalkylation reactions, the hydroxide is very hygroscopic so must be kept rigorously dry to ensure full reactivity. Alternatively caesium carbonate may also be used effectively in some reactions under milder conditions, generally avoiding molecular sieves, without the need for rigorous

drying before the reactions to produce acceptable yields and little evidence of overalkylation.<sup>3</sup> The authors of the phosphine addition reaction (Figure 2) do not state the reason for caesium acceleration, however the  $pK_a$  of the phosphine proton is likely to be too high for formal base abstraction, so the phosphine is expected to form P(V) on addition to the aryl bromide before reductive elimination of HBr forming the P(III) product.

## **1.2 Role of base in palladium catalysed coupling reactions**

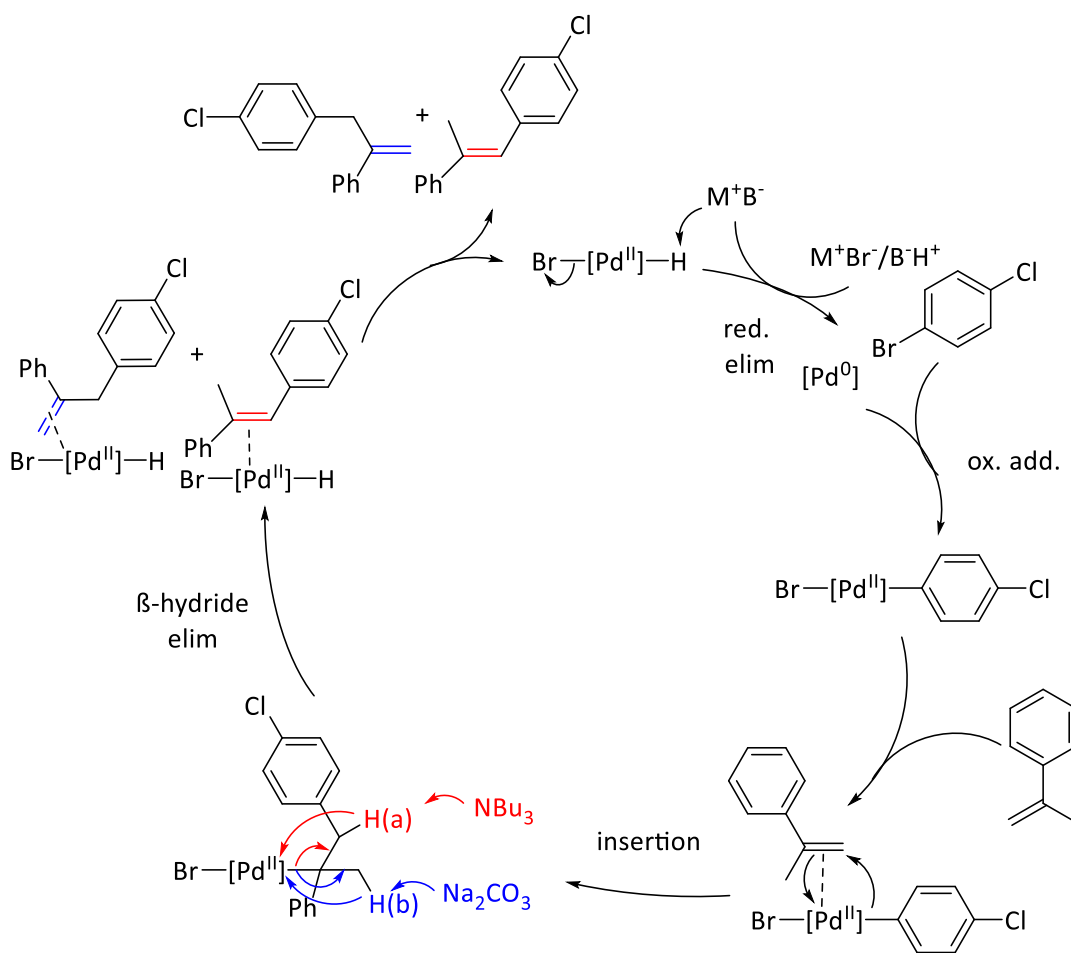
In several transition metal catalysed coupling reactions the base plays a vital role in the catalytic cycle. Whether that role is the reformation of the catalyst in an elimination step or to scavenge reactive intermediates or by-products, the choice of base in these reactions is crucial for optimisation, as the best base may have marked improvements to kinetics,<sup>28</sup> yield<sup>29</sup> and amount of by-products in the reaction.

Caesium bases, namely carbonate and fluoride, are commonly used in coupling reactions for their favourable performance over other group I bases.<sup>30, 31</sup> Numerous studies have been conducted to deduce the optimum base in palladium-catalysed coupling reactions including Suzuki-Miyaura cross coupling,<sup>32</sup> C-H activation,<sup>6, 10, 33</sup> and Sonogashira<sup>34</sup> reactions, with the caesium bases outperforming existing bases in certain reaction systems.

### **1.2.1 Heck Coupling reaction**

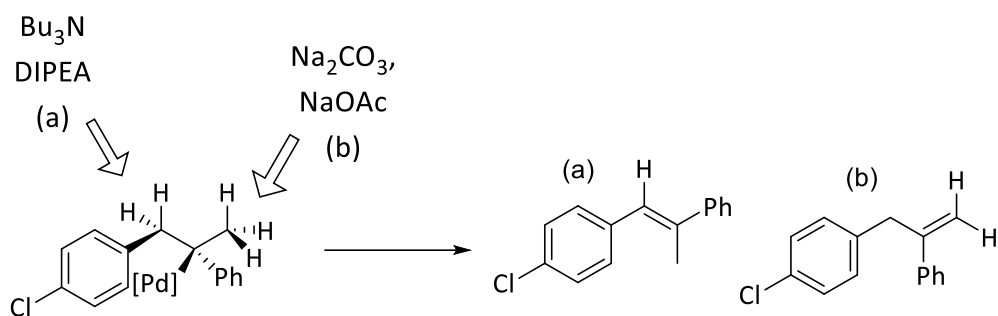
The Heck reaction is an important C-C bond forming reaction for coupling aryl halides or pseudohalides to activated alkenes to form substituted olefins with excellent *trans* selectivity using a palladium(0)-based catalyst in the presence of a weak base. The reaction earned Richard Heck a share of the 2010 Nobel Prize in Chemistry, alongside Suzuki and Negishi.<sup>35</sup> The use of the base in this reaction is to reductively eliminate the spent Pd(II) species. This then forms the active Pd(0) species and the protonated base along with the alkali metal halide. The choice of base in this reaction depends on the  $pK_a$  required to deprotonate the Pd(II) species after  $\beta$ -hydride elimination. For this reason weak bases such as alkali metal carbonates, as well as amine bases possessing  $pK_a$  values around 10-11 are traditionally used for optimum elimination conditions.<sup>36</sup> The reaction pH is affected by the amount of base dissolved in solution, as well as the

base  $pK_a$ . A more soluble base will give a higher reaction pH than a base which is sparingly soluble in the reaction solvent. Therefore it is important to consider that when bases are not fully soluble in the reaction media, that change of base cation or anion can affect the thermodynamic solubility, therefore changing the pH of solution and in turn, the rate of reaction. An additional role for the base in this reaction postulated by Beller and Riermeier<sup>29</sup> is that the base is directly involved in the  $\beta$ -hydride elimination step in the reaction by directly abstracting either the benzylic or methylic proton to afford the internal or external olefin regioisomers shown in Scheme 6. The products were not found to isomerise under the reaction conditions, suggesting the base mediated elimination was under kinetic control.



**Scheme 6:** Heck reaction cycle with different elimination pathways

The different products for this elimination are summarised in Scheme 7. It was found that coordinating bases such as DIPEA or  $Bu_3N$  favoured the internal olefin elimination pathway, and less coordinating bases such as  $NaOAc$  or  $Na_2CO_3$  favoured the external elimination.<sup>29</sup>

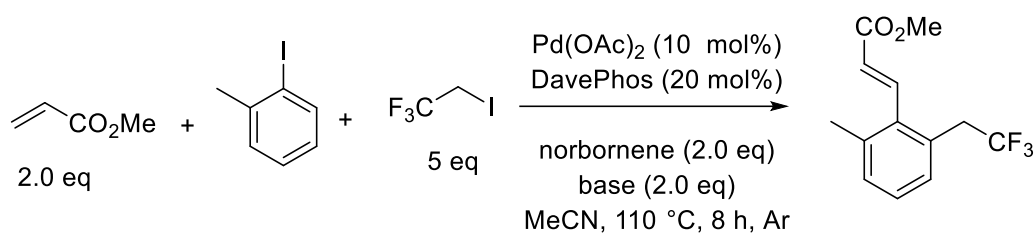


**Scheme 7:** Base effect on  $\beta$ -elimination products in Heck reactions<sup>29</sup>

The reason for this difference is thought to arise from the more coordinating amine bases being able to directly abstract the most acidic proton on the benzylic side during the  $\beta$ -hydride elimination step, but it is not known whether the less coordinating bases are able to interact at this step in the reaction cycle to form the unconjugated product. The difference in reaction between the two base types shows that the effect of base can cause further changes to a reaction than merely reaction yield and kinetics, and that different products can result from a reaction with the same reagents by changing only the base.

The seminal work published by Richard Heck in 1972 used triethylamine both as a base and a solvent,<sup>35</sup> which led on to the use of multiple organic and inorganic weak bases to facilitate the insertion mechanistic step (Scheme 6).<sup>32, 37-39</sup>

The majority of literature conducting a base screen in the Heck coupling reaction was conducted before caesium carbonate was a widely used base in palladium cross-coupling reactions, and therefore there is relatively little data directly comparing caesium carbonate or other caesium bases to potassium or sodium cations under similar reaction conditions.<sup>40</sup> Despite this, some work has been conducted illustrating an improvement in conversion when using caesium carbonate base in the cascade Heck-C-H trifluoroethylation of 2-iodotoluene.<sup>41</sup>



Entry	Base	Yield (%)
1	Na <sub>2</sub> CO <sub>3</sub>	4
2	K <sub>2</sub> CO <sub>3</sub>	5
3	Cs(OPiv) <sub>2</sub>	26
4	Cs <sub>2</sub> CO <sub>3</sub>	59

**Figure 3:** Conditions illustrating Cs effect in tandem Heck-C-H trifluoroethylation<sup>41</sup>

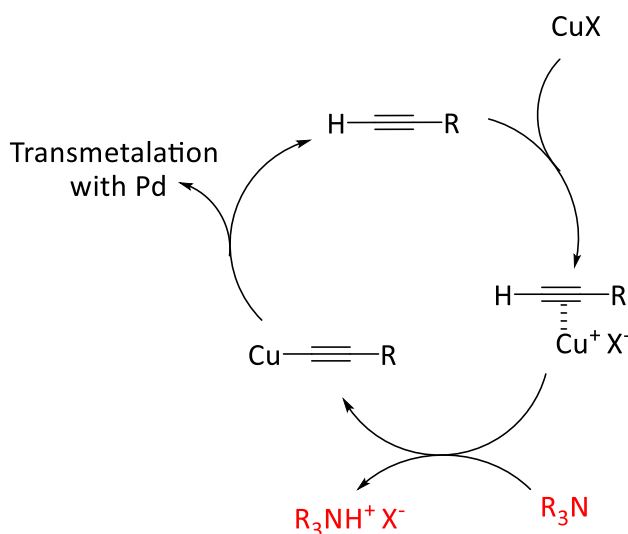
Both sodium and potassium carbonate fail to convert more than 5% of starting material to the desired Heck product, while caesium carbonate is able to convert over 50% in the 8 hour reaction time. The authors suggest that the caesium base is more effective due to it reducing the energy of the transition state in the reductive elimination step, forming caesium iodide from caesium carbonate after  $\beta$ -hydride elimination of the Heck product. The soft-hard interactions between the caesium cation and carbonate anion may allow the anion to better deprotonate the palladium hydride species, or the soft-soft interaction between the caesium cation and iodide anion may allow the caesium cation to stabilise the deprotonation step transition state and accelerate the reaction due to providing a less energetic pathway of reductive elimination.

### 1.2.2 Sonogashira coupling

The Sonogashira coupling reaction is significantly more complicated than palladium-only coupling reactions due to the presence of both a palladium and a copper catalytic cycle, which makes mechanistic analysis significantly more difficult. This reaction facilitates the catalytic connection of terminal alkynes to aryl or vinyl halides, and is generally run with an amine base which also functions as the solvent at room temperature.<sup>42</sup>

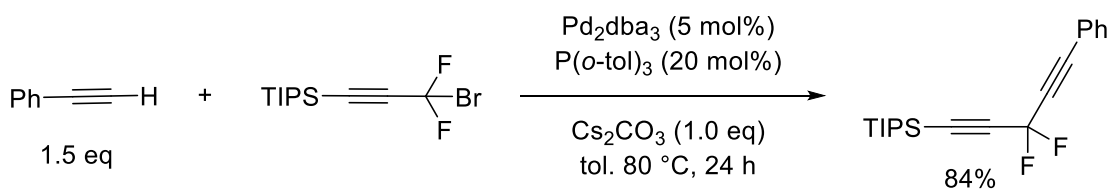
The function of the base in this reaction is to deprotonate the alkyne in favour of copper insertion, which can be transmetalated to palladium later in the catalytic cycle

(Scheme 8). It is thought that before the alkyne can be deprotonated, a  $\pi$ -alkyne complex is formed with the copper, which can be observed as an intermediate in analysis by  $^1\text{H}$  and  $^{31}\text{P}$  NMR.<sup>43</sup>



Scheme 8: Role of the base in traditional tandem Pd, Cu Sonogashira couplings

Sonogashira reactions are suspected to possess a measurable ‘caesium effect’ where caesium bases outperform all other tested bases in a given reaction. Zhang *et al.* discovered that in a Sonogashira reaction investigating formation of 1,4-diynes using a copper-free palladium catalyst caesium carbonate was the optimal base, with the reaction achieving 84% yield of the desired Sonogashira product.



Base	Solvent	Additive	Base loading (eq)	Yield (% , 24 h)
$\text{K}_2\text{CO}_3$	Cyclohexane	CuI	2.0	9
$\text{Cs}_2\text{CO}_3$	Cyclohexane	CuI	2.0	25
$\text{Cs}_2\text{CO}_3$	Cyclohexane	N/A	2.0	42
$\text{Cs}_2\text{CO}_3$	Toluene	N/A	1.0	84

Figure 4: Optimisation of caesium carbonate mediated Sonogashira coupling to form 1,4-diynes<sup>44</sup>

Interestingly this reaction does not appear to require a copper source to allow catalytic turnover and therefore facilitate the coupling reaction, which would suggest that the 'caesium effect' in this reaction is unrelated to the formal deprotonation step from the copper  $\pi$ -alkyne complex.

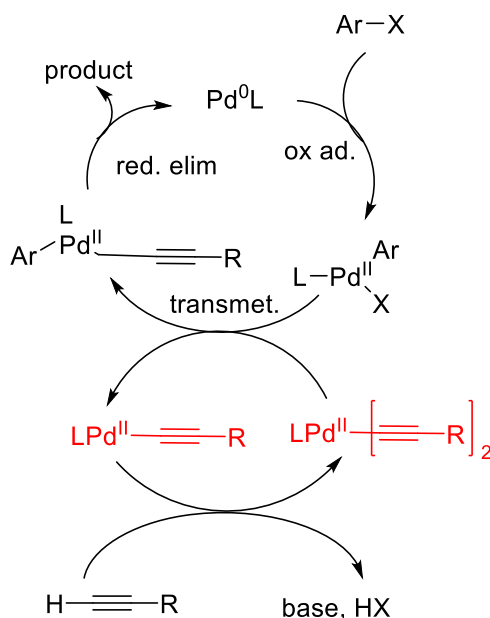


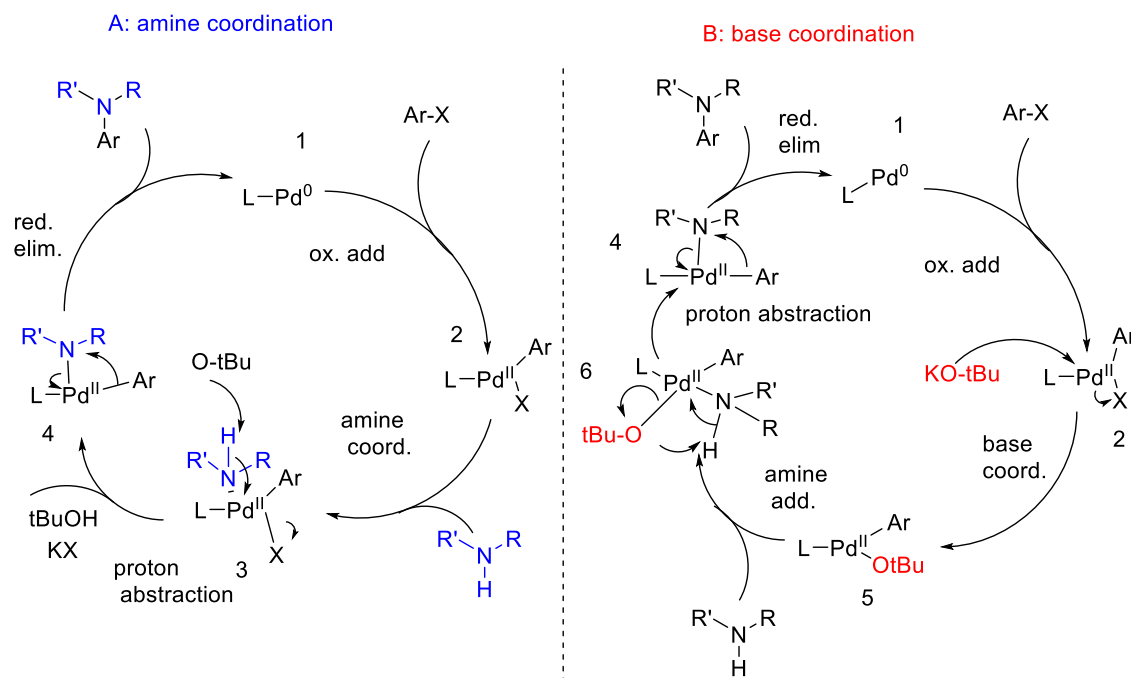
**Figure 5:** Copper-free Sonogashira mechanism with base-mediated step highlighted<sup>45</sup>

Because use of caesium carbonate can achieve increased yields over potassium carbonate using similar conditions, it is likely that the base cation can interact in some way with the base mediated transmetalation step. Evidence suggests that caesium bases are not actually more soluble in non-polar solvents *vide infra*, and therefore the cation is likely to influence the reaction and provide a lower energy pathway to increase the rate of the base mediated transmetalation step. Due to low solubility of the base in toluene solvent there may not be full dissociation of cation and anion which would allow close approach of the cation to the active catalyst.

### 1.2.3 Buchwald-Hartwig amination

Buchwald-Hartwig amination is a highly important, routinely used C-N coupling reaction.<sup>46</sup> In this reaction it is possible to couple a nitrogen directly to an aromatic ring system at lower temperatures than is routinely used in competing systems such as the Goldberg reaction.<sup>47</sup> Norrby *et al.* conducted DFT calculations to deduce the relationship between the strength of the base and the overall mechanism and found

two competing pathways that could switch depending on  $pK_a$ , leaving group and solvent. (Scheme 9).<sup>48</sup>



**Scheme 9:** Competing Buchwald-Hartwig amination reaction cycles

In amine coordination pathway A, after the palladium complex **1** has undergone oxidative addition to form **2**, the amine is able to coordinate to the palladium centre forming **3**. This step is followed by an external proton abstraction of the amido proton and dissociation of the leaving group forming **4**, where the destabilised amido moiety is labile to attack from the coordinated aryl group, producing the reductively eliminated arylated product and reforming active catalyst **1**.

The alternative base coordination pathway B, for this reaction involves an identical oxidative addition step to form **2**. At this stage the base can add to the palladium centre before the halide is able to dissociate to form complex **5**. From here the amine is able to add to the palladium centre to form **6** followed by internal abstraction of the amido proton to form **4**, which reductively eliminates in the same manner producing the arylated product and active catalyst **1** as in the previous mechanism.<sup>48</sup>

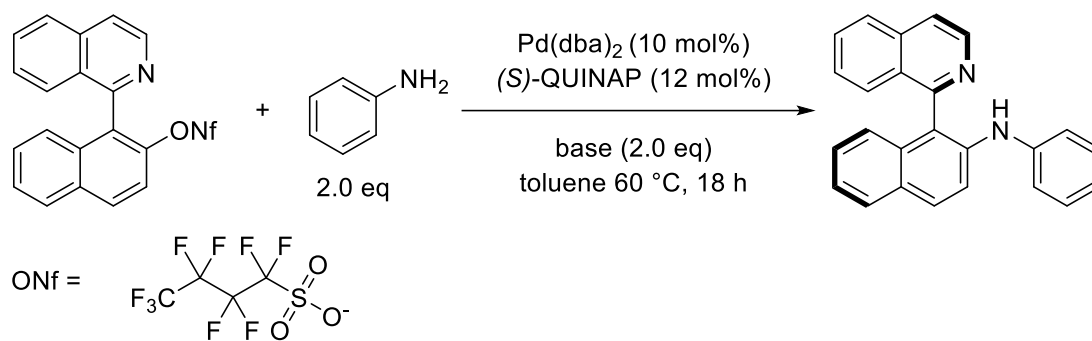
In a dipolar aprotic solvent such as DMF, the dissociation of the halide X is thought to be possible,<sup>48</sup> which allows the coordination of the base to palladium. When a nonpolar solvent such as toluene is used, the mechanism first coordinates the amine followed

by external proton abstraction, as the addition of the base to the palladium centre is not stabilised.

The base in this reaction must be of an appropriate  $pK_a$  to deprotonate the coordinated amine, but as the amine is only deprotonated after coordination to the palladium centre in both cases, the  $pK_a$  required is much lower than would be required for non-catalysed amines which require strong bases such as LDA. When using bases that are not freely soluble in the reaction solvent, the solubility of the bases must be taken into account when discussing the pH in the reaction solution. Caesium carbonate bases have been shown to be more soluble in dipolar aprotic solvents such as DMF,<sup>20</sup> so a reaction with caesium carbonate in this solvent will exhibit a higher pH than one with a less soluble base cation, which may increase or decrease the yield depending on the catalytic cycle and possible side reactions. When di-alkyl amines are used for Buchwald-Hartwig reactions, stronger alkoxide bases are needed and the reaction must be kept rigorously dry, as any water present will convert alkoxides to the relatively weak hydroxide.<sup>49</sup> Recent developments in the Buchwald-Hartwig reaction have allowed for weaker bases such as caesium carbonate to be used with simple substrates such as morpholine,<sup>48</sup> which can allow for more sensitive functional groups to be used.

In Buchwald-Hartwig amination reactions, caesium carbonate is sometimes used, as although it is generally marginally inferior for yield compared to conventional alkoxide bases, it has a much broader scope of functional group tolerance on account of being a weaker base, and as such will not deprotonate enolisable ketones and interact with other vulnerable acidic groups. For a significant amount of syntheses it may be used over the slightly more favourable alkoxides.<sup>50</sup>

A useful synthesis where caesium carbonate is a highly effective base is in the asymmetric Buchwald-Hartwig amination forming heterobiaryl amines conducted by Lassaletta *et al.*<sup>51</sup> Despite stronger *tert*-butoxide bases generally being more favoured than weaker carbonate and phosphate bases in Buchwald-Hartwig amination reactions due to it being better able to coordinate to the palladium catalyst,<sup>48, 52</sup> the reaction using caesium carbonate achieved higher yields than sodium *tert*-butoxide with very similar *ee*.



Entry	Base	Yield (%)	ee (%)
1	LiOtBu	44	89
2	NaOtBu	59	89
3	Cs <sub>2</sub> CO <sub>3</sub>	99	88

**Figure 6:** Illustration of caesium outperforming conventional *tert*-butoxide bases in B-H amination reaction<sup>51</sup>

To gain these yields the relatively obscure nonaflate leaving group is required. An explanation of the increased performance of caesium in this reaction is not given, however it could be attributed to the decreased ability for the carbonate anion to coordinate to the palladium centre which may slow the reaction down (Scheme 9). To gain a better picture of whether the cation or anion plays a bigger role in this rate increase a full screen of potassium and sodium carbonates would need to be conducted in addition to these reactions, so the exact interaction of the caesium cation is unknown.

#### 1.2.4 Pd catalysed C-H activation

C-H activations are a useful and relatively new class of carbon-carbon bond forming reactions that do not require addition of a reactive functional group to undergo chemical transformation.<sup>53-55</sup> These reactions involve varying metal based catalysts including cobalt,<sup>56</sup> rhodium,<sup>57</sup> ruthenium,<sup>54</sup> iridium,<sup>58</sup> platinum<sup>59</sup> and gold,<sup>60</sup> as well as commonly used palladium catalysts.<sup>8, 61, 62</sup> The mechanism for this reaction type depends on the metal catalyst involved, but palladium-catalysed reactions appear to undergo oxidative addition to the palladium catalyst, followed by exchange between the leaving group and the base anion and C-H palladation step, completed by reductive

elimination of the product.<sup>8, 63, 64</sup> The vital importance of the base cation in these reactions, and the possibility that the base mediated C-H palladation step may be rate determining lead to large base effects in these reaction systems, where caesium bases are routinely used after a base screen where found to be the optimal base for reaction conversion and product formation.<sup>6, 7, 63, 65</sup> The 'caesium effect' in these reactions is so large and commonly known that many publications do not report screening bases and move straight to caesium carbonate base without base optimisation.<sup>66-68</sup>

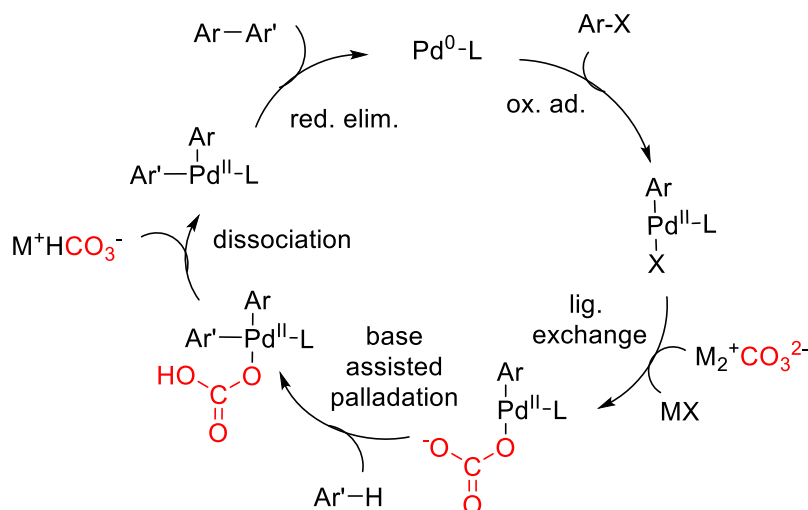
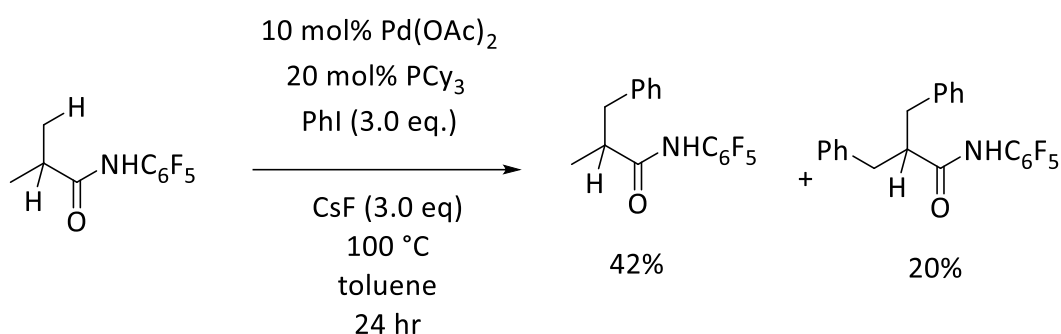


**Figure 7:** Base assisted C-H activation mechanism using carbonate anion<sup>63, 64</sup>

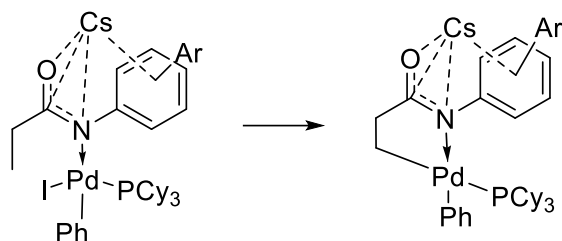
Due to the close interaction between the base anion and the palladium centre, clearly changes in the base anion will directly affect reaction performance. The base needs to be strong enough to facilitate the palladation step and abstract the aryl proton, but possess a weak enough nucleophilicity to allow dissociation from palladium to allow the catalytic cycle to proceed. The cation is important in these reactions as they are commonly performed in dipolar aprotic solvents,<sup>69, 70</sup> where caesium bases are up to 6 times as soluble as potassium equivalents.<sup>20</sup>

Both solubility of the base and the relative dissociation of the cation and anion will exert an effect on the palladation reaction. Not only must the anion be the correct  $\text{pK}_a$ , but the interaction between cation and anion is important for anion reactivity. The soft-hard interaction between the soft caesium cation and hard carbonate anion, leading to higher dissociation of the reactive base species and higher rates of ligand exchange may lead to higher reaction performance and therefore caesium carbonate base is regularly selected for inter and intramolecular C-H activation reactions.

The C-H bond arylation reaction of amides was conducted by Musaev and coworkers found that incorporation of a caesium cation into the mechanism of reductive elimination in DFT calculations gave a lower energy pathway by 15.1 kJ / mol over the use of potassium carbonate base, increasing the yield of the biaryl coupling from 32% to 67% and increasing the initial rate 3-fold.<sup>19</sup> This work provides evidence that the caesium cation can influence the reaction instead of being a spectator ion where the reactive anion facilitates the reaction alone. In this case the reductive elimination step is stabilised by addition of caesium cation to the reaction, speeding up the rate determining step and giving higher yields than potassium fluoride.



**Scheme 10:** Pd catalysed C-H arylation reaction with caesium fluoride<sup>18, 71</sup>

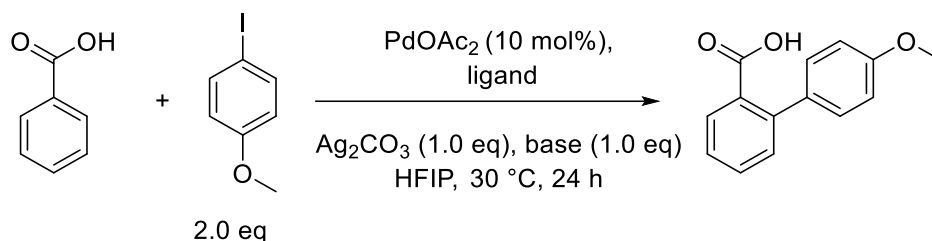


**Scheme 11:** Caesium-stabilised transition state for reductive elimination of C-H activation product

The presence of the caesium cation is vital for high yields in this reaction and the proposed Cs-stabilised transition state reduces the energy barrier for the C-H activation step by 17.6 kJ / mol, changing the mechanistic pathway from iodide-assisted to CsF-assisted. This was the first literature report of the addition of caesium cation able to not only improve the reaction but also open up a different mechanistic pathway to increase reaction rate.

In a mild C-H arylation reaction coupling benzoic acid to deactivated 4-iodoanisole, caesium carbonate was found to be the optimal base with a trend of increasing yields

as the size of the cation increased. This work conducted by Su and coworkers<sup>72</sup> stated that the large size of the caesium cation could provide more favourable interaction with the benzoic acid, and produce a more active Pd containing intermediate.



Entry	Base	ligand	Yield (%)
1	Li <sub>2</sub> CO <sub>3</sub>	N/A	31
2	Na <sub>2</sub> CO <sub>3</sub>	N/A	33
3	K <sub>2</sub> CO <sub>3</sub>	N/A	37
4	Na <sub>3</sub> PO <sub>4</sub>	N/A	33
5	CsOPiv	N/A	43
6	Cs <sub>2</sub> CO <sub>3</sub>	N/A	45
7	Cs <sub>2</sub> CO <sub>3</sub>		95

**Figure 8:** Observed Cs effect in C-H activation of benzoic acid with 4-iodoanisole<sup>72</sup>

The formation of a delocalised caesium carbonate-style structure is thought to increase the reaction rates using this base, with delocalisation of the benzoate group stabilising catalyst formation. Reactions with the preformed palladium complex were able to quantitatively generate the desired product, so it is likely that this caesium containing complex is an intermediate in catalysis.

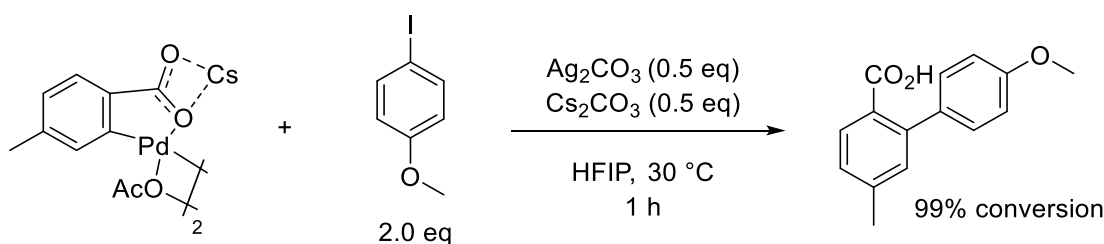
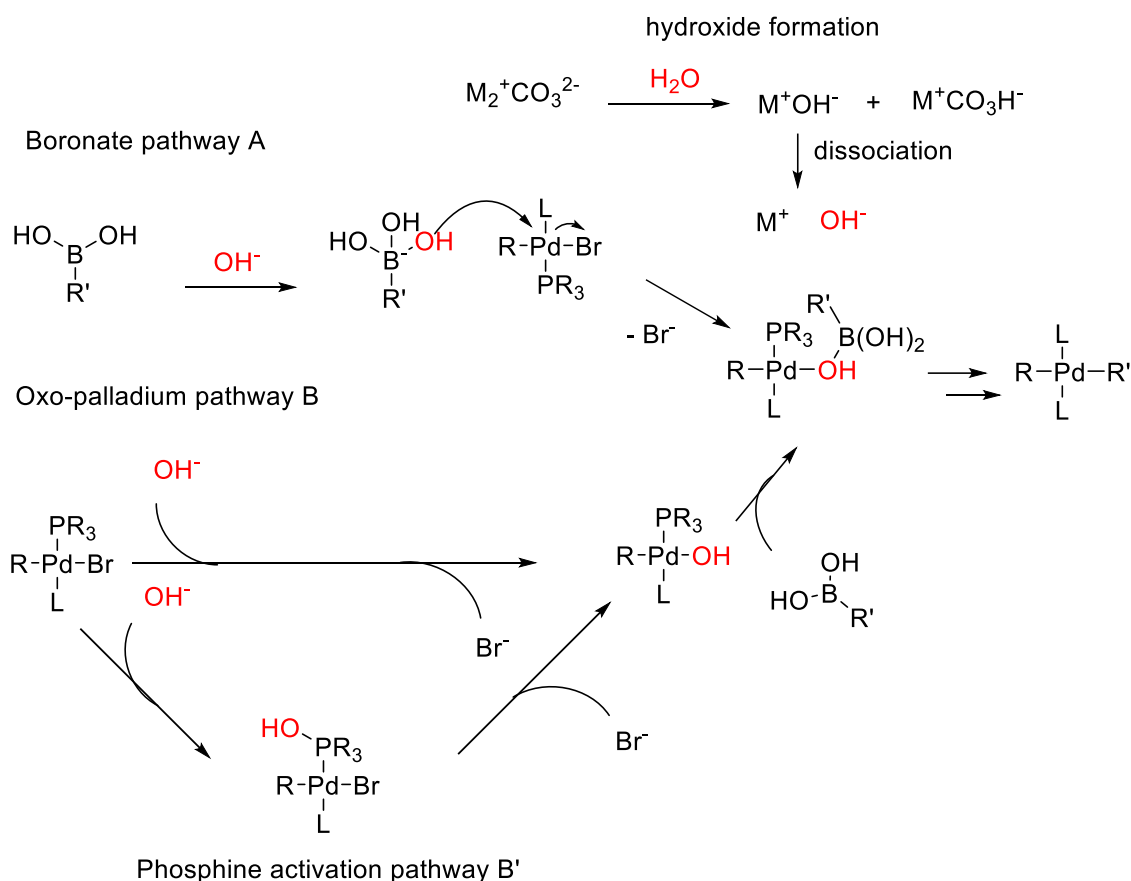


**Figure 9:** Proposed Cs containing catalytic intermediate facilitating quantitative conversion of coupling product when run stoichiometrically<sup>72</sup>

We can observe that not only can caesium bases increase conversions by utilising the size of the caesium cation, they can also be involved in facilitating catalytic steps and actively coordinating to catalytic species, increasing the rate of limiting steps and in some cases changing the mechanism entirely in C-H activation reactions.

### 1.2.5 Suzuki coupling

Bases have an important role in Suzuki coupling reactions and multiple pathways have been proposed.<sup>49, 73</sup> The most likely mechanism of action involves the basic anion deprotonating the boronic acid to form an active organoboronate species, which is more labile to the transmetalation step with a palladium halide intermediate than the base itself. This deprotonation step requires presence of water in the reaction mixture, so many Suzuki reactions involve wet conditions.<sup>28</sup>



**Scheme 12:** Competing base activation pathways of boronic acid in Suzuki Couplings, showing hydroxide formation step<sup>73</sup>

An alternative proposed mechanism involves the activation of the phosphine by a hydroxide anion from the water, producing an oxo-Pd complex which is able to attack

the boronic acid before the formal transmetallation to produce the di-substituted palladium species. DFT calculations found that the phosphine activation pathway is more favourable if a base is not present in the reaction, otherwise the boronate mechanism (Pathway A) is more favourable. An additional function of the base in both of these mechanisms is to break up the cyclic boroxine anhydride species which can be formed when reactions are run under rigorously dry conditions. These species are unreactive with respect to the catalytic cycle and need to be broken down into constituent boronic acids to function in the reaction.<sup>74</sup> A direct substitution is also possible where the hydroxide directly performs a substitution type reaction on the palladium centre, forgoing the phosphine activation step and directly forming the oxo-Pd complex before addition of the non-basic boronic acid.

Bases in the Suzuki reaction tend to be more varied than other coupling reactions,<sup>75</sup> with  $K_3PO_4$  performing particularly well in studies involving simple Suzuki reactions that could be modelled with several base systems.<sup>76</sup> The reason for this could be that the  $pK_a$  of the phosphate is most appropriate for the several different base functions within the reaction cycle.<sup>77</sup> The exact interactions in the transmetallation step have not been fully deduced, and continued optimisations occur.<sup>78</sup> One notable factor in the Suzuki coupling reaction is that an acidic by-product of boric acid is formed throughout the reaction, so for the base to remain effective throughout it should be applied in generous excess to neutralize the acidic by-product and maintain its effectiveness in the reaction mixture.<sup>49</sup>

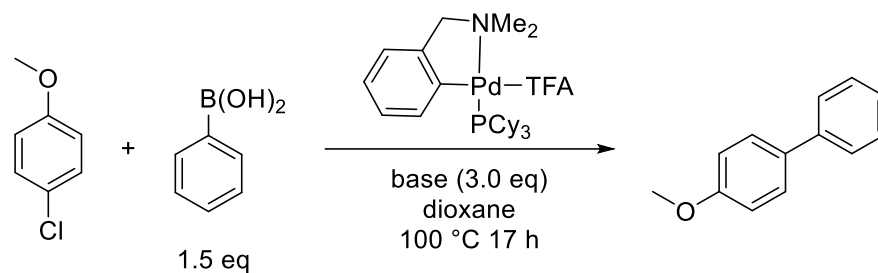
Suzuki reactions are relatively unique as they tend to incorporate either organic solvent which has not undergone a drying step, rendering it sufficiently wet to allow  $^-OH$  to form, or an aqueous / organic solvent mixture. Common reaction solvents include dioxane / water,<sup>79</sup> alcohol / water,<sup>80,81</sup> and THF / water systems.<sup>75,82,83</sup> Other palladium catalysed cross coupling reactions using anhydrous solvents and inorganic bases must take into account mass transfer between the solid and solution phase, as the base is not necessarily fully dissolved in the non-polar solution. As Suzuki-Miyaura cross couplings regularly involve aqueous solvent, all components of the reaction are generally fully soluble, however at high concentrations are known to 'salt out', forming two distinct phases incorporating the boronic acid and base in the aqueous phase and the catalyst and aryl halide in the less polar organic phase.

The exact concentration at which phase splitting occurs has not been studied previously, but work has been carried out in this project to elucidate the transition point at which splitting does occur, *vide infra*. Due to the two phases, mass transfer remains a factor in these reactions with mixing being crucial to ensure maximum amount of overlap between aqueous and organic layers. If steps are taken to ensure mixing remains high, Suzuki reactions can regularly gain high yields using inorganic bases.

Caesium bases are regularly used in Suzuki reactions that utilise iodide or bromide leaving groups,<sup>83</sup> though base screens are not routinely conducted in all cases. When base screens are conducted however, caesium carbonate or potassium phosphate are regularly found to be optimal bases.<sup>9, 84, 85</sup> Caesium carbonate tends to be more effective than potassium carbonate in these examples, and while potassium phosphate may be the most effective base studied, caesium phosphate was not used to fully deduce this trend. Synthesis of caesium phosphate would solve this problem and provide further insight into whether this trend was applicable in both phosphate and carbonate weak bases.

It can be suggested that when using coordinating solvents, such as DMF, DMAc or DMSO, caesium carbonate performs well for Suzuki couplings, and when less coordinating solvents such as acetone are used, phosphate bases tend to have better performance, with potassium phosphate being the most effective commercially available base.<sup>86</sup>

Bedford and Cazin found that palladacycles could perform well with high TONs when coupling deactivated aryl chlorides with phenylboronic acid. Despite the catalysts gaining over 75% yield at 0.01 mol% catalyst loading using caesium carbonate, the potassium carbonate reaction was only able to provide 6% conversion over the same reaction time.<sup>87</sup>

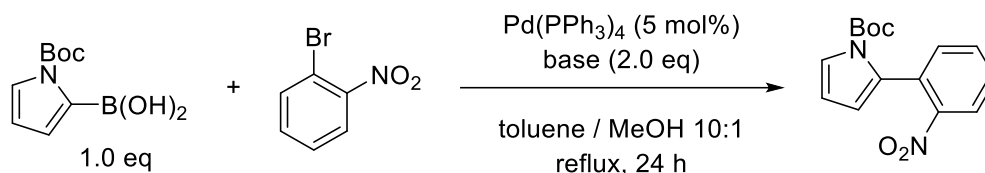


Entry	Base	Catalyst loading (mol %)	Conversion (%)
1	K <sub>2</sub> CO <sub>3</sub>	1.0	6
2	KF	1.0	22
3	NaOAc	1.0	25
4	K <sub>3</sub> PO <sub>4</sub>	1.0	60
5	Cs <sub>2</sub> CO <sub>3</sub>	1.0	100
6	Cs <sub>2</sub> CO <sub>3</sub>	0.1	99
7	Cs <sub>2</sub> CO <sub>3</sub>	0.01	80

**Figure 10:** Caesium effect in Suzuki-Miyaura cross coupling reactions using palladacycle catalyst

The publication did not state a possible mechanism for the improvement of the reaction using caesium bases, however due to the high stability of the boronic acid<sup>88</sup> it is likely that the base cation is able to interact in some way with the catalyst, improving the rate of the transmetallation step to achieve much higher yields.

In a base screen optimisation of a Suzuki cross coupling between *N*Boc-pyrroleboronic acid and 2-bromonitrobenzene, caesium carbonate was found to be the best base in a study conducted by Majerski *et al.*<sup>81</sup> In this system only caesium carbonate base could allow the reaction to achieve over 55% conversion.



Entry	Base	Yield (%)
1	Ba(OH) <sub>2</sub>	2
2	K <sub>3</sub> PO <sub>4</sub>	52
3	Na <sub>2</sub> CO <sub>3</sub>	15
4	Cs <sub>2</sub> CO <sub>3</sub>	74

**Figure 11:** Evidence of Cs effect in Suzuki-Miyaura cross coupling reactions using troublesome boronic acid<sup>81</sup>

After studying the reaction and gaining low yields initially, the boronic acid was added in 7 hours after the reaction start time, allowing all other components to equilibrate and preform the catalyst and oxidative addition product. The reason for the low yields was likely due to the relatively short half-life of the boronic acid, which has been measured by Lloyd-Jones *et al.* to be in the order of 15 mins.<sup>88</sup> The caesium effect in this case is unlikely to be related to solubility, as all bases are freely soluble in methanol, but could be due to either the caesium cation slowing the rate of protodeboronation of the boronic acid *vide infra*, or speeding up the transmetallation rate via stabilisation of the rate determining step or changing the mechanism itself via a lower energy pathway.

Protodeboronation is a significant problem in certain Suzuki reactions involving fluorinated and heteroaromatic boronic acids,<sup>88, 89</sup> so if the 'caesium effect' is able to negate these factors and provide higher yields we can expect caesium bases to have increased utility in this reaction area at process scale.

### **1.2.6 Protodeboronation reactions in Suzuki coupling**

The use of Suzuki reactions in industrial processes including pharmaceutical development is incredibly important and widely used. Brown & Bostrom reported that in 2014 Suzuki reactions were the 5<sup>th</sup> most used reaction in medicinal chemistry.<sup>46</sup> It is important, therefore, that these reactions are well understood and optimised for use

in industrial processes to make these reactions, and the manufacturing processes used to form compounds at scale, greener and more efficient.

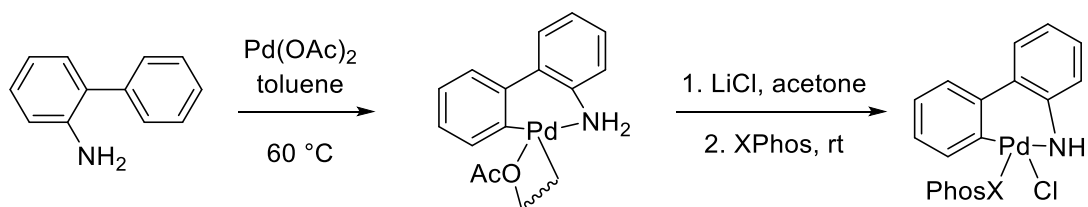
Generally, Suzuki cross couplings are sought after as high yielding and reliable ways to access C-C bond formation in biaryls.<sup>78</sup> One problem inherently associated with the coupling partners in these reactions is boronic acid synthesis which is usually carried out by a C-H borylation reaction, as the borylation reaction can suffer from low yields, especially when carried out on compounds with larger steric bulk and forcing or undesirable conditions.<sup>90</sup>

Another drawback of Suzuki cross couplings is the potential for a C-B protodeboronation reaction occurring under the basic aqueous reaction conditions to afford the inactive parent aryl and boric acid by-product.<sup>91</sup> Heteroaromatic and fluorinated starting materials are particularly prone to this decomposition, with half-lives as low as 2.6 ms under cross coupling conditions at high pH, where the boronic acid is exclusively in the boronate form.<sup>89</sup> Guy Lloyd Jones and coworkers found that there were as many as 5 different pathways of protodeboronation of heteroaromatic boronic acids with factors such as heteroatoms *ortho* to the boronic acid group which can stabilise the C-B fragmentation step, and orbital overlap with the formal carbanion after C-B cleavage.<sup>88</sup>

If the protodeboronation reaction occurs at a similar rate to the cross coupling reaction (half-lives of 0.5 - 6 hr), the reaction can suffer from lower yields and decreased reaction rates, owing to lower concentrations of boronic acid available to enter the catalytic cycle. When the half-life of the boronic acid decreases further and the protodeboronation reaction becomes much faster than the rate of the coupling ( $t_{1/2} < 30$  min), the Suzuki coupling reaction can suffer from very low yields or complete shutdown of conversion to the biaryl product.<sup>85</sup>

There are generally two common methods to overcome protodeboronation of labile boronic acids. The first involves preformation of an active catalyst to greatly increase turnover frequency and negate need of formation of the catalyst species from a precatalyst and ligand in solution.<sup>92, 93</sup> Buchwald and coworkers pioneered use of an XPhos containing palladacycle catalyst which allowed for coupling of nitrogen-rich heterocycles. However, while this increased rate could increase yields above that of

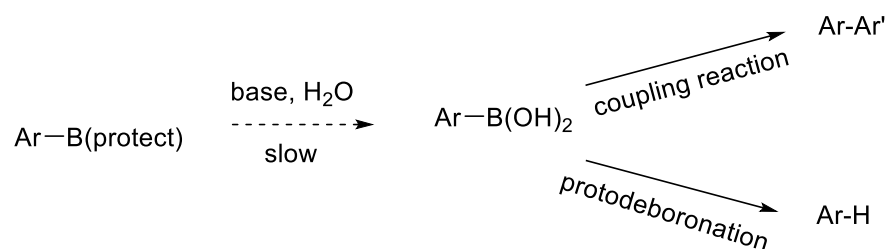
conventional 'one-pot' methodology, it has the drawbacks in that it was not applicable to boronic acids prone to fast protodeboronation, and that the precatalyst synthesis involved a 2-step process utilizing strictly inert reaction conditions, which added additional time, reagents and costs to the overall procedure.<sup>85</sup>



**Scheme 13:** Synthesis of Buchwald XPhos precatalyst<sup>85</sup>

The second method of combating the troublesome protodeboronation reaction involves protecting the boronic acid. This can be done during the borylation reaction, e.g. using bis(pinacolato)diboron to form the boronic acid pinacol ester instead of trimethyl borate, which would form the active boronic acid which may decompose under the reaction conditions.<sup>77, 94</sup>

While the number of different potential boronic esters and boronates is fairly numerous, all have the same general mechanism of hydrolysis of the B-Y bond by the basic OH<sup>-</sup> anion in the aqueous solution to form the active boronic acid *in-situ*.<sup>91</sup> As the boronates and boronic esters are not themselves active to the coupling reaction, the overall reaction rate is then dependant on the rate of hydrolysis to the active boronic acid. The rate of the reaction and the rate of protodeboronation is dependent on the concentration of the boronic acid in solution. In cases where the rate of hydrolysis from the protected boronate to the boronic acid, and the subsequent rate of protodeboronation of the boronic acid to the parent aryl are higher relative to the rate of the coupling reaction, a drop in overall conversions will result.



**Scheme 14** General scheme for protected boronic acid coupling<sup>95</sup>

An additional drawback of boronic acid protection is that once the protecting group is liberated in basic conditions the active boronic acid then undergoes a competitive reaction between protodeboronation and entering into the cycle of the coupling reaction itself. When using boronic acids which are particularly labile to protodeboronation under reaction conditions, using protecting groups such as trifluoroboronates may not be adequate due to the fast relative rate of protodeboronation with respect to the coupling reaction. These boronate salts including trifluoroboronates can be useful in reactions where the boronic acid protodeboronation rate remains within the same order of the coupling reaction and can be used successfully with numerous classes of boronic acids provided the rate of protodeboronation of the parent boronic acid is sufficiently low.

Caesium bases, particularly caesium carbonate, are routinely used in Suzuki cross couplings which conduct a base screen as it is frequently found to be superior to potassium and sodium carbonate when all three alkali metals are tested.<sup>9</sup> This increase in performance of caesium bases where the cation is generally thought to be a spectator is called the 'caesium effect'.<sup>96</sup> Reasons for this effect have been postulated and have been attributed to solubility, which has been proven in dipolar aprotic solvents, but is generally not a factor in homogenous Suzuki couplings, and intermediate stabilisation involving a M-Cs stabilised transition state.<sup>10, 97</sup> Transition states involving M-Cs interaction have been calculated by DFT but intermediates have never been isolated experimentally outside of *in silico* measurements.<sup>19, 21</sup>

Potassium phosphate is also a routinely used base in Suzuki couplings involving base screens. If the trend that caesium carbonate tends to perform better and give higher yields than potassium carbonate is also true for phosphates, we would expect caesium phosphate to be more active than potassium phosphate towards a broad range of conditions in Suzuki reactions.

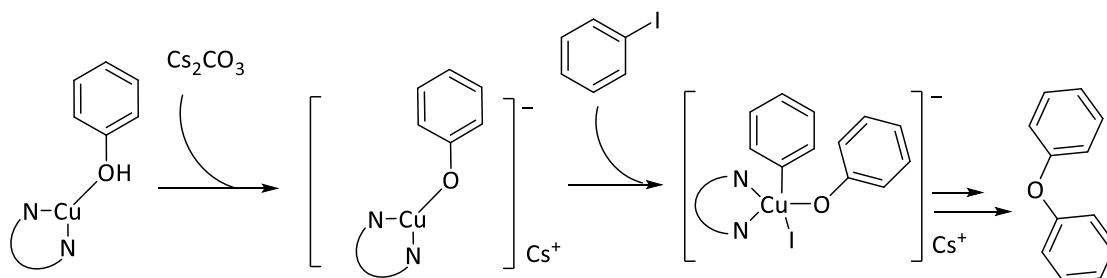
### **1.3 Evidence of direct Cs involvement in catalysis**

#### **1.3.1. Synthetic incorporation of caesium base in catalysis**

Previous research into the caesium effect has been conducted, however the vast majority of the research involved investigations into the increased solubility of caesium

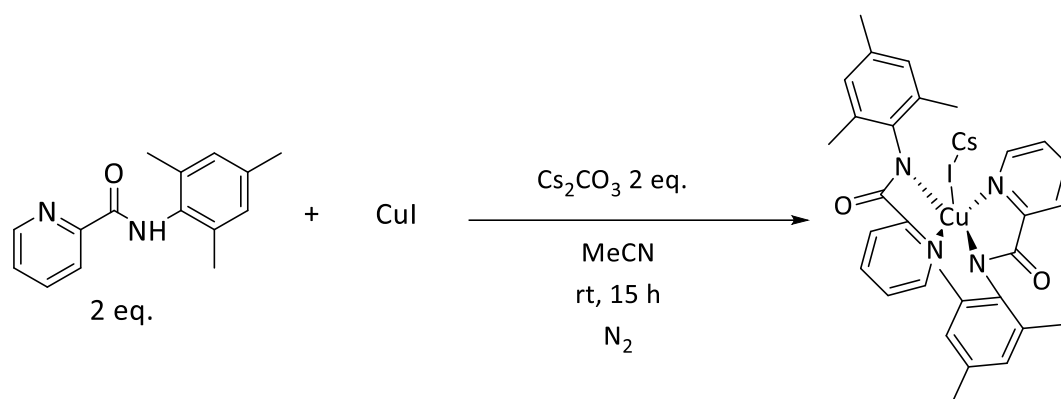
salts rather than any direct interactions involving the  $\text{Cs}^+$  cation.<sup>16, 27, 96</sup> No concrete evidence of the  $\text{Cs}^+$  ion interacting with either the reactive species or the catalyst had been found until recently. Results at University of Leeds have produced evidence of direct caesium involvement in the catalytic cycle, disputing the currently held beliefs that the caesium effect is related to the solubility of the  $\text{Cs}^+$  cation in organic solvents.

In a catalytic system involving arylation of phenols with a copper picolinamide complex, a reaction was conducted with a  $\text{CsI}$  fragment bonded directly to the copper atom of the catalyst with the starting material previously having been analysed to possess a  $\text{Cs-I-Cu}$  bond by XRD. The  $\text{Cs-I-Cu}$  complex was a by-product of previous catalytic reactions. The prevailing idea was that caesium bonded directly to the active catalyst would reduce reaction performance due to the caesium no longer acting as a base in solution, however the resulting complex proved to be more active than the standard  $\text{CuI}$  / ligand system, achieving a modest 40% yield over 20% for the  $\text{CuI}$  / ligand 1:2 ratio. This  $\text{Cu-I-Cs}$  complex was itself less reactive than a 1:1  $\text{CuI}$  / ligand system but gives evidence that  $\text{CsI}$  is directly involved in the catalytic cycle when bonded to the catalyst, and provides a beneficial effect to the reaction. In the hypothesized mechanism for this interaction, the  $\text{Cs}^+$  ion may provide a stabilizing interaction between the catalyst species and the reactants, lowering the activation barrier of the rate determining step. Specifically it is proposed that the  $\text{Cs}^+$  ion is able to reduce the energy of the rate limiting transition state of the oxidative addition step of the aryl halide before reductive elimination of the product.<sup>98</sup>



**Scheme 15:** Representation of caesium effect in arylation of phenols

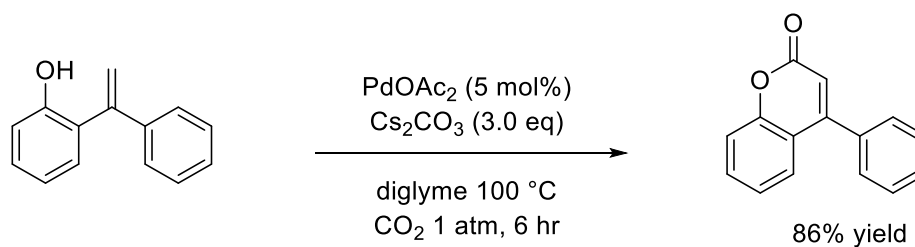
The synthesis of this  $\text{Cs-I-Cu}$  adduct was reported as a side product in the complexation reaction of the picolinamide ligand with copper iodide, with the two ligands arranged *trans* to each other and the  $\text{CsI}$  fragment bonded to the top face of the copper atom. This unusual structure is present as the product in Scheme 16.



**Scheme 16:** Synthesis of Cu-I-Cs species<sup>99</sup>

This type of bridged CsI complex is novel to catalytic reactions, and provides confirmation that catalytically active Cs-Cu bimetallic catalysts are plausible to synthesise.<sup>99</sup>

Despite multiple catalytic reaction classes suggesting a direct involvement between the caesium cation and the substrates or catalyst, there is only one synthetic example of a palladium-caesium bimetallic complex.<sup>100</sup> Iwasawa *et al.* discovered that in a C-H carboxylation reaction forming coumarin derivatives caesium carbonate was the optimal base in a base screen, but curiously potassium carbonate failed to convert any product at all (Scheme 17).



**Scheme 17:** 'caesium effect' exerted by Pd-Cs intermediate in C-H carboxylation reaction<sup>100</sup>

The authors were able to observe a bimetallic caesium-palladium intermediate by XRD which was catalytically active. Their proposed mechanism was direct carboxylation of the Pd-C bond in the intermediate followed by CO<sub>2</sub> transfer to the starting material producing the Pd-Cs species and the desired coumarin product.

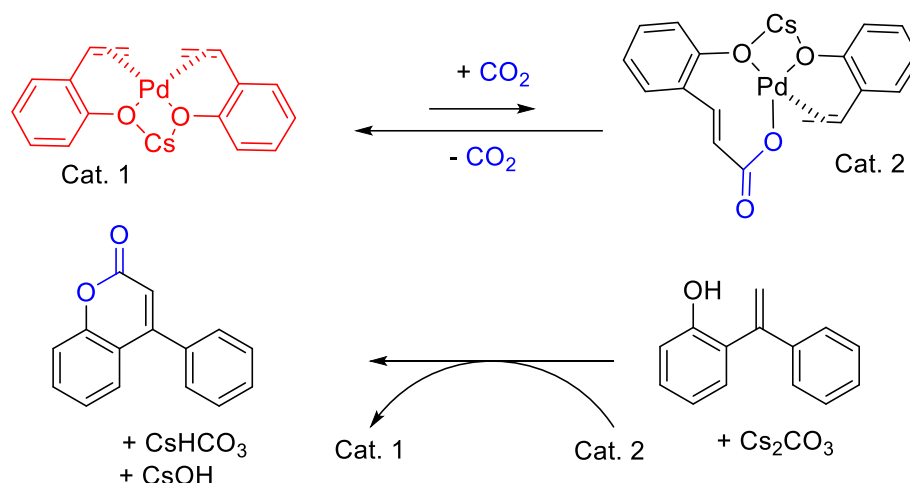
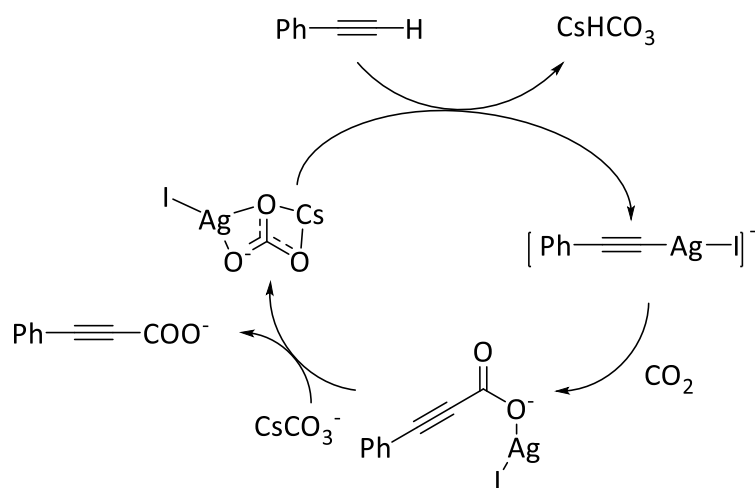


**Figure 12:** Caesium mediated C-H carboxylation reaction indicating isolated Pd-Cs species in red and CO<sub>2</sub> in blue

The caesium cation is required for this reaction to proceed, evidenced by the lack of any conversion using potassium carbonate base. The caesium cation is able to reduce the energy barrier to the CO<sub>2</sub> palladation step, allowing transfer of the activated CO<sub>2</sub> to the starting material providing the coumarin product.<sup>100</sup> Despite this being the only synthetic example of a caesium catalytic intermediate, numerous other reactions could incorporate similar species and allow for increased rates using caesium cations.

### 1.3.2 DFT calculations of caesium containing intermediates

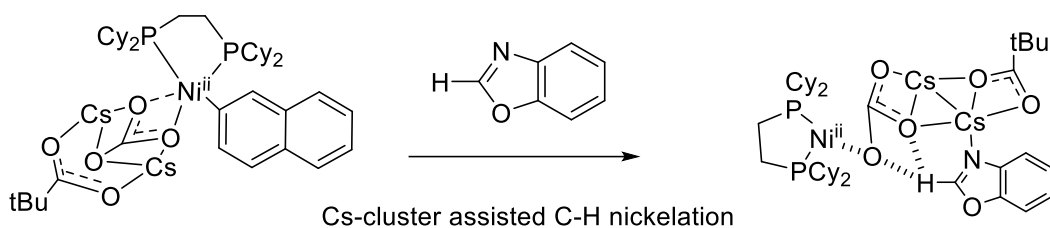
Multiple computational mechanistic studies have been recently conducted to confirm the active species in caesium-mediated transition metal catalysed reactions. Zhang *et al.* discovered that the lowest energy pathway in the silver-catalysed carboxylation reaction of phenylacetylene involves a Cs-Ag bimetallic intermediate.<sup>101</sup> The authors show that a CsCO<sub>3</sub><sup>-</sup> moiety is more computationally favourable than the previously considered silver carboxylate in this reaction by a margin of 21.8 KJ/mol, and the caesium containing intermediate is able to facilitate the deprotonation and oxidative addition of the acetylene molecule to the silver catalyst.



**Scheme 18:** Proposed catalytic cycle for carboxylation of phenylacetylene<sup>101</sup>

The complex nature of the caesium-mediated deprotonation step is supported by experimental findings, as caesium fluoride proves to be the best base for the reaction, outperforming caesium carbonate and other group I bases.<sup>18</sup> This data aligns with theoretical findings as the  $\Delta H$  value for the bond formation of H-F will be more favourable than for H-CO<sub>3</sub>. These findings are the first that provide any evidence for multiple instances of caesium ions in the active catalytic site in the form of a Cs<sub>2</sub>-I-F cluster, which may influence the C-H activation pathway, which also provides further evidence towards the catalytic activity of M-I-Cs moieties towards aryl substrates.

C-H activation reactions are affected by addition of caesium carbonate, and Musaev *et al.* discovered that not only did the addition of the base triple the rate constant and provide a higher yielding product in the C-H activation / nickelation step of the nickel catalysed coupling of benzoxazole with naphylen-2-yl pivalate, but the caesium ion was directly involved in the catalytic cycle by DFT calculations. They stipulated that the Cs-N and Cs-O interactions with the azole molecule play a crucial role in the energy barrier for reaction, with the addition of caesium providing a much easier pathway for coupling and higher yields of the coupled product from the rate determining C-H activation step by a factor of 15.1 KJ/mol.<sup>19</sup>



**Scheme 19:** Direct Cs<sup>+</sup> involvement in the rate determining nickelation step<sup>19</sup>

The authors also ran calculations on the reaction using potassium carbonate instead of the caesium base, finding that while the results were better than with no base, the smaller cation did not have as good interaction with the azole as caesium did, and therefore the C-H activation energy barrier was higher as a result. In experimental findings, the reaction was sped up by 1.1 fold on addition of potassium base, but was not nearly as effective as the 3 fold increase in rate on caesium base addition.

#### 1.4 Summary

Despite bases being highly important reagents for both traditional organic and transition metal-catalysed reactions, relatively little work has gone into assessing exactly how the base cation and anion can affect reaction performance. Caesium bases are routinely used in palladium catalysed coupling reactions,<sup>30</sup> and tend to perform better than other alkali metal bases.<sup>32</sup> While explanations such as increased solubility and the polarizability of the soft caesium cation have been suggested as possible reasons for this 'caesium effect',<sup>4</sup> very little hard evidence has been found to suggest the exact mechanism by which caesium bases can increase reactivity.

The role of the base in palladium catalysed coupling reactions is variable between the reaction classes, with bases able to change which product is formed, increase the rate of reaction by lowering the activation energy barrier, and alter the mechanistic pathway itself by direct coordination to the palladium centre.<sup>100</sup> We would usually expect that a reagent would only influence the reaction yield if it was involved in the rate determining step, but despite only the Buchwald-Hartwig amination reaction explicitly stating that the deprotonation step was rate limiting,<sup>102</sup> all reactions studied displayed some degree of base effect in the literature despite differences in reaction temperature, solvents, and base role. From this we can deduce that the base effect of a reaction, and therefore the 'caesium effect', does not appear to be dictated by the increased solubility of caesium bases in dipolar aprotic solvents. An alternative

reasoning behind this increase is likely to be due to stabilisation of transition states *via* the soft caesium cation.

Numerous DFT calculations in the literature have proposed caesium stabilised transition states in C-H activation reactions as well as C-O arylation reactions.<sup>18, 19, 101</sup> In these cases the caesium is not formally bound to the palladium atom, but allows an interaction which facilitates a mechanistic step by reducing the activation energy barrier below the level possible without any caesium cation stabilisation. Only one Pd-Cs species has been isolated and characterised formally by X-ray diffraction, in a C-H carboxylation reaction where the caesium cation facilitates addition of CO<sub>2</sub> to the palladium precatalyst.<sup>100</sup> This evidence of a bimetallic palladium-caesium catalyst provides sufficient evidence to further investigate how direct interaction of the caesium cation with both catalyst and reagents can allow for better understanding of these reactions. This therefore can result in greater optimisation, leading to higher rates and conversions by use of caesium bases in palladium catalysed coupling reactions.

This project aims to deduce which reactions the 'caesium effect' significantly affects, as well as elucidate the mechanism of action of any increase in rate or conversions where a change in the base cation can change the reaction rate or conversion. This will be completed *via* syntheses of non-commercial caesium species, as well as reaction monitoring and heteronuclear NMR experiments, to deduce how caesium bases can improve coupling reactions.

### **1.5 References**

1. T. Imamoto, T. Oshiki, T. Onozawa, M. Matsuo, T. Hikosaka and M. Yanagawa, *Heteroat. Chem.*, 1992, **3**, 563-575.
2. H. Kunz, R. Kullmann, P. Wernig and J. Zimmer, *Tetrahedron Lett.*, 1992, **33**, 1969-1972.
3. R. N. Salvatore, A. S. Nagle and K. W. Jung, *J. Org. Chem.*, 2002, **67**, 674-683.
4. G. Dijkstra, W. H. Kruizinga and R. M. Kellogg, *J. Org. Chem.*, 1987, **52**, 4230-4234.
5. P. S. J. Canning, K. McCrudden, H. Maskill and B. Sexton, *J. Chem. Soc., Perkin Trans.*, **2**, 1999, 2735-2740

6. M. Wang, X. Zhang, Y.-X. Zhuang, Y.-H. Xu and T.-P. Loh, *J. Am. Chem. Soc.*, 2015, **137**, 1341-1347.
7. T. W. Lyons, K. L. Hull and M. S. Sanford, *J. Am. Chem. Soc.*, 2011, **133**, 4455-4464.
8. L. Théveau, C. Verrier, P. Lassalas, T. Martin, G. Dupas, O. Querolle, L. Van Hijfte, F. Marsais and C. Hoarau, *Chem. - Eur. J.*, 2011, **17**, 14450-14463.
9. R. Grisorio and G. P. Suranna, *ACS Macro Lett.*, 2017, **6**, 1251-1256.
10. S. Yu, S. Liu, Y. Lan, B. Wan and X. Li, *J. Am. Chem. Soc.*, 2015, **137**, 1623-1631.
11. Q. A. McKellar and H. A. Benchaoui, *J. Vet. Pharmacol. Ther.*, 1996, **19**, 331-351.
12. H. Ikeda, T. Nonomiya, M. Usami, T. Ohta and S. Omura, *Proc. Natl. Acad. Sci. U. S. A.*, 1999, **96**, 9509-9514.
13. W. H. Kruizinga and R. M. Kellogg, *J. Am. Chem. Soc.*, 1981, **103**, 5183-5189.
14. J. Mitroy, M. S. Safronova and W. C. Charles, *J. Phys. B: At., Mol. Opt. Phys.*, 2010, **43**, 202001.
15. R. Shannon, *Acta Crystallogr. Sect. A*, 1976, **32**, 751-767.
16. A. de Lucas, L. Rodríguez, M. Pérez-Collado, P. Sánchez and J. F. Rodríguez, *Polym. Int.*, 2002, **51**, 1066-1071.
17. D. N. Bhattacharyya, C. L. Lee, J. Smid and M. Szwarc, *J. Phys. Chem.*, 1965, **69**, 612-623.
18. T. M. Figg, M. Wasa, J.-Q. Yu and D. G. Musaev, *J. Am. Chem. Soc.*, 2013, **135**, 14206-14214.
19. H. Xu, K. Muto, J. Yamaguchi, C. Zhao, K. Itami and D. G. Musaev, *J. Am. Chem. Soc.*, 2014, **136**, 14834-14844.
20. J. A. Cella and S. W. Bacon, *J. Org. Chem.*, 1984, **49**, 1122-1125.
21. D. G. Musaev, T. M. Figg and A. L. Kaledin, *Chem. Soc. Rev.*, 2014, **43**, 5009-5031.
22. R. Diaz-Torres and S. Alvarez, *Dalton Trans.*, 2011, **40**, 10742-10750.
23. R. N. Salvatore, A. S. Nagle, S. E. Schmidt and K. W. Jung, *Org. Lett.*, 1999, **1**, 1893-1896.
24. C. Chiappe and D. Pieraccini, *Green Chem.*, 2003, **5**, 193-197.
25. E. J. Corey, F. Xu and M. C. Noe, *J. Am. Chem. Soc.*, 1997, **119**, 12414-12415.
26. M. T. Honaker, B. J. Sandefur, J. L. Hargett, A. L. McDaniel and R. N. Salvatore, *Tetrahedron Lett.*, 2003, **44**, 8373-8377.

27. E. E. Dueno, F. Chu, S.-I. Kim and K. W. Jung, *Tetrahedron Lett.*, 1999, **40**, 1843-1846.
28. C. Amatore, A. Jutand and G. Le Duc, *Eur. J. Chem.*, 2011, **17**, 2492-2503.
29. M. Beller and T. H. Riermeier, *Eur. J. Inorg. Chem.*, 1998, **1998**, 29-35.
30. C. Meyers, B. U. W. Maes, K. T. J. Loones, G. Bal, G. L. F. Lemière and R. A. Dommissie, *J. Org. Chem.*, 2004, **69**, 6010-6017.
31. D. Tzalis and P. Knochel, *Angew. Chem. Int. Ed.*, 1999, **38**, 1463-1465.
32. Q. Xu, W.-L. Duan, Z.-Y. Lei, Z.-B. Zhu and M. Shi, *Tetrahedron*, 2005, **61**, 11225-11229.
33. M. B. Calvert and J. Sperry, *Org. Biomol. Chem.*, 2016, **14**, 5728-5743.
34. M. Carril, A. Correa and C. Bolm, *Angew. Chem. Int. Ed.*, 2008, **47**, 4862-4865.
35. R. F. Heck and J. P. Nolley, *J. Org. Chem.*, 1972, **37**, 2320-2322.
36. J. Kotz, P. Treichel, J. Townsend and D. Treichel, *Chemistry & Chemical Reactivity*, Cengage Learning, 2014.
37. V. Calò, A. Nacci, A. Monopoli and V. Ferola, *J. Org. Chem.*, 2007, **72**, 2596-2601.
38. J. G. de Vries, *Dalton Trans.*, 2006, 421-429.
39. Q. Yao, E. P. Kinney and Z. Yang, *J. Org. Chem.*, 2003, **68**, 7528-7531.
40. I. P. Beletskaya and A. V. Cheprakov, *Chem. Rev.*, 2000, **100**, 3009-3066.
41. H. Zhang, P. Chen and G. Liu, *Angew. Chem.*, 2014, **53**, 10174-10178.
42. R. Chinchilla and C. Najera, *Chem Rev*, 2007, **107**, 874-922.
43. C. Amatore and A. Jutand, *Acc. Chem. Res.*, 2000, **33**, 314-321.
44. W.-H. Guo, Z.-J. Luo, W. Zeng and X. Zhang, *ACS Catalysis*, 2017, **7**, 896-901.
45. M. Gazvoda, M. Virant, B. Pinter and J. Košmrlj, *Nat. Commun.*, 2018, **9**, 4814.
46. D. G. Brown and J. Boström, *J. Med. Chem.*, 2016, **59**, 4443-4458.
47. H. B. Goodbrand and N.-X. Hu, *J. Org. Chem.*, 1999, **64**, 670-674.
48. Y. Sunesson, E. Limé, S. O. Nilsson Lill, R. E. Meadows and P.-O. Norrby, *J. Org. Chem.*, 2014, **79**, 11961-11969.
49. C. F. R. A. C. Lima, A. S. M. C. Rodrigues, V. L. M. Silva, A. M. S. Silva and L. M. N. B. F. Santos, *ChemCatChem*, 2014, **6**, 1291-1302.
50. I. C. F. R. Ferreira, M.-J. R. P. Queiroz and G. Kirsch, *Tetrahedron*, 2003, **59**, 975-981.
51. P. Ramírez-López, A. Ros, A. Romero-Arenas, J. Iglesias-Sigüenza, R. Fernández and J. M. Lassaletta, *J. Am. Chem. Soc.*, 2016, **138**, 12053-12056.

52. K. O. Kirlikovali, E. Cho, T. J. Downard, L. Grigoryan, Z. Han, S. Hong, D. Jung, J. C. Quintana, V. Reynoso, S. Ro, Y. Shen, K. Swartz, E. Ter Sahakyan, A. I. Wixtrom, B. Yoshida, A. L. Rheingold and A. M. Spokoyny, *Dalton Trans.*, 2018, **47**, 3684-3688.
53. X. Chen, K. M. Engle, D.-H. Wang and J.-Q. Yu, 2009, *Angew. Chem. Int. Ed.*, **48**, 5094-5115.
54. V. Ritleng, C. Sirlin and M. Pfeffer, *Chem. Rev.*, 2002, **102**, 1731-1770.
55. J. Wencel-Delord, T. Dröge, F. Liu and F. Glorius, *Chem. Soc. Rev.*, 2011, **40**, 4740-4761.
56. D. Wei, X. Zhu, J.-L. Niu and M.-P. Song, *ChemCatChem*, 2016, **8**, 1242-1263.
57. G. Song, F. Wang and X. Li, *Chem. Soc. Rev.*, 2012, **41**, 3651-3678.
58. J.-Y. Cho, M. K. Tse, D. Holmes, R. E. Maleczka and M. R. Smith, *Science*, 2002, **295**, 305-308.
59. M. Lersch and M. Tilset, *Chem. Rev.*, 2005, **105**, 2471-2526.
60. C. Wei and C.-J. Li, *J. Am. Chem. Soc.*, 2003, **125**, 9584-9585.
61. B.-J. Li, S.-D. Yang and Z.-J. Shi, *Synlett*, 2008, **2008**, 949-957.
62. M. Chaumontet, R. Piccardi, N. Audic, J. Hitce, J.-L. Peglion, E. Clot and O. Baudoin, *J. Am. Chem. Soc.*, 2008, **130**, 15157-15166.
63. P. M. Holstein, M. Vogler, P. Larini, G. Pilet, E. Clot and O. Baudoin, *ACS Catalysis*, 2015, **5**, 4300-4308.
64. C. E. Kefalidis, O. Baudoin and E. Clot, *Dalton Trans.*, 2010, **39**, 10528-10535.
65. R. N. P. Tulichala and K. C. K. Swamy, *Org. Biomol. Chem.*, 2016, **14**, 4519-4533.
66. B. B. Touré, B. S. Lane and D. Sames, *Org. Lett.*, 2006, **8**, 1979-1982.
67. K. M. Gericke, D. I. Chai, N. Bieler and M. Lautens, *Angew. Chem. Int. Ed.*, 2009, **48**, 1447-1451.
68. B. Mariampillai, J. Alliot, M. Li and M. Lautens, *J. Am. Chem. Soc.*, 2007, **129**, 15372-15379.
69. N. W. Y. Wong and P. Forgione, *Org. Lett.*, 2012, **14**, 2738-2741.
70. S. Sharma, J. Park, E. Park, A. Kim, M. Kim, J. H. Kwak, Y. H. Jung and I. S. Kim, *Adv. Synth. Catal.*, 2013, **355**, 332-336.
71. M. Wasa, K. M. Engle and J.-Q. Yu, *J. Am. Chem. Soc.*, 2009, **131**, 9886-9887.
72. C. Zhu, Y. Zhang, J. Kan, H. Zhao and W. Su, *Org. Lett.*, 2015, **17**, 3418-3421.

73. A. A. C. Braga, N. H. Morgon, G. Ujaque and F. Maseras, *J. Am. Chem. Soc.*, 2005, **127**, 9298-9307.
74. A. J. J. Lennox and G. C. Lloyd-Jones, *Angew. Chem. Int. Ed.*, 2013, **52**, 7362-7370.
75. D. D. Dolliver, B. T. Bhattarai, A. Pandey, M. L. Lanier, A. S. Bordelon, S. Adhikari, J. A. Dinser, P. F. Flowers, V. S. Wills, C. L. Schneider, K. H. Shaughnessy, J. N. Moore, S. M. Raders, T. S. Snowden, A. S. McKim and F. R. Fronczek, *J. Org. Chem.*, 2013, **78**, 3676-3687.
76. C. Baillie, L. Zhang and J. Xiao, *J. Org. Chem.*, 2004, **69**, 7779-7782.
77. A. J. J. Lennox and G. C. Lloyd-Jones, *Chem. Soc. Rev.*, 2014, **43**, 412-443.
78. A. Suzuki, *Chem. Commun.*, 2005, 4759-4763.
79. I. Hoffmann, B. Blumenroder, S. Onodi nee Thumann, S. Dommer and J. Schatz, *Green Chem.*, 2015, **17**, 3844-3857.
80. Z. Yinjun, Y. Guizhou, X. Jianwei and Z. Jianrong, *Eur. J. Org. Chem.*, 2014, **2014**, 5901-5905.
81. M. Alešković, N. Basarić and K. Mlinarić-Majerski, *J. Heterocycl. Chem.*, 2011, **48**, 1329-1335.
82. B. P. Carrow and J. F. Hartwig, *J. Am. Chem. Soc.*, 2011, **133**, 2116-2119.
83. M. Butters, J. N. Harvey, J. Jover, A. J. Lennox and G. Lloyd-Jones, *Angew. Chem. Int. Ed.*, 2010, **49**, 5156-5160.
84. A. Thakur, K. Zhang and J. Louie, *Chem. Commun.*, 2012, **48**, 203-205.
85. M. A. Oberli and S. L. Buchwald, *Org. Lett.*, 2012, **14**, 4606-4609.
86. C. Chen and L.-M. Yang, *Tetrahedron Lett.*, 2007, **48**, 2427-2430.
87. R. B. Bedford and C. S. J. Cazin, *Chem. Commun.*, 2001, 1540-1541.
88. P. A. Cox, A. G. Leach, A. D. Campbell and G. C. Lloyd-Jones, *J. Am. Chem. Soc.*, 2016, **138**, 9145-9157.
89. P. A. Cox, M. Reid, A. G. Leach, A. D. Campbell, E. J. King and G. C. Lloyd-Jones, *J. Am. Chem. Soc.*, 2017, **139**, 13156-13165.
90. L. Xu, G. Wang, S. Zhang, H. Wang, L. Wang, L. Liu, J. Jiao and P. Li, *Tetrahedron*, 2017, **73**, 7123-7157.
91. A. J. Lennox and G. Lloyd-Jones, *Isr. J. Chem.*, 2010, **50**, 664-674.
92. G.-R. Peh, E. A. B. Kantchev, J.-C. Er and J. Y. Ying, *Eur. J. Chem.*, 2010, **16**, 4010-4017.

93. L. Chen, H. Francis and B. P. Carrow, *ACS Catalysis*, 2018, **8**, 2989-2994.
94. K. M. Clapham, A. S. Batsanov, M. R. Bryce and B. Tarbit, *Org. Biomol. Chem.*, 2009, **7**, 2155-2161.
95. A. J. J. Lennox and G. C. Lloyd-Jones, *J. Am. Chem. Soc.*, 2012, **134**, 7431-7441.
96. M. Honaker, Master of Science Thesis, Western Kentucky University, 2004.
97. M. Crescenzi, C. Galli and L. Mandolini, *J. Phys. Org. Chem.*, 1990, **3**, 428-434.
98. C. Sambigiagio, PhD Thesis, University of Leeds, 2015.
99. G. J. S. Carlo Sambigiagio, Bao N. Nguyen, and Patrick C. McGowan, unpublished work.
100. K. Sasano, J. Takaya and N. Iwasawa, *J. Am. Chem. Soc.*, 2013, **135**, 10954-10957.
101. C. Liu, Y. Luo, W. Zhang, J. Qu and X. Lu, *Organometallics*, 2014, **33**, 2984-2989.
102. F. Wang, L. Zhu, Y. Zhou, X. Bao and H. F. Schaefer, *Chem. -Eur. J.*, 2015, **21**, 4153-4161.

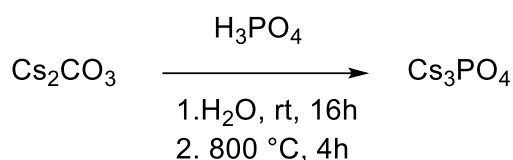
## Chapter 2: Synthesis and reactivity of non-commercial caesium species

Weak bases, defined as basic species which do not fully dissociate in aqueous solution, such as alkali metal carbonates, phosphates, and fluorides are widely used in catalytic cross coupling reactions.<sup>1</sup> The standard bases used in catalysed coupling reactions tend to be carbonates ( $pK_a$  10.3) and phosphates ( $pK_a$  12.3). If a stronger base is needed, potassium *tert*-butoxide ( $pK_a$  17) is generally used to drive the equilibrium towards deprotonation of the substrate.<sup>2, 3</sup> While the entire range of alkali metal carbonates and fluorides are commercially available, caesium phosphate is not and must be synthesised from commercially available starting materials. In numerous base screen studies in the literature, caesium bases have been found to provide access to higher reaction performance than cheaper potassium or sodium equivalents.<sup>1, 4-6</sup> We would expect therefore, that if caesium carbonate and fluoride tended to be superior to the potassium base equivalent, the phosphate base would behave in a similar way.

Due to the lack of commercial availability, caesium phosphate has only been used in two literature procedures in catalytic reactions.<sup>7, 8</sup> This represents a large knowledge gap of the performance of this base in catalytic reactions.

### 2.1 Synthesis of caesium phosphate monohydrate

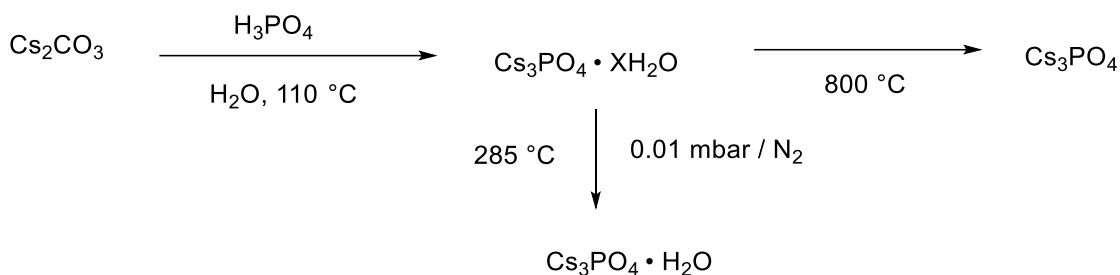
The synthesis of caesium phosphate was adapted from a procedure from Cordfunke and Ouweltjes, who provided a useful one-step chemical reaction forming caesium phosphate which evolved  $CO_2$  as a by-product.<sup>9</sup> Due to the extremely harsh conditions required for calcination to remove the bound water molecules, specialist furnaces were used and the dry base cooled under inert gas to avoid deliquescence.<sup>10</sup>



**Scheme 20:** Literature synthesis of caesium phosphate

To avoid the issues with heating the sample to extremely high temperatures, a different approach to drying the caesium phosphate was taken which allowed more control of the reaction using standard fume hood procedures. The base hydrate was added to a round bottom flask and heated to 285 °C in a sand bath under vacuum using a

diaphragm pump (~10 mbar) overnight. The vacuum line was then changed to a rotary vane style pump (~0.01 mbar) to remove the remaining free moisture to give dry tricaesium phosphate as a monohydrate.



**Scheme 21:** Comparison of literature and BNN caesium phosphate drying methods

Despite the reduction in temperature from 800 °C to 285 °C, allowing the drying step to be done in a sand bath rather than specialist furnace, we elected to investigate means of drying by azeotropic distillation. After the initial heating step at 110 °C, which gave a caesium phosphate slurry, ethanol was added to reduce the boiling point of the solvent mixture. The solubility of caesium phosphate in ethanol was enough to fully dissolve the slurry, at which point the azeotrope was heated to 200 °C in a sand bath *in vacuo* to give dry caesium phosphate powder. The reduction in temperature required for this synthesis represents the difference between needing specialist equipment and extremely forcing conditions, to allow reliable synthesis on multi-gram scale with easily available equipment in any research laboratory. The base must be kept dry, which was accomplished by flushing with inert gas after use to stop water uptake.

## **2.2 Analysis and characterisation of caesium phosphate monohydrate**

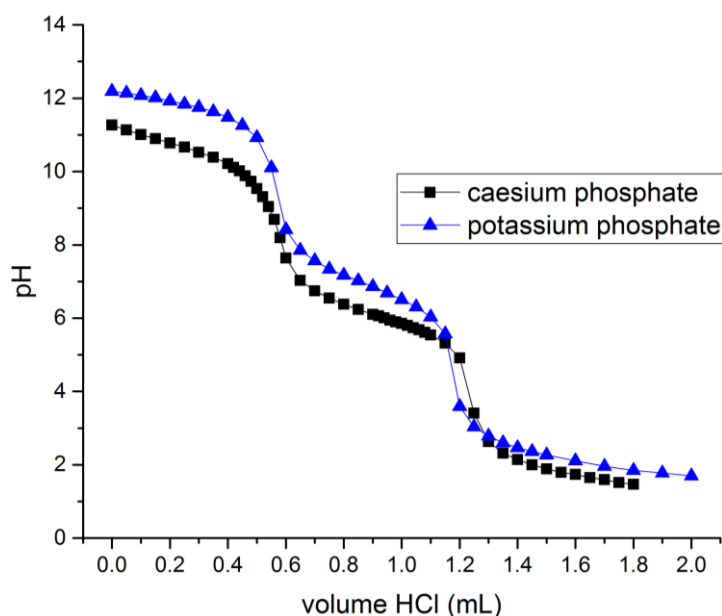
Salts are a class of compounds that are relatively difficult to characterise. While caesium phosphate has two spin active nuclei ( $^{133}\text{Cs}$  and  $^{31}\text{P}$ ), due to splitting into component ions when dissolved this analysis becomes problematic, and the chemical shift directly correlates with concentration rather than shielding.<sup>11, 12</sup> In the same fashion mass spectrometry is difficult and the caesium ion itself remains as the main peak. Atomic absorption spectroscopy (AAS) is a useful way to find the atomic composition of a sample, particularly metal salts, and provides insights into impurities and water content. This method of analysis is particularly useful for caesium salts, as it does not matter if the compound is dissociated into cation and anion for accurate results to be found.

Pure tricaesium phosphate has a theoretical caesium content of 80.7%, with caesium content of 77.9% calculated for caesium phosphate monohydrate. The experimental result agreed with this figure at 77.9% Cs. The monohydrate analysis was then confirmed with Karl-Fischer titration, with 3.8% water expected for a monohydrate base and 4.0% measured experimentally.

The other facet of tricaesium phosphate that must be investigated is the possibility of formation of dicaesium hydrogen phosphate ( $\text{Cs}_2\text{HPO}_4$ ) and caesium dihydrogen phosphate ( $\text{CsH}_2\text{PO}_4$ ). The potassium equivalent of these compounds act as buffers at physiological pH in solution, but as with the tricaesium base the salts are seldom used synthetically. While AAS analysis provides evidence of tricaesium salt formation, a titration is the easiest way to confirm these findings.

The measured  $\text{pK}_a$  of any base relies on both the anion and the assumption that the base is fully dissociated, as is the case with most bases in water. Due to the full dissociation coupled with only the anion having an effect on measured pH, we can compare different alkali metals through a  $\text{pK}_a$  measurement comparison between potassium and caesium phosphate. 0.5 mmol of the caesium species was dissolved in 10 mL water and titrated against 1M HCl in comparison with tripotassium phosphate to deduce the starting pH, and the number of equivalence points.

**Figure 13:** Titration of caesium phosphate species and comparison with tripotassium phosphate



Tripotassium phosphate and tricaesium phosphate in this experiment behave similarly. Both the initial pH of the solution are within a unit of each other, and the equivalence points occur at near identical points in the titration. In corroboration with the AAS data we are able to conclude that tricaesium phosphate is the sole species present, and that the exact species is likely to behave as a monohydrate base, similar to commercially available caesium hydroxide monohydrate.

### **2.2.1 Investigation of caesium phosphate monohydrate solubility in organic solvents**

Despite the prevailing hypothesis of the 'caesium effect' attributing the increased performance of caesium bases to solubility,<sup>13</sup> very little work has gone into solubility studies of inorganic bases in organic solvents, except for dipolar aprotic examples.<sup>14</sup> We elected to test the existing solubility hypothesis for both potassium and caesium phosphate in protic, dipolar aprotic and non-polar solvents routinely used for catalytic coupling reactions.

Solubility measurements for drug compounds and organic species are usually calculated using either HPLC or UV-Vis detection methods due to their high throughput, low detection limit properties.<sup>15</sup> The downsides of these methods are that they are difficult to keep dry, especially with hygroscopic samples and solvent, and require significant calibration and filtration steps, all of which must be done in dry atmosphere and solvent to avoid moisture ingress.

While both of the widely used methods of solubility detection are well documented and capable of precision of up to  $\pm 2\%$ , we elected to develop a new method involving solubility detection by heteroatomic NMR spectroscopy.

Alkali metal phosphate bases are not detectable by routine  $^1\text{H}$  and  $^{13}\text{C}$  NMR, but  $^{31}\text{P}$  is an NMR active isotope with 100% relative abundance. Phosphorus NMR can be referenced against  $\text{H}_3\text{PO}_4$  acid dissolved in  $\text{D}_2\text{O}$  and give chemical shifts along with solubility data by NMR. For caesium phosphate itself, we are able to use  $^{133}\text{Cs}$  NMR which in addition to  $^{31}\text{P}$  which due to a shorter  $T_1$  relaxation time of 25s along with a lower  $\Delta\nu$  of 0.6 Hz we can gain more precise data in a shorter time than  $^{31}\text{P}$  data.<sup>16</sup> Due to the presence of 3 Cs atoms in each molecule of base, our detection threshold for

solubility drops by about 25x from approximately 2.5 mM to 0.1 mM when changing from phosphorus to caesium nuclei if the NMR experiment is run overnight.

Non routine deuterated NMR solvents such as  $d^9$ -Dimethylacetamide tend to be prohibitively expensive to procure for a small run of samples, with prices commonly up to £100 / g for less commonly used solvents. To avoid this we elected to use a coaxial NMR insert tube to gain a  $^2D$  lock on  $D_2O$  containing 100 mM triphenylphosphine oxide or caesium nitrate standard respectively. The machine can then lock and shim on the deuterated solvent, and the signal relative to the external standard gives us solubility.

Samples were made up by oven drying NMR tubes and weighing 0.02 mmol phosphate base under inert atmosphere, followed by syringing in 1.0 mL of dry protic solvent. The sample was then sonicated for 10 minutes to ensure sufficient kinetic dissolution, and then the coaxial NMR tube with  $D_2O$  and internal standard inserted and covered in parafilm. It is important that at this stage a small amount of solid remains in the solvent, at a position below the NMR coil to ensure the solution is saturated and an accurate solubility reading is found. Results of these reactions are found in (Table 2). The experiments were repeated using the same sample with two unique runs on the NMR, giving an experimental error of 0.1 mM for both nuclei.



**Figure 14:** Coaxial insert NMR tube for solubility measurements

**Table 2:** Cs<sub>3</sub>PO<sub>4</sub>.H<sub>2</sub>O solubility in reaction solvents

Solvent	DMSO	DMAc	Toluene	DMF	MeCN	MeOH
Polarity index	7.2	6.5	2.4	6.4	5.8	5.1
Solubility (mM, ± 0.1)	1.7	0.3	<0.1	2.0	0.6	1300

It is evident here that solubility is not necessarily directly related to polarity of the solvent, and that whether a solvent is protic makes much more of a difference. There is no clear trend between the dipolar aprotic solvents as more polar DMAc has 7x lower solubility than marginally less polar DMF. Every reasonable precaution was taken to ensure reaction solvent dryness including purchasing fresh anhydrous solvents and utilizing the solvent purification system when applicable.

An interesting result gained from this data is that while base-mediated coupling reactions are well known in less polar solvents such as toluene, the extremely low solubility below the detection limit for overnight <sup>133</sup>Cs NMR would suggest that the deprotonation step may occur heterogeneously on the surface of the caesium base, similar to the templating mechanism present in polymerisation reactions. Alternatively the step could proceed homogeneously with a very low concentration of base in solution which is in equilibrium, with more base being pulled into the solution phase as the substrate is deprotonated forming dicaesium phosphate and caesium halide by-products.

Though knowing the value of caesium phosphate solubility in organic solvents is useful, to fully ascertain whether the existing solubility reasoning behind the caesium effect is corroborated with experimental evidence, we elected to run potassium phosphate base with the same methodology using <sup>31</sup>P NMR and phosphoric acid standard (Table 3).

**Table 3:** K<sub>3</sub>PO<sub>4</sub> solubility in organic reaction solvents by NMR

Solvent	DMSO	DMAc	Toluene	DMF	MeCN
Polarity index	7.2	6.5	2.4	6.4	5.8
Solubility (mM, ± 0.1)	0.3	0.3	6.4	<0.2	0.2

Previous literature conducted on carbonate bases by Cella and Bacon found that caesium carbonate was up to 15 times more soluble than potassium carbonate in dipolar aprotic solvents.<sup>14</sup> Clearly from the data we have acquired using heteroatomic NMR, there is not such a clear trend of solubility between the phosphate bases. While generally in dipolar aprotics the caesium base tended to be more soluble, with a 6 fold increase in solubility in DMSO, in less polar toluene however the potassium base was at least 60x more soluble, indicating that any caesium effect in this solvent was not due to solubility reasons. The much higher solubility found using potassium phosphate in toluene, while repeated to ensure reproducibility, may have arisen from trace amounts of water in the sample. While every reasonable precaution was taken to dry the solvent, utilising molecular sieves and inert atmosphere, even a very small amount of water would cause a large effect due to the high solubility of phosphate salts in aqueous solvent.

The majority of palladium-catalysed coupling reactions occur at elevated temperatures to overcome the activation energy barrier of the rate determining step. Generally upon increase of temperature the solubility of solids in the reaction solvent also increase, as this additional kinetic energy can overcome the crystal lattice energy and allow for increased solubility.

We decided to run NMR measurements of caesium phosphate and potassium phosphate in organic solvents using the coaxial insert method at varying temperatures (VT) to deduce whether increased temperature would cause an effect of increased base solubility. Potassium phosphate was run in toluene due to its relatively high solubility in this solvent, whereas caesium phosphate was run in both toluene and DMF (Table 4).

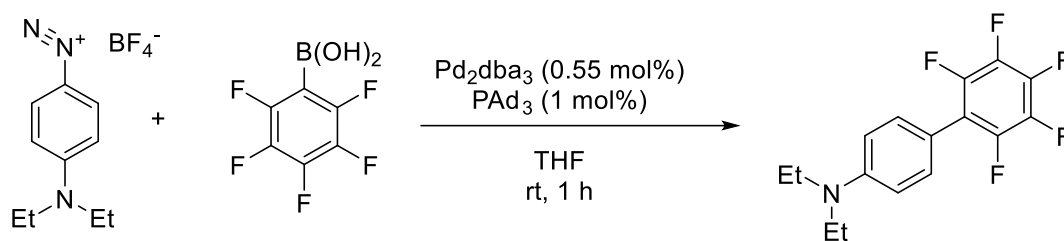
**Table 4:** NMR VT solubility of phosphate bases using coaxial insert method (N/C = Not completed due to instrument constraints)

Solubility in reaction solvent at T (mM, $\pm 0.1$ )							
Base (solvent)	25 °C	35 °C	45 °C	55 °C	65 °C	75 °C	85 °C
K <sub>3</sub> PO <sub>4</sub> (Toluene)	5.7	N/C	N/C	5.8	5.3	5.7	N/C
CS <sub>3</sub> PO <sub>4</sub> (toluene)	<0.5	<0.5	<0.5	<0.5	<0.5	<0.5	<0.5
CS <sub>3</sub> PO <sub>4</sub> (DMF)	3.3	3.4	3.7	3.6	3.0	2.0	4.2

Due to time constraints on facility access, individual experiments were only available to run for 4 hours which resulted in a 0.5 mM detection threshold for  $^{133}\text{Cs}$  and 2.5 mM for  $^{31}\text{P}$ . In both phosphate bases there does not seem to be a clear trend of solubility at increased temperatures. While there appears to be a small trend towards increasing solubility using caesium phosphate in DMF (Table 4), the effect appears to be quite subtle, with a possible outlier at 75 °C. This evidence shows that the solubility data gained at room temperature for each organic solvent (Table 2, Table 3) for both caesium and potassium phosphate is unlikely to change at increased reaction temperatures, and that the solubility of these bases is relatively temperature independent.

The entropy of a reaction system is increased by dissolution, due to the increased number of species in the reaction. On dissolution of the base, the cation and anion are free as ions in solution (assuming full dissociation), but partial dissociation still increases entropy to a lesser extent. This then results in a positive  $\Delta S$  value due to the breaking of the ionic lattice. As there appears to be little temperature dependence on solubility with both studied salts, the enthalpy change appears to be near zero, as the solubility appears to neither be endo or exothermic, which would present as a solubility change based on temperature due to Le Chatelier's principle. This then renders  $\Delta G$  negative which means solubility is thermodynamically favourable, which we can observe in small quantities ranging from sub mM to multi mM concentrations in organic solvents.

We can therefore state that in catalytic coupling reactions using phosphate bases, solubility is unlikely to play a major factor for any increase in performance of caesium bases, and that any increase in yield, reaction rate or product composition is intrinsic to the specific properties of the caesium cation. A likely hypothesis for the increased performance using the caesium cation in cross coupling reactions is due to a templating effect allowing the catalytic reaction to occur on the positively charged surface of the caesium cation. The Carrow group has had recent success with coupling base sensitive boronic acids to cationic aryldiazonium salts in a Suzuki type reaction.<sup>17</sup> If the positively charged caesium cation surface can perform a similar role to the aryldiazonium, where the positive charge of the nitrogen cation was hypothesised to facilitate acceleration of the coupling reaction, this may go some way to explain the presence of a caesium effect in these types of reactions.



**Scheme 22:** Carrow group diazonium Suzuki coupling of sensitive boronic acids<sup>17</sup>

The other likely possibility for caesium mediated reaction improvements in coupling reactions is that of direct caesium cation involvement in the rate determining step, either by reducing the energy of a rate limiting transition state or facilitating a change in the intermediate substrates themselves. Numerous examples have been found in DFT studies of Cs-M bimetallic transition states and intermediates but no species has ever been isolated for XRD or other conclusive analysis.<sup>4, 18, 19</sup>

### **2.3 Assessment of base mediated palladium catalysed coupling reactions for base screen**

Very little previous work has been conducted on the use of caesium phosphate in catalytic reactions. Only two literature preparations involving a palladium catalysed reaction have used caesium phosphate as the base.<sup>3, 8</sup> For this reason we elected to choose five commonly-used base-mediated palladium-catalysed coupling reactions applicable in industry and investigate both whether caesium phosphate monohydrate was an effective base, and in which examples it would improve the reaction over conventional inorganic carbonate and phosphate bases.

For caesium phosphate monohydrate to be applicable for wide scale use in coupling reactions it would need to impart some improvement on the reaction, as the extra cost associated with synthesis and calcination would need to be offset by a reduction in unit cost of the product. Moreover, it is only if caesium phosphate monohydrate is clearly better than other bases in a specific reaction that it would be economically viable to undergo a base synthesis prior to the coupling reaction itself.

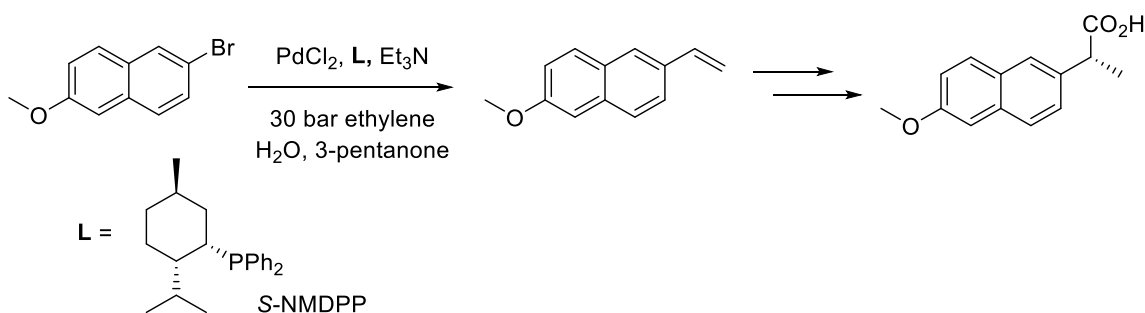
The reactions classes selected for screening caesium phosphate monohydrate were selected based on their use in medicinal chemistry. All of which use a coupling partner along with an aryl halide to reach the desired product (Table 5).

**Table 5:** Reactions for caesium phosphate monohydrate base screening

Reaction type	Coupling partner	Product
Heck Reaction	$R-\text{CH}=\text{CH}_2$	$R-\text{CH}=\text{CH}-\text{Ar}$
C-H activation	$\text{Ar}-\text{H}$	$\text{Ar}-\text{Ar}'$
Sonogashira reaction	$R-\text{C}\equiv\text{C}-\text{H}$	$R-\text{C}\equiv\text{C}-\text{Ar}$
Buchwald-Hartwig amination	$\begin{array}{c} \text{H} \\   \\ \text{R}-\text{N}-\text{R}' \end{array}$	$\begin{array}{c} \text{Ar} \\   \\ \text{R}-\text{N}-\text{R}' \end{array}$
Suzuki-Miyaura coupling	$\begin{array}{c} \text{OR}' \\   \\ \text{R}-\text{B} \\   \\ \text{OR}' \end{array}$	$\text{R}-\text{Ar}$

According to Brown and Boström, Suzuki-Miyaura cross couplings, Sonogashira coupling reactions and Buchwald-Hartwig aminations were all within the top 20 most common reactions used in *J. Med. Chem.* papers in 2014.<sup>20</sup> These reactions have demonstrable utility in biaryl coupling reactions, and each traditionally requires a base to mediate the catalyst reformation and/or the deprotonation of the substrate itself after oxidative addition.

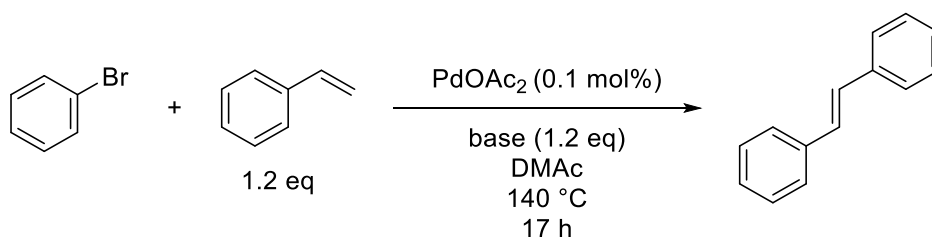
In addition to these three reactions we elected to investigate a C-H arylation reaction, as the use of this class of reactions has increased in recent years as a facile method to form C-C bonds on unactivated aryl rings. Lastly we selected the Heck coupling reaction, as while high temperatures and emphasis on dipolar aprotic solvents generally decrease the scope in substrates that the reaction can be applied to, it is still a highly important reaction in industry, providing a key step in the synthesis of Naproxen, a widely used anti-inflammatory drug sold under the brand name Aleve<sup>21</sup> (Scheme 23).

**Scheme 23:** Heck reaction key step in synthesis of Naproxen<sup>22</sup>

Individual reactions were chosen from literature reports which had all undergone a base screen involving potassium phosphate or carbonate bases. Each was selected based on criteria including ease of analysis, reproducibility, starting material availability and potential for base effect due to change of cation or anion. This gave an adequate starting point to benchmark both known commercially available bases as well as relatively unstudied caesium phosphate monohydrate base.

### **2.3.1 Heck coupling reaction**

The Heck reaction requires the base to reform the active Pd(0) catalyst and mediate the reductive elimination step forming the coupling reaction product.<sup>23</sup> We would argue that given its active role in the reductive elimination and  $\beta$ -hydride elimination step, the base is likely to have a significant effect on reaction rates.<sup>24</sup> As Heck reactions are generally more efficient with aryl iodides than chlorides, the oxidative addition step was thought to be rate determining.<sup>24</sup> However, there has been some evidence that when using more labile leaving groups such as bromides and iodides, Heck reactions the reductive elimination step may be rate limiting, allowing the base to directly affect the reaction rate.<sup>25</sup> We investigated whether caesium bases would be the most effective base in the ligand-free palladium catalysed coupling of styrene with bromobenzene (Scheme 24).



**Scheme 24:** Heck cross coupling reaction chosen for base screen<sup>26</sup>

The reaction was selected due to the low catalytic loading required in addition to the simple substrates and low equivalences of base and styrene, so any differences between the bases would be highlighted as well as being relatively inexpensive. In addition to this the dipolar aprotic solvent dimethyl acetamide (DMAc) would allow observations as to whether the increased solubility of caesium bases would increase the reaction rate.

The authors found that DMAc was the optimised solvent for the reaction and potassium phosphate the optimised base, though the authors did not investigate potassium carbonate in the base screen.<sup>26</sup>

We adapted the reaction, doubling the scale from 1 mL to 2 mL and halving the excess of base by reducing the base loading from 1.4 to 1.2 equivalents, with the intention of increasing the relative differential of base performance in the screening reaction. We found that for both phosphate and carbonate bases the potassium cation was superior to caesium (Table 6).

**Table 6:** Overnight conversion (GC) of Heck reaction, referenced against *p*-xylene internal standard after calibration (Scheme 24)

Base	K <sub>2</sub> CO <sub>3</sub>	Cs <sub>2</sub> CO <sub>3</sub>	K <sub>3</sub> PO <sub>4</sub>	Cs <sub>3</sub> PO <sub>4</sub> ·H <sub>2</sub> O
Conversion (% , ±2%)	92	13	68	13

The reason for this may be due to the pH of the solution inhibiting the reaction. The caesium salts, particularly the carbonate salt, are known to be much more soluble than other alkali bases in dipolar aprotic solvents such as DMF and DMSO.<sup>14</sup> This increased solubility of the base cation will increase the pH of the solution as the concentration of the anion will be higher. Heck reactions are known to be pH dependent when conducted in aqueous conditions,<sup>27</sup> and an increase in the pH of the solution in dipolar aprotics caused by additional base solubility could cause a decrease in turnover frequency and therefore overall reaction yield.

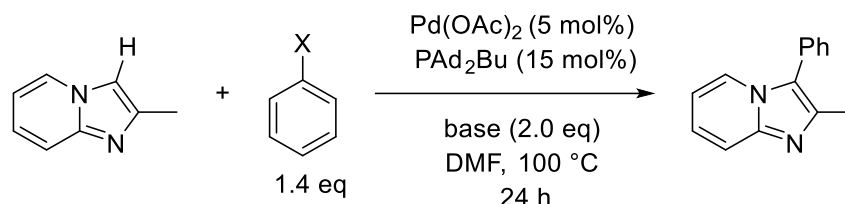
If the concentration of the anion was a factor in the overall yield, we could reduce reaction concentration and therefore decrease the pH of the reaction. This would then improve the reaction with more soluble caesium bases, however reduction in concentration of the substrates with respect to the solvent would decrease the rate, possibly by an equal or larger amount. Therefore ensuring pH remains constant with reduction in base concentration makes the correlation harder to study.

As the reaction was not improved using caesium bases, and Heck reactions traditionally do not incorporate caesium bases, we chose to move on to a palladium catalysed

coupling reaction which had been optimised with a caesium cation incorporated in the selected base.

### **2.3.2 C-H Arylation reaction**

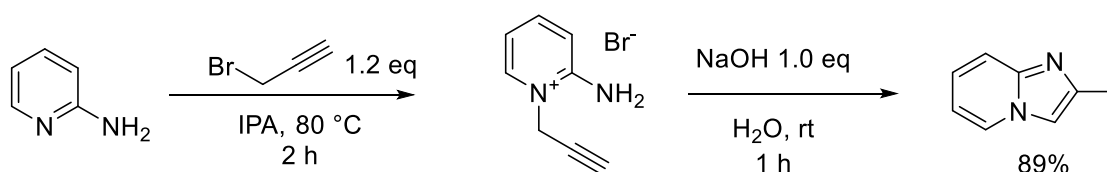
In traditional C-H arylation reactions, the base is thought to support the C-H palladation step after oxidative addition of the aryl halide, *vide supra*. While the rate limiting step in C-H arylation reactions using aryl chlorides is most likely the oxidative addition step,<sup>28</sup> we can investigate whether base cation would affect the overall reaction rate,<sup>29</sup> and therefore which base would be optimal for the coupling of 2-methylimidazo(1,2-a)pyridine with chlorobenzene (Scheme 25).<sup>30</sup>



**Scheme 25:** Investigation into base effect in palladium catalysed C-H arylation<sup>31</sup>

The substrates for the palladium catalysed C-H activation reaction were chosen due to the use of a dipolar aprotic solvent (DMF), the relatively inexpensive catalyst system and the ease of analysis, as the reaction could be easily followed by <sup>1</sup>H and <sup>13</sup>C NMR experiments. In addition to this, the literature investigated both caesium and potassium carbonate as well as potassium phosphate, so benchmarking conditions against the literature was relatively simple.

The route to the imidazopyridine starting material required a facile 2 step synthesis starting from 2-aminopyridine and propargyl bromide. The reaction proceeded well on gram scale followed by a cyclisation step giving 89% yield over 1 h at room temperature (Scheme 26).<sup>32</sup>



**Scheme 26:** Facile synthesis of imidazopyridine starting material for C-H activation reaction<sup>32</sup>

The authors found caesium carbonate to be the optimal base by 2% over potassium carbonate in DMF, achieving 78% conversion overnight. This small difference would indicate that the base cation is not present in the rate determining step. When we repeated the literature reaction with the aryl chloride to assess caesium phosphate reaction performance, we found potassium carbonate to be superior (Table 7), which is likely due to mass transfer effects. The caesium carbonate was likely to be slower due to slow dissolution in the reaction solvent due to larger particle size. Maes and coworkers investigated that in low solubility environments such as toluene the surface area of the base would impact reaction rate, as the kinetic solubility of larger particles is lower than with fine powders with larger surface area. Fine milled bases therefore led to faster rates in a palladium catalysed amination reaction.<sup>33</sup>

**Table 7:** Base screen of C-H arylation reaction using chloride leaving group with alkali metal carbonate and phosphate bases (Scheme 25), referenced against *p*-xylene internal standard

Base	K <sub>2</sub> CO <sub>3</sub>	Cs <sub>2</sub> CO <sub>3</sub>	K <sub>3</sub> PO <sub>4</sub>	Cs <sub>3</sub> PO <sub>4</sub> ·H <sub>2</sub> O
GC conversion(% ±2)	67	25	24	35

Potassium carbonate is available as a pre-milled very fine powder due to this base being much less hygroscopic than caesium carbonate. To prevent additional moisture uptake the caesium equivalent is generally supplied as a coarse granular powder which provides a much lower surface area and therefore much lower kinetic solubility. As the authors made no mention of supplier, milling or base preparation, along with order of addition to the reaction, we were unable to directly replicate the important methodology when repeating the reaction. Any additional milling or drying steps would change the experimental procedure from the literature protocol. While we could repeat the potassium carbonate reaction, which used pre milled commercially available base, we could not repeat the caesium carbonate entry. We therefore deduce that it is likely the authors used pre-milled caesium carbonate base for their methods but did not make a note of it in the manuscript.

The rate determining step with aryl chlorides is usually expected to be either the oxidative addition of the aryl halide to the active palladium catalyst or reductive

elimination of the product which both involve the aryl halide in the rate limiting step. We therefore elected to rerun the C-H arylation reaction using the aryl bromide to shift the rate determining step towards the C-H palladation step which directly involves the base.

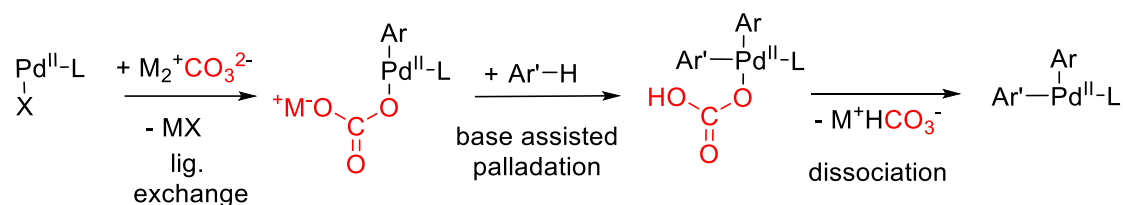
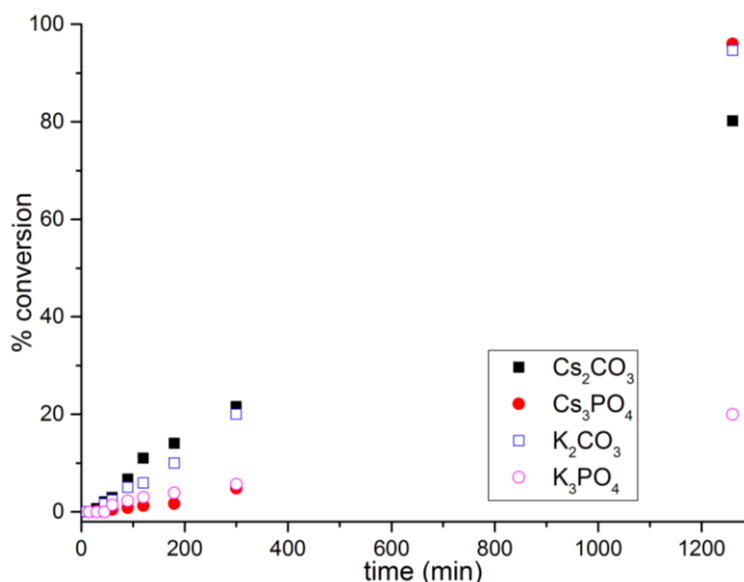


**Figure 15:** Representation of base effect in C-H activation reactions using carbonate anion

Due to the close interaction between the base anion and cation to the palladium catalyst, base selection is paramount and therefore thought must be given to the net nucleophilicity as well as the  $\text{pK}_a$  of the basic anion and the solubility of the base in solution formed by dissociation of cation and anion. We may also see an increase in rate when using differing cations due to possible caesium-assisted C-H activation reported in the literature, *vide supra*.<sup>4, 19, 34</sup> These results are reported in Figure 16.

**Figure 16:** Kinetic plot of C-H activation base screen using bromobenzene



We can observe that the reactions involving caesium phosphate monohydrate, potassium carbonate and caesium carbonate all achieve yields of over 75%, while the potassium phosphate reaction converts under 20% of starting material to product. The

carbonate bases both allow increased initial rates over the phosphate bases, however after 300 minutes the caesium phosphate monohydrate base increases in rate dramatically to achieve over 90% of the desired coupling product.

The reason for the carbonate effectiveness is likely to be due to the lower nucleophilicity of the carbonate base. If the phosphate anion slows the dissociation step (Figure 15), it can slow the turnover frequency and reduce overall reaction rate. Caesium phosphate monohydrate appears to undergo this same reduction in rate relative to the carbonates, but may form some kind of caesium assisted intermediate to then speed the reaction up later due to a small concentration of active substrate being present at the reaction start. The more active proposed Caesium assisted catalyst may take a significant time to form, or it may be dependant on concentration of CsBr or Cs<sub>2</sub>HPO<sub>4</sub> formed as by-products of the reaction. If the initial rate is low, then [by-product] will also be low at reaction start and therefore take time before a critical point where the reaction rate is increased, where the by-product stabilises the catalyst and increases conversion rate in an autocatalytic type process.

### **2.3.3 Sonogashira cross coupling**

The Sonogashira cross coupling reaction provides a highly useful, industrially relevant method to impart *sp* hybridised centres onto an aryl ring.<sup>35, 36</sup> These reactive alkynes can then undergo additional functionalisation after the C-C coupling reaction is complete allowing for late stage derivatisation reactions.

Sonogashira reactions traditionally involve both palladium and copper catalysts, though recent work has been carried out to remove the copper element allowing for less air and moisture-sensitive conditions.<sup>37</sup> The copper-free mechanism is thought to proceed *via* a coupled catalytic cycle of Pd(0)/Pd(II), involving the oxidative addition of the aryl halide and reductive elimination of the product. The second Pd(II)-only cycle involves a base mediated transmetallation of the acetylene and elimination of the halide, giving the transmetallated product and base halide as products of the reaction. The authors state that in this mechanism the rate determining steps are either the transmetallation step or the reductive elimination of the product and generation of Pd(0), as DFT calculations showed that the activation energy barriers were very similar.<sup>38</sup>

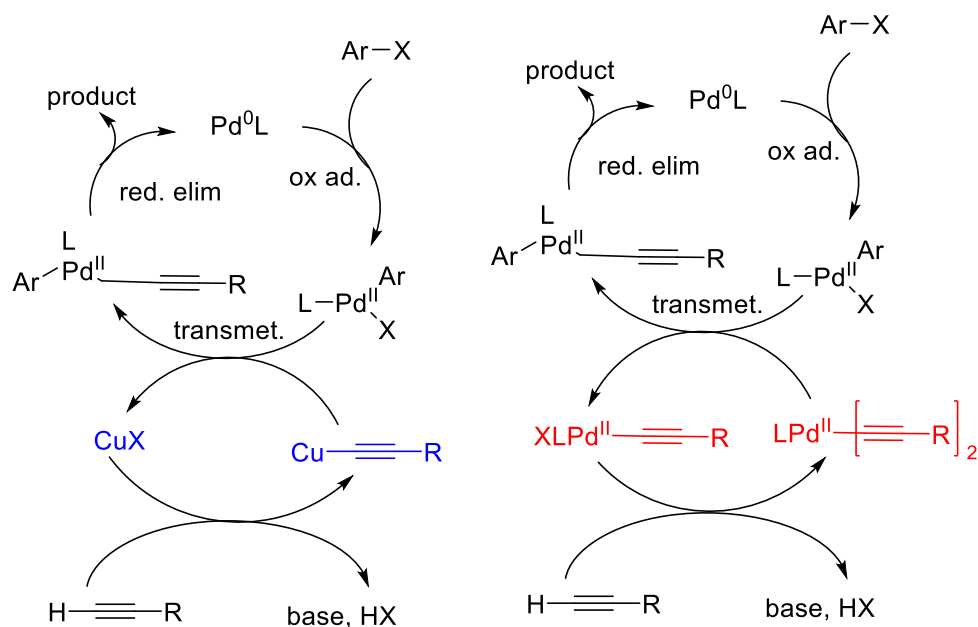
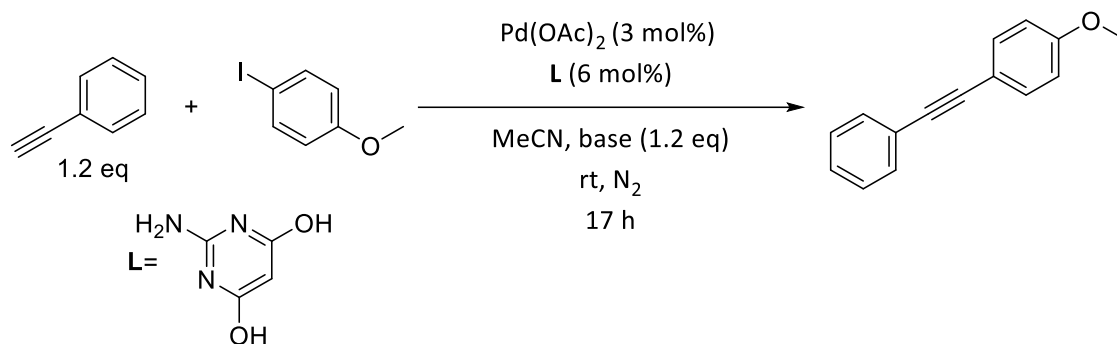


**Figure 17:** Cu assisted (blue) and palladium only (red) Sonogashira mechanistic proposals<sup>38</sup>

While organic amine bases such as triethylamine are still widely used for Sonogashira couplings due to their ease of use and the ability to combine both solvent and base roles,<sup>39</sup> use of conventional solvents and alkali metal bases has recently increased, with multiple literature reactions employing alkali metal carbonate bases after optimisation.<sup>40, 41</sup>

The reaction chosen for the initial probe was a coupling of phenylacetylene and 4-iodoanisole using a pyrimidine ligand and alkali metal base. This reaction was selected due to the ease of analysis using the methoxy group on the aryl iodide, allowing for easy conversion determination via  $^1\text{H}$  NMR, as well as using readily available phenylacetylene starting material and a low catalyst and base equivalence, to ensure any differences between the bases was apparent. In addition to this, Li *et al.* found that caesium carbonate was superior to potassium carbonate, with the reaction gaining 80% conversion over 8 hours, 15% more than using potassium carbonate base, suggesting a small but significant cation effect.<sup>42</sup>



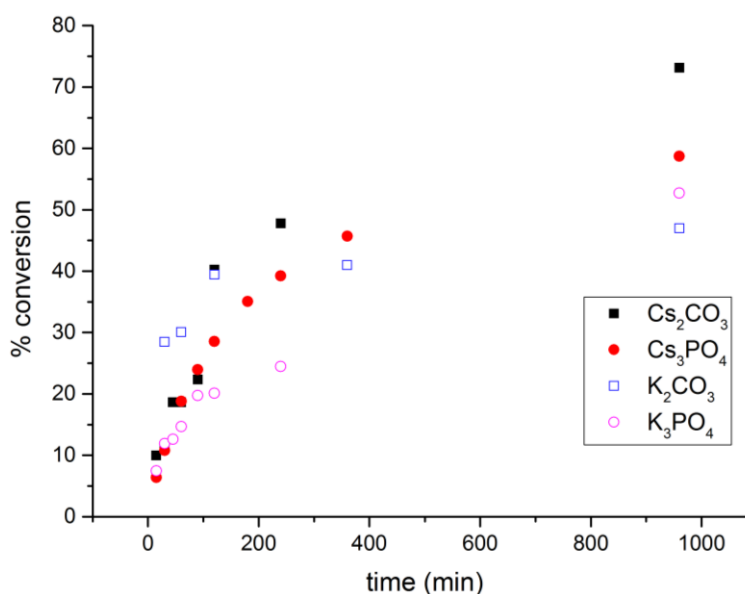
**Scheme 27:** Sonogashira coupling reaction selected for base screen<sup>42</sup>

We were able to replicate the literature results, finding that caesium carbonate was the superior base under literature conditions, followed by caesium phosphate (Table 8).

**Table 8:** Results of initial Sonogashira base screen experiments

Base	$\text{K}_2\text{CO}_3$	$\text{Cs}_2\text{CO}_3$	$\text{K}_3\text{PO}_4$	$\text{Cs}_3\text{PO}_4 \cdot \text{H}_2\text{O}$
Conversion(%)	47	73	53	59

Due to the increased performance of caesium bases over potassium bases in this reaction system we elected to run the reactions using kinetic sampling, to deduce any difference in initial rate, and any inductive effects. We would expect that if the reaction was mass transfer-limited, the superior base would display zero order kinetics until equilibrium is reached and then obey a conventional first order profile. If the base solubility was not the limiting factor however, we would expect a first order rate profile initially. If the base was interacting with the rate determining step of the reaction, in this case thought to be the transmetallation step, we would expect a difference in rate between the two cations. If the base was not directly effecting the RDS, we expect to only see a difference due to base anion, which would change the pH of the solvent mixture and therefore alter the rate indirectly.

**Figure 18:** Kinetic profiles of Sonogashira base screen

We are able to observe that caesium carbonate does not have a significantly higher initial rate than the other bases, it is however able to provide additional conversion later in the reaction. Both caesium bases demonstrate significant conversion rates throughout the reaction, whereas the potassium bases, especially potassium carbonate, appear to have a faster initial rate and then slow down after approximately 2 hours. This may indicate a possible mechanism by which the caesium cation is able to stabilize the catalyst for a longer time period allowing for a longer period of high catalytic turnover, while the potassium bases, unable to stabilize the active catalyst, have lower conversions due to a slow catalyst deactivation. The alternative possibility stated in a recent paper by Pinter *et al.* noted that if the transmetalation step is disfavoured, for example when using aryl chlorides, the Glaser-Hay homocoupling product forming the acetylene dimer is favoured over the Sonogashira product.<sup>38</sup> If the potassium bases were disavouring this reaction step we would expect to observe this product in analysis, however we were unable to observe the expected homocoupling product 1,4-diphenylbutadiyne by GC or <sup>1</sup>H NMR. Both these analysis methods were sensitive enough to detect the homocoupling product, which was observed using commercial material at the expected concentration possible due to catalyst deactivation.

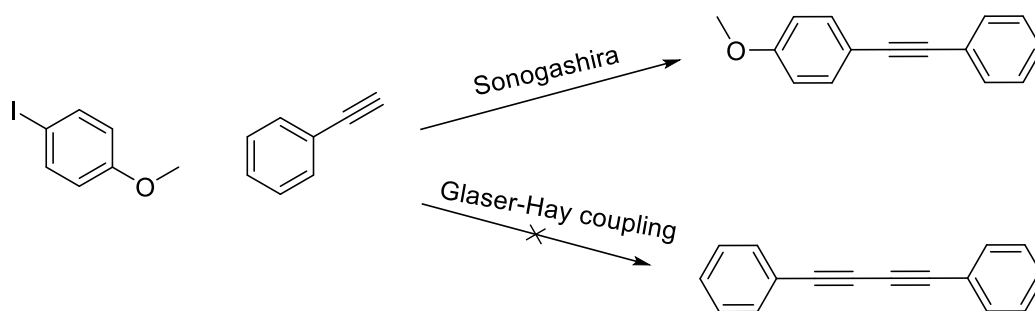
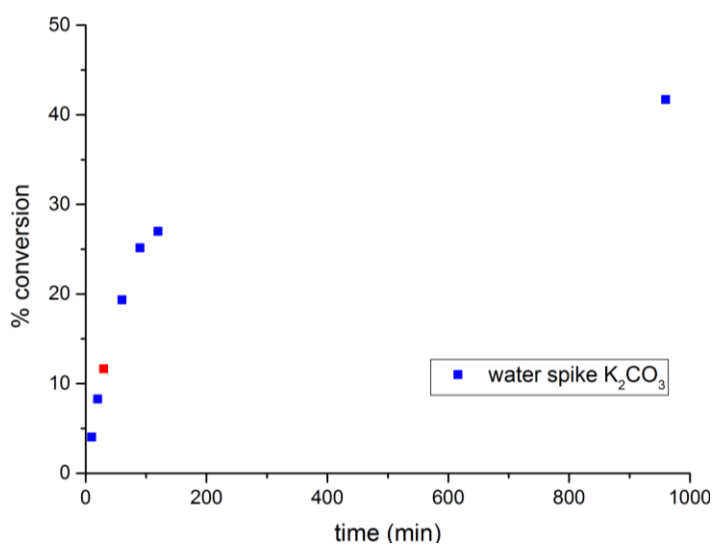


**Figure 19** Sonogashira coupling product, and Glaser-Hay homocoupling product (not observed)

An additional consideration for the relative performance of these bases is the presence of water in the caesium phosphate monohydrate. While solubility in dry acetonitrile is expected to be relatively low (0.6 mmol at 25 °C), the water may dissociate and oxidise the catalyst, rendering it inactive. In the kinetic plot (Figure 18) we do not see conclusive evidence that the water in the monohydrate is adversely affecting the reaction which suggests that caesium phosphate monohydrate does not appear to cause significant catalyst deactivation.

We elected to run a water spiking reaction with potassium carbonate, as of the 4 bases this was the least hygroscopic, and therefore is likely to have minimal water content reducing yield in the case of aqueous catalytic oxidation and deactivation. While a number of aqueous Sonogashira reactions have been carried out, these generally involve specific non-commercially available catalysts which are robust to water (Figure 20).<sup>43, 44</sup>

**Figure 20:** Sonogashira water spike at t = 30 min using potassium carbonate base



2 mmol water was added at 30 minutes (red) to see if any reduction in rate would occur indicating catalyst deactivation. 1.2 equivalents of caesium phosphate monohydrate would provide 1.2 mmol of water to the reaction assuming full dissociation, so the lack of rate decrease after addition of water to the reaction would indicate that the reaction is water stable at max concentration of water possible under reaction conditions. We would therefore conclude that the caesium phosphate monohydrate would not deactivate the catalyst through moisture from the dissociation of water, and the active catalyst is robust to stoichiometric water addition.

Despite the promising results gained from the Sonogashira base screen which indicated caesium bases were likely to be more effective at the cross coupling reaction, we elected to continue profiling additional coupling reactions with the goal of taking forward the most promising two systems forward for more rigorous study.

#### **2.3.4 Buchwald-Hartwig amination**

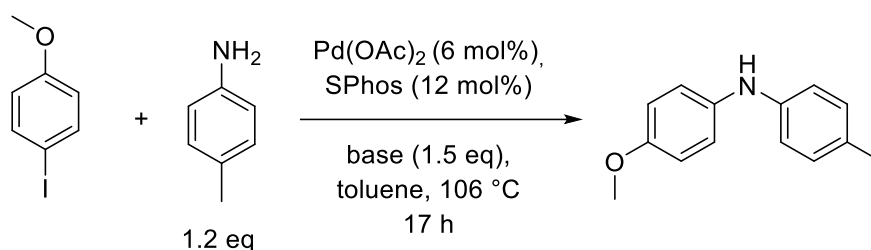
The Buchwald-Hartwig amination reaction is a widely used C-N  $sp^2$  bond forming reaction. Since its discovery in 1994 it remains the only reaction introduced after 1990 that has broken into the top 20 medicinal chemistry reactions according to a meta-analysis by Brown and Boström in 2014.<sup>20</sup> For this reason it is of great importance that we understand the reaction to optimise procedures in medicinal and process chemistry.

Due to the two possible mechanisms of amine and base cation coordination *vide supra*, the choice of base is very important to the outcome of the reaction, as a change of base may be able to allow the reaction to adopt a different mechanistic pathway.<sup>45</sup> In Buchwald-Harwtig amination reactions the rate limiting step is expected to be oxidative addition when using the aryl chloride due to the higher activation energy of the palladium insertion. When using aryl bromide or iodides however, the rate limiting step is expected to be amine addition after base anion coordination.<sup>45</sup> In cases where the amine coordination mechanism is favoured, the rate limiting step is thought to be the external deprotonation of the amine by the base anion.<sup>33</sup>

As the base is likely to be involved directly in the rate determining step of the reaction we would expect a significant increase in reaction rate if the base anion or cation was

able to reduce the activation barrier of amine coordination or deprotonation. Any increase in initial rate along with higher conversions should be noted as a potential interaction between the base and the catalytic cycle.

The reaction we chose to study for an initial base screen was the coupling of *p*-toluidine to 4-iodoanisole studied by Knölker *et al* (Scheme 28).<sup>46</sup> The reaction was chosen due to the ease of analysis of the methoxy and aniline proton groups by <sup>1</sup>H NMR, the readily available catalytic system, and the literature-optimised base of caesium carbonate. Toluene solvent also represents a non-polar aprotic solvent where caesium bases are not more soluble than potassium bases, so any increase in rate gained by use of the caesium cation would be unrelated to increased solubility and therefore must be due to direct interaction between the cation and the substrates.



**Scheme 28** Buchwald-Hartwig amination reaction chosen for base screen<sup>46</sup>

The authors originally ran the reaction with *rac*-BINAP at reflux, but the reaction was run for 7 days at reflux to achieve maximum conversion using caesium carbonate base gaining 97% conversion. They then optimised the ligand to the more active SPhos Buchwald ligand which achieved 88% conversion over 4 days.

We elected to reduce the temperature from reflux to 106 °C to allow for easier sampling and reduce the extent of condensation altering the concentration, as well as running the reaction overnight to highlight any differences between the bases (Table 9).

**Table 9:** Base screen for initial Buchwald-Hartwig amination reaction (Scheme 28) GC conversion aided by *p*-xylene internal standard

Base	K <sub>2</sub> CO <sub>3</sub>	Cs <sub>2</sub> CO <sub>3</sub>	K <sub>3</sub> PO <sub>4</sub>	Cs <sub>3</sub> PO <sub>4</sub> ·H <sub>2</sub> O	KOtBu
GC conversion(% , ±2)	3	45	8	80	83

In this case both caesium bases were able to convert ten times as much product compared to their potassium equivalents. This is an unprecedented result in coupling reactions as the base cation is not thought to directly interact with the catalyst or the mechanism. There are no current mechanistic analyses of palladium-catalysed coupling reactions which include the base cation in the rate equation, though we can observe in this case that the caesium cation can clearly improve the overall conversion over potassium bases. The current solubility reasoning behind the caesium effect in this case would indicate that higher solubility and therefore higher concentration of base anion would increase the reaction rate, though as observed in NMR solubility studies caesium phosphate is up to 60x less soluble than potassium phosphate in dry toluene. We can observe that a higher  $pK_a$  base can facilitate higher conversions by using potassium *tert*-butoxide. For these reasons we argue that the increased rate observed in this Buchwald-Hartwig amination reaction is unlikely to be due to solubility, and the more likely possibility is that either the caesium cation is able to alter the mechanism between the amine coordination pathway and the base coordination pathway, or alternatively that the base cation itself is able to directly interact with the catalyst and reduce the energy barrier of the rate determining step of the reaction.

These interesting results led us to study this reaction in more depth, probing the change in solvent, aryl halide and presence of spiking agents, *vide infra*.

### **2.3.5 Suzuki-Miyaura cross-coupling**

Suzuki-Miyaura couplings are one of the most widely utilized palladium-catalysed reactions in process chemistry, and could rightly be considered the most useful transition metal catalysed reaction in medicinal chemistry.<sup>20</sup> The reaction allows direct C-C  $sp^2$  coupling using prefunctionalised boronic acid substrates and aryl halides. These biphenyl motifs are widely used in drug molecules which allows Suzuki cross couplings to be an incredibly useful late stage functionalization reaction, with great importance in convergent syntheses.

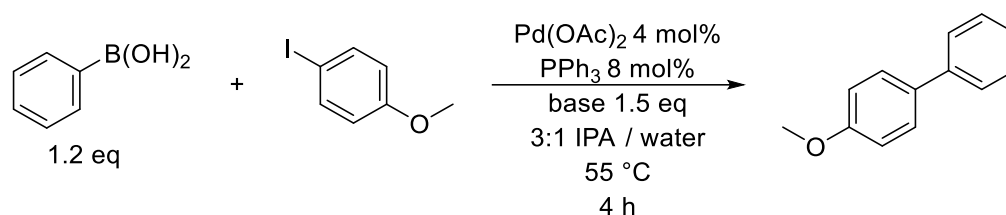
The rate determining step for the majority of Suzuki cross coupling reactions is thought to be transmetallation of the boronic acid onto the palladium centre. This step also incorporates the base which can facilitate the attack of the boronic acid to the palladium centre. Additionally, the base must deprotonate the water causing a

hydroxyl attack on the boronic acid, giving a  $\text{B}(\text{OH})_3^-$  moiety which is destabilised to form the transmetallated product on the palladium and boric acid byproduct.<sup>47, 48</sup>

The alternative pathway of transmetallation however involves a hydroxyl exchange with the halide after oxidative addition forming a Pd-OH moiety, before addition of the boronic acid forming the same  $\text{B}(\text{OH})_3^-$  group on the palladium atom itself (*vide infra*, Figure 58). Both of these pathways however do not directly incorporate the alkali metal base anion or cation, which would suggest the role of this 'pre-base' would mainly be to activate the hydroxyl anion, break up the boroxine anhydride species and scavenge the aryl halide anion. If this was the case we would expect that the base cation would not play any role in facilitating the reaction, as mass transfer effects along with solubility differentials would be effectively nullified due to the reaction being carried out in aqueous conditions.<sup>49</sup>

We would expect the base cation to alter the reaction rate based on  $\text{pK}_a$ , as at higher pH in aqueous solution,  $[\text{OH}^-]$  would increase which then would increase reaction rate. However, curiously few Suzuki reactions require strong bases such as hydroxides to facilitate the reaction. Therefore we can conclude that despite the literature not directly referring to an active role of the base anion or cation, the interaction between the base and the substrates as well as the catalyst may facilitate a change in reaction rate in addition to the most likely mechanism *vide infra*.

The reaction we elected to study to probe the effect of base in Suzuki-Miyaura cross couplings was the reaction of 4-iodoanisole with benzene boronic acid (Scheme 29), adapted from a procedure by Amali and Rana who investigated the stabilisation of Pd(0) on iron oxide nanoparticles.<sup>50</sup> This reaction was selected because it was run below reflux temperatures in the azeotropic solvent mixture, in addition to use of industrially relevant catalyst, ligand and solvents. The methoxy group on the aryl iodide also allowed for facile determination of conversion based on the  $\text{CH}_3$  group in  $^1\text{H}$  NMR. As benzeneboronic acid is unlikely to undergo protodeboronation, with measured half-lives in the order of months,<sup>51</sup> protodeboronation is not a factor and therefore any stabilisation of the boronic acid was not required. Any improvement in reaction yield or rate by the base cation or anion can be linked to the reaction itself, rather than reducing the rates of any side reactions or stabilisation of the reactants.



**Scheme 29:** Suzuki-Miyaura cross coupling selected for initial base screen

The outcome of the base screen with caesium and potassium carbonates and phosphates gave highly interesting results which appeared to negate previously held dogma surrounding the Suzuki cross coupling reaction. We found that increased anion pK<sub>a</sub> (specifically the change in pK<sub>a</sub> of the conjugate acid of the anion) from carbonate to phosphate would allow for increased [OH<sup>-</sup>]. This did increase the initial reaction rate, however there was a marked difference between caesium and potassium bases both with the carbonate and phosphate anion (Table 10).

**Table 10:** Observable caesium base cation effect in Suzuki cross coupling (Scheme 29) utilising *p*-xylene internal standard

Base	K <sub>2</sub> CO <sub>3</sub>	Cs <sub>2</sub> CO <sub>3</sub>	K <sub>3</sub> PO <sub>4</sub>	Cs <sub>3</sub> PO <sub>4</sub> ·H <sub>2</sub> O
GC conversion (% , 30 min ±2)	8	53	43	87
GC conversion(% , 17 h, ±2)	45	72	90	99

There are two possibilities for the large increase in rate achieved using caesium bases in this reaction. The first possibility is that the caesium cation is able to change the mechanistic pathway for transmetallation of the palladium species, changing it from the palladium hydroxide pathway to the activated boronic acid pathway or *vice versa*. This change in mechanism would in turn change the activation energy of the reaction and allow access to higher initial rates.

The alternative hypothesis for increased rate is that the caesium cation can actually directly interact and reduce the energy of the reactive palladium transition states, which reduces the activation barrier of the transition state and increases turnover frequency. Previous bimetallic Cu-I-Cs species and Pd-O-Cs have been observed experimentally by XRD, but no caesium species has ever been isolated in a Suzuki type reaction.<sup>52-54</sup>

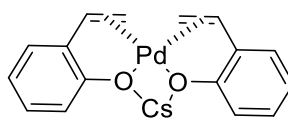


**Figure 21:** Evidence of Pd-Cs catalytic species in C-H carboxylation reactions observed by XRD<sup>54</sup>

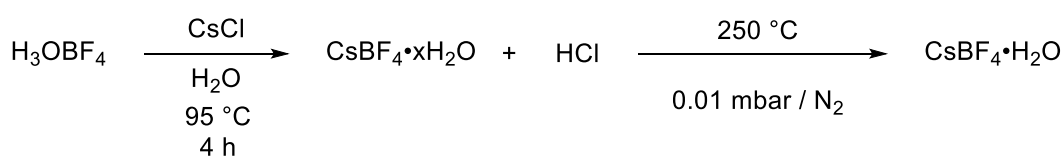
We elected to investigate the Suzuki-Miyaura reaction further and elected to probe how changes to the aryl halide, boronic acid and temperature effected the reaction, along with investigation of the protodeboronation of troublesome boronic acids in these coupling reactions, *vide infra*.

#### **2.4 Synthesis and characterization of caesium tetrafluoroborate monohydrate**

Synthesis of caesium phosphate base and screening of different alkali metal bases with multiple cations is an important step towards elucidating the magnitude and scope of the caesium effect in catalytic cross coupling reactions. However if we synthesise a substance with the goal of 'spiking' in concentrations of caesium cation without adding additional base, ensuring that only the caesium cation can affect reaction performance and not the anion, we may get additional data on whether the presence of the caesium cation, or increased concentration of the cation in absence of anion concentration increase can affect the reaction performance.

We identified caesium tetrafluoroborate as a non-basic ionic caesium species which can dissociate to form the Cs<sup>+</sup> cation, allowing for additional concentration of caesium in reactions without increasing [base], and therefore without increasing the solution pH in solvents where the bases are fully soluble. As the pK<sub>b</sub> of tetrafluoroborate is 0.5, no additional basicity is imparted on the reaction mixture upon addition of CsBF<sub>4</sub>.

We adapted a synthesis originally proposed by Clark and Lynton,<sup>55</sup> who were interested only in the crystal structures of alkali metal tetrafluoroborates.



**Scheme 30:** synthesis of caesium tetrafluoroborate monohydrate<sup>55</sup>

We adapted the synthesis to incorporate an extensive drying step reducing the water content down to a monohydrate. An additional factor was to remove all traces of HCl as a gas, without addition of base to neutralize the reaction mixture. The product was analysed by AAS and 56.0% Cs was observed with 55.9% calculated for showing the product was likely to behave as a monohydrate. The presence of water in the crystal lattice does raise the issue that any water sensitive reaction will be affected by the water content as well as the caesium base. The addition of  $\text{CsBF}_4 \cdot \text{H}_2\text{O}$  does however allow us allows us to increase  $[\text{Cs}^+]$  for greater understanding of how cation concentration can influence the rate determining step of palladium catalysed coupling reactions.

#### **2.4.1 Utilization of caesium tetrafluoroborate in Buchwald-Hartwig amination reactions**

The Buchwald-Hartwig amination reactions *vide supra* were suggested as a good initial starting point to model for evidence of caesium effect in a reaction where the caesium cation appears to provide a marked increase in reaction rate and overall conversion. We chose to run the amination reaction with aryl iodide to conclude whether presence of caesium would increase the reaction rate.

**Table 11:** Effect of  $\text{CsBF}_4$  spiking agent on Buchwald-Hartwig amination reaction

Base (additive)	$\text{K}_3\text{PO}_4$	$\text{K}_3\text{PO}_4$ ( $\text{CsBF}_4$ 1 eq.)	$\text{K}_3\text{PO}_4$ ( $\text{CsBF}_4$ 3 eq.)	$\text{Cs}_3\text{PO}_4 \cdot \text{H}_2\text{O}$
% conversion ( $\pm 2$ )	8	12	6	80

We can observe an increase in conversion when an equimolar ratio of  $\text{CsBF}_4$  to  $\text{K}_3\text{PO}_4$  are present in the reaction mixture, however when a 3:1 ratio of the tetrafluoroborate salt was added with respect to the phosphate base, ensuring  $[\text{Cs}^+]$  and  $[\text{K}^+]$  would be the same assuming equal levels of dissociation, the reaction performance fell below what would be expected using only potassium phosphate base due to lower effective solubility of the phosphate anion due to competition with the tetrafluoroborate salt additive. Caesium phosphate was not investigated with the tetrafluoroborate additive

due to additional caesium cation concentration being unnecessary for the reaction to proceed with good yields.

The likely reason for this is that initial addition of caesium cation to the system will allow for increased rate, though not to the level found using caesium phosphate itself which would suggest the mechanism was not changed to the faster base coordination mechanistic pathway of transmetalation. We argue that an equilibrium between the two mechanisms is likely, with increased  $[\text{Cs}^+]$  pushing the mechanism towards the base coordination pathway and decreasing  $[\text{PO}_4^{3-}]$  would make the faster base coordination mechanism disfavoured due to slow coordination of  $\text{PO}_4^{3-}$ . This then has the effect of pushing the equilibrium towards the slower amine coordination mechanism.

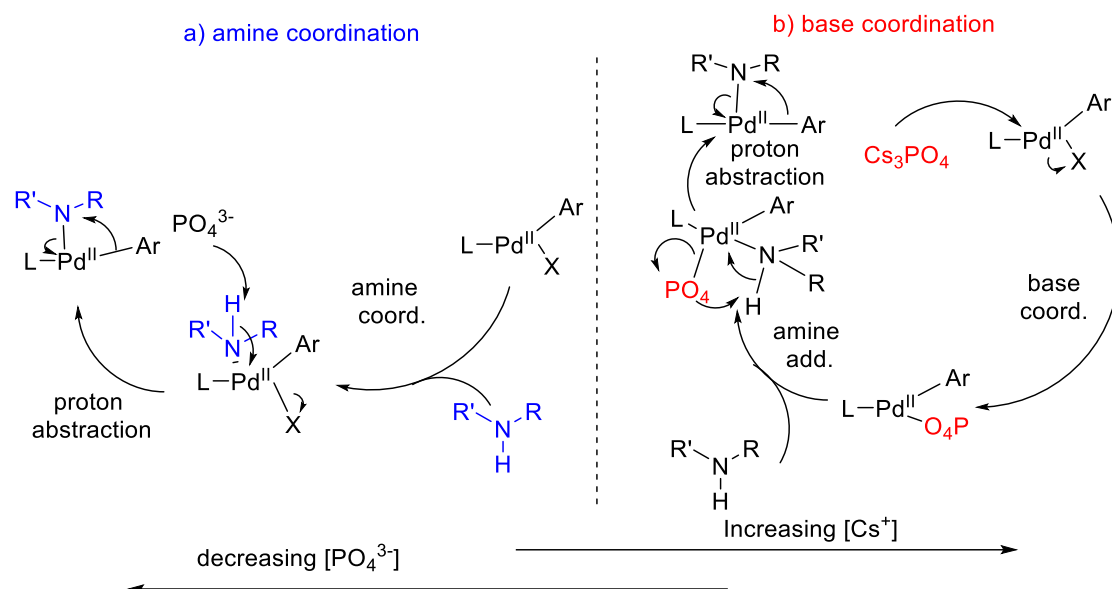


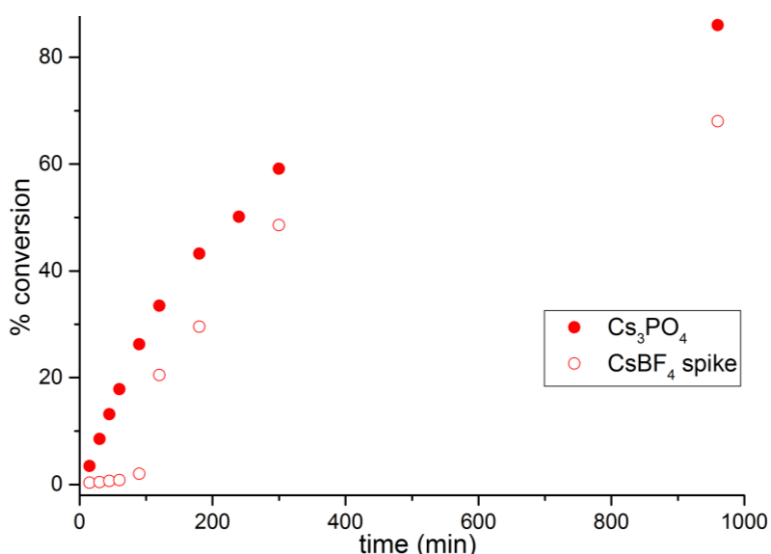
**Figure 22** Proposed changes of mechanistic pathways based on [anion] and [cation]

The reduced concentration of the basic anion stems from the  $\text{CsBF}_4$  species being able to replace a proportion of the potassium phosphate in solution at higher concentrations due to the solubility limits of salts within the organic solvent. This then reduces  $[\text{PO}_4^{3-}]$  and therefore reduces transmetalation rate. As the reaction in dry toluene is fully saturated with alkali metal salts without any additional concentration of salt species using the spiking agent, this suggests that the reaction has a slower initial rate and conversion because the base anion concentration is reduced due to addition of the spiking agent.

Due to the presence of water in the form of the monohydrate, an additional reasoning behind the reduced yield of the 3:1 addition ratio is due to poisoning of the catalyst by water present in the  $\text{CsBF}_4$  monohydrate. While this is a possibility, Dallas and Gothelf found that Buchwald-Hartwig aminations using a  $\text{Pd}(0)$  Xantphos catalyst were stable to up to 150 mol% of water with respect to the aryl halide when using 6 mol% catalyst.<sup>56</sup> This would indicate that while presence of water in the reaction could affect overall conversion, the spiking agent would need to dissolve and dissociate to release free water which, due to the low solubility of basic salts in organic solvents such as toluene, is unlikely. A more rigorous study of catalytic deactivation by water in this system has been conducted *vide infra*.

To further understand how addition of caesium tetrafluoroborate would affect both reactivity and solubility in Buchwald-Hartwig amination reactions where the inorganic base was not fully soluble, we elected to conduct the reaction using the optimal base in the study of caesium phosphate monohydrate (Scheme 28) in addition to one equivalent of caesium tetrafluoroborate. We would expect that if the concentration of the phosphate anion was a more important factor for conversion, the caesium phosphate would perform better as  $[\text{PO}_4^{3-}]$  would be higher. However, if the caesium atom was more important in achieving high conversions, the spiked caesium tetrafluoroborate reaction would achieve higher yields.

**Figure 23:** Kinetic plot of amination reaction showing slowdown on addition of  $\text{CsBF}_4$  spiking agent (present at reaction start)

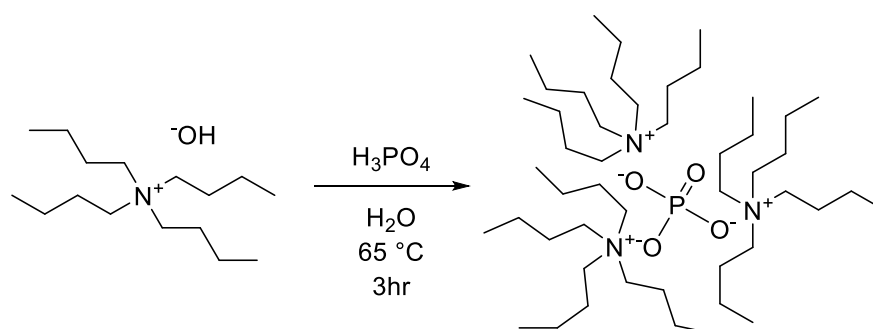


We can observe that when including the spiking agent in the reaction, thereby increasing  $[\text{Cs}^+]$ , the initial reaction rate decreases dramatically. The competition between the tetrafluoroborate and phosphate salts are expected to decrease  $[\text{PO}_4^{3-}]$ , thereby decreasing the initial rate of the reaction. As the reaction proceeds, more phosphate can dissolve in the solution and increase the rate slightly, but the overall conversion remains lower than the un-spiked reaction conditions using caesium phosphate monohydrate.

We can observe that use of caesium tetrafluoroborate can be effective to increase rates if used in small quantities which then in turn can increase reaction yield in palladium catalysed coupling reactions where  $[\text{Cs}^+]$  is critical to increasing reaction rates. However when used in reactions where the solution is already saturated with the basic salt, addition of  $\text{CsBF}_4$  may actually decrease the amount of basic anion in solution and therefore reduce the reaction pH and the overall reaction rate. Use of a sub-stoichiometric concentration of  $\text{CsBF}_4$  may be more effective than 1.0 equivalent and would be a useful reaction in non-solubility limited reactions in future work.

### **2.5 Synthesis of tetrabutylammonium phosphate**

Whilst  $\text{CsBF}_4$  represents a simple method of increasing  $[\text{Cs}^+]$  without increasing concentration of the basic anion, we attempted to synthesise a species where [anion] would be increased without additional concentration of alkali metal cation. This led us to synthesise tetrabutylammonium phosphate (TBAP) as a highly soluble organic phosphate base for use in organic solvents.

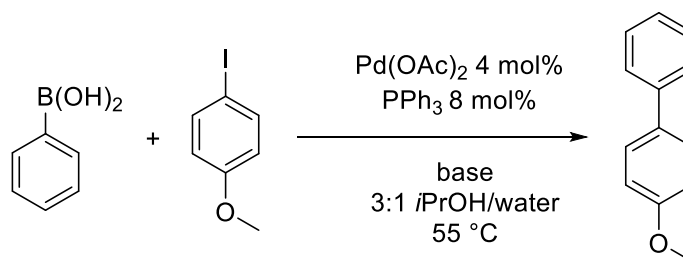


**Scheme 31:** Synthesis of more soluble organobase TBAP

Tetrabutylammonium salts are notoriously hygroscopic, therefore drying the product became difficult. A glove box could not be used due to all literature preparations

utilising water as a solvent due to solubility of the product and starting material salts. Relatively dry TBAP can be obtained by lyophilisation for several days, however the product does not remain sufficiently dry for use in water sensitive reactions. The product was known to decompose above 90 °C so extended high temperature drying was not possible to remove excess moisture.

The organic base should have increased solubility in organic solvents over alkali metal bases, however the hygroscopicity of the base made it particularly difficult to identify a relevant reaction in which it would both benefit from increased solubility in less polar solvents, and also not be negatively impacted by the water content. Organic tetrabutylammonium bases are rarely used in coupling reactions over simpler and easier to handle alkali metal or amine bases, so despite synthesis of TBAP we were unable to replicate results using equal concentrations of phosphate which were possible using alkali metal basic salts.



Base =  $\text{K}_3\text{PO}_4$ ,  $\text{Cs}_3\text{PO}_4 \cdot \text{H}_2\text{O}$ , TBAP

**Scheme 32:** Initial test of TBAP reaction performance

**Table 12:** Conversion figures using TBAP organic base

Base	TBAP	$\text{K}_3\text{PO}_4$	$\text{Cs}_3\text{PO}_4 \cdot \text{H}_2\text{O}$
Conversion (%)	35	98	98

Based on this data along with difficulties of keeping the base sufficiently dry for accurate weighing, we concluded that TBAP base is unlikely to be applicable for larger scale palladium catalysed coupling reactions in industry and therefore elected to continue the study solely using alkali metal base cations.

## **2.6 Conclusions & Future work**

Despite caesium bases being used in numerous classes of palladium-catalysed cross coupling reactions, and potassium phosphate regularly being found to be optimal when a base screen is run in these reactions, caesium phosphate has only been utilised as a base in two transition metal catalysed reactions with base screens only regularly utilising caesium carbonate.<sup>7, 8</sup> A useful and milder synthesis of caesium phosphate monohydrate has been provided which is robust up to 25 gram scale using standard laboratory techniques and equipment (Scheme 21).

Caesium phosphate monohydrate and potassium phosphate were tested for solubility in organic solvents and measured by heteronuclear <sup>133</sup>Cs and <sup>31</sup>P NMR relative to an internal standard (Table 2). One of the main theories behind the caesium effect is that increased solubility of caesium bases arises due to hard-soft interactions between the soft caesium cation and hard anion which allows for increased reaction rates and yields. We found that caesium phosphate was only more soluble in dipolar aprotic solvents such as DMF and DMAc, and was actually less soluble than potassium phosphate in less polar solvents such as toluene. Therefore, we can discount solubility as being the major factor facilitating the caesium effect, as numerous reactions studied exhibit significant caesium effect in protic or non-polar solvents.

When a base screen was conducted for five common palladium-catalysed coupling reactions using commercially available carbonate and phosphate salts, as well as newly synthesised caesium phosphate monohydrate, we found that Sonogashira reactions, Buchwald-Hartwig amination reactions and Suzuki-Miyaura cross couplings were most susceptible to the caesium effect. This effect was most evident when utilising caesium phosphate monohydrate as the base in two of the three reactions. Of the aforementioned reactions, Buchwald-Hartwig amination gave the most dramatic increase in yield, allowing conversion of up to 10 times the amount of product in an overnight reaction involving iodoanisole using caesium bases than the potassium cation (Table 9). Despite this, stronger bases such as potassium *tert*-butoxide can be utilised in Buchwald-Hartwig amination reactions which possess a rate limiting deprotonation step, and are able to increase yields above that attainable using weak bases.

A particularly interesting result in the base screen reactions was that the Suzuki cross coupling reaction involving caesium phosphate monohydrate was able to produce 87% conversion in 30 minutes, over double the conversion attained in the reaction using potassium phosphate over the same timescale (Table 10). This highlights a niche where caesium phosphate monohydrate could be strategically utilised in reactions where a faster rate is required, and may subsequently mitigate the need for protected boronic acids or the use of expensive highly activated catalysts in Suzuki-Miyaura cross couplings involving boronic acids which are prone to protodeboronation.

Caesium phosphate, a previously obscure base in palladium catalysed reactions, was synthesised and purified for the first time at gram scale using standard techniques and equipment available to the research chemist. The previous solubility argument for the 'caesium effect' was disproven *via* solubility studies using insert NMR tubes and protic solvent, which had not been attempted prior to this project. The large 'caesium effect' present in Buchwald-Hartwig amination and Suzuki-Miyaura cross coupling reactions represents a useful tool for research chemists, where caesium phosphate base was shown to greatly improve experimental yields in these model reactions

Further study would benefit the C-H arylation reaction which was profiled (Scheme 25). This reaction did not appear to have any obvious trend in base cation or anion when the aryl chloride was used (Table 7), however when the more labile aryl bromide was used almost all bases performed well, gaining over 80 % conversion overnight except potassium phosphate (Figure 16). To assess whether a trend could be identified using the even more labile aryl iodide, further work on this C-H arylation reaction would be beneficial to deduce any cation effect is present in this reaction class.

Similar to the C-H arylation reaction, the studied Sonogashira coupling reaction appeared to show some level of caesium acceleration, with caesium carbonate the optimal base in the studied reaction (Table 8). Changing the leaving group to a less labile aryl halide, or using a more activated aryl halide such as 4-nitroiodobenzene rather than 4-methoxyiodobenzene would change the reaction sufficiently to alter the reaction rate and therefore possibly the rate determining step. If we could alter the rate limiting step by changing the strength of the C-X bond, and therefore the rate of oxidative addition, we would be able to determine in which step this caesium acceleration did occur, and investigate possible intermediates.

When using the caesium tetrafluoroborate monohydrate spiking agent, the reagent was included in the reaction in 1 and 3 equivalent reactions (Table 11). However, an increase in rate was only found when using 1 equivalent, which was thought to be due to competing base solubility and subsequent reduction in concentration of the phosphate anion. If the caesium cation was increasing the rate, we would expect a larger increase if a catalytic amount of caesium was added, for example 10 mol%.

## **2.7 Experimental details**

Unless otherwise noted, all materials were obtained from commercial suppliers and used as received.  $\text{Cs}_2\text{CO}_3$ ,  $\text{K}_2\text{CO}_3$  and  $\text{K}_3\text{PO}_4$  were oven dried at 100 °C overnight before use. Unless otherwise noted, all reactions were performed under an atmosphere of  $\text{N}_2$  gas using standard vacuum-line techniques. All work-up and purification procedures were carried out with reagent-grade solvents in air.

Column chromatography was carried out on prepacked flash columns on a Biotage purification unit.  $^1\text{H}$  NMR spectra were recorded in  $\text{CDCl}_3$  (TMS, no IS integration) at 300 or 500 MHz on Bruker Avance spectrometers. All chemical shift values are reported in ppm ( $\delta$ ).  $^1\text{H}$  and  $^{13}\text{C}$  NMR assignments were aided by COSY, DEPT and HMBC NMR. NMR spectra were assigned in order of decreasing chemical shift of  $^{13}\text{C}$  peaks. Gas chromatography was conducted on Hewlett Packard HP 6890 Gas Chromatography apparatus, equipped with HP-5 chromatography columns (mobile phase:  $\text{H}_2$ , column length 30 m, film thickness 0.25  $\mu\text{m}$ , injection volume 1.0  $\mu\text{L}$ , split ratio 100:1, split flow 71.5 ml/min.) For kinetic experiments unless otherwise stated 50  $\mu\text{L}$  sample taken via syringe after inerting and quenched into 1 mL acetonitrile at room temperature.

### **Synthesis of $\text{Cs}_3\text{PO}_4 \cdot \text{H}_2\text{O}$**

A round bottom flask was charged with caesium carbonate (5.0 g, 15.3 mmole, 1.005 equivalent) in water (10 mL). Concentrated phosphoric acid (14.9 M 696  $\mu\text{L}$ , 10.23 mmole, 1.0 equivalent) was added dropwise to the solution to allow for steady evolution of  $\text{CO}_2$ . The mixture was stirred for 22 hours followed by heating *in vacuo* (40 mbar) at 105 °C, then heating to 285 °C *in vacuo* (0.05 mbar) for 4 hours. Tricaesium phosphate monohydrate was received as a highly hygroscopic colourless powder. Yield 4.99 g, 96%.  $^{31}\text{P}$  NMR (160 MHz, MeOD)  $\delta$  3.89  $^{133}\text{Cs}$  NMR (67 MHz, MeOD)  $\delta$ : -23.1.

FTIR  $\text{cm}^{-1}$ : 3058 br (O-H), 2331, 1688, 1444, 1347 (P-O), 970, 842, 817, 649, 522, 427.  
AAS analysis Cs: 77.9%; calc: 77.9%. Karl Fisher analysis: 4.0% water; calc: 3.7%.

### **Titration of $\text{Cs}_3\text{PO}_4\cdot\text{H}_2\text{O}$**

$\text{Cs}_3\text{PO}_4\cdot\text{H}_2\text{O}$  (0.5 mmole) was added to deionized water (10.0 mL) in a round bottom flask equipped with a digital pH sensor. A solution of HCl 1.0 M was added to the solution via automatic pipette. The equivalence points are:

$\text{Cs}_3\text{PO}_4\cdot\text{H}_2\text{O}$ : pH 9.0 and 4.2 at 0.6 mL and 1.2 mL of HCl 1.0 M.

$\text{K}_3\text{PO}_4$ : pH 8.0 and 4.1 at 0.58 mL and 1.15 mL of HCl 1.0 M.

These confirm the tribasic nature of the salt  $\text{Cs}_3\text{PO}_4\cdot\text{H}_2\text{O}$ .

### **Solubility measurements of alkali metal phosphates in organic solvents**

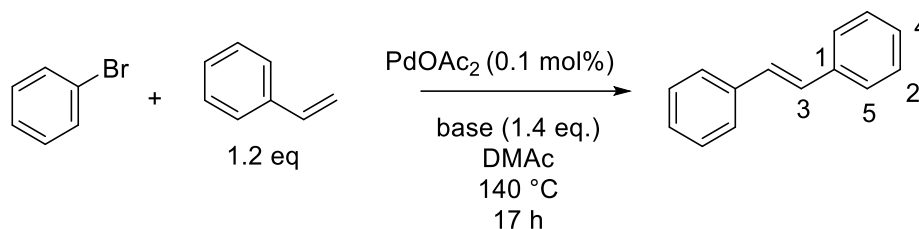
Alkali metal phosphate salt (0.02 mmole) was added to an NMR tube under inert atmosphere to avoid moisture ingress. Dry organic solvent (1.0 mL) was added under inert atmosphere followed by sonication for 10 min to ensure maximum dissolution. A NMR tube insert, filled with  $\text{CsNO}_3$ , or  $\text{H}_3\text{PO}_4$  standard (50 mM) in  $\text{D}_2\text{O}$  (1.0 mL) was inserted into the experimental NMR tube to give a signal lock and a standard to measure against.  $^{133}\text{Cs}$  and  $^{31}\text{P}$  NMR data were collected for 512 scans. The concentrations of phosphate salt were calculated using the integration of its signal against that of the standard solution in the insert tube.

### **Standard sampling protocol**

The reaction stirring was stopped for ~5 seconds to encourage solids to settle at the bottom of the Schlenk flask. An oven dried needle attached to a luer lock syringe was purged by drawing up 1 mL of nitrogen atmosphere from the reaction and dispensing it to atmosphere and repeating 5 times. 50  $\mu\text{L}$  of reaction mixture was drawn into the syringe and diluted in 1 mL acetonitrile in a GC vial. The vial was left open to atmosphere to ensure to additional conversion would take place and the vial ran on GC without further purification

## Procedure and characterisation of Palladium catalysed coupling reactions

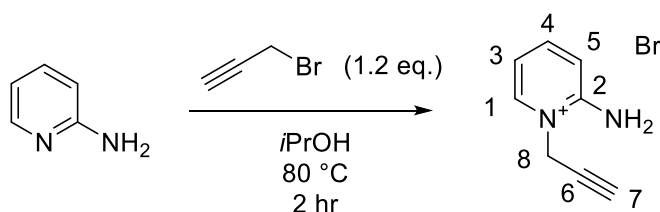
### General procedure for *E*-Stilbene<sup>26</sup>



An oven dried Schlenk tube was charged with palladium(II) acetate (3.0 mg, 0.01 mmol) and dry degassed dimethyl acetamide (2.0 mL) was added and stirred at room temperature for 10 min. A second dried Schlenk tube was charged with base (1.4 mmol, 1.4 equivalents), and biphenyl internal standard (15.4 mg, 0.1 mmol). Styrene (137  $\mu$ L, 1.2 mmol, 1.2 equivalents) and bromo benzene (105  $\mu$ L, 1.0 mmol, 1.0 equivalent) were added followed by addition of an aliquot of the catalyst solution (0.2 mL, 0.3 mg, 0.001 mmol, 0.1 mol%) and dry degassed dimethyl acetamide (1.8 mL). The vessel was sealed and heated to 140  $^{\circ}$ C for 17 h. The mixture was allowed to cool to room temperature and the crude filtered through celite and silica gel to give crude *E*-Stilbene as a light brown solid giving 92% conversion using  $K_2CO_3$  as base by NMR and GC.  $^1H$  NMR (400 MHz,  $CDCl_3$ )  $\delta$  7.48-7.52 (m, 4H, H-5), 7.32-7.40 (m, 4H, H-2), 7.23-7.27 (m, 2 H, H-4), 7.11 (s, 2H, H-3);  $^{13}C$  NMR (125 MHz,  $CDCl_3$ )  $\delta$  137.2 (C-1), 128.6 (C-2), 128.5 (C-3), 127.5 (C-4), 126.4 (C-5).

Literature data:<sup>57</sup>  $^1H$  NMR (400 MHz,  $CDCl_3$ )  $\delta$  7.50-7.52 (d,  $J = 7.2$  Hz, 4 H, ArH), 7.33-7.37 (t,  $J = 7.6$  Hz, 4H, ArH), 7.22-7.27 (m, 2H, ArH), 7.10 (s, 2H, =CH).

### 2-Amino-1-(2-propynyl)pyridinium bromide<sup>32</sup>

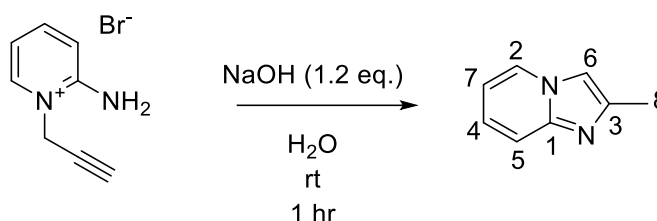


2-Aminopyridine (20 mmol, 1.0 eq), propargyl bromide (80% w/w toluene, 24.0 mmol, 1.2 eq.), and 2-propanol (40 mL) were added to a round bottom flask under air and stirred at 80  $^{\circ}$ C for 2 hours. The mixture was allowed to cool to room temperature and the excess solvent and bromide removed *in vacuo* to afford a light brown solid, which

was then washed with petroleum ether (4 x 50mL) and recrystallized from the minimum amount of 2-propanol in a cardice bath at -25 °C. The recrystallized product was dried *in vacuo* to afford the desired product as a cream solid. 1.82 g yield, 43%. <sup>1</sup>H NMR (500 MHz, D<sub>2</sub>O) δ 8.02 (dd, *J*<sub>1,3</sub> = 6.9 Hz, *J*<sub>1,4</sub> = 1.0 Hz, 1H, H-1), 7.88 (td, *J*<sub>3,1</sub> = 7.3 Hz, *J*<sub>3,4</sub> = 7.3 Hz, *J*<sub>3,5</sub> = 1.5 Hz, 1H, H-3), 7.12 (d, *J*<sub>5,4</sub> = 8.0 Hz, 1H, H-5), 6.96 (td, *J*<sub>4,3</sub> = 7.0 Hz, *J*<sub>4,5</sub> = 7.0 Hz, *J*<sub>4,1</sub> = 1.3 Hz, 1H, H-4), 5.01 (d, *J*<sub>8,7</sub> = 2.7 Hz, 2H, H-8), 3.11 (t, *J*<sub>7,8</sub> = 2.7 Hz, 1H, H-7); <sup>13</sup>C NMR (125 MHz, CDCl<sub>3</sub>) δ 153.8 (C-1), 143.0 (C-2), 138.5 (C-3), 115.2 (C-4), 113.8 (C-5), 78.6 (C-6), 73.2 (C-7), 43.4 (C-8).

Literature data: <sup>1</sup>H NMR (300 MHz, D<sub>2</sub>O) δ 8.08 (d, *J* = 6.9 Hz, 1H, pyH), 7.93 (t, *J* = 8.4 Hz, 1H, pyH), 7.17 (d, *J* = 8.4 Hz, 1H, pyH), 7.01 (t, *J* = 6.9 Hz, 1H, pyH), 5.06 (d, *J* = 2.7 Hz, 2H, CH<sub>2</sub>), 3.18 (t, *J* = 2.7 Hz, 1H, C≡CH); <sup>13</sup>C NMR (100 MHz, D<sub>2</sub>O) δ 153.8, 143.1, 138.5, 115.2, 113.9, 78.6, 73.2, 43.5.

### 2-Methylimidazo(1,2-a)pyridine<sup>32</sup>

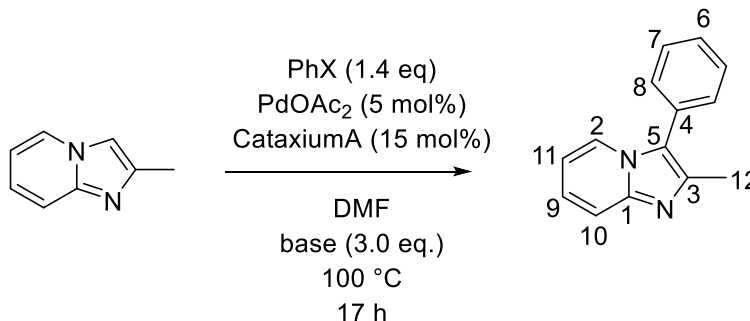


A round bottom flask was charged with ultrapure water (80 mL), followed by addition of sodium hydroxide pellets (420 mg, 10.5 mmol, 1.2 equivalents) in portions with stirring for 20 min. 2-amino-1-(2-propynyl)pyridinium bromide (1.80 g, 8.8 mmol, 1.0 equivalent) was added in portions and the solution stirred at room temperature for 1 hr. The crude product was obtained via extraction in ethyl acetate (150 mL x 4) to give crude product as a brown oil. 950 mg yield, 81%, 95% conversion by NMR. <sup>1</sup>H NMR (500 MHz, CDCl<sub>3</sub>) δ 8.02 (dt, *J*<sub>2,7</sub> = 6.8 Hz, *J*<sub>2,4</sub> = 1.2 Hz, 1H, H-2), 7.50 (dd, *J*<sub>5,4</sub> = 9.1 Hz, *J*<sub>5,1</sub> = 0.7 Hz, 1H, H-5), 7.32 (s, 1H, H-6), 7.10 (m, 1H, H-4), 6.71 (td, *J*<sub>7,2</sub> = 6.8 Hz, *J*<sub>7,4</sub> = 1.1 Hz, 1H, H-7), 2.45 (d, *J*<sub>8,6</sub> = 0.9 Hz, 3H, H-8); <sup>13</sup>C NMR (125 MHz, CDCl<sub>3</sub>) δ 143.4 (C-1), 137.8 (C-2), 125.2 (C-3), 124.0 (C-4), 116.9 (C-5), 111.8 (C-6), 109.5 (C-7), 14.3 (C-8).

Literature data: <sup>1</sup>H NMR (300 MHz, CDCl<sub>3</sub>) δ 8.24 (dt, *J* = 6.6, 2.1, 0.9 Hz, 1H, pyH), 7.58 (d, *J* = 9.0 Hz, 1H, pyH), 7.49 (s, 1H, imH), 7.20 (m, 1H, pyH), 6.80 (td, *J* = 9.0, 6.6, 0.9 Hz,

$^1\text{H}$ , pyH), 2.41 (d,  $J = 0.9$  Hz, 3H,  $\text{CH}_3$ );  $^{13}\text{C}$  NMR (75 MHz,  $\text{CDCl}_3$ )  $\delta$  143.2, 140.2, 126.5, 126.1, 115.2, 113.3, 110.2, 13.1.

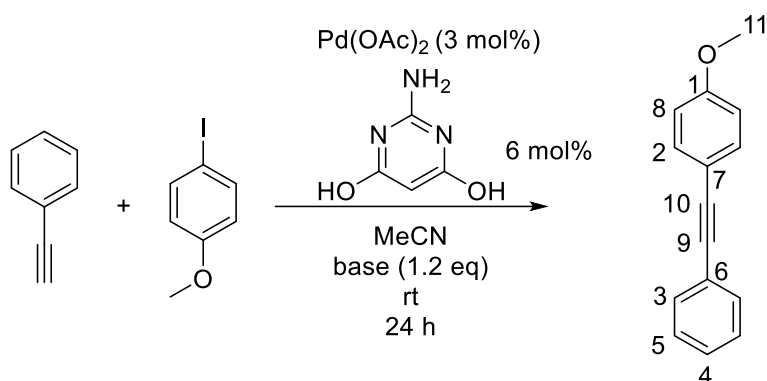
General procedure for 2-Methyl-3-phenylimidazo[1,2-a]pyridine<sup>58, 59</sup>



An oven dried Schlenk tube was charged with palladium(II) acetate (6 mg, 0.025 mmol, 5 mol%), Cataxium A (27 mg, 0.075 mmol, 15 mol%) and base (1.5 mmol, 3.0 equivalents). 2-Methylimidazo(1,2-a)pyridine (67  $\mu\text{L}$ , 0.5 mmol, 1.0 equivalent), halobenzene (0.7 mmol, 1.4 equivalents) was added followed by addition *p*-xylene internal standard (12.4  $\mu\text{L}$ ) and anhydrous degassed DMF (2 mL). The vessel was sealed and heated with stirring to 100  $^\circ\text{C}$  for 17 h and sampled using the general procedure before being cooled to room temperature and the solution filtered through celite and silica before evaporation to give crude 2-methyl-3-phenylimidazo[1,2-a]pyridine as a light brown oil. Representative 67% conversion using potassium carbonate as base by NMR.  $^1\text{H}$  NMR (500 MHz,  $\text{CDCl}_3$ )  $\delta$  8.10 (d,  $J_{2,11} = 6.8$  Hz, 1H, H-2), 7.57-7.52 (m, 3H, H-8,9), 7.46-7.39 (m, 3H, H-6,7), 7.15 (dd,  $J_{11,2} = 7.2$  Hz,  $J_{11,9} = 6.8$  Hz, 1H, H-11), 6.74 (d,  $J_{10,9} = 6.1$  Hz, 1H, H-10), 2.47 (s, 3H, H-12);  $^{13}\text{C}$  NMR (125 MHz,  $\text{CDCl}_3$ )  $\delta$  140.7 (C-1), 132.3 (C-2), 129.4 (C-3), 129.0 (C-4), 128.0 (C-5), 125.2 (C-6), 124.0 (C-7), 123.8 (C-8), 123.0 (C-9), 116.6 (C-10), 111.8 (C-11), 14.0 (C-12).

Literature data:  $^1\text{H}$  NMR (400 MHz,  $\text{CDCl}_3$ )  $\delta$  8.08 (d,  $J = 6.8$  Hz, 1H), 7.56–7.50 (m, 3H), 7.45–7.39 (m, 3H), 7.15 (t,  $J = 6.8$ , Hz, 1H), 6.70 (t,  $J = 6.8$ , Hz, 1H), 2.47 (s, 3H);  $^{13}\text{C}$  NMR (100 MHz,  $\text{CDCl}_3$ )  $\delta$  144.4, 132.1, 132.0, 129.4, 129.2, 128.6, 128.1, 124.1, 123.0, 116.9, 111.9, 13.9.

General procedure for 1-methoxy-4-(phenylethynyl)benzene

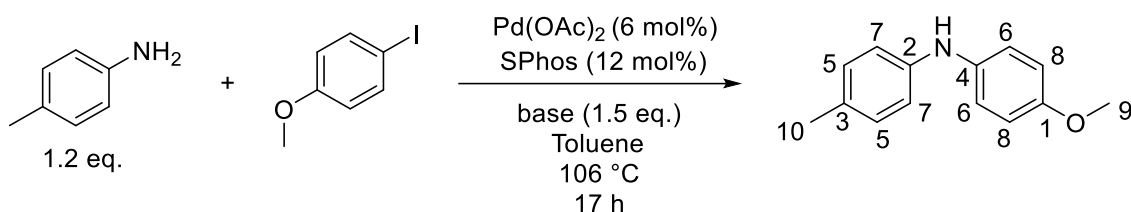


An oven dried Schlenk tube was charged with palladium(II) acetate (4.0 mg, 0.012 mmol 3 mol%), 4-iodoanisole (117 mg, 0.5 mmol), 2-Amino-4,6-dihydroxypyrimidine (4.0 mg, 0.03 mmol, 6 mol%) and base (0.6 mmol, 1.2 equivalents). Phenylacetylene (66  $\mu$ L, 0.6 mmol, 1.2 equivalents) was added with stirring followed by dry degassed acetonitrile (4.0 mL). The vessel was sealed and stirred at room temperature for 17 h. The mixture was quenched with 0.1 M acetic acid, and the crude filtered through celite and silica gel to give crude 1-methoxy-4-(phenylethynyl)benzene as a light brown solid (68 mg) giving 73% conversion using Cs<sub>2</sub>CO<sub>3</sub> as base by <sup>1</sup>H NMR and GC. <sup>1</sup>H NMR (500 MHz, CDCl<sub>3</sub>)  $\delta$  7.52-7.50 (dd,  $J_{1,2}$  = 9.6 Hz,  $J_{1,3}$  = 1.9 Hz, 2H, H-3), 7.47 (d,  $J_{2,4}$  = 8.9 Hz, 2 H, H-5), 7.34-7.31 (m, 3H, H-2,4), 6.88 (d,  $J_{5,3}$  = 8.8 Hz, 2H, H-8), 3.83 (s, 3H, H-11); <sup>13</sup>C NMR (75 MHz, CDCl<sub>3</sub>)  $\delta$  159.6 (C-1), 133.0 (C-2), 131.4 (C-3), 128.3 (C-4), 127.9 (C-5), 123.6 (C-6), 115.4 (C-7), 114.0 (C-8), 89.4 (C-9), 88.1 (C-10), 55.3 (C-11).

Literature data: (400 MHz, CDCl<sub>3</sub>)  $\delta$  7.52–7.51 (m, 2H), 7.48 (d,  $J$  = 9.0 Hz, 2H), 7.34–7.32 (m, 3H), 6.88 (d,  $J$  = 8.8 Hz, 2H), 3.83 (s, 3H); <sup>13</sup>C NMR (100 MHz, CDCl<sub>3</sub>)  $\delta$  159.6, 133.0, 131.4, 128.3, 127.9, 123.6, 115.4, 114.0, 89.4, 88.1, 55.3.

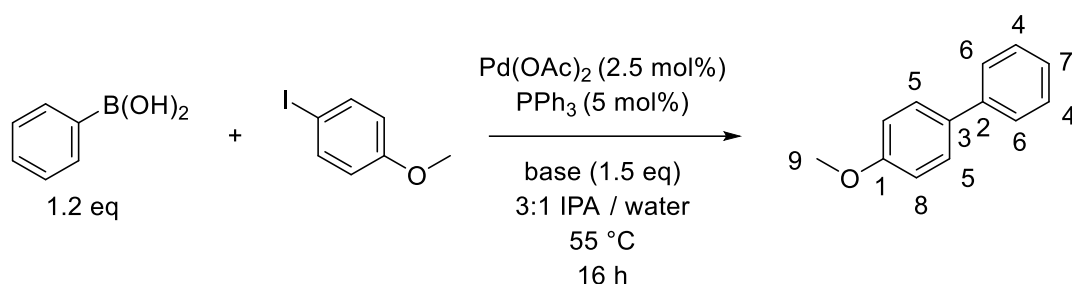
Water spiking experiments of 1-methoxy-4-(phenylethynyl)benzene

The reaction was conducted using the general method, with addition of degassed water (22  $\mu$ L, 1.22 mmol, 1.22 equivalents) after 30 minutes. The reaction was run sampled using the general method, giving 41% conversion using potassium carbonate base by <sup>1</sup>H NMR and GC.

General procedure for 4-methoxy-*N*-(4-methylphenyl)aniline<sup>46</sup>

An oven dried Schlenk tube was charged with 4-iodoanisole (176 mg, 0.75 mmol, 1.0 equivalents), 4-toluidine (97 mg, 0.9 mmol, 1.2 equivalents), base (1.125 mmol, 1.5 equivalents), palladium(II) acetate (10.1 mg, 0.045 mmol 6 mol%) and SPhos (37 mg, 0.09 mmol, 12 mol%), followed by addition of degassed toluene (6 mL). The vessel was sealed and heated to 106 °C for 17 h. The mixture was allowed to cool to room temperature and the crude extracted in DCM (3 x 20 mL) before filtering through celite and silica gel to give crude 4-methoxy-*N*-(4-methylphenyl)aniline as a light brown solid which was eluted in a silica column (3:1 petroleum ether 40-60 °C / ethyl acetate) and evaporated to give purified product (93 mg) as an off white solid giving 68% conversion using  $\text{Cs}_2\text{CO}_3$  as base. Conversions analysed using NMR and calibrated GC.  $^1\text{H}$  NMR (500 MHz, acetone- $d_6$ )  $\delta$  7.01 (d,  $J_{6,8} = 8.9$  Hz, 2H, H-6), 6.96 (d,  $J_{5,7} = 8.1$  Hz, 2H, H-5), 6.85 (d,  $J_{7,5} = 8.3$  Hz, 2H, H-7), 6.81 (d,  $J_{8,6} = 8.9$  Hz, 2H, H-8), 3.71 (s, 3H, H-9), 2.18 (s, 3H, H-10);  $^1\text{H}$  NMR (500 MHz,  $\text{CDCl}_3$ )  $\delta$  7.03 (m, 4H, H-5,6), 6.84 (m, 4H H-7,8), 5.39 (s, 1H, NH), 3.79 (s, 3H, H-9), 2.25 (s, 3H, H-10);  $^{13}\text{C}$  NMR (125 MHz,  $\text{CDCl}_3$ )  $\delta$  154.9 (C-1), 142.4 (C-2), 136.7 (C-3), 129.9 (C-4), 129.4 (C-5), 121.2 (C-6), 116.7 (C-7), 114.7 (C-8), 55.6 (C-9), 20.6 (C-10); m.p. 77 – 80 °C; HRMS ESI<sup>+</sup>: 214.1217 [M + H]<sup>+</sup> Calculated value for  $\text{C}_{14}\text{H}_{16}\text{NO}^+$  214.1220.

Literature data<sup>46 60</sup>:  $^1\text{H}$  NMR (400 MHz,  $\text{CDCl}_3$ )  $\delta$  7.05 (d  $J = 8.6$  Hz, 2H), 6.99 (d  $J = 8.3$  Hz, 2H), 6.89 (d,  $J = 8.3$  Hz, 2H), 6.83-6.86 (m, 2H), 5.62 (s, 1H), 3.74 (s, 3H), 2.21 (s, 3H);  $^{13}\text{C}$  NMR (125 MHz,  $\text{CDCl}_3$ )  $\delta$  154.8, 142.4, 136.6, 129.8, 129.3, 121.1, 116.5, 114.6, 55.6, 20.6; mp 79 – 80 °C.

General procedure for 4-methoxybiphenyl<sup>61, 62</sup>

An oven dried Schlenk tube was charged with 4-iodoanisole (117 mg, 0.5 mmol, 1.0 equivalents), benzene boronic acid (73 mg, 0.6 mmol, 1.2 equivalents), base (0.75 mmol, 1.5 equivalents), palladium acetate (6.0 mg, 0.025 mmol, 2.5 mol%) and triphenylphosphine (13.1 mg, 0.05 mmol, 5 mol%), followed by addition of degassed isopropanol/water (3:1 ratio, 5 mL). The vessel was sealed and heated to 55 °C for 16 hr. The mixture was allowed to cool to room temperature and the crude extracted in DCM (3 x 20 mL) before filtering through celite and silica gel to give crude 4-methoxybiphenyl, which was eluted in a silica column (70 mg, 72% conversion using  $\text{Cs}_2\text{CO}_3$  4:1 petroleum ether 40-60 °C / DCM) and evaporated to give as colourless needles, 77 mg, 84% yield using  $\text{Cs}_2\text{CO}_3$  as base. Conversions determined by NMR and calibrated GC.  $^1\text{H}$  NMR (500 MHz,  $\text{CDCl}_3$ )  $\delta$  7.53 (m, 2H, H-5), 7.51 (m, 2H, H-6), 7.41 (dd,  $J_{3,2} = J_{3,4} = 7.8$  Hz, 2H, H-4), 7.30 (t,  $J_{4,3} = 7.4$  Hz, 1H, H-7), 6.98 (d,  $J_{5,1} = 8.7$  Hz, 2H, H-8), 3.85 (s, 3H H-9);  $^{13}\text{C}$  NMR (125 MHz,  $\text{CDCl}_3$ )  $\delta$  159.1 (C-1), 140.8 (C-2), 133.8 (C-3), 128.7 (C-4), 128.5 (C-5), 126.8 (C-6), 126.7 (C-7), 114.2 (C-8), 55.4 (C-9); m.p. 81 – 83 °C; GCMS (EI<sup>+</sup>) ( $m/z$ ):  $[\text{M} + \text{H}]^+$  calcd. For  $[\text{C}_{13}\text{H}_{12}\text{O} \text{H}]$  184.5; found 184.5.

Literature data<sup>61, 62</sup>:  $^1\text{H}$  NMR (300 MHz,  $\text{CDCl}_3$ )  $\delta$  7.55-7.28 (m, 7H), 6.96 (d,  $J = 9.1$  Hz, 2H), 3.81 (s, 3H);  $^{13}\text{C}$  NMR (100 MHz,  $\text{CDCl}_3$ )  $\delta$  159.0, 140.7, 133.7, 128.6, 128.0, 126.6, 126.5, 114.1, 55.3; ESI<sup>+</sup> MS (ESI<sup>+</sup>) ( $m/z$ ):  $[\text{M} + \text{H}]^+$  184.4.

Caesium tetrafluoroborate monohydrate

A round bottom flask was charged with tetrafluoroboric acid (754  $\mu\text{L}$ , 5.9 mmol) in water (10 mL). Caesium chloride (1.0 g, 5.9 mmol) was added in portions and solution went cloudy, followed by stirring at 40 °C for 60hr to evaporate water slowly. Crude product was visible as a colourless powder. 1.03 g, 79% yield.  $\text{AgNO}_3$  test for halides:  $\text{CsBF}_4 \cdot \text{H}_2\text{O}$  (5 mg, 0.02 mmol) was added to a solution of silver nitrate (55 mg) in water

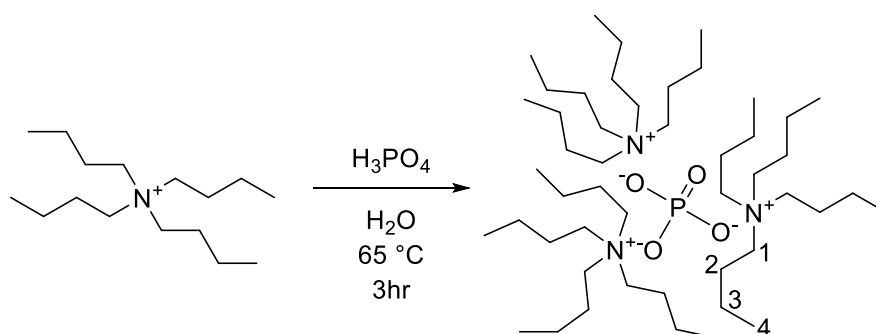
(5 mL). Negative, very slightly cloudy on addition of product, immediate white opaque precipitate on addition of 0.01 mol CsCl. FTIR  $\text{cm}^{-1}$ : 2183, 2002, 1089, 1034, 650, 517, 584, 419;  $^{19}\text{F}$  NMR (375 MHz,  $\text{D}_2\text{O}$ )  $\delta$  -150.3; AAS analysis Cs: 56.0%. Calc: 60.5%. Calc for  $\text{CsBF}_4 \cdot \text{H}_2\text{O}$  55.9%.

Literature data:<sup>63</sup> FTIR  $\text{cm}^{-1}$ : 1500, 1250, 1085, 1030, 524, 423;  $^{19}\text{F}$  NMR (neat)  $\delta$ : -147.

#### Procedure for $\text{CsBF}_4 \cdot \text{H}_2\text{O}$ spiking experiments to form 4-tolyl-p-anisidine

The reaction was run using the general method with addition of  $\text{CsBF}_4 \cdot \text{H}_2\text{O}$  (1.0 equivalents or 3.0 equivalents) to the reaction before addition of degassed toluene. The reaction was sampled according to the general sampling method. 12% representative conversion using  $\text{K}_3\text{PO}_4$  base.

#### Tetrabutylammonium phosphate<sup>64</sup>



A round bottom flask was charged with degassed ultrapure water (7.5 mL), followed by addition of tetrabutyl ammonium hydroxide (40% w/w 12.5 mL, 19.3 mmol, 3.01 equivalents), followed by slow addition of phosphoric acid (85 w/w, 430  $\mu\text{L}$ , 6.4 mmol). The vessel was sealed and stirred at 65 °C for 3 hr. The solution was freeze dried to yield crude product as a highly hygroscopic cream powder. The powder was washed with DCM/cyclohexane solution (10% v/v, 3 x 3 mL) to remove residual tributylamine. 4.51 g yield, 86%, 95% conversion by NMR.  $^1\text{H}$  NMR (500 MHz,  $\text{CDCl}_3$ )  $\delta$  3.37 (t,  $J_{1-2} = 8.5$  Hz, 24 H, H-1), 1.67 (m, 24 H, H-2), 1.46 (tq,  $J_{3-2} = 7.8$  Hz,  $J_{3-4} = 7.1$  Hz, 24 H, H-3), 0.99 (t,  $J_{4-3} = 7.3$  Hz, 36 H, H-4);  $^{13}\text{C}$  NMR (125 MHz,  $\text{CDCl}_3$ )  $\delta$  58.7 (C-1), 24.2 (C-2), 19.7 (C-3), 13.8 (C-4);  $^{31}\text{P}$  NMR (160 MHz,  $\text{CDCl}_3$ )  $\delta$  3.70.

Literature data:  $^1\text{H}$  NMR (400 MHz,  $\text{D}_2\text{O}$ )  $\delta$  3.12 (t,  $J = 6.6$  Hz, 24H), 1.58 (m, 24H), 1.29 (dt,  $J = 16.5, 5.4$  Hz, 24H), 0.87 (dt,  $J = 10.2, 0.9$  Hz, 36H);  $^{13}\text{C}$  NMR (100 MHz,  $\text{D}_2\text{O}$ )  $\delta$  58.2, 25.2, 19.2, 12.9 ppm.

## **2.8 References**

1. T. Okitsu, K. Iwatsuka and A. Wada, *Chem. Commun.*, 2008, 6330-6332.
2. V. Calò, A. Nacci, A. Monopoli and V. Ferola, *J. Org. Chem.*, 2007, **72**, 2596-2601.
3. M. B. Calvert and J. Sperry, *Org. Biomol. Chem.*, 2016, **14**, 5728-5743.
4. D. G. Musaev, T. M. Figg and A. L. Kaledin, *Chem. Soc. Rev.*, 2014, **43**, 5009-5031.
5. D. Tzalis and P. Knochel, *Angew. Chem., Int. Ed.*, 1999, **38**, 1463-1465.
6. Z. Qiao, J. Wei and X. Jiang, *Org. Lett.*, 2014, **16**, 1212-1215.
7. L. D. Tran and O. Daugulis, *Angew. Chem. Int. Ed.*, 2012, **51**, 5188-5191.
8. D. Shabashov and O. Daugulis, *J. Am. Chem. Soc.*, 2010, **132**, 3965-3972.
9. E. H. P. Cordfunke and W. Ouweltjes, *J. Chem. Therm.*, 1993, **25**, 1011-1016.
10. G. Zhang, Z. Peng and C. Li, *J. Therm. Anal. Calorim.*, 2016, **124**, 1063-1070.
11. D. Cuc, D. Canet, J.-P. Morel, N. Morel-Desrosiers and P. Mutzenhardt, *ChemPhysChem*, 2007, **8**, 643-645.
12. G. V. Lagodzinskaya, M. V. Loginova, N. G. Yunda, V. O. Zavel'skii and G. B. Manelis, *Russ. J. Coord. Chem.*, 1998, **24**, 142-149.
13. G. Dijkstra, W. H. Kruizinga and R. M. Kellogg, *J. Org. Chem.*, 1987, **52**, 4230-4234.
14. J. A. Cella and S. W. Bacon, *J. Org. Chem.*, 1984, **49**, 1122-1125.
15. C. A. Lipinski, F. Lombardo, B. W. Dominy and P. J. Feeney, *Adv. Drug Delivery Rev.*, 2001, **46**, 3-26.
16. J. Rena and A. Dean Sherry, *Inorg. Chim. Acta.*, 1996, **246**, 331-341.
17. L. Chen, D. R. Sanchez, B. Zhang and B. P. Carrow, *J. Am. Chem. Soc.*, 2017, **139**, 12418-12421.
18. T. M. Figg, M. Wasa, J.-Q. Yu and D. G. Musaev, *J. Am. Chem. Soc.*, 2013, **135**, 14206-14214.
19. S. Yu, S. Liu, Y. Lan, B. Wan and X. Li, *J. Am. Chem. Soc.*, 2015, **137**, 1623-1631.
20. D. G. Brown and J. Boström, *J. Med. Chem.*, 2016, **59**, 4443-4458.
21. S. Jagtap, *Catalysts*, 2017, **7**, 267.
22. J. G. de Vries, *Can. J. Chem.*, 2001, **79**, 1086-1092.
23. J. G. de Vries, *Dalton Trans.*, 2006, 421-429.
24. M. Beller and T. H. Riermeier, *Eur. J. Inorg. Chem.*, 1998, **1998**, 29-35.
25. I. D. Hills and G. C. Fu, *J. Am. Chem. Soc.*, 2004, **126**, 13178-13179.

26. Q. Yao, E. P. Kinney and Z. Yang, *J. Org. Chem.*, 2003, **68**, 7528-7531.
27. S. Ogo, Y. Takebe, K. Uehara, T. Yamazaki, H. Nakai, Y. Watanabe and S. Fukuzumi, *Organometallics*, 2006, **25**, 331-338.
28. I. J. S. Fairlamb and A. F. Lee, *Organometallics*, 2007, **26**, 4087-4089.
29. L.-C. Campeau, M. Parisien, A. Jean and K. Fagnou, *J. Am. Chem. Soc.*, 2006, **128**, 581-590.
30. L. Théveau, C. Verrier, P. Lassalas, T. Martin, G. Dupas, O. Querolle, L. Van Hijfte, F. Marsais and C. Hoarau, *Chem. - Eur. J.*, 2011, **17**, 14450-14463.
31. H. Cao, Y. Lin, H. Zhan, Z. Du, X. Lin, Q.-M. Liang and H. Zhang, *RSC Advances*, 2012, **2**, 5972-5975.
32. M. R. Chapman, M. H. T. Kwan, G. E. King, B. A. Kyffin, A. J. Blacker, C. E. Willans and B. N. Nguyen, *Green Chem.*, 2016, **18**, 4623-4627.
33. C. Meyers, B. U. W. Maes, K. T. J. Loones, G. Bal, G. L. F. Lemièrre and R. A. Dommissie, *J. Org. Chem.*, 2004, **69**, 6010-6017.
34. C. Liu, Y. Luo, W. Zhang, J. Qu and X. Lu, *Organometallics*, 2014, **33**, 2984-2989.
35. D. G. Musaev, T. M. Figg and A. L. Kaledin, *Chem. Soc. Rev.*, 2014, **43**, 5009-5031.
36. R. Chinchilla and C. Najera, *Chem Rev*, 2007, **107**, 874-922.
37. H. Zhong, J. Wang, L. Li and R. Wang, *Dalton T.*, 2014, **43**, 2098-2103.
38. M. Gazvoda, M. Virant, B. Pinter and J. Košmrlj, *Nature Commun.*, 2018, **9**, 4814.
39. M. Schilz and H. Plenio, *J. Org. Chem.*, 2012, **77**, 2798-2807.
40. J. Cheng, Y. Sun, F. Wang, M. Guo, J.-H. Xu, Y. Pan and Z. Zhang, *J. Org. Chem.*, 2004, **69**, 5428-5432.
41. C. A. Fleckenstein and H. Plenio, *Eur. J. Chem.*, 2007, **13**, 2701-2716.
42. J.-H. Li, X.-D. Zhang and Y.-X. Xie, *Eur. J. Org. Chem.*, 2005, **2005**, 4256-4259.
43. M. Bakherad, A. Keivanloo, B. Bahramian and M. Hashemi, *Tetrahedron Lett.*, 2009, **50**, 1557-1559.
44. H. Peng, Y.-Q. Chen, S.-L. Mao, Y.-X. Pi, Y. Chen, Z.-Y. Lian, T. Meng, S.-H. Liu and G.-A. Yu, *Org. Biomol. Chem.*, 2014, **12**, 6944-6952.
45. Y. Sunesson, E. Limé, S. O. Nilsson Lill, R. E. Meadows and P.-O. Norrby, *J. Org. Chem.*, 2014, **79**, 11961-11969.
46. R. Hesse, A. W. Schmidt and H.-J. Knoelker, *Tetrahedron*, 2015, **71**, 3485-3490.
47. A. A. C. Braga, N. H. Morgon, G. Ujaque and F. Maseras, *J. Am. Chem. Soc.*, 2005, **127**, 9298-9307.

48. B. P. Carrow and J. F. Hartwig, *J. Am. Chem. Soc.*, 2011, **133**, 2116-2119.
49. N. Miyaura, *J. Organomet. Chem.*, 2002, **653**, 54-57.
50. A. J. Amali and R. K. Rana, *Green Chem.*, 2009, **11**, 1781-1786.
51. P. A. Cox, M. Reid, A. G. Leach, A. D. Campbell, E. J. King and G. C. Lloyd-Jones, *J. Am. Chem. Soc.*, 2017, **139**, 13156-13165.
52. C. Sambigiato, PhD, University of Leeds, 2015.
53. C. Sambigiato, R. H. Munday, S. P. Marsden, A. J. Blacker and P. C. McGowan, *Chem. - Eur. J.*, 2014, **20**, 17606-17615.
54. K. Sasano, J. Takaya and N. Iwasawa, *J. Am. Chem. Soc.*, 2013, **135**, 10954-10957.
55. M. J. R. Clark and H. Lynton, *Can. J. Chem.*, 1969, **47**, 2579-2586.
56. A. S. Dallas and K. V. Gothelf, *J. Org. Chem.*, 2005, **70**, 3321-3323.
57. J. Yang, D. Wang, W. Liu, X. Zhang, F. Bian and W. Yu, *Green Chem.*, 2013, **15**, 3429-3437.
58. H. Cao, Y. Lin, H. Zhan, Z. Du, X. Lin, Q.-M. Liang and H. Zhang, *RSC Advances*, 2012, **2**, 5972-5975.
59. C. Cheng, L. Ge, X. Lu, J. Huang, H. Huang, J. Chen, W. Cao and X. Wu, *Tetrahedron*, 2016, **72**, 6866-6874.
60. K. Matsuo, Y. Shichida, H. Nishida, S. Nakata and M. Okubo, *J. Phys. Org. Chem.*, 1994, **7**, 9-17.
61. M. Trivedi, Bhaskaran, G. Singh, A. Kumar and N. P. Rath, *Inorg. Chim. Acta.*, 2016, **449**, 1-8.
62. I. Hoffmann, B. Blumenroder, S. Onodi nee Thumann, S. Dommer and J. Schatz, *Green Chem.*, 2015, **17**, 3844-3857.
63. R. E. J. Sears, *J. Chem. Phys.*, 1980, **72**, 2888-2889.
64. C.-T. Yang, Y. Fu, Y.-B. Huang, J. Yi, Q.-X. Guo and L. Liu, *Angew. Chem. Int. Ed.*, 2009, **121**, 7534-7537.

### Chapter 3: Investigation into the effectiveness of caesium bases in Buchwald-Hartwig amination reactions

Numerous literature investigations into the Buchwald-Hartwig (B-H) amination reaction have included a base screen to optimise the reaction conditions. In a significant proportion of these screening reactions caesium bases, especially caesium carbonate, were found to be the optimal weak base for the reaction.<sup>1-4</sup>

Buchwald-Hartwig amination reactions are able to proceed *via* two different mechanistic pathways, with the dominant mechanism dictated by the cycle with a lower rate limiting activation energy. Both amine coordination and base coordination pathways have been observed in the literature,<sup>5</sup> so being able to influence the mechanistic pathway by altering the reaction pathway, and therefore increase the overall reaction rate would be a useful method to provide increased yields in process chemistry and reaction optimisation (Figure 22, Figure 24).

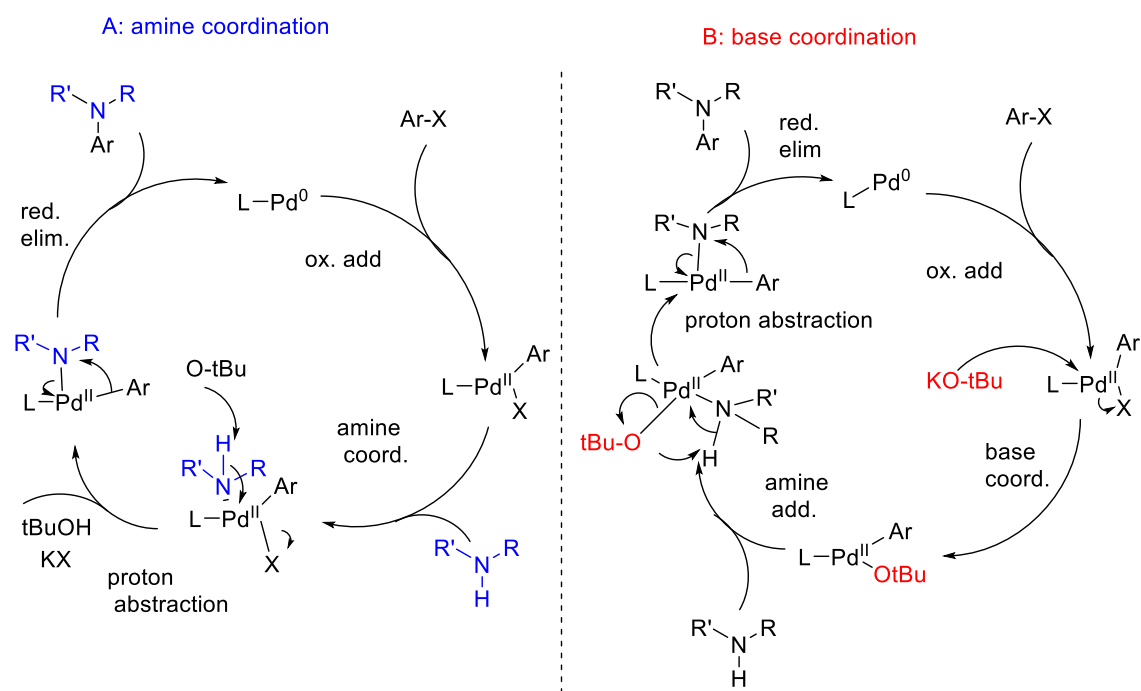


**Figure 24:** Possible mechanistic pathways in Buchwald-Hartwig amination

The rate limiting step in B-H amination reactions is largely dependent on the the aryl halide, as stronger C-X bonds disfavour oxidative addition so this step becomes more favourable as the halides proceed down the group. The turnover frequency and number of a given catalyst greatly affects the mechanistic pathway, as a more active

and stabilised catalyst can increase the rate of all catalytic steps as the palladium atom is involved at each point. Maes *et al.* found that the proton abstraction step can also be rate limiting, with the particle size of the base being highly important to reaction rate.<sup>2</sup> When using a weak base, the proton abstraction step is thought to be rate limiting due to poor solubility or low  $pK_b$  of the base anion,<sup>6</sup> whereas when stronger bases such as potassium *tert*-butoxide are used, either the oxidative addition or reductive elimination step are thought to be rate limiting, which would be dependent on the leaving group of the aryl halide.<sup>7</sup>

To gain additional data investigating the less well-known rate limiting proton abstraction step using weak bases, we conducted a base screen (Figure 25) for the reaction of *p*-toluidine with 4-iodoanisole where caesium phosphate was found to be the optimal weak base, and herein found that both caesium phosphate and carbonate reactions gave over 10x the conversion than the respective potassium bases (Figure 26).

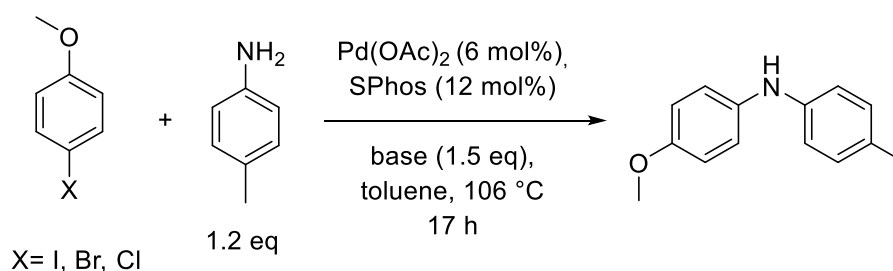


**Figure 25:** Conditions for amination reaction base screen<sup>8</sup>

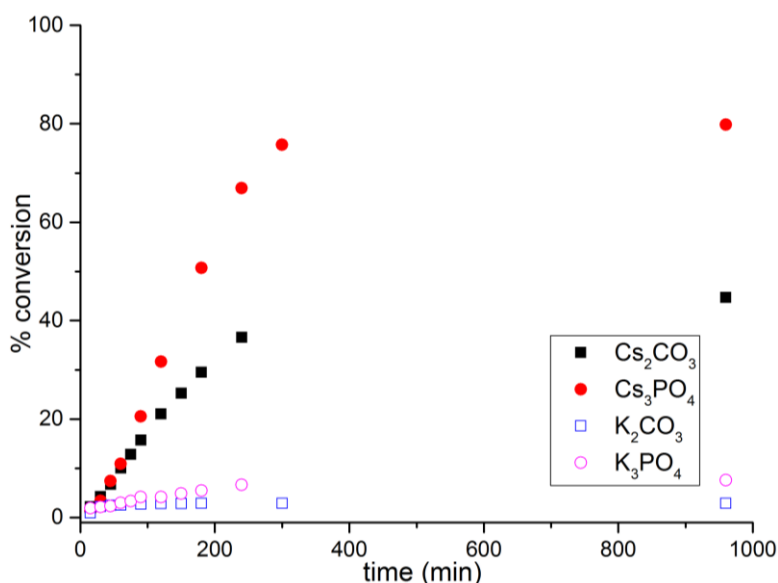
### **3.1 Investigation into the rate determining step of Buchwald-Hartwig amination reactions and the influence of base**

It is important that reaction sampling is robust and repeatable in order to provide a reliable method of elucidating reaction conversion in a time efficient manner. We elected to analyse reactions by calibrated GC, as both the starting material and product had boiling points below 300 °C and would easily separate allowing for facile analysis. In addition, we reduced the temperature used in the literature reaction from reflux to 106 °C to minimize issues with solvent condensation on the reactor walls which would change both the reaction concentration itself, and the reaction concentration relative to the internal standard. The methoxy group on the aryl halide also allowed for <sup>1</sup>H analysis so end point conversions were aided by <sup>1</sup>H NMR to ensure the results were

reproducible and accurate. *p*-Xylene was used as an internal standard at 0.05 M concentration as it is chemically similar to toluene solvent, and observable by GC.

### 3.1.1 Reactions with aryl iodides

**Figure 26:** Base screen comparison of B-H amination with aryl iodide (conversion  $\pm 2\%$ )



In this reaction we can observe that the optimal base is caesium phosphate monohydrate by overall conversion. We can observe over 10x the conversion % using caesium bases than potassium for both carbonate and phosphate anions.

For the first 90 minutes, the initial rate appears to be similar using both caesium carbonate and phosphate, at which point the reaction using caesium phosphate monohydrate is able to maintain the reaction rate while the caesium carbonate reaction decreases slightly. The presence of similar rates with both the anions would suggest that the major component of the reaction increasing rates is the caesium cation (*vide infra*), rather than the cation and anion together that improves the rate in this reaction, so any rationalisation of the increased performance of the caesium bases in this reaction example must involve the caesium cation specifically.

The existing solubility reasoning behind the 'caesium effect' pointing to existing data of increased solubility of caesium carbonate over other alkali metal carbonates in dipolar aprotic solvents does not apply here.<sup>9</sup>  $^{31}\text{P}$  and  $^{133}\text{Cs}$  NMR measurements of caesium phosphate monohydrate and potassium phosphate in toluene *vide supra*

show that caesium phosphate monohydrate base actually has lower solubility in the reaction solvent than potassium phosphate at room temperature, and that there does not appear to be a temperature dependence on solubility of phosphate bases in this solvent.

The reason for this very large increase in reaction performance when using caesium could be because there is a change in the mechanism due to the formation of the metal halide salt by-product at the end of the reaction. The difference in  $\Delta H_{\text{formation}}$  of KI and CsI is 8.5 kJ/mol more favourable for CsI,<sup>10</sup> so this additional energy may allow a change between the base and amine coordination mechanism which is only possible due to formation of CsI. An alternative hypothesis is that the caesium is in some way influencing the catalyst, allowing for a formation of a more favourable intermediate species which requires the caesium cation to form.

Previous work in the literature had suggests that if strong bases are not used, in addition to using an iodide leaving group, oxidative addition is unlikely to be rate limiting.<sup>7</sup> The expected rate limiting step in both base and amine coordination mechanisms is therefore the internal and external proton abstraction steps respectively.

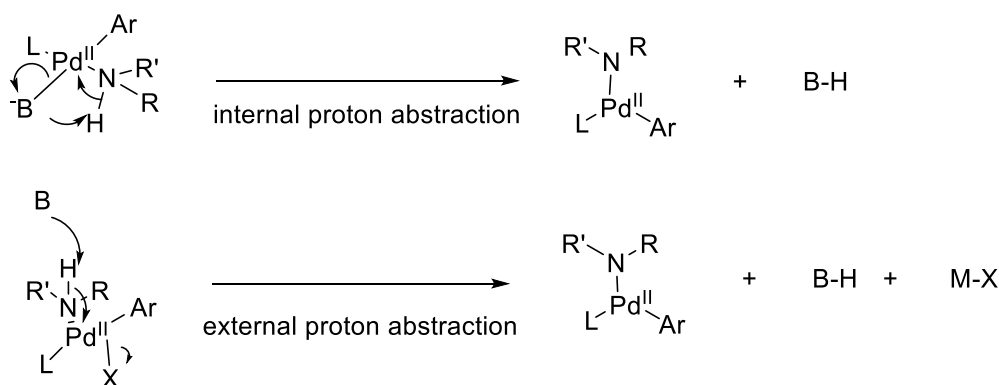


**Figure 27:** Comparison between internal and external proton abstraction rate limiting steps

The cation is not present in either of the proposed rate limiting steps, so either the caesium cation can facilitate a change in mechanism (Figure 24) changing the rate determining step between the internal and external proton abstraction step, or it can reduce the activation energy of the existing rate limiting abstraction step sufficiently to gain increased reaction yields.

Previous literature results in alkylation and macrocyclic ring closure hypothesised that the reaction could occur on the positively charged surface of the caesium cation.<sup>11, 12</sup> This is more likely to occur in cases where the base is not fully dissolved and the deprotonation step is able to occur heterogeneously. Numerous examples of caesium incorporation into the catalyst have been found by Density Functional Theory (DFT), suggesting that the caesium cation itself may be able to directly bind to the catalyst allowing for lower activation energy. In turn, this causes higher reaction rates due to stabilisation of the transition state by the cation.<sup>13-15</sup> This may explain why caesium phosphate increases the yield after 90 minutes of reaction time, as the tribasic caesium contains 50% more cation than the dibasic carbonate equivalents assuming the same solubility. The higher equivalents of the caesium cation using the phosphate base lead to a larger amount of caesium to template the deprotonation step and therefore keep the rate as high as at the start of the reaction.

In contrast to rate increases attained by use of the caesium cation, potentially due to the increased ionic character of CsI over potassium iodide, we elected to probe whether a much harder lithium cation would reduce the reaction yield. Lithium is more electronegative than caesium and potassium by 0.19 Pauling units, which means there is a smaller differential between the cation and anion electronegativity, causing a higher covalent character to the Li-I bond from the increased power of polarisation of the lithium cation as the metal is more able to withdraw electron density from the halide. In addition to this the  $\Delta H_{\text{formation}}$  for lithium iodide is only -65 kJ/mol, over 19 kJ/mol less favourable than caesium iodide meaning that the solid lattice has less ionic character than the softer caesium cation.<sup>10</sup>

Taking this data into account along with the rationalisation of the increased performance of reactions using caesium bases we would expect much lower yields when using lithium bases with the iodide leaving group. When using lithium phosphate base in the amination reaction, the overall conversion at the end of the reaction was only 2% which suggests that the formation of CsI may be increasing reaction rate if the amine coordination mechanism was preferred.

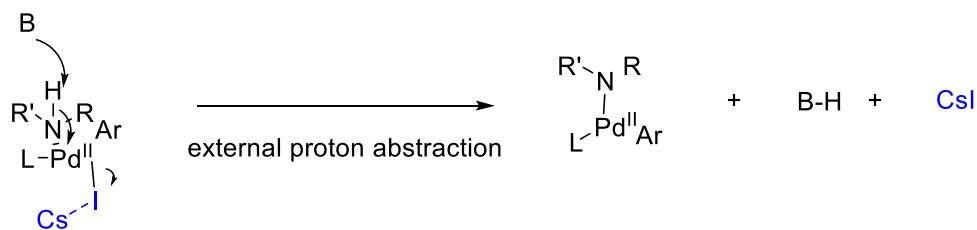


**Figure 28:** External proton abstraction step illustrating caesium destabilisation of Pd-I bond

Due to the strong soft-soft interaction between the caesium cation and iodide anion, the Pd-I bond may be destabilised by the caesium, allowing for improved rate of the rate limiting external proton abstraction step when using caesium bases in this reaction. It is not clear whether all bases undergo the external proton abstraction step and the caesium cation improves the rate, or whether the presence of the caesium cation actually reduces the energy barrier of the amine coordination pathway sufficiently to change the mechanistic cycle from the base coordination to amine coordination pathway (Figure 24), allowing for cation interaction.

In addition to this, because of the more covalent character of the lithium base and the relative strength of the ionic bonds, the solubility of lithium bases is very low. Due to the lowered conversion using this effectively insoluble base we can argue that the deprotonation by the base must occur homogeneously with the base in solution, rather than heterogeneously on the surface of the base particles in a reaction suspension. The presence of some turnover however does indicate that once the base anion has been protonated, the solubility equilibrium allows for more base to dissolve, as the solvent is no longer saturated, which allows for continuation of reaction turnover. This explains why high conversions are still possible in cases where the solubility of the base is less than 1 equivalent of amine starting material.

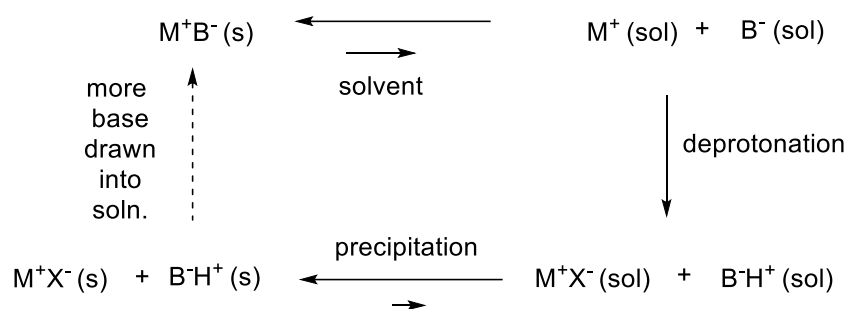


**Figure 29:** Illustration of how low solubility bases can be drawn into solution via precipitation of base by-products

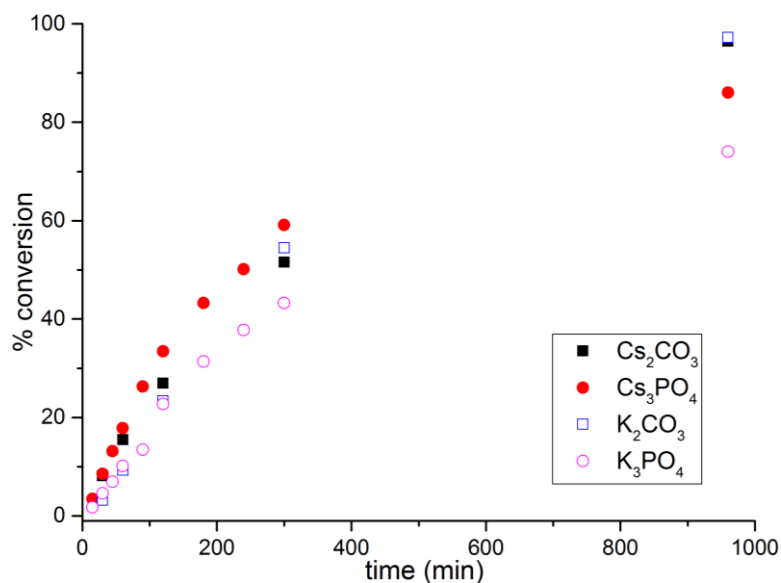
For the reactions using low solubility bases to gain high conversions, the base must be more soluble than the deprotonation by-products, otherwise the reaction solvent will remain at saturation after one catalytic turnover. If the by-products do precipitate however, additional base can be drawn into solution to perform the deprotonation step, which allows for further catalytic turnovers and higher yields.

### **3.1.2 Reactions using aryl bromides and chlorides**

To assess the effect of the by-product salt on the reaction, we chose to alter the leaving group of the aryl halide from iodide to bromide. If CsI formation and destabilisation of the Pd-I bond was driving the reaction, we would expect that upon a change to the smaller bromide anion, we would see a difference in performance of caesium bases relative to potassium because of the reduction in soft-soft interactions between the large caesium cation and large iodide anion.<sup>16</sup>

In contrast to the 8.5 kJ/mol difference between caesium and potassium iodide formation, we observe a much smaller difference when changing to the bromide leaving group, as the  $\Delta H_{\text{formation}}$  is 0.2 kJ/mol more favourable for caesium bromide than potassium bromide, therefore the formation enthalpy difference is only 2% of the iodide example.<sup>10</sup> From this we would expect the reaction to behave similarly with caesium and potassium cations.

**Figure 30:** Buchwald-Hartwig Amination reaction with bromide leaving group base screen



We observe that the change from iodide to bromide leaving group can cause a large change in initial rate and overall conversion when changing the base cation. Despite the reactions with the potassium cation only achieving at most 8% conversion using the iodide leaving group, which usually has a lower activation energy barrier for oxidative addition due to the C-I bond strength being weaker by approximately 25 kJ/mol,<sup>17</sup> we see a large increase in conversion when changing to the more difficult bromide leaving group. We are currently unaware of any previous examples of base cations allowing a reaction to achieve better yields and initial rates when switching to a less labile aryl halide in palladium catalysed cross coupling reactions.

It is likely that due to similar conversions and rates using different base cations, the mechanistic pathway is likely to be the base coordination cycle (Figure 24) where the base cation is not involved in the internal proton abstraction rate limiting step.

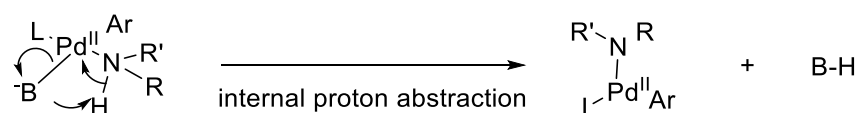


**Figure 31:** Internal rate limiting proton abstraction step which does not involve base cation

While the proton abstraction step is still likely to be rate limiting due to using weak bases,<sup>7</sup> the anion nucleophilicity will play a major role in determining any differential on using different bases in these reactions, which due to exhibiting similar rates appears to be relatively similar. If the amine coordination pathway was still dominant, we can deduce that any destabilisation of the Pd-Br bond by the alkali metal cations was similar between the caesium and potassium cations, which agrees with the data that the formation enthalpy is very similar for both CsBr and KBr.

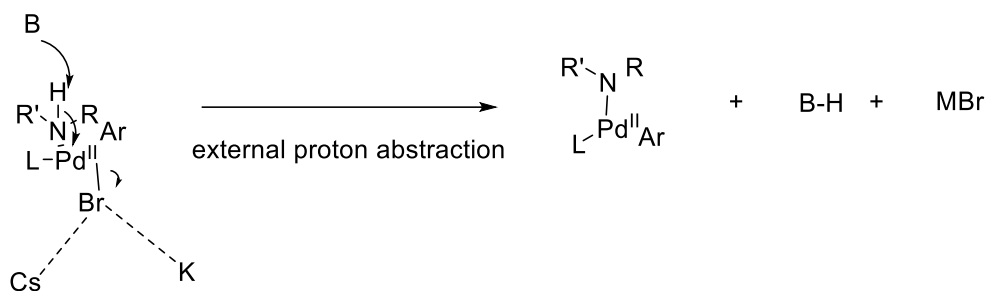


**Figure 32:** Rate limiting external proton abstraction step illustrating similar Cs and K destabilisation of the Pd-Br bond

One way we can explain the change in performance of the amination reaction when changing from iodide to bromide leaving groups is that the ion pairing allows caesium bases to perform much better when using iodide but not bromide due to the Cs-I interaction destabilising the Pd-I bond (Figure 28) which allows the reaction to gain higher conversions due to increased rate of external proton abstraction. To investigate this we chose to use lithium phosphate as the most covalent and hardest anion available in this reaction to provide minimal orbital overlap with the relatively soft bromide anion.

When we elected to use lithium phosphate in the reaction with the bromide leaving group, only 1% conversion was observed. Despite potassium and caesium bromides possessing almost equal formation enthalpies, the formation of lithium bromide is over 11 kJ/mol higher,<sup>10</sup> and therefore less favourable than both potassium and caesium bromide. This very large differential explains why reactions using more covalent lithium bases cannot achieve similar conversions relative to the softer caesium and potassium cations.

To further investigate the possibility of base pairing we elected to change the leaving group to the chloride. While we would expect lower conversions using the aryl chloride than the bromide and iodide due to the stronger bond strength slowing the oxidative addition step, if the ion pairing effect were the predominant explanation for the increase in reaction conversion in the iodide example, we would expect the reverse to be true when using the chloride as the  $\Delta H_{\text{formation}}$  of KCl is 3.9 kJ/mol lower than CsCl. Based on the values in the iodide case of 8.5 kJ/mol we would expect a small but noticeable increase in overall conversion using potassium bases in the chloride reaction (Table 13).<sup>10</sup>

**Table 13:** Buchwald-Hartwig amination (Figure 25) reaction with chloride leaving group

Base	Cs <sub>3</sub> PO <sub>4</sub> .H <sub>2</sub> O	Cs <sub>2</sub> CO <sub>3</sub>	K <sub>3</sub> PO <sub>4</sub>	K <sub>2</sub> CO <sub>3</sub>
Conversion (%)	5.0	46.8	17.1	67.3

We can see from this table that as expected, potassium bases are better than the caesium bases, likely due to the more favourable salt by-product enthalpy of formation which indicates that the proton abstraction step remains rate limiting in the amine coordination mechanism. Interestingly, when changing leaving group from iodide to chloride, we would expect the rate of oxidative addition to slow down significantly. However, if oxidative addition to the palladium catalyst was the rate determining step, we would expect the bases to perform equally regardless of pK<sub>a</sub> or cation, provided the pK<sub>b</sub> of the base was sufficiently high to abstract the proton and form the MX salt. Consequently, these results show that regardless of which aryl halide is used, the rate determining step of this Buchwald-Hartwig amination reaction is not the oxidative addition step. Due to the substantial effect changing cations has in both iodide and chloride examples the evidence points towards a rate limiting proton abstraction step, in line with previous findings in the literature.<sup>6</sup>

The change in reaction conversion caused by the change in cation is clearly important to the understanding of the base effect in Buchwald-Hartwig amination reactions. A more subtle change in addition to this larger effect is how the phosphate and carbonate anions influence the reaction rate. We can observe that when using the iodide leaving

group, the phosphates give approximately twice the conversion than the carbonates. With the bromide this then changes to the carbonate bases being more favourable by approximately 20%, and finally with the chloride we see an almost 50% increase in conversion using the carbonates over the phosphate bases. Buchwald-Hartwig amination reactions can usually be improved when increasing the  $pK_b$  of the anion, for example using  $KOtBu$  as the base instead of weaker bases such as carbonates, phosphates or fluorides.<sup>18</sup>

It is thought that the explanation for this change is related to the higher affinity of the phosphate anion to the palladium centre compared to the carbonate anion. The higher  $pK_b$  of the phosphate may be able to stabilise the palladium in the base coordination mechanism more than the carbonates which allows for a faster rate as the base anion is present in the rate limiting internal proton abstraction step. When using the chloride leaving group the opposite is true, which suggests the amine coordination mechanism may be preferred limiting the role of the anion to an external proton abstraction with minimal catalytic cycle involvement. In the amine coordination mechanism the phosphate anion may compete between palladium coordination and proton abstraction of the bound amine, slowing the reaction down, whereas the carbonate anion will readily undergo the external proton abstraction step.

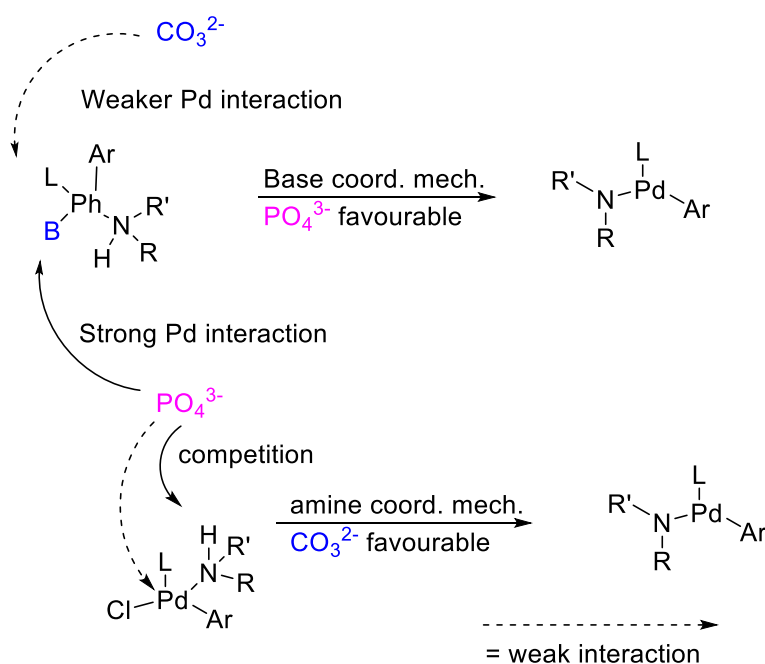


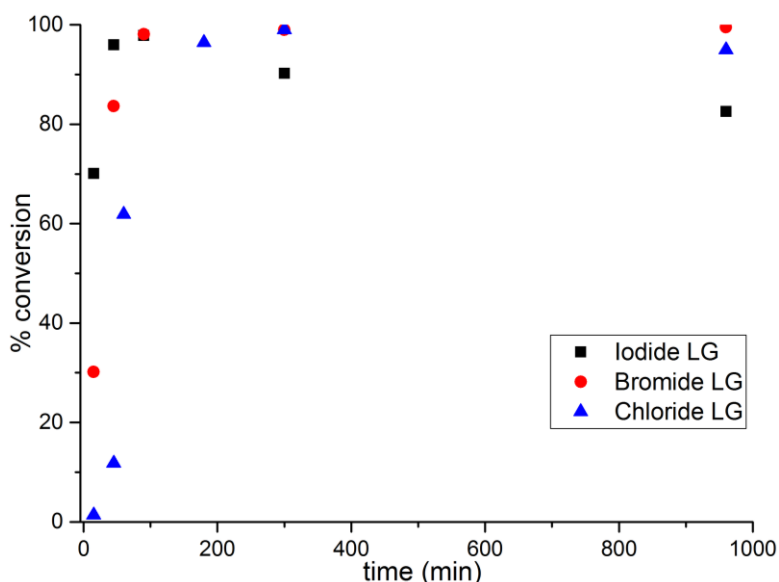
**Figure 33:** Relative interactions of carbonate and phosphate anions in rate limiting proton abstraction steps based on change in mechanistic pathway

To further investigate the effect of anion on the reaction we elected to run all three reactions with the stronger base potassium *tert*-butoxide. Consequentially the rate limiting step may shift from the proton abstraction step to oxidative addition.<sup>7</sup> This will significantly change the relative reaction rates. We would then expect an improvement in rate as the deprotonation step is expected to occur very quickly.

### **3.2 Use of KOtBu in Buchwald-Hartwig amination reaction**

The higher  $pK_b$  of 17 due to the basic butoxide anion in potassium *tert*-butoxide allows the base to increase the rate of deprotonation relative to weaker bases, and increase reaction rate in reactions in which deprotonation is the rate determining step. The more basic anion is therefore highly useful in base mediated coupling reactions. If the basic anion was involved in the rate determining step the increased  $pK_b$  would accelerate the reaction. Stronger bases are not always compatible with Buchwald-Hartwig amination reactions as they often produce unwanted side products,<sup>19</sup> or overarylation of the amine.<sup>1</sup> In this case we do observe significant overarylation of the aniline using the stronger base of 17% using the aryl iodide, causing a decrease in desired product formation (Figure 34).

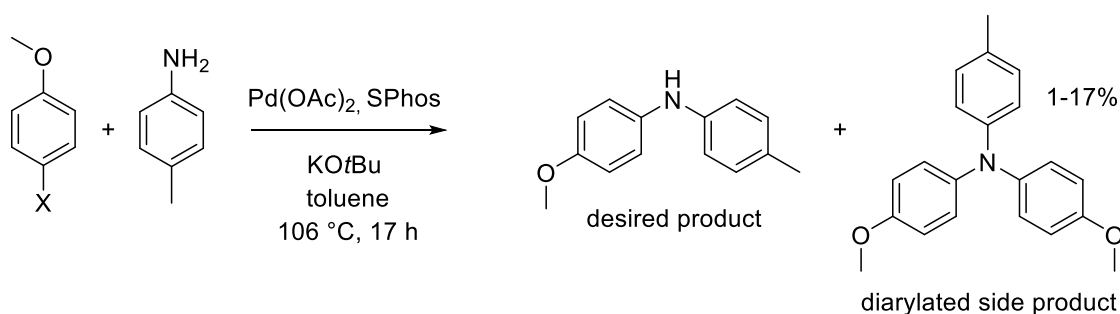
**Figure 34:** Potassium *tert*-butoxide in Buchwald-Hartwig amination



We do observe much faster initial rates using the *tert*-butoxide anion, with even the slowest halide leaving group of the chloride achieving over 90% conversion at  $t = 120$  min. The conversion is comparable with the best weak base case of caesium phosphate monohydrate when using the aryl iodide which had an initial rate of approximately half

of that using KO $t$ Bu iodide reaction. This would therefore suggest that the highly basic anion is increasing the rate of the reaction. This is likely achieved by increasing the rate of proton abstraction sufficiently that it is no longer rate limiting.

Using the less labile aryl chloride, the stronger *tert*-butoxide base is better than the weak phosphate or carbonate bases. However, in the case of the bromide and particularly the iodide the increased rates of reaction appear to actually reduce the conversion by forming the diarylated product, reducing the amount of desired product in the reaction mixture. The overall conversion at 16 h to the desired product is 83% using both caesium phosphate and potassium *tert*-butoxide, however the stronger base is observed to convert the remaining 17% into the diarylated side product (Scheme 33).



**Scheme 33:** Side product formation in Buchwald-Hartwig amination

The rationalisation behind this increased reactivity which allows for conversion of both the aniline and the diarylated product is that the basic anion can stabilise the amine coordinated palladium. This lowers the pK<sub>a</sub> of the aniline proton which is able to be abstracted more easily by the butoxide anion (Figure 35).

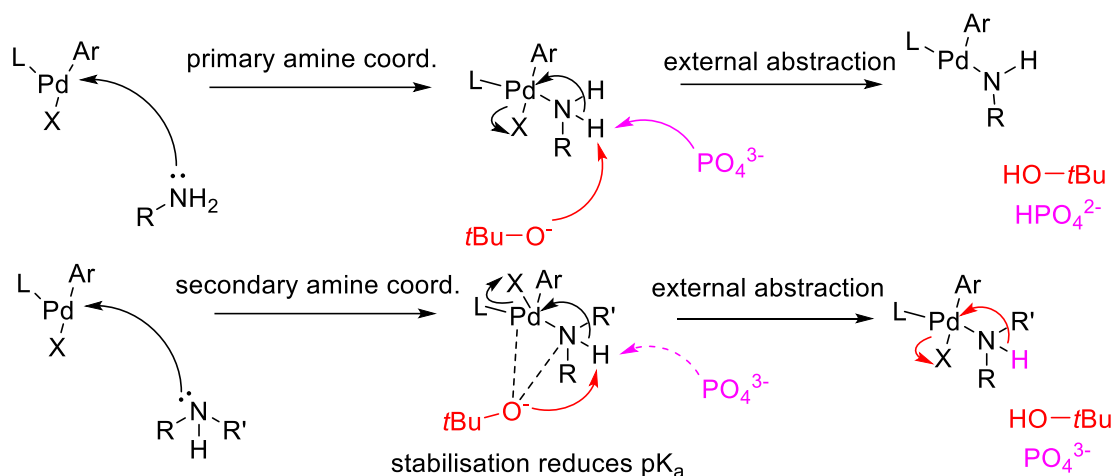


**Figure 35:** Representation of overarylation of anilines using KOtBu

Each base can stabilise the complex enough to reduce the pK<sub>a</sub> sufficiently for monoarylation, however only the *tert*-butoxide can stabilise the palladium halide enough to perform the second arylation reaction to form the diarylated side product. This stabilisation then ensures the external proton abstraction step is favourable.

When the leaving group is less favourable this overarylation does not occur to the same degree, and when using the aryl chloride the total amount of diarylated product drops to below 1% (Table 14).

**Table 14:** Side product in amination reaction with KOtBu based on leaving group

Leaving group	Iodide	Bromide	Chloride
Diarylated product (%)	16.5	5.0	0.8

Despite KOtBu being a more effective base in this reaction and allowing for increased yields using shorter reaction times, other bases, particularly caesium phosphate monohydrate have utility in Buchwald-Hartwig aminations where the product is liable to undergo further reaction or when base sensitive functional groups are present. This reduction in unwanted side reactions and products present caesium phosphate monohydrate as the best weak base in amination reactions where the iodide leaving group is used.

### **3.3 Increasing solubility of bases via crown ether complexation**

The previous reasoning behind the caesium effect in organic reactions had been that caesium bases were more soluble than other alkali metals due to the soft-hard interactions between the cation and anion. Based on our research *vide supra* we do not believe caesium bases to be more soluble in non dipolar-aprotic solvents, and argue that any caesium effect in these solvents would be caused by another factor unrelated to solubility. Despite solubility not appearing to directly influence reaction performance, we elected to attempt to alter the solubility of potassium bases by introducing crown ethers into the reaction.

Crown ethers are known to increase solubility of alkali metal bases by complexing the alkali metal cation inside the 'crown' ring.<sup>20</sup> The oxygen atoms can donate electron density to the metal centre as the core hole inside the ether is a very similar size to the cation itself, which allows for complexation and stabilization of the positively charged cation.

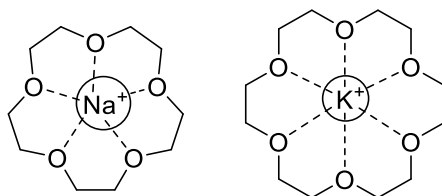


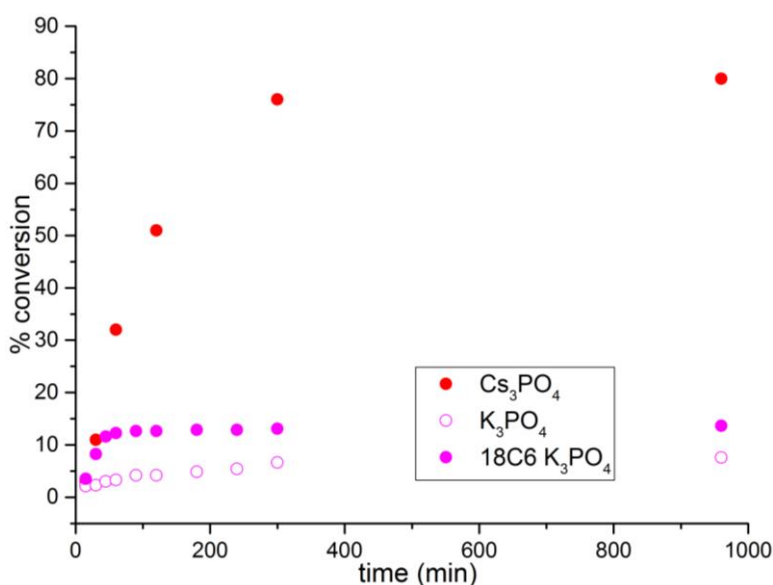
**Figure 36:** Representation of crown ether complexation of sodium and potassium cations

The complexation of the cation suppresses ion pairing and allows for increased solubility of the base as the anion and cation are dissociated into parent ions. This then allows the anion to freely react in solution as the cation is bound by the crown ether molecule. This is referred to in the literature as the 'naked anion effect'.<sup>21</sup>

The crown ether with the strongest binding affinity for both caesium and potassium cations is 18-crown-6. Despite it being best for both cations the ligand cavity is much more akin to the size of the potassium cation than the caesium cation, with a radius of 143 pm expected for the cavity, while the cationic radius of  $K^+$  is slightly smaller at 138 pm. The much larger caesium cation at 170 pm radius is much harder to ligate well, and therefore possesses much lower binding energies, with the binding constant  $K$  being over 20 times higher using ethanol solvent and 6 times higher using DMF solvent.<sup>22</sup>

Given this information we would expect any increase in solubility or rate enhancement using 18-crown-6 to be much higher using potassium bases than caesium bases. However, as caesium bases were much more effective using the iodide leaving group, it is important to test whether crown ether mediated solubility increases accompanied with the 'naked anion effect' would increase reaction rate.

**Figure 37:** Increase in performance using crown ethers in amination reaction with iodide leaving group (Figure 25)



We can observe an initial increase in rate from 0 to 30 minutes in the crown ether complex system, however after this time the reaction appears to level off in conversion indicating no further catalysis had taken place. Interestingly this 3.7 fold increase in initial rate is very similar to the initial rate using the best case caesium phosphate base. We then argue that after this initial period of higher catalytic activity, the residual water in the reaction caused catalyst oxidation and deactivation of the catalyst preventing any further turnover from occurring. We can rationalise this deactivation by understanding the hygroscopicity of crown ethers, which are notoriously difficult to dry. The relatively low boiling point of 116 °C makes vacuum drying and lyophilisation difficult, and despite undergoing desiccation *in vacuo* at 30 mbar overnight the crown ether appeared 'jelly-like' indicating some water remained. More rigorously dry 18-crown-6 can be made by drying with NaK and decomposing the ligated product under low pressure to sublime 18-crown-6.<sup>23</sup> This method involves significant safety concerns for anything but very slightly wet crown ether, as any more will react violently with

NaK.<sup>24</sup> For this reason we elected to maintain our drying method as the bases themselves were not dried as rigorously, but instead by oven drying overnight at 110 °C.

What the increased initial rate would suggest is that the complexed cation renders the anion freer to react in solution due to the higher solubility and the more facile breaking of the crystal lattice. This 'naked anion effect' appears to increase the rate similarly to the caesium phosphate monohydrate example, which provides evidence that the rate limiting step can increase in rate *via* changing both the cation and anion. Ion pairing between cation and anion is also highly important to reaction performance.

The water in caesium phosphate monohydrate appears to not affect reaction rate when in water sensitive reactions due to the low solubility of the caesium cation in these solvents which means low ionic dissociation and therefore lower concentration of water in the reaction. When using the much more soluble crown ether reagents this bound water will be liberated and free to react with the active catalyst, causing oxidation and deactivation which can be observed after 30 minutes. We would expect a large increase in conversion using either rigorously dried crown ether, or in a reaction with a similar mechanism but using a non-water sensitive catalyst.

### **3.4 Elucidating rate limiting step of Buchwald-Hartwig amination reactions by changing concentration of limiting reagents**

The rate of a reaction, assuming mass transfer limitations are negligible and the reaction itself is homogenous, depends purely on the reactants present in the rate determining step. Previous research has indicated the Buchwald-Hartwig amination reaction was first order in both catalyst, and aryl halide.<sup>25, 26</sup> More recent work has suggested however, that in most cases the proton abstraction step is rate limiting which involves: the palladium source, ligand, base anion, aryl halide and amine.<sup>7</sup>

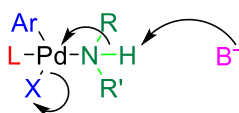


**Figure 38:** External proton abstraction step showing multiple components present in rate limiting step

No study attempting to provide a rate equation for the amination reaction had included a term for the base, or the cation or anion of the base separately, though both clearly can effect reaction performance as base screens have shown in literature.<sup>2</sup> The drastic change in relative rates when switching from the iodide to bromide leaving group led us to investigate the effect of concentration using the bromide further and deduce whether a term would be required for the base in the rate equation.

The rate of a reaction is proportional to the concentration of the reactants present in the rate determining step. If a reaction was first order in aryl halide we would expect the reaction rate to halve when [aryl halide] was reduced by half. Based on this information we created a number of reactions altering the concentrations of species in the reaction to probe which had a direct effect on the rate of reaction.

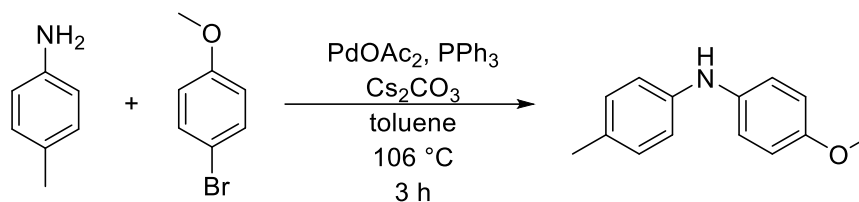
The reactions were carried out on a Mettler Toledo EasySampler apparatus, allowing for uniform sampling at specified times via a 20  $\mu\text{L}$  pocket which was pumped directly into a quenched vial. This then reduced errors in sample volume and reaction time to below 1%, which gave superior results than manually sampling the reaction for offline GC analysis (Figure 39).



**Figure 39:** EasySampler setup showing sampling arm, vials and inerted flask

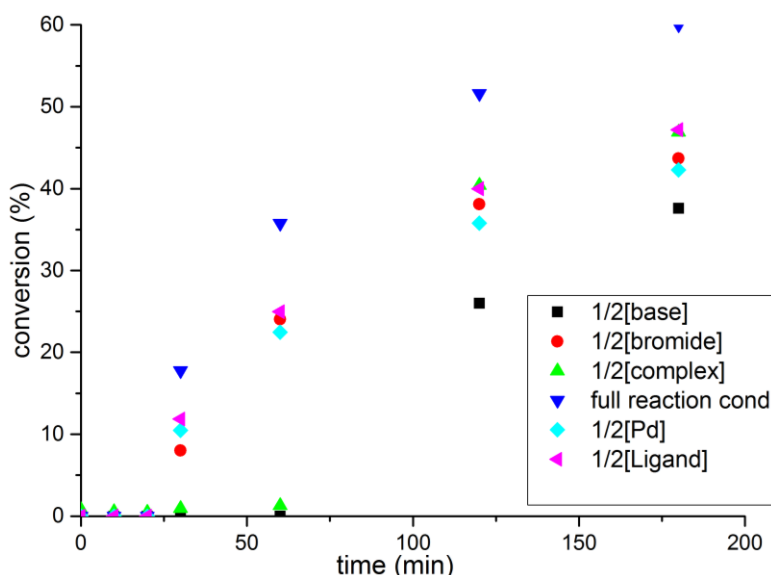
The base we elected to use for the rate determination experiments was caesium carbonate, as it performed well in the bromide reactions gaining over 90% conversion

after 17 h, and was not as hygroscopic as the phosphate bases so any potential for water ingress into the reaction was minimized (results in Figure 40).



**Scheme 34:** Standard conditions for EasySampler reactions forming 4-tolyl-*p*-anisidine

**Figure 40:** Rate determination experiments found from changing reagent concentrations



The first thing to consider in this figure is that all of the reactions had an induction period of approximately 30 minutes which is likely to correspond to the time required to form the active catalyst because the reactions were all done 'one-pot' with addition of all reagents followed by addition of solvent and aryl halide at the reaction temperature. There is also a change in induction period on reduction of concentration of base and complex (see p.103). To avoid this induction period in subsequent reactions *vide infra*, we performed the catalyst by mixing in solvent at room temperature followed by evacuation of the flask to dryness and the addition of solid reagents following the general method. Nevertheless, to ensure repeatability, all EasySampler reactions were run using standard conditions resulting in an induction period due to time constraints on using the EasySampler equipment.

As we would expect, the highest rate is attained by the full reaction conditions (Figure 25), which suggests that every component of the reaction influences the rate. This is in contrast to previous research which indicated reaction order was only dependant on concentration of catalyst and aryl halide.<sup>25, 26</sup> Our results would suggest that the real reaction order is more complicated, as reduction in concentration of the base, aryl bromide, complex (defined as palladium precursor and ligand in this context) and both palladium and ligand all reduce reaction rate by 25-35% as observed by measuring the initial rate once the induction period was complete. This data indicates two possible explanations for each reaction component influencing the post induction period initial rate. We can rationalise that the actual rate determining step in this reaction includes a step where every component of the reaction is active in the mechanism, so oxidative addition and reductive elimination are ruled out as they do not include the base, as is the base coordination step in the base coordination mechanism for the same reason.

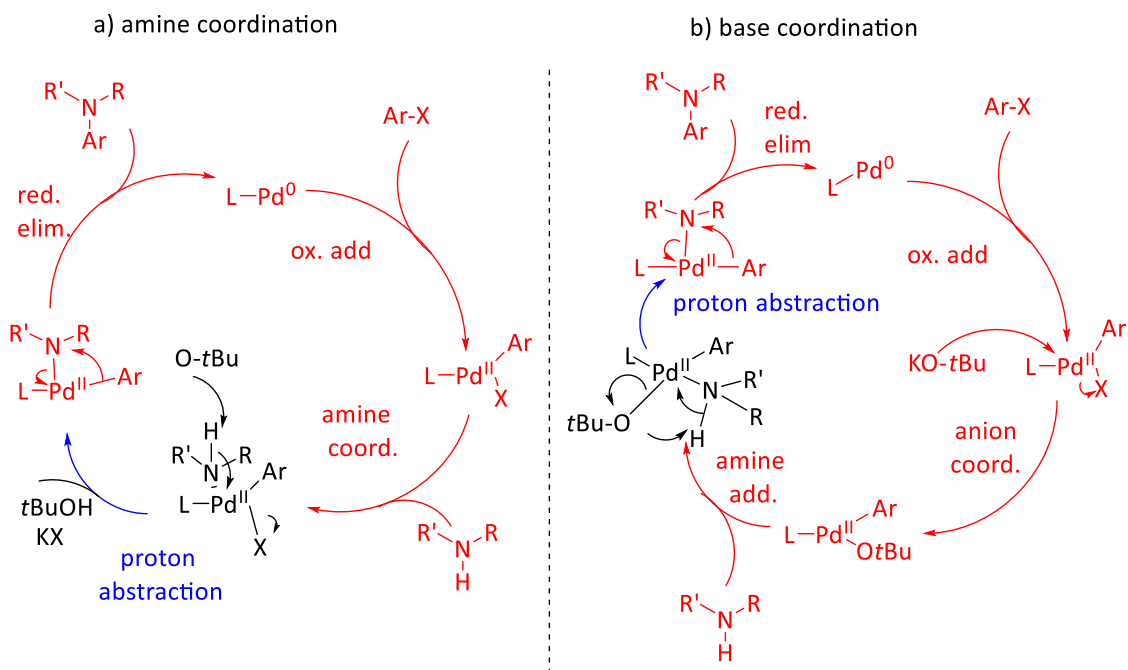


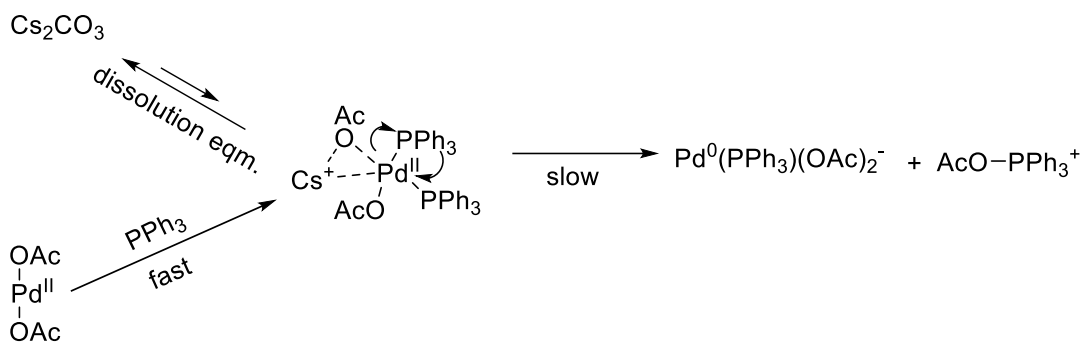
**Figure 41:** Proposed Buchwald-Hartwig mechanism indicating unlikely rate determining steps in red and viable rate determining steps in blue

Proton abstraction is not traditionally a rate limiting step as the deprotonation step is usually expected to be mechanistically fast. Reactions with rate limiting deprotonation are known however, and due to the low  $pK_b$  and low solubility of caesium bases in non-polar toluene solvent the proton abstraction step is likely to be rate limiting.<sup>27,28</sup> The external proton abstraction step in the amine coordination mechanism involves the

base anion abstracting the amine proton which can transfer electron density to the palladium atom and eliminate the halide. This contrasts with the base coordination mechanism internal proton abstraction step where the anion attacks the proton while bound to the palladium after anion coordination. Of the two mechanisms we would argue that the most likely mechanism when using caesium carbonate base in this system is the amine coordination pathway as the base, amine, complex and aryl halide are all active with regards to transfer of electron density.

We must also consider the presence of equilibria in the system. While the true rate determining step may well be proton abstraction, this is likely also influenced by the solubility equilibrium of both the base and catalyst, neither of which are fully soluble under the reaction conditions. It may well be due to the very low solubility of the base that forces the proton abstraction step to be rate determining, which would agree with results (Figure 40) that reduction in concentration of each reaction component results in a decrease in rate.

In addition to the reduction in rate when reducing concentrations of reaction components, we see an increase in the induction period from 30 minutes to 1 hour when reducing the concentration of the base and the complex (which involved reducing the palladium and ligand concentration by half). This result can be rationalised as reduced catalyst concentration decreases the rate of active catalyst formation and ligation due to lower probabilities of collision in solution making the equilibrium shift towards the individual catalyst components rather than the preformed complex. Due to the base also increasing the length of the induction period, it is likely that the base is required for formation of the active catalyst from the palladium acetate precursor. Reduced base concentration leads to longer ligation time which increases the induction period as it is then more difficult to reduce the palladium(II)  $\text{PdX}_2$  precursor to the  $\text{PdL}_2$  triphenylphosphine complex, via the square planar  $\text{PdX}_2\text{L}_2$  complex. To form this active  $\text{PdL}_2$  palladium(0) complex, the acetate must attack the triphenylphosphine ligand, forming a negatively charged palladium(0) triphenylphosphine species, along with a positively charged triphenylphosphine acetate species.<sup>29-31</sup> The reduction in concentration of caesium base results in less  $\text{Cs}^+$  in solution, which may reduce the stabilisation of the formation of the Pd(0) complex and speeding up the slow step of the catalyst formation (Scheme 35).

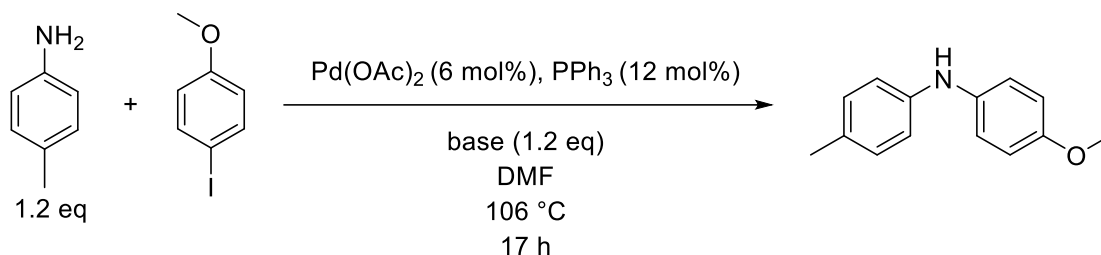


**Scheme 35:** Literature proposed mechanism for caesium cation stabilisation of Pd(0) formation influencing induction period observed in DFT calculations<sup>32</sup>

This kind of caesium cation stabilisation has been observed before by Musaev and co-workers, who found that the most likely reaction pathway for transmetallation involved a caesium cation cluster observed in DFT calculations.<sup>13</sup> While it may be difficult to observe these intermediates experimentally by isolation for crystal structure determination, the experimental results support the theory that the cation is active in speeding up the rate of formation of Pd(0) catalyst.

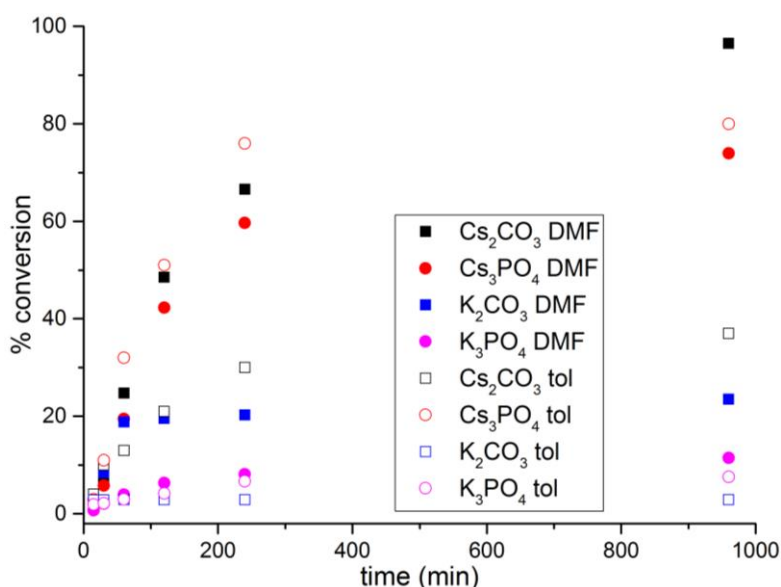
### **3.5 Effects of coordinating solvent on amination reaction rates and yields**

The polarity of a solvent can change many factors in a reaction, both immediately visible changes such as solubility, viscosity and mixing, as well as more subtle effects including coordination of substrates and catalyst. We found a large difference in rates and overall yield in toluene when changing base when using the aryl iodide (Scheme 36), so we would expect a similar change in reactivity when changing towards the more polar and more coordinating solvent DMF. Based on our work studying solubility by NMR *vide supra* we would expect much higher solubility for caesium phosphate than potassium phosphate, with the caesium base increasing in solubility from below 0.1 mM to 2.0 mM, and potassium phosphate reducing from 6.4 mM to <0.2 mM at room temperature relative to toluene solvent. Using this information we can deduce that [base] will be higher for caesium phosphate monohydrate than for potassium phosphate in DMF, so we would expect the induction period, if any, to be reduced due to increased base concentration. Additionally if the existing previous solubility hypotheses about the 'caesium effect' being largely related to increased solubility in dipolar aprotic solvents was to hold up, we would expect a large increase in reaction rate when using caesium bases in DMF over less soluble potassium bases (Scheme 36).



**Scheme 36:** Investigation into reaction performance using DMF solvent

**Figure 42:** Change in reaction performance of iodide leaving group amination reaction relative to solvent polarity



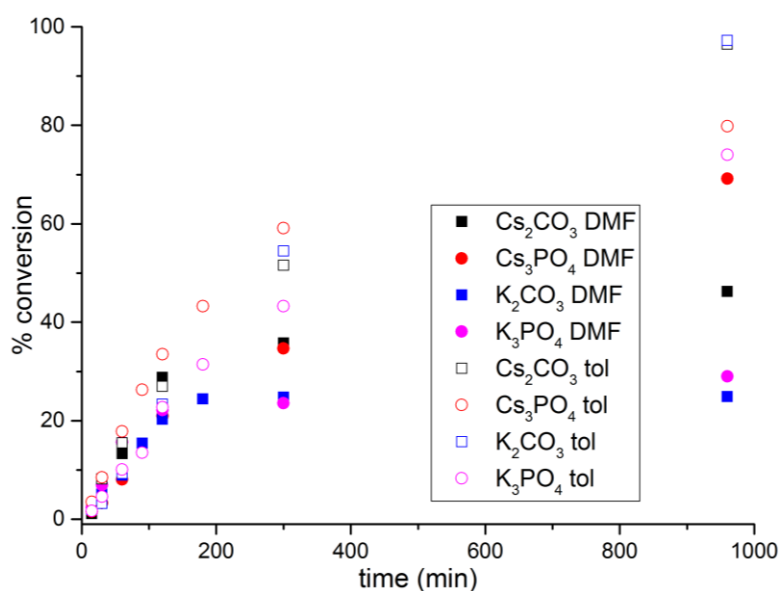
We can observe that in all cases the change in solvent affects the reaction performance relative to the base. In carbonate bases the reaction rate is improved dramatically, showing 96% conversion using caesium carbonate in DMF overnight compared to 38% in toluene. The converse is true using the phosphate anion, which suggests that the DMF solvent better facilitates the amine coordination mechanism and slows the base coordination mechanism favoured by the phosphates (Figure 33). The more nucleophilic phosphate anion can competitively coordinate to the palladium, and slow down the reaction, however the weaker carbonate anion does not have the coordinating power of the phosphate and does not slow the reaction rate (Figure 33).

DMF has been known to act as a coordinating ligand which can stabilise transition states and reduce activation energies in palladium-catalysed coupling reactions.<sup>33, 34</sup> In addition to this, the DMF ligated complex could push the monomer-dimer equilibrium of the catalyst towards the active monomer. The resting state of palladium catalysts

are usually in dimeric form, which can be observed in XRD measurements.<sup>35-37</sup> If the DMF coordination blocks an active site, this can prevent the dimer from forming and increasing reaction rate due to the increased relative concentration of the active monomeric catalyst.

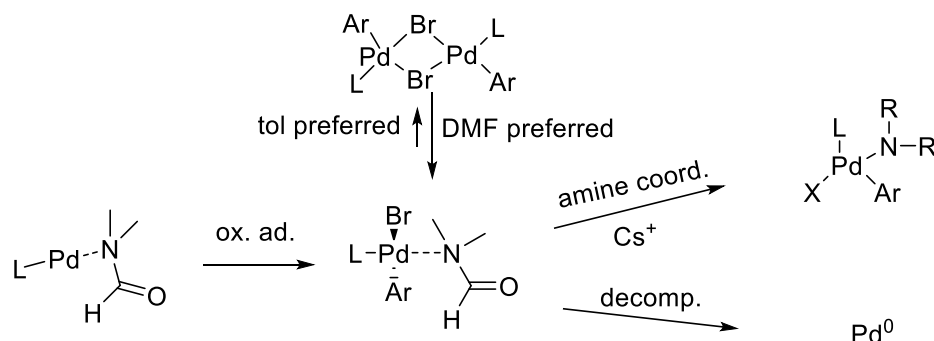
We elected to also run the reaction using the bromide leaving group in DMF solvent. When using toluene all bases gave similar initial rates, with potassium carbonate found to be the best base with 96% conversion overnight.

**Figure 43:** Change in reaction performance of bromide leaving group amination reaction relative to solvent polarity



The figure shows that in DMF solvent the bases have similar initial rates, which appears to reduce as the reaction time increases. As the initial rates are similar we would argue that similar to toluene, the M-Br interaction is similar between the two cations (Figure 32). Caesium phosphate monohydrate is more advantageous in this example as the reaction undergoes turnover for an extended period of time relative to the potassium bases, which points towards some kind of caesium cation stabilisation of the catalyst allowing to reach higher conversions than using potassium bases. In addition to this the conversions using DMF are lower than using toluene in all cases, which can be attributed to the active DMF ligated monomeric catalyst being more susceptible to decomposition than the dimeric catalyst possible using toluene. Hor *et al.* has shown that use of coordinating solvents can force palladium catalytic dimers to dissociate

more readily into the active monomer, so this may be occurring in the amination reaction using DMF to give a higher concentration of the catalytic monomer.<sup>33</sup>

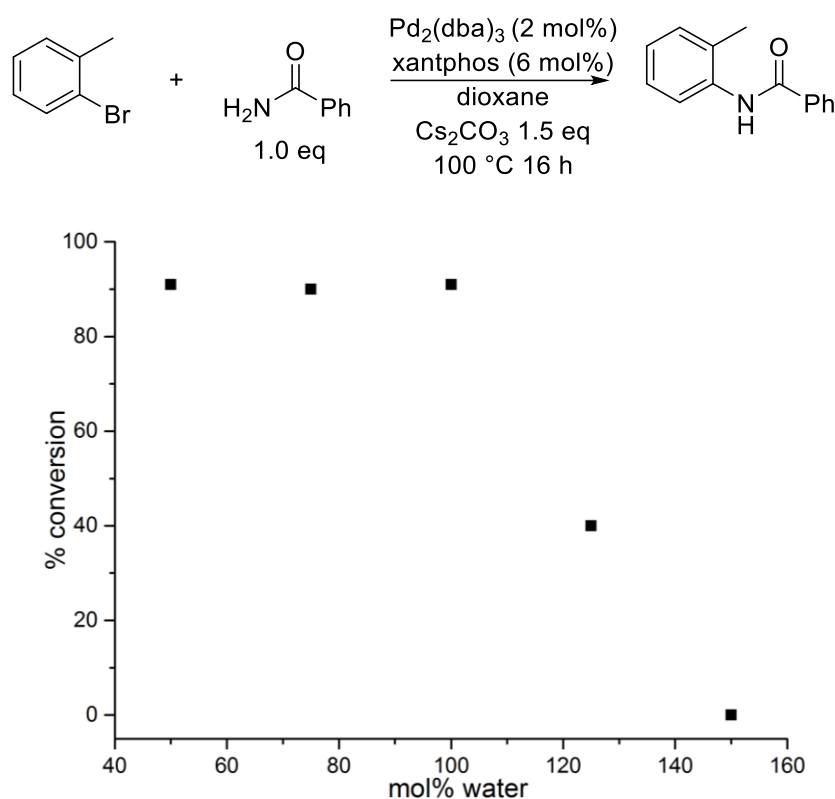


**Figure 44:** Figure showing plausible method of action enabling DMF solvent to increase [monomer], along with caesium cation reducing decomposition rate<sup>33</sup>

The oxidative addition step cleaving the C-Br bond is more challenging for the catalyst which may increase the amount of deactivation reactions, reducing yield over time compared to the toluene solvent where [monomer] remains lower which enables conversion over longer periods of time.

### 3.6 Investigation into catalyst stability due to water content of Cs<sub>3</sub>PO<sub>4</sub>·H<sub>2</sub>O

Due to the presence of water in the reaction using caesium phosphate monohydrate it is important to deduce whether this water will slow down the reaction relative to a non-hygroscopic dry base. Some Buchwald-Hartwig amination reactions have been shown to be inert towards up to 150 mol% of water with respect to the aryl halide. Dallas and Gothelf found that in the reaction of 2-bromotoluene with benzamide there was very little change in reaction yield on addition of below 1 equivalent of water.<sup>38</sup>

**Figure 45:** Buchwald-Hartwig amination reaction robust to 100 mol% water addition<sup>38</sup>

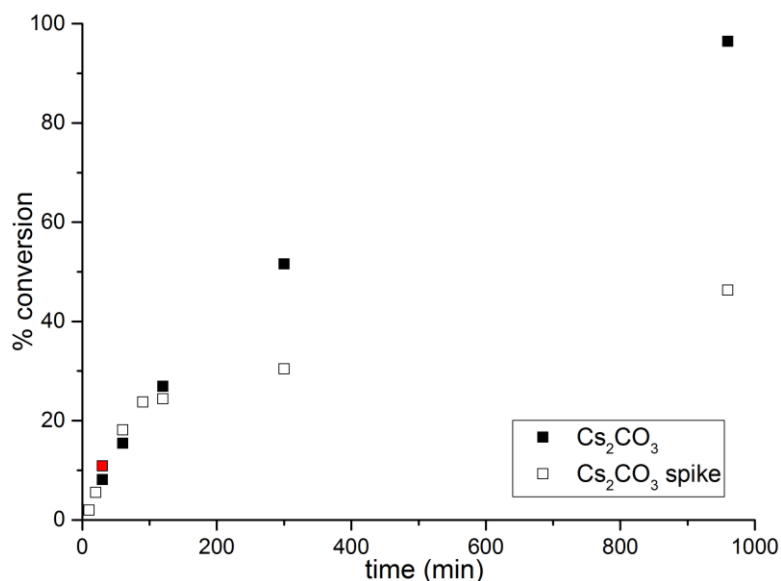
While the presence of water in the reaction flask will reduce catalytic turnover as [water] increases, the amount of water present in the reaction using caesium phosphate monohydrate is directly proportional to the equivalents of this base in the reaction. In the standard conditions of 1.5 equivalents base (Figure 45), as 150 mol% water, we would expect a decrease in reaction conversion relative to the dry conditions using caesium phosphate monohydrate, based on the literature reaction. Despite this, we observed caesium phosphate monohydrate to be the optimal base in toluene using the iodide leaving group, which would suggest that the reaction is not being slowed by addition of water content. Our hypothesis is that due to the low solubility of caesium phosphate monohydrate in toluene very little of the water content is able to dissociate in solution to oxidise the catalyst and prevent further catalytic turnover, which leads to higher conversions relative to direct water addition.

### **3.6.1 Water spiking experiments using non hygroscopic base**

To deduce whether the caesium phosphate monohydrate water content is likely to remain bound to the base rather than be free in solution in toluene solvent, we elected to run a water spiking experiment using less hygroscopic caesium carbonate base. We

ran the reaction under anhydrous conditions using the bromide leaving group, followed by a spike of 1.5 equivalents of water via direct syringe injection at 30 minutes which was equivalent to the total amount of water in the reaction flask present in caesium phosphate monohydrate.

**Figure 46:** Caesium carbonate spiking reaction in bromide leaving group with water spike shown in red at 30 minutes



This figure shows the anhydrous reaction and the water spiking reaction have similar reaction rates until the water spike after the sample at 30 minutes. The reaction rate does not appear to reduce until approximately 60 minutes where the conversion levels off somewhat, to give over 50% less conversion than the anhydrous reaction.

Despite these factors we can observe that after 1 hr of reaction time the rate decreases below the anhydrous conditions, so we have evidence that water does negatively affect reaction performance. As the reaction using caesium phosphate monohydrate base performs similarly to all other anhydrous bases in the bromide leaving group amination example this would suggest that water present in this base does not negatively affect the rate. This is likely due to the equilibrium of solubility causing very little base to be present in solution at any given time. Therefore very little water is solvated at any given time in the reaction, with the vast majority remaining bound to the insoluble base rather than free in solution where it is able to reduce reaction rate.

In this experiment the reduction in rate after addition of water to the reaction is observable, however additional conversion does appear to occur after the reaction rate

reduces at 60 minutes. The reason for the rate not reducing initially may be due to mass transfer effects of the small concentrations of both water and catalyst in the reaction. In addition, the reaction was run above the boiling point of water at 106 °C so condensation of water was possible on the side of the reaction flask which reduces effective concentration of water in solution.

The other possibility may be due to the palladium centre undergoing oxidation to palladium oxide or palladium hydroxide nanoparticles. Observations in the reaction were that after addition of the water the reaction colour changed from dark orange to dark brown, which may indicate formation of nanoparticles which were less reactive than the palladium complex but still able to turn over the reaction, albeit slowly. The palladium catalyst will decompose via a Pd-OH pathway, followed by further decomposition to the palladium nanoparticles. At this hydroxide stage it may be possible that the palladium can be reduced and regenerate the active species by forming the palladium(II) oxidative addition product Ar-Pd-X, and forming the phenol from the aryl bromide.

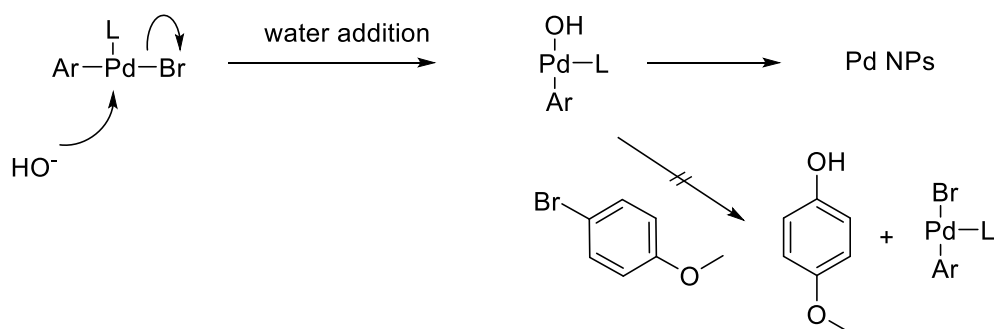


**Figure 47:** Disproven proposed palladium 'resurrection' reaction via halide exchange

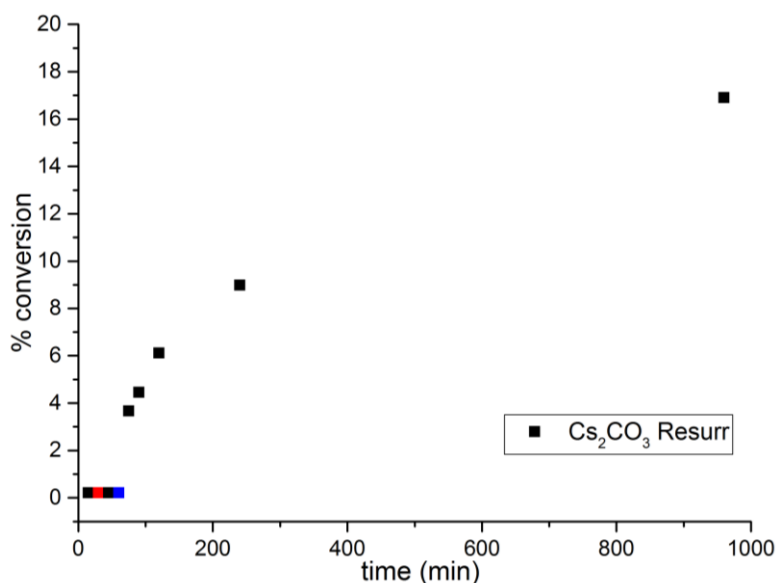
This resurrection reaction would occur slowly and explain the reduced reaction rate. We would expect to see quantities of the phenol by MS and NMR analysis when running the spiking reaction, which we did not observe under standard coupling conditions.

To probe the presence of the phenol after water spiking we ran the reaction without the aniline coupling partner, ensuring no reaction would take place and the catalyst would not be subject to any step after oxidative addition. No phenol was observed indicating the catalyst was not 'resurrected' to an active palladium species by the aryl halide and underwent decomposition to palladium nanoparticles. In this reaction the

addition of water promoted a change in colour from dark orange to black, providing more evidence of nanoparticle formation.

While ‘resurrection’, or reformation of the palladium catalyst was proposed to occur *via* the aryl halide, a catalyst reformation reaction facilitated by the basic aniline could also occur, providing a method to halt the reaction before decomposition into palladium nanoparticles and facilitate further reaction turnover. To probe this possibility we repeated the reaction without the aniline, spiking in water at 30 minutes with stirring. This changed the reaction colour from orange to brown, indicating palladium hydroxide had formed, followed by waiting for 30 further minutes for the palladium species to reach steady state. At this point 0.2 equivalents of aniline, 3.3 equivalents relative to the catalyst, was added to the flask under strong nitrogen flow.

**Figure 48:** Resurrection of oxidised palladium by aniline addition showing water spike (red) and aniline spike (blue)



We can observe that when the aniline was added, the reaction begins to turnover, gaining 17% conversion, equating to 85% of the total aniline addition. Using this data we can infer that the aniline itself effectively reduces the palladium hydroxide species and successfully facilitates additional turnover of the complex. This would also explain the presence of conversion after the water spiking experiment, as the reduction by aniline and oxidation by water would be in equilibrium, with some of the palladium undergoing further decomposition to nanoparticles which are likely to be much less active than the catalyst in this reaction.

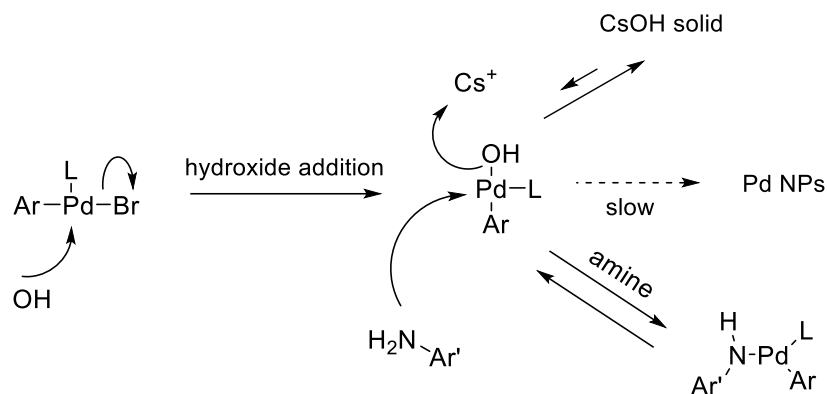


**Figure 49:** Plausible mechanism for palladium resurrection by aniline

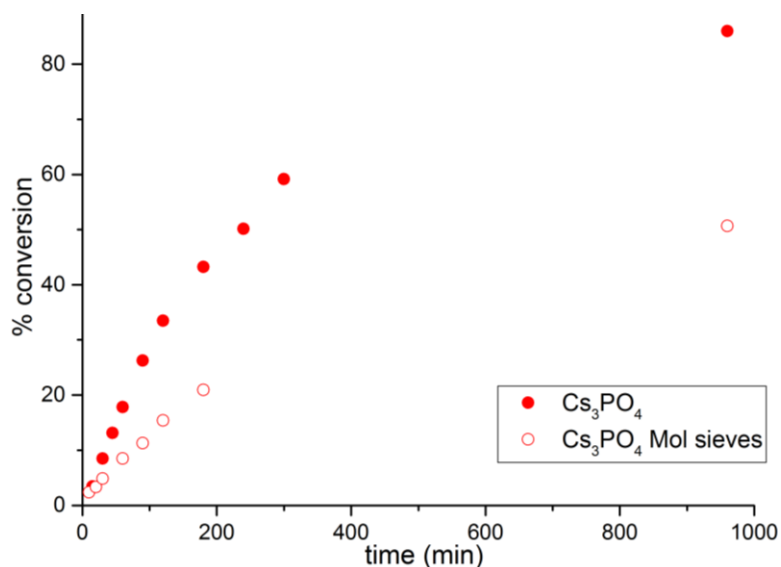
When the aniline is present in the reaction it is able to displace the inactive hydroxide and undergo the amine addition step of the mechanism which can then undergo the external deprotonation step. The hydroxide can attack the caesium cation to form  $\text{CsOH}$  which, due to the low solubility of caesium hydroxide in toluene, crystallises out to remove hydroxide anion from the reaction and allow for catalytic turnover.

### **3.6.2 Use of molecular sieves to reduce $[\text{H}_2\text{O}]$ in reaction**

To fully investigate how the water content present in caesium phosphate monohydrate affects reaction rate, we must deduce whether the reaction performs similarly to the other potassium and caesium bases. Either the water is not in solution and therefore not affecting the reaction rate, or the water does affect the rate but the increased performance of the caesium phosphate monohydrate base allows the rate to appear similar. This positive effect imparted by the caesium cation may be cancelling out negative effects imparted by the water content. To do this we identified molecular sieve addition of 5% w/v as a facile method to remove any residual water from the reaction. The sieves were activated via flame drying before addition to the reaction flask with other reagents including caesium phosphate monohydrate.

The bromide reaction was chosen for analysis with molecular sieves because reactions involving all studied bases displayed similar rates. We would expect that if the caesium phosphate monohydrate base was accelerating the reaction and the water decelerating the rate by a similar amount, the reaction including molecular sieves would result in a higher rate than the slower water affected reaction.

**Figure 50:** Bromoanisole reaction using molecular sieves, showing decreased performance on addition of drying agent



From our results we can observe that surprisingly, the molecular sieves actually decrease the reaction rate rather than increase it. This may be due to the sieves reducing mass transfer in the reaction. As both the base and the catalyst are not fully soluble in the reaction solvent, the rate of mixing in the reaction is important. Addition of molecular sieve beads increases the solution viscosity and interferes with the stirring rate, decreasing the rate of mass transfer in the reaction, which decreases the rate at which base and catalyst are drawn into solution and therefore decreases the reaction rate.

As the rate was lower with molecular sieves than without we argue that it is unlikely that the water present in caesium phosphate monohydrate was affecting the reaction in any significant way, and that for the water to dissociate from the base, the molecule must be significantly soluble.

### **3.7 NMR studies**

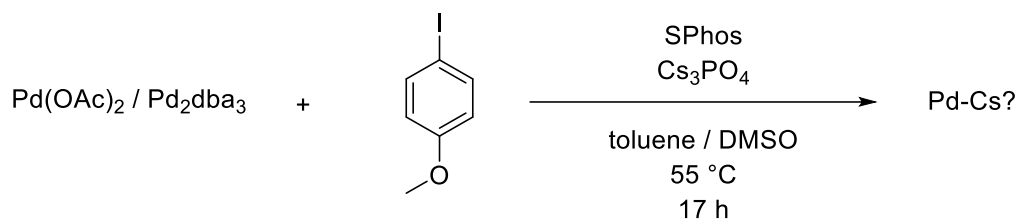
Based on the results gained in the initial iodide amination run (Figure 26) along with evidence that the base is involved in the rate determining step of the reaction (Figure 40) we elected to investigate the possibility of caesium involvement in the active catalyst species. DFT calculations had previously indicated caesium cation presence in the rate determining reaction step in catalytic reactions, however no experimental analysis, such as NMR or XRD has shown caesium cation involvement in catalytic

species in Buchwald-Hartwig amination reactions. We identified  $^{133}\text{Cs}$  and  $^{31}\text{P}$  NMR as a possible method of elucidating whether there was direct caesium cation involvement in the active catalyst, without having to crystallise the product. This is an especially useful method of analysis as the species does not have to be in solid state to gain experimental data. Palladium(II) catalysts are known to dimerise or enter a resting state when crystallised, making it difficult to know the active catalytic species by single crystal X-Ray diffraction.

Alternatively, high resolution mass spectrometry can be used to elucidate the structure of catalysts, though the weak strength of the proposed Pd-Cs bond is likely to break even under weak electrospray ionisation techniques, yielding the caesium cation and the palladium catalyst species separately. Based on this previous research the technique of heteronuclear NMR spectroscopy was chosen as the most likely analytical technique to result in evidence of caesium interaction with the active palladium catalyst.

Previous work *vide supra* had been conducted where addition of caesium carbonate to a copper iodide catalyst in the Ullman type C-O arylation of phenols produced an isolable Cu-I-Cs complex which was catalytically active. Despite the different properties of palladium and copper catalysts, the results of the amination reaction using iodide leaving groups had shown that caesium bases were much more effective than potassium bases under the reaction conditions. This suggests base involvement in the catalytic cycle allowing for faster initial reaction rates due to a reduction in the activation energy barrier using the caesium cation.

The general method to investigate this phenomenon involved stopping the reaction at a point in the catalytic cycle and attempting to probe the catalytic species present at that point in the cycle by NMR. While palladium does not possess an NMR active nucleus,  $^{31}\text{P}$  NMR can be used to investigate the behaviour of the palladium centre, as the region of 20-45 ppm is generally referred to as the ligated or palladium region for catalysts studied by phosphorus NMR. Therefore, once we have a figure for the ligated palladium species we can monitor the concentration of this and other species in the palladium region to deduce whether oxidative addition of the aryl halide or caesium adduction has occurred.



**Scheme 37:** General scheme of NMR measurements to follow caesium catalytic involvement

We elected to use  $\text{Pd}_2\text{dba}_3$  for some of the reactions as the  $\text{Pd(0)}$  reagent did not have to undergo reduction from  $\text{Pd(II)}$  to  $\text{Pd(0)}$  to become active. Without the presence of the reducing aniline reagent the active catalyst may not reduce to  $\text{Pd(0)}$  which can then allow oxidative addition of the aryl halide reforming  $\text{Pd(II)}$ . Therefore, a  $\text{Pd(0)}$  species is needed in cases where the aniline is not present. Additionally  $\text{DMSO-d}_6$  was used in certain cases to increase solubility of the base, as caesium phosphate solubility in toluene is minimal, whereas solubility in dipolar aprotic solvents has been shown to be as high as 6 mM. Additionally, the temperature of the reaction was reduced from 106 °C to 55 °C to reduce unwanted side reactions and decomposition of any catalytic species, as well as mimic the highest temperature the NMR experiments could be conducted at for an extended timescale without loss of data quality.

An issue with  $^{133}\text{Cs}$  NMR in solvents where complete ion dissociation occurs is that due to dissociation of the ions, the caesium atom behaves as  $\text{Cs}^+$  rather than the parent species, so only one peak is detected which can shift based on average chemical shifts of substances in equilibrium. In addition to this, the solubility of caesium species below saturation point can change the chemical shift relative to the standard, so to gain good data of  $^{133}\text{Cs}$  NMR reactions need to be conducted at the saturation point of that solvent.

In a reaction where caesium phosphate monohydrate was saturated in DMSO, followed by addition of the catalyst and other reagents we found a 5.1 ppm increase in chemical shift of the  $\text{Cs}^+$  cation above what can be attained at maximum solubility of the caesium species. This suggests that the caesium cation is more deshielded than when in a saturated DMSO solution, which suggests formation of a bond between the cation and another reagent. Based on previous data we can argue that it is likely that this increase in chemical shift is likely due to interaction with the palladium catalyst, as proposed by

DFT calculations in the literature *vide supra*. Due to the  $pK_a$ 's of the species involved, no deprotonation had occurred to change the  $Cs_3PO_4 \cdot H_2O$  to  $Cs_2HPO_4$  which would cause a change in chemical shift, so it is likely the caesium species had bound more formally to a reagent in the reaction.

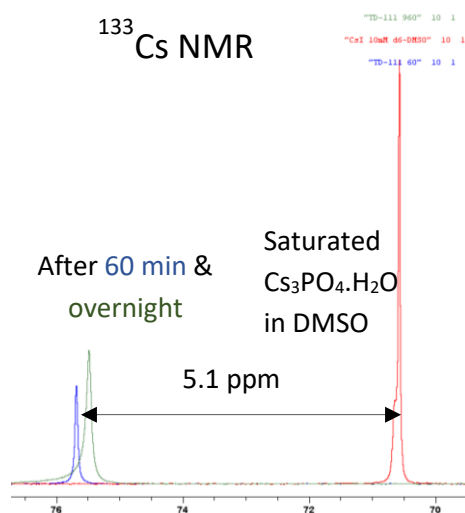


**Figure 51:** <sup>133</sup>Cs NMR showing the difference between Cs salt and Cs species in reaction

This reaction also yielded an interesting result in <sup>31</sup>P NMR whereby three unknown phosphorus environments were found, two of which appeared to be coupled together with a *coupling constant* of  $J = 395$  Hz, which would be expected if the phosphorus atoms were *trans* to the palladium centre by <sup>3</sup>J coupling.

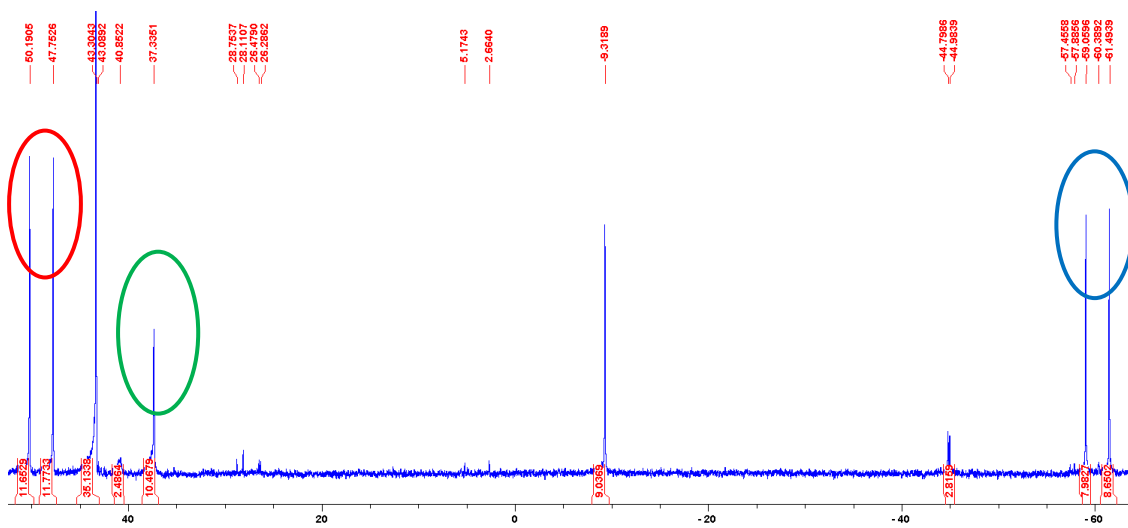


**Figure 52:** <sup>31</sup>P NMR spectra of assumed *trans* P-Pd-P species TD-136 A (green) and TD-136 B (red), with unknown (blue)

The known phosphorus species in this reaction were SPhos starting material at -9 ppm and PdSphos complex at 42 ppm. The three unknowns were peaks with doublets at -60 ppm and 49 ppm respectively with an additional singlet peak at 37 ppm. The NMR tube was then put in the freezer with hope of producing crystals suitable for X-Ray diffraction techniques to deduce the exact species responsible for these peaks. The first crystals found were orange and rectangular which were taken to XRD and solved to be PdSPhosdba.

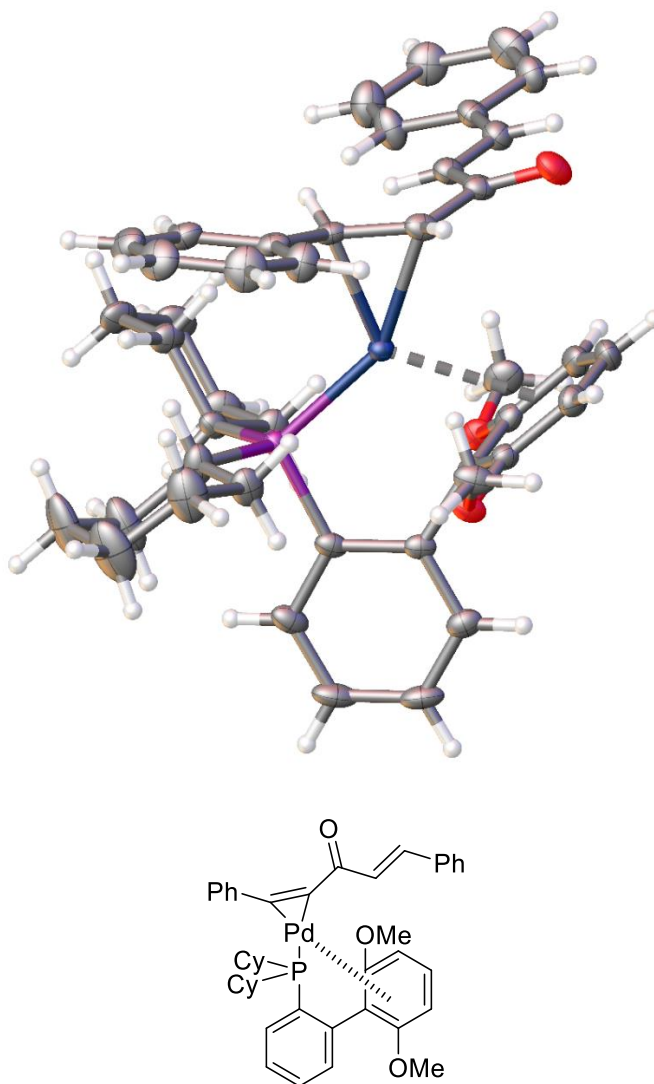


**Figure 53:** X-Ray diffraction structure (top) and representation (bottom) of TD-136 A (PdSPhosdba)

This structure is thought to correspond to the peak in  $^{31}\text{P}$  NMR at 37 ppm, as the environment is similar to PdSphos alone which occurs at 42 ppm with electron density taken away from the Pd atom by its bonds to the C=C carbon of the

dibenzylideneacetone compound, thus reducing the chemical shift to 37 ppm. This structure had not been previously observed in the Cambridge Structural Database (CSD), and represents a novel structure with both starting material and reaction ligands in one molecule.

In the NMR tube there were also some orange-red crystals which looked slightly different to the previous TD-136 A compound. These were also analysed by XRD to deduce the structure of this compound.

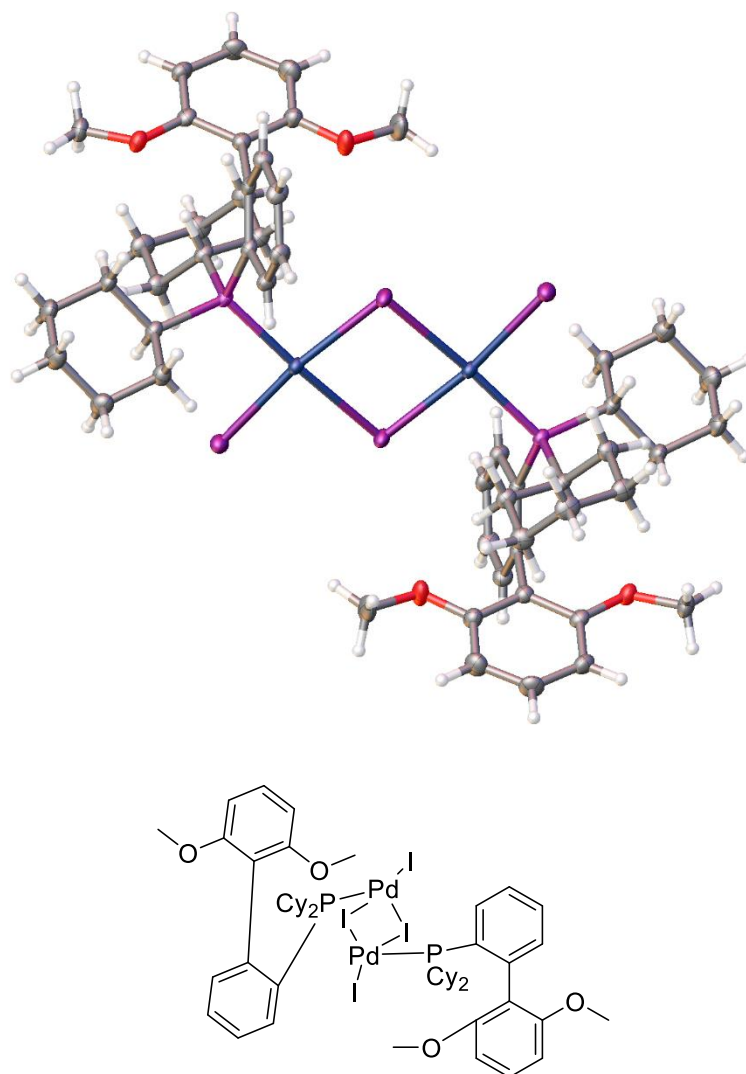


**Figure 54:** X-Ray diffraction structure (top) and representation (bottom) of TD-136 B

This structure agrees with one of the doublets in the <sup>31</sup>P NMR. It is likely that this corresponds to the more deshielded doublet at 49 ppm and the more shielded doublet at -60 ppm is more likely to be a conventional X-Pd-L oxidative addition product expected in these reactions. Numerous species of form X-Pd-L have been synthesised

by Buchwald and co-workers and characterised by XRD and NMR.<sup>39</sup> The phosphorus peaks can be split by both Pd and I which are 5/2 spin active nuclei to give the doublets as observed. The high coupling constant of up to 500 Hz is caused by the bridging palladium centre. *Trans* phosphorus ligands usually have a constant of approximately 500 Hz, whereas *cis* species are closer to 250 Hz.

In this example, not only do we see the relatively rare case of bridging iodines between the two palladium centres, but more surprisingly there is another iodine instead of the aryl group positioned *trans* to the palladium (Figure 54). This type of system is novel within the type of reaction as no elemental iodine or other iodine containing compounds were present to form this species aside from the aryl halide, which suggests homocoupling is possible. We propose that the caesium iodide formed from iodoanisole is able to exchange with the solvent molecule in the monomeric catalyst, which then encourages the anisole to dimerise with another oxidative addition product. The end product in this system is a twofold dimerization: of the anisole, giving 4-4'-dimethoxybiphenyl, and the isolated palladium dimerised catalyst species. The crystallised product may not itself be active with respect to the catalytic cycle, however it does require the oxidative addition product to form prior to dissociation of SPhos and dimerization to give the coupled catalyst. We can detect the Pd(SPhos)<sub>2</sub>Arl oxidative addition product by High Resolution Mass Spectrometry (HRMS) at 1159.14 m/z, so despite not forming crystals appropriate for XRD the formation is observed by mass spectrometry proving that the oxidative addition product does form before functionalisation and dimerization.

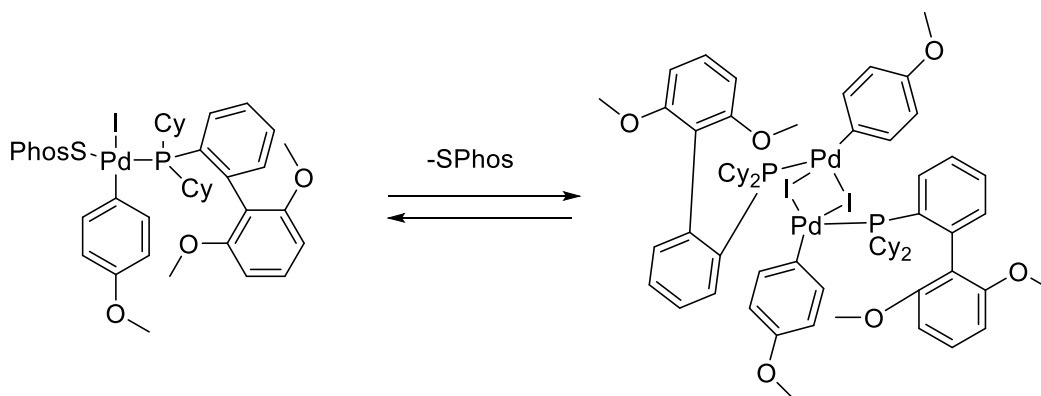


**Figure 55:** Expected oxidative addition product and dimer relationship

This product is likely to be the unknown doublet at -49 ppm in the  $^{31}\text{P}$  NMR (Figure 52), as the phosphorus ligands are arranged *trans* to the palladium centre, which can allow high coupling constants observed in the NMR measurements.

The proposed pathway is supported by evidence of the homocoupling product in  $^{13}\text{C}$  and  $^1\text{H}$  NMR, which suggests that if the catalyst is exposed to caesium in addition to absence of amine, the reactive species allows for dimerization of the anisole itself rather than cross coupling of the amine to the aryl halide.

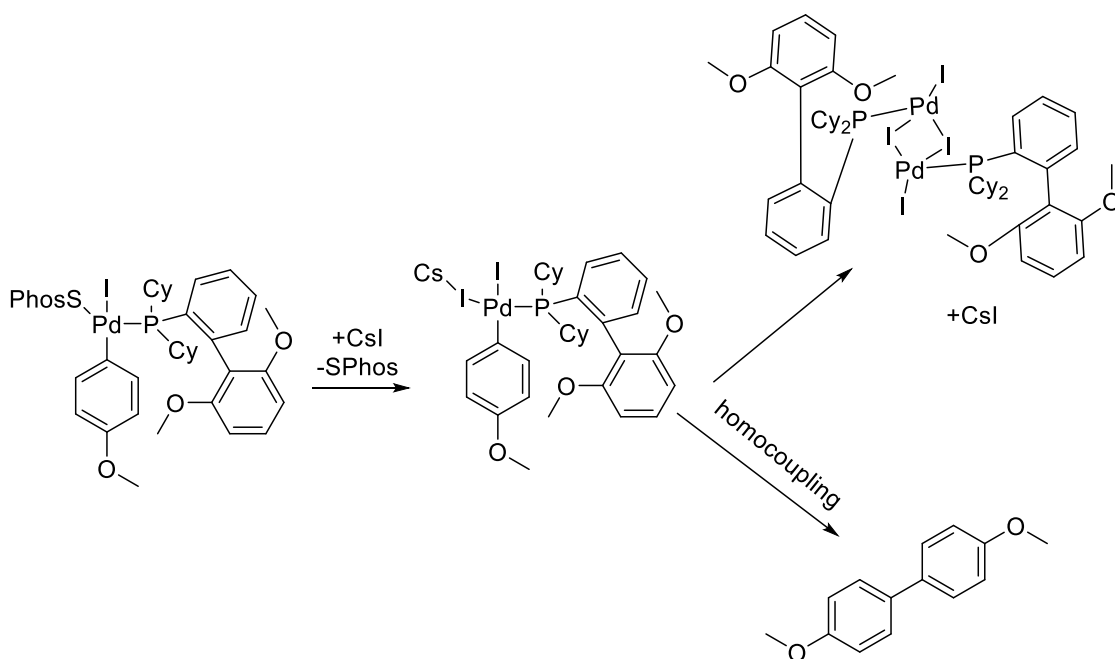


**Figure 56** Proposed homocoupling pathway to form dimerised catalyst TD-136 B species (Figure 53)

This Cs-I interaction provides some insight into the mechanism of action of increased performance of caesium bases using an iodide leaving group in these reactions. While we were unable to trap the caesium ion bonded directly to the catalyst species, the X-Ray diffraction and NMR analysis, along with the lack of any evidence of homocoupling without caesium present, suggests that for the dimerization to occur the caesium cation is needed. From this secondary evidence of a palladium-caesium bonded species, we can begin to paint a picture of how the activation energy in these amination reactions can be reduced by caesium addition to the catalyst, and that the most likely reasoning behind increased performance of amination reactions using caesium bases is due to caesium itself binding to an open active site on the catalyst and reducing the energy of the rate limiting transition state in Buchwald-Hartwig amination reactions.

### **3.8 Conclusions & future work**

Buchwald-Hartwig amination reactions are relatively unique palladium-catalysed coupling reactions as they are the only common class of catalytic reactions with an expected rate limiting step involving the base (Figure 27).<sup>6</sup> Caesium phosphate monohydrate was incorporated into a base screen for the synthesis of 4-tolyl-*p*-anisidine (Figure 25), and was found to be the optimal weak base in a reaction involving the labile aryl iodide (Figure 26). The caesium cation was superior both in initial rate and overall conversion using the iodide, which is expected to be due to caesium destabilisation of the Pd-I bond due to soft-soft interactions (Figure 28). This then suggests that the amine coordination mechanism is preferred in this reaction example as the external proton abstraction step is rate limiting.

When the less labile aryl bromide was used, there did not appear to be as great a difference between the bases (Figure 30). This points to an internal proton abstraction rate limiting step and base coordination mechanism due to the cation not having a large effect on the initial rate, or an external proton abstraction step where the caesium and potassium destabilisation of the Pd-Br bond are similar, due to similar formation enthalpies of CsBr and KBr.

Conversions were reduced using the aryl chloride reagent, as the strength of the C-Cl bond is higher than using the softer halides (Table 13). We saw an increase in conversion using potassium bases in this reaction, which suggests that the amine coordination mechanism remains favoured, and that the halide has a more favourable interaction with the potassium cation than caesium.

Reactions were conducted using a Mettler Toledo EasySampler apparatus to assess which reagents were present in the rate limiting step of the reaction (Scheme 34). We found that when reducing any reaction component concentration, the rate would decrease relative to the full reaction conditions. We can deduce from this that the aryl halide, amine coupling partner, catalyst, and base are all present in the rate limiting step which narrows the possibility for this step to the internal or external proton abstraction step, which would agree with previous literature (Figure 41).<sup>27, 28</sup>

A water spiking reaction was conducted to test if the water in caesium phosphate monohydrate would cause a significant change in reaction performance. Caesium

carbonate was spiked with 1.5 equivalents of water to replicate the maximum amount of water present in the reaction using caesium phosphate monohydrate, and a significant drop in conversion occurred after addition of water (Figure 46). Based on this reaction it is likely that the water in caesium phosphate monohydrate either remains bound to the base in solution, or the solubility of the base is so low at any time that the amount of water present in solution is insignificant.

$^{31}\text{P}$  and  $^{133}\text{Cs}$  NMR studies were conducted to elucidate possible catalytic intermediates which require caesium to form. Two unknown species were observed in  $^{31}\text{P}$  NMR, one of which appeared to relate to a change in  $^{133}\text{Cs}$  NMR (Figure 52). The NMR tubes were placed in the freezer to encourage crystal growth and a novel iodine bridging palladium complex was found in XRD measurements (Figure 54). While this species did not contain the caesium atom bound to the complex, it appears to require the presence of CsI to form, and therefore provides evidence that caesium cation interaction can occur directly on the palladium centre in catalysis.

Work on the Buchwald-Hartwig amination reaction has shown that the most likely rate limiting step is the external proton abstraction of the amine coordination mechanism. This is highly important for chemists who conduct these reactions as the base cation ion pairing plays a large factor in overall reaction rate and yield. Caesium phosphate can be utilised in reactions involving aryl iodide as the optimal base to gain increased yields over other alkali metal bases. Conversely the results found in this project show that when aryl bromides and chlorides are used, changes in the base cation to pair the halide leaving group will allow for increased conversions in research chemistry.

Future work could be carried out to elucidate whether the use of sodium carbonate and phosphate would be a useful way to further understand how bond destabilisation caused by cation interaction in solution changes the reaction based on formation of the salt by-product. In addition to this, using an activated secondary amine as a coupling partner would provide insight into how steric interactions can change the reaction, as the bulk of the basic anion may then change the rate of external proton abstraction and therefore overall yield.

Previous computational work had indicated that involving the caesium cation in the transition state of C-H arylation reactions would lower the activation energy barrier

and therefore increase reaction rate.<sup>13, 15</sup> Future work on this project would benefit from DFT calculations assessing the optimal pathway of the rate limiting proton abstraction step, and how cation interaction with the aryl halide occurs at transition state.

Coordinating solvent DMF has been shown to favour more reactive catalytic monomers due to its ability to bind to a vacant coordination site on the palladium before coordination of a reagent, so future work should assess whether the oxidative addition product in toluene and DMF solvents would favour the catalytic monomer or dimer and therefore possibly change catalyst reactivity. X-Ray diffraction analysis and XAS would be the ideal way to gain insight into these structures and elucidate either the defined catalyst structure or an important catalyst resting state.

### **3.9 Experimental procedures**

Unless otherwise noted, all materials were obtained from commercial suppliers and used as received. Cs<sub>2</sub>CO<sub>3</sub>, K<sub>2</sub>CO<sub>3</sub> and K<sub>3</sub>PO<sub>4</sub> were oven dried at 100 °C overnight before use. Unless otherwise noted, all reactions were performed under an atmosphere of N<sub>2</sub> gas using standard vacuum-line techniques. All work-up and purification procedures were carried out with reagent-grade solvents in air. Column chromatography was carried out on prepacked flash columns on a Biotage purification unit. <sup>1</sup>H NMR spectra were recorded in CDCl<sub>3</sub> (TMS, no IS integration) at 300 or 500 MHz on Bruker Avance spectrometers. All chemical shift values are reported in ppm (δ). <sup>1</sup>H and <sup>13</sup>C NMR assignments were aided by COSY, DEPT and HMBC NMR. NMR assignments were made in order of decreasing chemical shift of <sup>13</sup>C nuclei. Gas chromatography was conducted on Hewlett Packard HP 6890 Gas Chromatography apparatus, equipped with HP-5 chromatography columns (mobile phase: H<sub>2</sub>, column length 30 m, film thickness 0.25 μm, injection volume 1.0 μL, split ratio 100:1, split flow 71.5 ml/min.) For kinetic experiments unless otherwise stated 50 μL sample taken via syringe after inerting and quenched into 1 mL acetonitrile at room temperature.

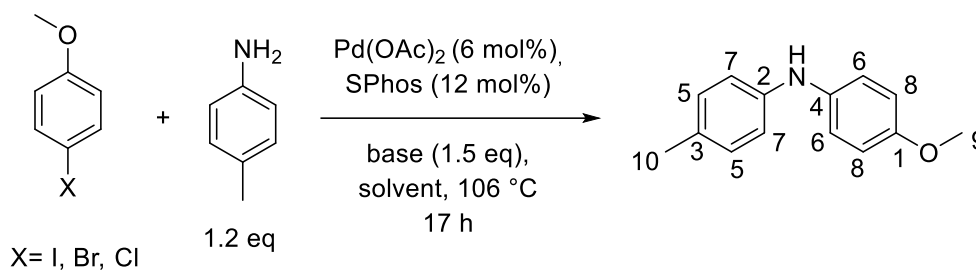
#### **Standard sampling protocol**

The reaction stirring was stopped for ~5 seconds to encourage solids to settle at the bottom of the Schlenk flask. An oven dried needle attached to a luer lock syringe was purged by drawing up 1 mL of nitrogen atmosphere from the reaction and dispensing

it to atmosphere and repeating 5 times. 50  $\mu\text{L}$  of reaction mixture was drawn into the syringe and diluted in 1 mL acetonitrile in a GC vial. The vial was left open to atmosphere to ensure no additional conversion would take place and the vial ran on GC without further purification. Conversion was analysed via GC (50  $^{\circ}\text{C}$  hold for 1 minute, ramp 20  $^{\circ}\text{C}/\text{min}$  to 300  $^{\circ}\text{C}$ , hold for 5 minutes.)

### **Synthesis and characterisation of reaction products**

#### **General procedure for 4-methoxy-*N*-(4-methylphenyl)aniline**<sup>8</sup>

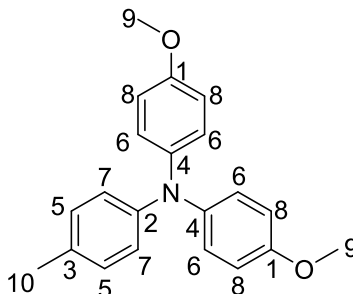


An oven dried Schlenk tube was charged with 4-haloanisole (0.75 mmol, 1.0 equivalents), *p*-toluidine (97 mg, 0.9 mmol, 1.2 equivalents), base (1.125 mmol, 1.5 equivalents), palladium(II) acetate (10.1 mg, 0.045 mmol 6 mol%) and SPhos (37 mg, 0.09 mmol, 12 mol%), followed by addition of degassed solvent (6 mL). The vessel was sealed and heated to 106  $^{\circ}\text{C}$  for 17 h and sampled according to the general method. The mixture was allowed to cool to room temperature and the crude extracted in DCM (3 x 20 mL) before filtering through celite and silica gel to give crude 4-methoxy-*N*-(4-methylphenyl)aniline as a light brown solid which was eluted in a silica column (3:1 petroleum ether 40-60  $^{\circ}\text{C}$  / ethyl acetate) and evaporated to give purified product as an off white solid giving 68% conversion using  $\text{Cs}_2\text{CO}_3$  as base. Conversions analysed using NMR and calibrated GC.  $^1\text{H}$  NMR (500 MHz, acetone- $d_6$ )  $\delta$  7.01 (d,  $J_{6,8} = 8.9$  Hz, 2H, H-6), 6.96 (d,  $J_{5,7} = 8.1$  Hz, 2H, H-5), 6.85 (d,  $J_{7,5} = 8.3$  Hz, 2H, H-7), 6.81 (d,  $J_{8,6} = 8.9$  Hz, 2H, H-8), 3.71 (s, 3H, H-9), 2.18 (s, 3H, H-10);  $^1\text{H}$  NMR (500 MHz,  $\text{CDCl}_3$ )  $\delta$  7.03 (m, 4H, H-5,6), 6.84 (m, 4H H-7,8), 5.39 (s, 1H, NH), 3.79 (s, 3H, H-9), 2.17 (s, 3H, H-10);  $^{13}\text{C}$  NMR (125 MHz,  $\text{CDCl}_3$ )  $\delta$  154.9 (C-1), 142.4 (C-2), 136.7 (C-3), 129.9 (C-4), 129.4 (C-5), 121.2 (C-6), 116.7 (C-7), 114.7 (C-8), 55.6 (C-9), 20.6 (C-10); m.p. 77 – 80  $^{\circ}\text{C}$ ; HRMS ESI<sup>+</sup>: 214.1217 [M + H]<sup>+</sup> Calculated value for  $\text{C}_{14}\text{H}_{16}\text{NO}^+$  214.1220.

Literature data:<sup>8, 40</sup>  $^1\text{H}$  NMR (400 MHz,  $\text{CDCl}_3$ )  $\delta$  7.05 (d,  $J = 8.6$  Hz, 2H), 6.99 (d,  $J = 8.3$  Hz, 2H), 6.89 (d,  $J = 8.3$  Hz, 2H), 6.83-6.86 (m, 2H), 5.62 (s, 1H), 3.74 (s, 3H), 2.21 (s, 3H);

$^{13}\text{C}$  NMR (125 MHz,  $\text{CDCl}_3$ )  $\delta$  154.8, 142.4, 136.6, 129.8, 129.3, 121.1, 116.5, 114.6, 55.6, 20.6; m.p. 79 – 80 °C.

#### 4,4'-Dimethoxy-4''-methyltriphenylamine



$^1\text{H}$  NMR (500 MHz,  $\text{CDCl}_3$ )  $\delta$  6.96-6.98 (m, 6H, H-5,6), 6.83-6.87 (m, 2H H-7), 6.78 (d,  $J_{8,6}$  = 8.9 Hz, 4H, H-8), 3.77 (s, 6H, H-9), 2.24 (s, 3H, H-10);  $^{13}\text{C}$  NMR (125 MHz,  $\text{CDCl}_3$ )  $\delta$  157.8 (C-1), 136.7 (C-2), 130.5 (C-3), 129.2 (C-4), 126.3 (C-5), 116.1 (C-6), 114.0 (C-7), 55.6 (C-8), 30.9 (C-9), 24.7 (C-10); HRMS: 320.1634  $[\text{M} + \text{H}]^+$  Calculated value for  $\text{C}_{21}\text{H}_{22}\text{NO}_2^+$ : 320.1640.

Literature data:<sup>1</sup>  $^1\text{H}$  NMR (300 MHz,  $\text{CDCl}_3$ )  $\delta$  6.98-7.00 (m, 6H), 6.87 (d,  $J$  = 8.2 Hz, 2H), 6.78 (d,  $J$  = 8.9 Hz, 4H), 3.76 (s, 6H), 2.26 (s, 3H).

#### Crown ether complexation in reactions to form 4-methoxy-*N*-(4-methylphenyl)aniline

The reaction was run according to the general procedure, with 18-crown-6 (297 mg, 1.125 mmol, 1.125 equivalents) added to the reaction before addition of degassed toluene solvent (6 mL). The reaction was sampled according to the general method, with 8% representative conversion using  $\text{K}_3\text{PO}_4$  as the base.

#### General procedure for EasySampler reactions

Full reaction conditions: An oven dried round bottom flask was charged with  $\text{PdOAc}_2$  (20.2 mg, 0.09 mmol, 6 mol%), SPhos (74 mg, 0.18 mmol, 12 mol%), *p*-toluidine (194 mg, 1.8 mmol, 1.2 equivalents), caesium carbonate (2.25 mmol, 1.5 equivalents) and 4-bromoanisole (182  $\mu\text{L}$ , 1.5 mmol, 1.0 equivalent). This was followed by addition of dry degassed toluene (12 mL) spiked with *p*-xylene (0.05 M). Reaction conditions involving reduced concentration of reagents half the equivalents above. The vessel was sealed and the autosampler arm attached, with heating and stirring to 106 °C for 17 hr. The reaction was sampled via the robot at regular intervals to quenched GC vials

containing 0.1M acetic acid in acetonitrile for GC analysis. The mixture was allowed to cool to room temperature and the crude extracted in DCM (3 x 20 mL) before filtering through silica to give crude product, which was eluted on a biotage purification system (15-35% ethyl acetate – petroleum ether) and evaporated to give purified product. Conversions determined by  $^1\text{H}$  NMR and calibrated GC.

#### General procedure for water spiking experiments

The reaction was run according to the general procedure for 4-tolyl-*p*-anisidine using caesium carbonate base and 4-bromoanisole in toluene solvent. The reaction was sampled according to the general sampling protocol. Water was added (21  $\mu\text{L}$ , 1.17 mmol, 1.56 eq) via microsyringe after the reaction time had reached 30 min. Conversion 42% by GC. Reaction was not purified.

#### General procedure for 'resurrection' experiments

The reaction was run according to the general procedure for 4-tolyl-*p*-anisidine using caesium carbonate base and 4-bromoanisole in toluene solvent, without addition of *p*-toluidine. The reaction was sampled according to the general sampling protocol. Water (21  $\mu\text{L}$ , 1.17 mmol, 1.56 eq) was added via microsyringe after the reaction time had reached 30 min. *p*-Toluidine (17 mg, 0.16 mmol, 0.2 equivalents) was added when the reaction time had reached 60 minutes. Conversion 17% by GC. Reaction was not purified.

#### General procedure for reactions involving molecular sieves

The reaction was run according to the general procedure for 4-tolyl-*p*-anisidine using caesium phosphate monohydrate base and 4-bromoanisole in toluene solvent. Activated 4Å molecular sieves (300 mg, 5% w/v) were added before addition of solvent and the reaction sampled according to the general sampling protocol. Conversion 48% by GC. Reaction was not purified.

#### General procedure for $^{133}\text{Cs}$ and $^{31}\text{P}$ NMR experiments

Palladium source (0.09 mmol, 1.0 equivalent), SPhos (72 mg, 0.18 mmol, 2.0 equivalents) and degassed deuterated solvent (2 mL) were added to an oven dried Schlenk tube under inert gas. The reaction was heated to 55 °C for 30 minutes before addition of caesium phosphate monohydrate (100 mg, 0.2 mmol, 2.0 equivalents). The

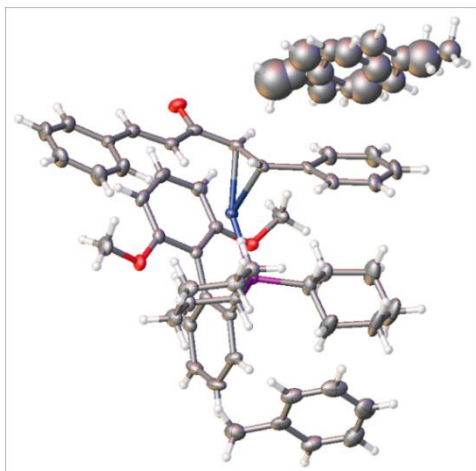
reaction stirred at 55 °C for a further 30 minutes before an aliquot (0.4 mL) of the reaction was syringed into an oven dried NMR tube under inert gas and sealed for NMR study of  $^1\text{H}$ ,  $^{31}\text{P}$  and  $^{133}\text{Cs}$  nuclei at room temperature. The main reaction was then left to stir, with addition of 4-iodoanisole (42 mg, 0.2 mmol, 2.0 equivalents) was added under strong flow of inert gas and the reaction stirred for 30 minutes. A further aliquot (0.4 mL) of the reaction was syringed into an oven dried NMR tube under inert gas and sealed for NMR study of  $^1\text{H}$ ,  $^{31}\text{P}$  and  $^{133}\text{Cs}$  nuclei at room temperature. After analysis the NMR tubes were sealed with parafilm and left in the freezer for 3 days to encourage crystal formation suitable for single crystal XRD.

### **3.10 References**

1. L. Cai, X. Qian, W. Song, T. Liu, X. Tao, W. Li and X. Xie, *Tetrahedron*, 2014, **70**, 4754-4759.
2. C. Meyers, B. U. W. Maes, K. T. J. Loones, G. Bal, G. L. F. Lemièrè and R. A. Dommissè, *J. Org. Chem.*, 2004, **69**, 6010-6017.
3. F. Bonnaterre, M. Bois-Choussy and J. Zhu, *Org. Lett.*, 2006, **8**, 4351-4354.
4. M. Wolter, A. Klapars and S. L. Buchwald, *Org. Lett.*, 2001, **3**, 3803-3805.
5. Y. Sunesson, E. Limé, S. O. Nilsson Lill, R. E. Meadows and P.-O. Norrby, *J. Org. Chem.*, 2014, **79**, 11961-11969.
6. F. Wang, L. Zhu, Y. Zhou, X. Bao and H. F. Schaefer, *Chem. - Eur. J.*, 2015, **21**, 4153-4161.
7. K. H. Hoi, S. Çalimsiz, R. D. J. Froese, A. C. Hopkinson and M. G. Organ, *Chem. – Eur. J.*, 2011, **17**, 3086-3090.
8. R. Hesse, A. W. Schmidt and H.-J. Knoelker, *Tetrahedron*, 2015, **71**, 3485-3490.
9. J. A. Cella and S. W. Bacon, *J. Org. Chem.*, 1984, **49**, 1122-1125.
10. J. Zhang, J. Chen, M. Liu, X. Zheng, J. Ding and H. Wu, *Green Chem.*, 2012, **14**, 912-916.
11. D. N. Bhattacharyya, C. L. Lee, J. Smid and M. Szwarc, *J. Phys. Chem.*, 1965, **69**, 612-623.
12. R. N. Salvatore, A. S. Nagle, S. E. Schmidt and K. W. Jung, *Org. Lett.*, 1999, **1**, 1893-1896.
13. T. M. Figg, M. Wasa, J.-Q. Yu and D. G. Musaev, *J. Am. Chem. Soc.*, 2013, **135**, 14206-14214.

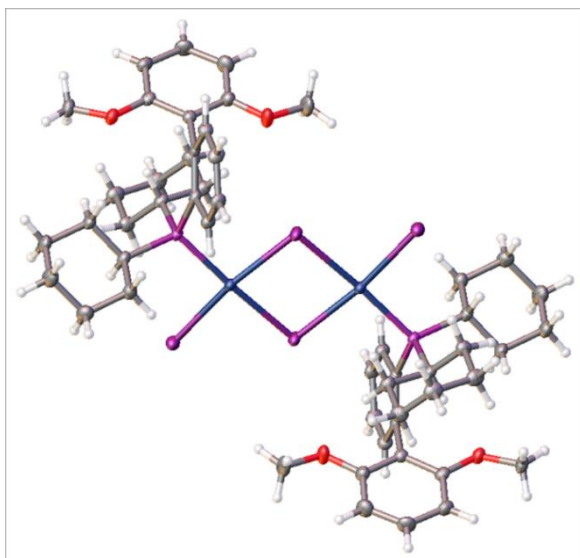
14. C. Liu, Y. Luo, W. Zhang, J. Qu and X. Lu, *Organometallics*, 2014, **33**, 2984-2989.
15. D. G. Musaev, T. M. Figg and A. L. Kaledin, *Chem. Soc. Rev.*, 2014, **43**, 5009-5031.
16. R. G. Pearson, *Coord. Chem. Rev.*, 1990, **100**, 403-425.
17. S. J. Blanksby and G. B. Ellison, *Acc. Chem. Res.*, 2003, **36**, 255-263.
18. B. R. Kim, S.-D. Cho, E. J. Kim, I.-H. Lee, G. H. Sung, J.-J. Kim, S.-G. Lee and Y.-J. Yoon, *Tetrahedron*, 2012, **68**, 287-293.
19. U. Scholz and B. Schlummer, *Tetrahedron*, 2005, **61**, 6379-6385.
20. C. M. Goff, M. A. Matchette, N. Shabestary and S. Khazaeli, *Polyhedron*, 1996, **15**, 3897-3903.
21. C. L. Liotta and H. P. Harris, *J. Am. Chem. Soc.*, 1974, **96**, 2250-2252.
22. A.-N. Francoise and S. Chaves, *Pure Appl. Chem.*, 2003, **75**, 71-102.
23. N. R. Council, *Prudent Practices in the Laboratory: Handling and Management of Chemical Hazards, Updated Version*, The National Academies Press, Washington, DC, 2011.
24. D. B. G. Williams and M. Lawton, *J. Org. Chem.*, 2010, **75**, 8351-8354.
25. B. P. Fors and S. L. Buchwald, *J. Am. Chem. Soc.*, 2010, **132**, 15914-15917.
26. M. G. Organ, M. Abdel-Hadi, S. Avola, I. Dubovyk, N. Hadei, E. A. B. Kantchev, C. J. O'Brien, M. Sayah and C. Valente, *Chem. – Eur. J.*, 2008, **14**, 2443-2452.
27. M. J. Schultz, R. S. Adler, W. Zierkiewicz, T. Privalov and M. S. Sigman, *J. Am. Chem. Soc.*, 2005, **127**, 8499-8507.
28. J. A. Mueller, D. R. Jensen and M. S. Sigman, *J. Am. Chem. Soc.*, 2002, **124**, 8202-8203.
29. S. Shekhar, P. Ryberg, J. F. Hartwig, J. S. Mathew, D. G. Blackmond, E. R. Strieter and S. L. Buchwald, *J. Am. Chem. Soc.*, 2006, **128**, 3584-3591.
30. C. Amatore, E. Carre, A. Jutand and M. A. M'Barki, *Organometallics*, 1995, **14**, 1818-1826.
31. C. C. C. Johansson Seechurn, T. Sperger, T. G. Scrase, F. Schoenebeck and T. J. Colacot, *J. Am. Chem. Soc.*, 2017, **139**, 5194-5200.
32. P. R. Melvin, D. Balcells, N. Hazari and A. Nova, *ACS Catalysis*, 2015, **5**, 5596-5606.
33. S. K. Yen, L. L. Koh, H. V. Huynh and T. S. A. Hor, *Aust. J. Chem.*, 2009, **62**, 1047-1053.

34. B. Vaz, R. Pereira, M. Pérez, R. Álvarez and A. R. de Lera, *J. Org. Chem.*, 2008, **73**, 6534-6541.
35. C. M. So, C. P. Lau and F. Y. Kwong, *Angew. Chem. Int. Ed.*, 2008, **47**, 8059-8063.
36. R. B. Bedford, C. S. J. Cazin, S. J. Coles, T. Gelbrich, P. N. Horton, M. B. Hursthouse and M. E. Light, *Organometallics*, 2003, **22**, 987-999.
37. K. O. Kirlikovali, E. Cho, T. J. Downard, L. Grigoryan, Z. Han, S. Hong, D. Jung, J. C. Quintana, V. Reynoso, S. Ro, Y. Shen, K. Swartz, E. Ter Sahakyan, A. I. Wixtrom, B. Yoshida, A. L. Rheingold and A. M. Spokoyny, *Dalton Trans.*, 2018, **47**, 3684-3688.
38. A. S. Dallas and K. V. Gothelf, *J. Org. Chem.*, 2005, **70**, 3321-3323.
39. M. R. Biscoe, T. E. Barder and S. L. Buchwald, *Angew. Chem. Int. Ed.*, 2007, **46**, 7232-7235.
40. K. Matsuo, Y. Shichida, H. Nishida, S. Nakata and M. Okubo, *J. Phys. Org. Chem.*, 1994, **7**, 9-17.

**Appendix: XRD data****TD-136 A**

Empirical formula	C <sub>56.44</sub> H <sub>63.36</sub> O <sub>3</sub> PPd
Formula weight	927.08
Temperature/K	120.02(10)
Crystal system	triclinic
Space group	P-1
a/Å	11.0712(4)
b/Å	12.2460(4)
c/Å	18.2883(6)
α/°	94.461(3)
β/°	106.755(3)
γ/°	103.240(3)
Volume/Å <sup>3</sup>	2283.44(14)
Z	2
ρ <sub>calc</sub> /cm <sup>3</sup>	1.348
μ/mm <sup>-1</sup>	0.487
F(000)	974
Crystal size/mm <sup>3</sup>	0.41 × 0.24 × 0.18
Radiation	MoKα (λ = 0.71073)
2θ range for data collection/°	5.674 to 62.714
Index ranges	-16 ≤ h ≤ 13, -16 ≤ k ≤ 17, -24 ≤ l ≤ 25
Reflections collected	29375
Independent reflections	13092 [R <sub>int</sub> = 0.0414, R <sub>sigma</sub> = 0.0686]
Data/restraints/parameters	13092/14/535
Goodness-of-fit on F <sup>2</sup>	1.045
Final R indexes [ I  ≥ 2σ (I)]	R <sub>1</sub> = 0.0523, wR <sub>2</sub> = 0.1143
Final R indexes [all data]	R <sub>1</sub> = 0.0668, wR <sub>2</sub> = 0.1241
Largest diff. peak/hole / e Å <sup>-3</sup>	1.44/-0.73

## TD-136 B



Empirical formula	C <sub>87</sub> H <sub>110</sub> I <sub>4</sub> O <sub>4</sub> P <sub>2</sub> Pd <sub>2</sub>
Formula weight	2002.08
Temperature/K	119.99(15)
Crystal system	triclinic
Space group	P-1
a/Å	10.5482(3)
b/Å	14.9255(4)
c/Å	15.4054(4)
α/°	112.493(3)
β/°	102.769(2)
γ/°	101.787(2)
Volume/Å <sup>3</sup>	2070.15(10)
Z	1
ρ <sub>calc</sub> /cm <sup>3</sup>	1.606
μ/mm <sup>-1</sup>	15.944
F(000)	998
Crystal size/mm <sup>3</sup>	0.08 × 0.04 × 0.03
Radiation	CuKα (λ = 1.54184)
2θ range for data collection/°	6.58 to 147.674
Index ranges	-13 ≤ h ≤ 12, -18 ≤ k ≤ 15, -18 ≤ l ≤ 19
Reflections collected	16688
Independent reflections	7814 [R <sub>int</sub> = 0.0322, R <sub>sigma</sub> = 0.0396]
Data/restraints/parameters	7814/28/433
Goodness-of-fit on F <sup>2</sup>	1.029
Final R indexes [I >= 2σ (I)]	R <sub>1</sub> = 0.0352, wR <sub>2</sub> = 0.0891
Final R indexes [all data]	R <sub>1</sub> = 0.0404, wR <sub>2</sub> = 0.0930
Largest diff. peak/hole / e Å <sup>-3</sup>	1.81/-0.88

## Chapter 4: Investigation into the effectiveness of caesium bases in Suzuki-Miyaura cross coupling reactions

Base screens are highly prevalent in Suzuki-Miyaura cross coupling reactions.<sup>1-4</sup> This palladium cross-coupling reaction represents one of the most important C-C bond forming reactions in both academic research and industrial chemical production.<sup>5-7</sup> It is therefore important to understand any effect bases have on influencing reaction rate, yield and formation of side products in these reaction systems.

Numerous Suzuki reactions have found caesium carbonate to be the best base following a base screen,<sup>1-3</sup> and due to the aqueous nature of traditional Suzuki reactions, use of stronger bases to increase reaction rates is not possible, due to the deprotonation of water and formation of the hydroxide anion, resulting in a maximum solution pH of 15.4.<sup>6, 8</sup>

The basic mechanism of a Suzuki coupling involves oxidative addition of the aryl halide to the palladium(0) centre, followed by transmetalation of the boronic acid, then reductive elimination to give the bi-aryl product. Much research has been undertaken into elucidating the interactions between the catalyst, boronic acid and base in the transmetalation step, with multiple pathways proposed both experimentally and computationally.<sup>6, 8-10</sup>

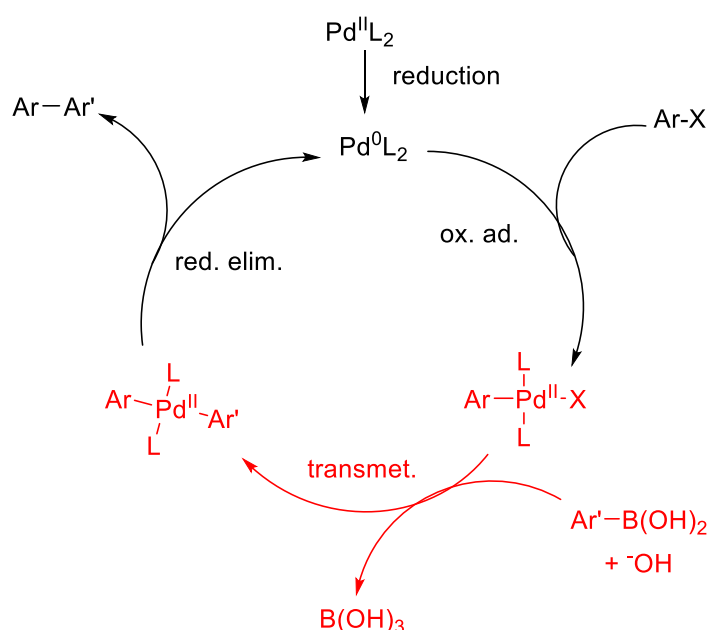


**Figure 57:** Overall Suzuki-Miyaura cross coupling mechanism highlighting less well understood transmetalation step<sup>11</sup>

The transmetallation step itself is proposed to go via two major pathways, with the route dependant on the relative reactivity of the boronic acid itself in addition to the catalyst structure. Both pathways involve hydroxide activation producing a Pd-O-B species, however whether the oxo-palladium species attacks the boronic acid, or the negatively charged boronate attacks the palladium centre is still not well understood.<sup>8</sup>

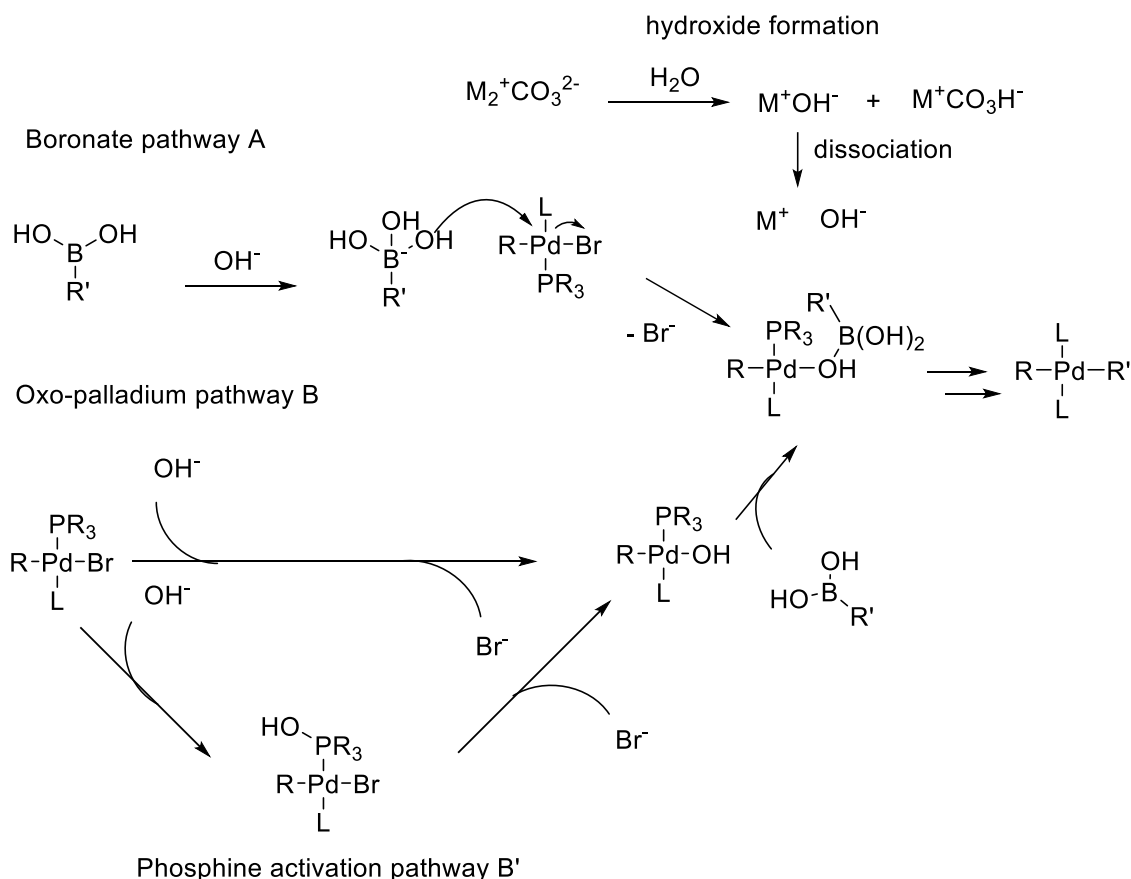
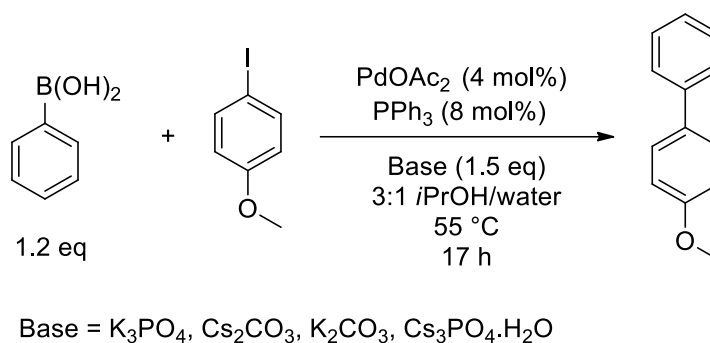


**Figure 58:** Proposed transmetallation pathways of Suzuki-Miyaura cross coupling<sup>9, 12</sup>

The oxo-palladium pathway either occurs directly by external substitution with the bromide, forming the oxo-palladium species, or *via* an addition to the phosphine followed by internal addition of the hydroxide to the palladium, removing the bromide. This pathway is generally known as the phosphine activation route.<sup>8</sup>

We chose to investigate this transmetallation step and attempt to understand how the addition of bases to the reaction would affect reaction performance. A literature Suzuki coupling of 4-iodoanisole with benzenboronic acid was selected and adapted for use with the common bis(triphenylphosphine)palladium(II) diacetate catalyst because of its mild conditions and reproducibility, as well as for easy <sup>1</sup>H NMR analysis of conversion via the methoxy group.<sup>13</sup>



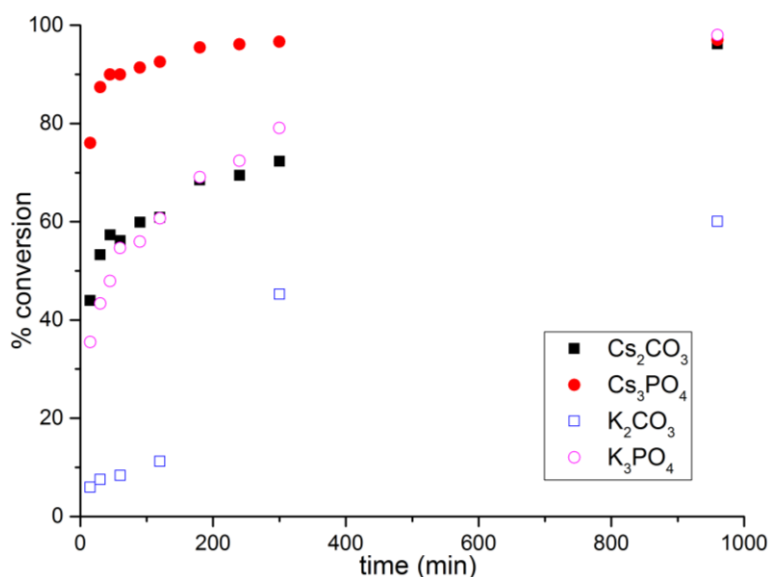
**Scheme 38:** Reaction scheme of initial base effect test of Suzuki coupling<sup>13</sup>

#### **4.1 Investigation into the transmetallation step of Suzuki-Miyaura coupling reactions and influence of base on reaction performance**

Due to the boiling points of both aryl halide starting material and product being below 300 °C we elected to analyse the reactions by calibrated GC, as well as confirming conversions using <sup>1</sup>H NMR relative to the CH<sub>3</sub> methoxy group. *p*-Xylene was chosen as a suitable internal standard as it would not overlap in GC nor in NMR analysis, and could be added directly to the solvent mixture in bulk before degassing an appropriate quantity.

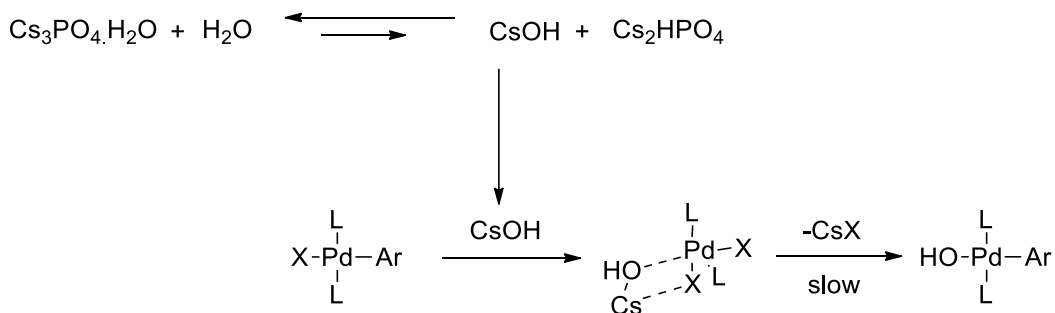
##### **4.1.1 Reactions with 4-iodoanisole**

**Figure 59:** Base effect of Suzuki-Miyaura coupling reaction using iodide leaving group



When caesium phosphate monohydrate base was used in the coupling reaction with 4-iodoanisole the initial rate increased by 2.1 fold compared to potassium phosphate, and 1.7 fold over the next fastest base, caesium carbonate. The caesium carbonate reaction can access a higher initial rate than potassium carbonate in similar conditions by 7.1 fold. These findings may suggest an interaction between the caesium cation and the iodide leaving group, allowing for easier oxidative addition of the aryl halide across the Pd atom due to reduced C-I bond strength. This could be caused by the soft-soft interactions between the caesium cation and iodide anion in this step. The orbital overlap between the caesium cation and iodide anion is larger than with harder cations such as potassium or sodium which results in a lower enthalpy of formation of 8.5 kJ / mol for CsI, over KI.<sup>14</sup>

Previous research has indicated that alkali metals are able to stabilise the formation of the oxo-palladium species, forming the Pd-OH moiety and M-X.<sup>12</sup> Due to the soft-soft interaction between caesium and iodide we propose that the caesium cation is able to reduce the activation energy of the rate determining step of the reaction, which is likely to be the substitution reaction forming the oxo-palladium species.



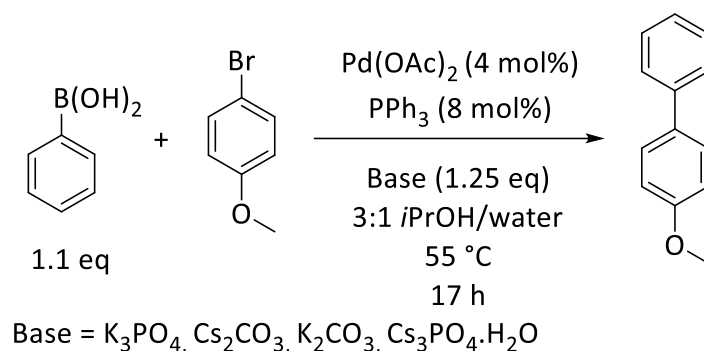
**Scheme 39:** M-X species where caesium cation accelerates formation of oxo-palladium rate determining step<sup>12</sup>

While the overall concentration of the caesium hydroxide will be relatively low due to the triphosphate  $\text{pK}_b$  being 12.3, the relative concentration of  $\text{OH}^-$ , and therefore CsOH will be sufficient to not make the hydroxide formation the rate determining step. As both caesium bases perform better than their potassium equivalents, we can interpret this as the caesium cation stabilising the formation of the Pd-OH species before addition of boronic acid. The observation that phosphate bases possess a faster initial rate than the carbonate bases therefore indicates that the equilibrium between water

and metal hydroxide lies further to the basic form using phosphate bases, which agrees with the relative  $pK_a$ 's in water, where carbonate bases are 2.0 units lower than phosphate bases at 25 °C.<sup>15</sup>

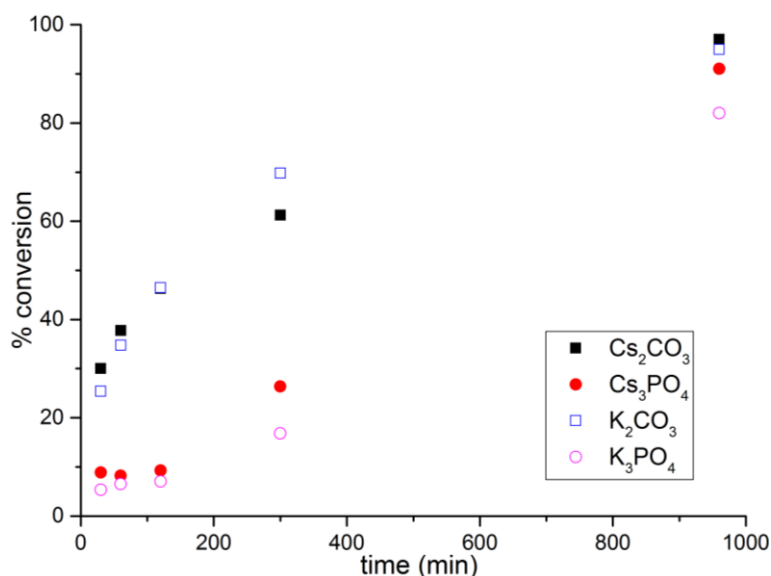
Caesium phosphate monohydrate base was by far the best base using the aryl iodide, which has utility in reactions where faster initial rates are needed due to reagents which are liable to decompose under the reaction conditions *vide infra*. However to understand the transmetallation step further, more understanding can be found by changing to a more challenging aryl halide, which will not have the same soft-soft interactions possible using the aryl iodide.

#### 4.1.2 Reactions using 4-bromoanisole



**Scheme 40:** Standard Suzuki reaction conditions with bromide leaving group

The Suzuki reaction was relatively easy to conduct using 4-iodoanisole, achieving over 70% conversion using each base using calibrated GC as the primary analytical tool, and poor using 4-chloroanisole, with less than 10% conversion using all weak bases overnight at 55 °C. It can be assumed then that using 4-bromoanisole, a leaving group with lability in between iodo and chloro would be somewhere in the middle of these two scenarios giving good conversions, while slower than the iodide leaving group. It would also be expected that if the increase in performance using caesium bases was because of soft-hard interactions between the aryl halide and the cation, this effect would be diminished due to the harder bromide group, as the enthalpy of formation of caesium and potassium bromide only differs by 0.2 kJ / mol.<sup>14</sup>

**Figure 60:** Standard Suzuki reaction screen with 4-bromoanisole substrate

We are able to observe that the phosphate bases are less active than carbonate bases using the bromide group. The fastest initial rate was observed using caesium carbonate followed closely by potassium carbonate. Both phosphate base reactions achieved below 90% conversion while carbonate bases give nearly quantitative conversion overnight using a more challenging aryl halide than iodide.

The reaction with potassium carbonate is actually faster with a worse leaving group in this example, so it appears that the carbonate bases speed up the rate determining step relative to the iodide leaving group. This would suggest that the carbonate anion allows a change between the different transmetallation pathways due to decreased [OH<sup>-</sup>] in solution as a result of the lower pK<sub>a</sub> of the carbonate anion. We argue that due to the higher concentration of hydroxide in the solution using phosphate bases, the boronate pathway is favoured due to the acidity of the boronic acid, whereas with a lower hydroxide concentration the direct substitution to the palladium is favoured, allowing for a faster reaction. Specifically the higher hydroxide concentration imparted by the phosphate bases allows for the boronic acid – boronate equilibrium to shift further towards the basic species, which facilitates the slower transmetallation pathway. The weaker carbonate bases allow less of the boronate to form and allow for direct addition of the hydroxide to palladium, speeding up the reaction.

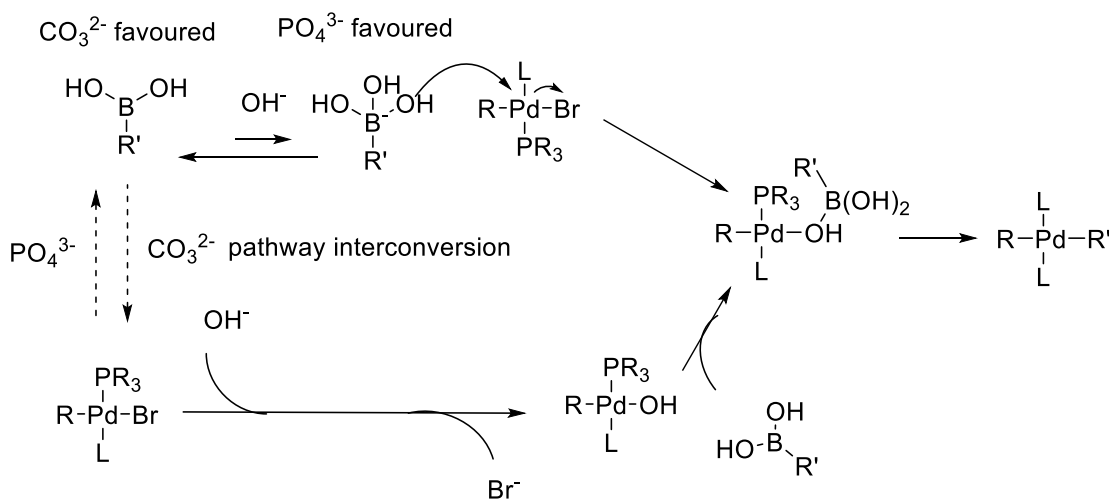


**Figure 61:** Figure detailing transmetalation pathway interconversion based on base anion using bromide leaving group

The reason pathway interconversion can affect the reaction so drastically and allow potassium carbonate to gain higher conversions using a less labile halide appears to be that the Pd-Br bond is stronger than Pd-I, which means that the hydroxyl attack can reduce the energy of the reaction transition state when the oxo-palladium pathway is favoured (Figure 60). When using the more basic phosphate anion, the boronate pathway is preferred; this increase in rate visible using the iodide (Figure 59) disappears when switching to the bromide, which we can observe in the kinetic plot.

We chose to run the reactions ‘one-pot’ rather than with catalyst preformation and premixing to further understand if any change in the base anion or cation would change the formation rate of the Pd-OH intermediate. In cases where the reagents were liable to decompose and therefore required a preformed catalyst to gain satisfactory yields *vide infra*, preformation of the catalyst was used.

As well as an increase in conversion using potassium carbonate using the aryl bromide, we observe an induction period with both phosphate bases. This appears to be due to the one-pot nature of the reaction, whereby the catalyst takes time to form the active species. The phosphate bases appear to slow the formation of the Pd-OH intermediate, which may be observable using  $^{31}\text{P}$  NMR of the bound phosphine. This reduction in rate of formation is likely due to competition between the hydroxide substitution and the phosphate anion in the reaction solvent. This then pushes the reaction further towards

the boronate pathway when using phosphate bases, providing evidence for slower reactivity using a stronger basic anion (Figure 62).

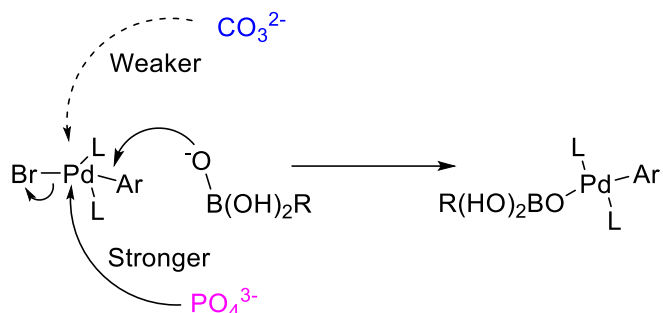


**Figure 62:** Proposed competition between phosphate anion and hydroxide slowing formation of oxo-Pd species

We propose that the phosphate interaction causing the lower rate likely occurs while the bromide is still attached to the palladium atom. As the bromide is usually a less labile leaving group than the iodide, the phosphate may coordinate to the palladium, which must first unbind before substitution of the halide to liberate the bromide. This then slows the initial rate before the boronic acid can coordinate, liberating alkali metal bromide as the by-product. While XRD would be the ideal way to investigate this induction period, we can observe a peak which agrees with the experimental induction period. We hypothesise this peak to be the Pd-OB(OH)<sub>2</sub>R species (Figure 61) visible in <sup>31</sup>P NMR in a reaction monitoring experiment using caesium phosphate (Figure 63).

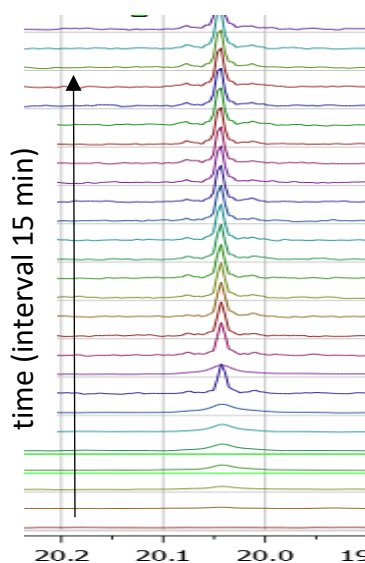


**Figure 63:** Proposed formation of active P-Pd-OB(OH)<sub>2</sub>R species in aryl bromide Suzuki reaction involving caesium phosphate by <sup>31</sup>P NMR

Each spectrum is 15 minutes apart and focussed on the Pd-P region, with subsequent spectra stacking on top of the previous. This shift compares to the  $^{31}\text{P}$  NMR shift of the phosphate anion of around 6 ppm depending on solvent. It appears that the phosphate bases inhibit the formation of the palladium boronate under these circumstances until about  $t=120$  minutes, which corroborates the kinetic run data and suggests a direct interaction between the phosphate anion and palladium complex, slowing down active catalyst formation and reducing turnover frequency at the start of the reaction. The induction period observed in the reaction using phosphate bases therefore agrees with the  $^{31}\text{P}$  NMR data as both point to a slow formation of active Pd-OH catalyst, which provides evidence towards the phosphate competition effect proposed (Figure 62).

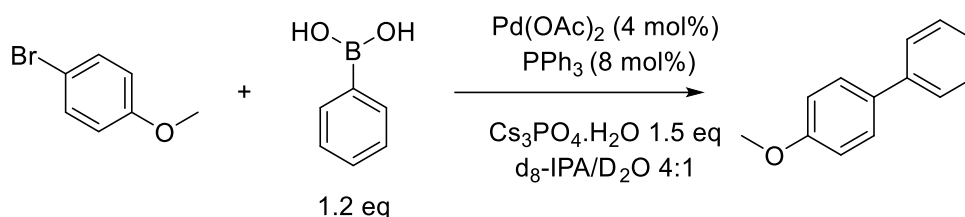
When changing the order of addition of the reaction, which allows the palladium precursor, ligand, base and boronic acid to be present in the reaction before addition of the aryl halide, we see a change in the reaction kinetics by  $^{31}\text{P}$  NMR. The presence of base and boronic acid together without the oxidative addition product appears to force the boronate mechanism, so the reaction was fast once addition of the aryl halide occurred once the reactants were fully in solution and the reaction was at temperature.

Heteronuclear NMR was found to be a successful way to monitor the induction period when using phosphate bases. It also allowed us to further understand the transmetallation step in Suzuki reactions, as well as provide evidence that the transmetallation pathway could change depending on base cation. Using the bromide leaving group, we elected to search for possible intermediates which would confirm whether the caesium cation was able to influence the reaction by coordinating to the active catalyst via  $^{31}\text{P}$  and  $^{133}\text{Cs}$  NMR.

#### **4.1.3 NMR monitoring experiments**

We initially conducted on-line NMR monitoring experiments to deduce the mechanism of the induction period observed when using phosphate bases in the bromide leaving group reaction. An upshot of the online nature of these experiments allows us to investigate potential catalytically active species, especially proposed Pd-Cs intermediates by  $^{133}\text{Cs}$  and  $^{31}\text{P}$  NMR. If a Pd-Cs species was present we would likely see a correlation between an increase or decrease in the integration of peaks in both the  $^{133}\text{Cs}$  NMR, and the  $^{31}\text{P}$  NMR corresponding to the phosphorus ligand. When

investigating the phase split point of Suzuki reactions involving dual solvent mixtures (p. 144), it was discovered that all Suzuki reactions tested were ran above the phase splitting point for this reaction class resulting in a biphasic mixture. Despite this all reactions, including the NMR monitoring reactions were homogenous with respect to solid-liquid dissolution equilibria, so all of the reagents were fully soluble in the biphasic mixture.



**Scheme 41:** Conditions for NMR monitoring reaction mimicking standard Suzuki conditions

Numerous Pd-P species were present in the reaction observed by NMR, visible using <sup>31</sup>P measurements judging from peaks present in the palladium region of 15-45 ppm. As Suzuki reactions contain multiple Pd-P species at various stages at the reaction cycle including Pd-L, Pd-L<sub>2</sub>, HO-Pd-L, HO-Pd-L<sub>2</sub>, Ar-Pd-X, Ar-Pd-B(OH)<sub>2</sub>R, as well as possible dimers of each, there is likely to be numerous species in the palladium region of the <sup>31</sup>P experiments in low concentrations visible in NMR spectra. Due to the nature of the study only the peaks correlating to proposed bimetallic palladium-caesium species were investigated provided they were in the Pd-P region. Two observable intermediate species were present in both <sup>31</sup>P and <sup>133</sup>Cs at early points in the reaction which appear to correlate to each other (Figure 64).

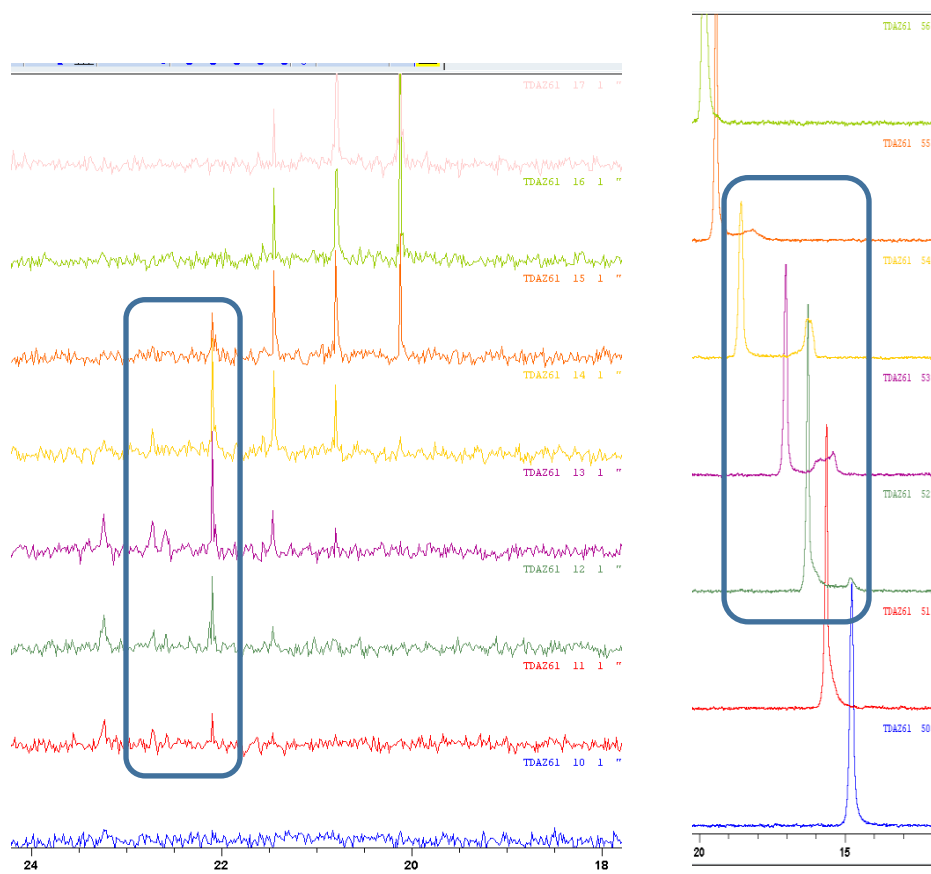
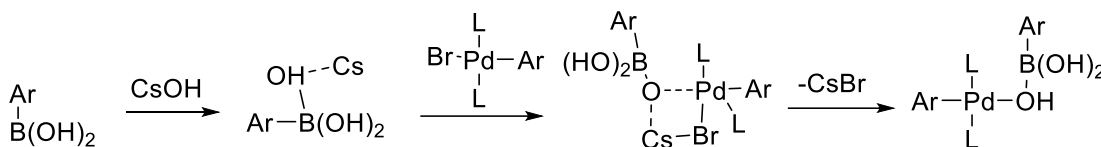


**Figure 64:** Observable Cs-P intermediates in  $^{31}\text{P}$  (left) and  $^{133}\text{Cs}$  (right) NMR

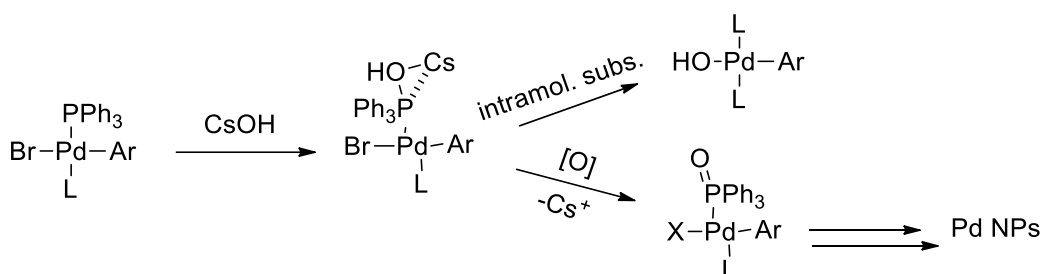
The NMR spectra were each taken at 15 minute intervals relative to each nuclei, in the order  $^{133}\text{Cs}$ - $^{31}\text{P}$ - $^1\text{H}$ . We can observe a species in spectrum 11 (red) at 22.1 ppm in the  $^{31}\text{P}$  measurements which is observable until spectrum 15 (orange). The corresponding  $^{133}\text{Cs}$  spectrum 52 (green) possesses a shoulder at 14.5 ppm which shifts right relative to the main caesium phosphate peak due to changing concentrations.<sup>16</sup> The peak itself disappears after spectrum 15 and 55 (orange) showing the species are correlated, and therefore likely to be a Pd-P-Cs species of some description influencing the reaction conversion. This species appears to form approximately 20 minutes into the reaction with a lifetime of 90 minutes. The observed species is likely to occur after ligation of the palladium centre of  $\text{PPh}_3$  as the species was not present before 20 minutes. It is not clear however whether the proposed Pd-Cs bimetallic molecule speeds up or slows down the reaction, as it is hard to deduce whether the caesium atom would reduce the energy of the transition state, speeding up the reaction, or deactivate the catalyst thereby reducing the rate. The most likely intermediate based on the proposed mechanism is related to the palladium boronate species after addition of the boronate to the palladium centre in the boronate pathway where the caesium atom facilitates

addition of the hydroxide anion to palladium. (Scheme 39). Previous work in the Grisorio group had found that by in DFT calculations a M-X-Pd-OH species was a key factor within the oxo-palladium pathway, so it is likely similar complexes can be formed using the boronate pathway also.<sup>12</sup>



**Scheme 42:** Proposed Pd-Cs species visible by heteronuclear NMR<sup>12</sup>

There is also a short lived intermediate which appears in spectrum 11 (green) in the <sup>31</sup>P NMR at 22.7 ppm but only has a lifetime of 45 minutes (3 spectra). This can be observed in the <sup>133</sup>Cs NMR as a shoulder on the left of the Cs-P 1 peak in spectra 53-54, but as <sup>133</sup>Cs NMR are subject to peak broadening due to switching of the Cs<sup>+</sup> cation between molecules, showing the peak as the average chemical shift of the bulk solution, this is less pronounced than the phosphorus data. The likely identity of this would be an intermediate leading to catalyst deactivation, possibly related to a palladium oxide species. The fall of both the caesium and phosphorus peaks would indicate both detach from the palladium, causing catalyst deactivation and a corresponding decrease in reaction rate. As triphenylphosphine oxide is present in this reaction in small quantities, we argue that the Pd-Cs species responsible for catalyst deactivation is likely to be an intermediate in the phosphine activation pathway B' (Figure 58), where the activated phosphorus is then oxidised to triphenylphosphine oxide and decomposes the palladium catalyst.



**Scheme 43:** Proposed Pd-Cs species allowing for catalyst decomposition<sup>17</sup>

Despite observing these species in caesium and phosphorus NMR, the overall yield for the NMR tube reaction was lower than the standard Schlenk tube reaction under

nitrogen atmosphere. The NMR tube suffers from poor mixing, as only convective mixing will be possible with stirring within the NMR machine being impractical, providing poor phase transfer contact area which may actually influence the transmetallation pathway due to poor mass transfer and therefore low mixing between the organic layer containing catalyst and aryl halide with the aqueous layer containing base and boronic acid. In addition the NMR machine was pre-shimmed and tuned and matched to a blank tube so the reaction could be observed as soon as the sample was taken from the bulk reaction mixture. This means that the tube took some time to equilibrate at the correct reaction temperature in the VT NMR which would indicate possible slower kinetics than in the bulk system. Previous work has shown that the metal cation may slow down the transmetallation step in some circumstances, though the exact makeup of the decomposed catalytic species was not made apparent.<sup>17</sup>

#### **4.1.4 Investigation into phase separation of dual solvent Suzuki-Miyaura cross couplings**

Based on the poor phase transfer between the organic and aqueous layer present in NMR tube experiments using the biphasic Suzuki solvent system, the decision was made to investigate at which point 'salting out' occurs in the reaction mixture. Isopropanol is usually miscible with water, however if sufficient solute is dissolved in the miscible solvent mixture, the solvent phases split into organic and aqueous, leaving the charged base ions and boronic acid in the aqueous layer, and the aryl halide and catalyst complex in the organic layer. Using NMR as an analytical technique is useful to elucidate at what reaction concentration the phases are likely to split, as there is a minimal amount of mixing.

In order to experimentally elucidate the boundary for miscibility and 'salting out' the decision was made to make up a 3:1 solution of IPA and water and using potassium phosphate as a surrogate for the reaction mixture, as the main components of the reaction causing this phase split are the boronic acid and the base itself. The reaction was investigated at temperatures from 50 °C to 75 °C. As solubility of solids in solution tends to increase with temperature, we would expect miscibility to increase as well. Each equivalent of potassium phosphate will contain 4 charged species after dissociation, the three potassium cations and the tribasic phosphate anion. The boric

acid by-product from the boronic acid exists as a further charged species, so every mole of potassium phosphate added to this reaction represents 80% of the total salt species present in the full reaction conditions.

When running the tests confirming the concentration required to break the miscibility of the organic and aqueous layers, we found that 0.05 mM potassium phosphate would cause a salt out at 50 °C, while 0.06 mM was required at 75 °C. This then means that 0.25 mM and 0.3 mM total ion concentration is required to break miscibility when factoring in the anions, cations and boric acid by product.

The standard loading of salts in Suzuki reactions used in this chapter is 1.0 mmol boronic acid and 1.25 mmol base in 10 mL. This then confirms that all reactions conducted in this chapter at the standard concentration do in fact salt out, and the threshold required to negate this and run the reactions completely homogeneously would require a reduction in concentration by factor of 2.5 (60%). The reduction in concentration of all components of the reaction by this much would cause a large decrease in rate, as rate is directly proportional to the concentration of the reactants present in the rate determining step and therefore the rate order. The downside to having a non-homogeneous mixture is that mixing becomes a large factor in reaction kinetics, as was observed when using NMR tubes as a reaction vessel *vide supra*. Cross bladed stirrer bars are a useful way to increase reaction shear rate, and therefore ensure the mass transfer between the aqueous and organic layers remain high at all times. This is especially important where reactions are scaled up, and therefore require increased mass transfer as the volume of the reaction increases much faster than the size of the container by a square cubed law. Given this knowledge of the importance of mixing due to phase splitting of the reaction mixture, cross bladed stirrer bars with high shear rates were used in all experiments to ensure mass transfer was not a factor reducing reaction rate in these Suzuki coupling examples.

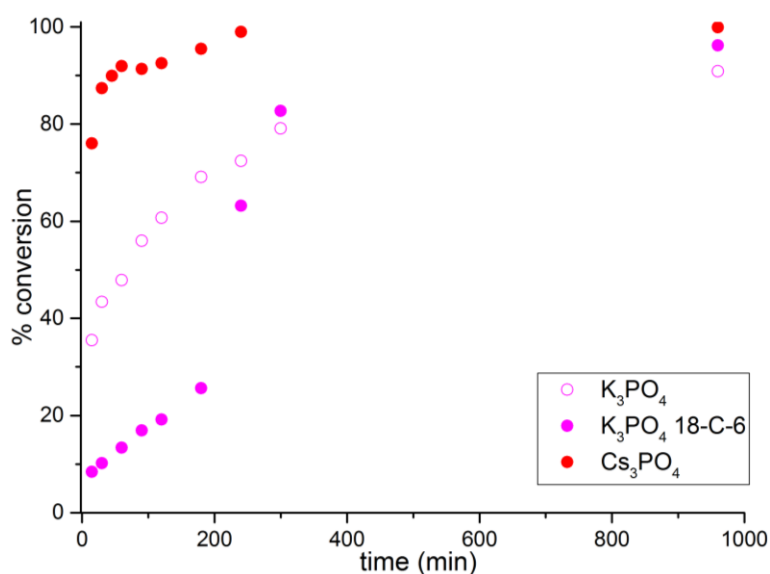
#### **4.1.5 Crown ether complexation of alkali metal cations**

The existing dogma behind the caesium effect points to increased performance due to solubility effects caused by soft-hard interactions between the soft caesium cation and hard anion. To investigate this, we chose to increase solubility of alkali metal bases by complexing the cation to a crown ether, resulting in increased reactivity of the anion

as the base becomes dissociated into cation and anion elements.<sup>18</sup> Increased organic phase solubility of the basic anion should increase reaction rate if mixing and phase transfer were rate limiting. It is important to deduce whether the crown ether would increase reaction performance by facilitating base dissociation by complexing to the alkali metal cation, providing a 'naked anion' effect by dissociating the cation from the anion. The crown ether complex could also increase reaction rate by encouraging phase transfer between the aqueous and organic layer allowing for the anion to further mix with the reactants in the organic layer. Crown ethers have particularly large affinities to alkali metal cations due to the donating powers of the oxygen atoms around the ring *vide supra*. The oxygen atoms are able to impart electron density around the metal cation and suppress ion pairing between the anion and cation, allowing the anion to be free to react in solution, and the base as a whole to become more soluble. 18-Crown-6 has a high binding affinity for the  $K^+$  cation and should elucidate any solubility related increase in reaction performance.

A useful reaction to investigate if addition of 18-crown-6 would increase the performance of reactions in Suzuki couplings would be the aryl iodide reaction using potassium phosphate base. The difference between caesium and potassium phosphate bases in this reaction are significant and if the complexation of the cation allows for better reaction rates this will be evident in the kinetic profile.

**Figure 65:** Suzuki iodide coupling rates when using 18-crown-6 additive

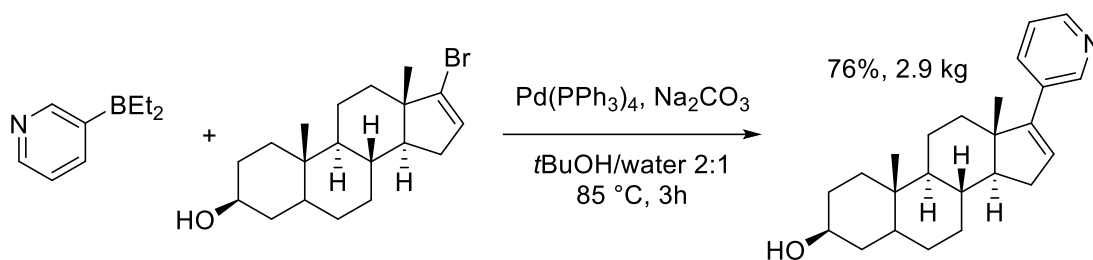


Despite obtaining a similar yield to the unaltered reaction (Scheme 38), the reaction using 18-crown-6 additive has a much slower initial rate at only 30% as fast as the original reaction. What we then see is an induction type effect where after 180 minutes the reaction accelerates and overtakes the reaction without additive. The proposed mechanism of action for the induction period is that the crown ether allows increased solubility of the base in the organic phase, however the anion must deprotonate water to form the active Pd-OH species, which must occur in the aqueous phase. Lower anion concentrations in the aqueous phase lead to lower pH in aqueous solution which lowers the concentration of the OH anion, slowing formation of Pd-OH (Figure 58) and therefore reaction rate.

Despite the crown ether increasing the rate of potassium phosphate base in this reaction, it did not increase the rate using caesium phosphate. This is likely due to the fact that the binding constant for the caesium cation in a methanol/water mixture is 31 times higher using a potassium cation than a caesium one, so any addition of 18-crown-6 will affect the reaction kinetics using the potassium cation to a much larger degree. Larger crown ethers are available, but 18-crown-6 has the highest binding affinity for the Cs<sup>+</sup> cation of all crown ethers measured.<sup>18</sup>

#### **4.2 Troublesome heteroaromatic boronic acids in Suzuki reactions**

Heteroaromatic rings are common in candidates for drug molecules as they allow manipulation of pharmacological properties such as lipophilicity and hydrogen bonding. A common, widely used, and relatively reliable reaction generally used in these medicinal chemistry syntheses is the Suzuki reaction and numerous drug molecules have been synthesised through this synthetic route.<sup>7, 19</sup> One particularly notable example of a blockbuster drug molecule synthesised through a heteroaromatic boronic acid Suzuki reagent is abiraterone acetate (trade name Zytiga®) used in the treatment of metastatic prostate cancer. This drug, boasting over £2.3 billion dollars of sales in 2015, has a C-C bond forming key step optimized using a diethylborane group (Scheme 44).

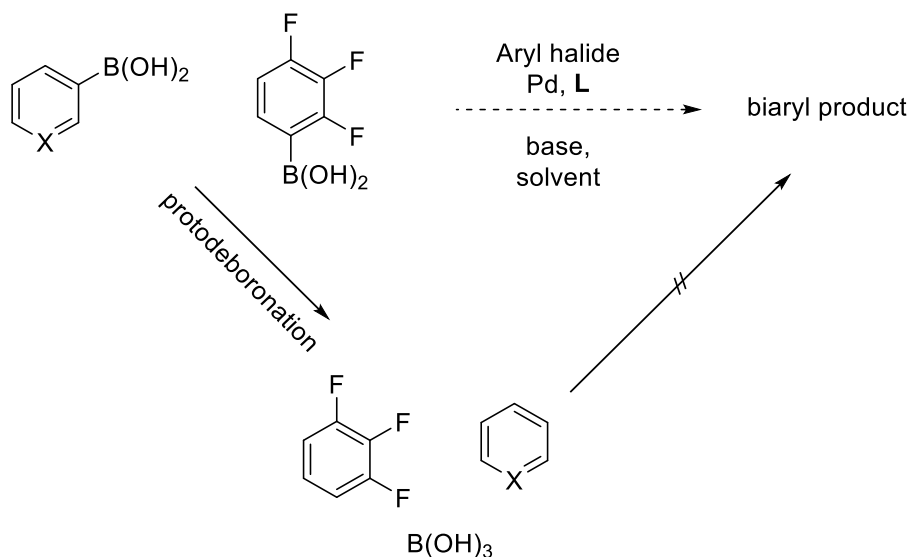


**Scheme 44:** Heteroaromatic Suzuki key step in Synthesis of Zytiga<sup>20, 21</sup>

It is therefore necessary that in order to access these motifs, heteroaromatic reagents for Suzuki reactions are available. These are usually boronic acids and boroxine anhydrides and must be effective and high yielding to access the chemical space needed for API and pharmaceutical intermediate synthesis. The main issue with these systems however, is that they are typically prone to protodeboronation reactions under aqueous reaction conditions, forming the heteroaromatic ring and boric acid from the starting material and  $\text{OH}^-$  from water.

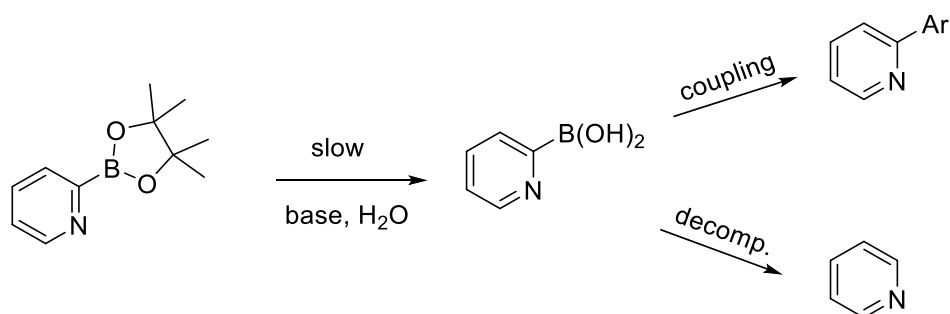
Lloyd-Jones and co-workers stipulated that the rate of protodeboronation of these boronic acids correlates with the pH of the system, and that a higher pH would generally increase the rate of protodeboronation within the system, decreasing reaction yield.<sup>22</sup> In palladium-catalysed base-mediated coupling reactions such as Buchwald-Hartwig aminations, stronger bases such as potassium *tert*-butoxide are used to increase the reaction rate *vide supra*. This is not generally possible in Suzuki-Miyaura couplings as the rate of protodeboronation of boronic acids to boric and parent aryl is generally increased at high pH, as well as the ubiquitous use of aqueous solvents in these reactions. Weak bases must be used because the  $\text{pK}_a$  of  $\text{KO}^t\text{Bu}$  is above 15.4 and therefore effectively deprotonates water forming  $\text{OH}^-$  anion regardless of the  $\text{pK}_b$  of the base itself. If bases with a  $\text{pK}_b$  above the limit of water are used, alcoholic solvents or dioxane are generally more appropriate.<sup>23</sup>

Weak bases are therefore the only alternative in these troublesome Suzuki reactions. Caesium bases may be more effective if there is a potential increase in reaction performance gained by use of caesium cation in these reactions. If we can increase reaction performance above existing techniques using novel caesium bases, this then provides a pathway for use of these bases on a wider scale.



**Scheme 45:** General scheme of protodeboronation reactions of heteroaromatic and fluorinated boronic acids

To avoid this protodeboronation, two methods have had some success in providing high yielding reactions. Numerous boronic acid protecting groups exist, from trifluoroboronate salts to MIDA and DABO boronates.<sup>11</sup> All of these go through the pathway of hydrolysis slowly in solution to yield the active boronic acid, which undergoes reaction competition between the coupling reaction and transmetallation step to the palladium, and protodeboronation. As the concentration of the boronic acid is low at all times, the concentration of catalyst and other reagents relative to the boronic acid is high, which increases the rate of the coupling reaction relative to the decomposition reaction.



**Scheme 46:** Scheme showing how boronic acid protecting groups can increase reaction yields

The downside of these methods is that either the protected boronic acid must be formed before the coupling reaction which requires an extra synthetic step to form the

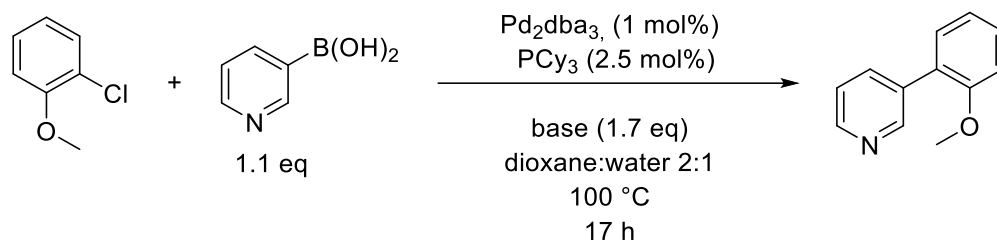
final product, usually *via* an expensive palladium catalysed Miyaura borylation reaction, or preformed protected boronic acids must be purchased, which can be as much as 20 times the cost of the boronic acid itself, which becomes prohibitive on scale.<sup>24</sup>

The alternative option for increased yields of troublesome Suzuki couplings is to use a highly active catalyst, making the rate of the coupling reaction itself more favourable than the protodeboronation reaction. This can either involve highly specialised ligands which are able to stabilise the transition state sufficiently to increase reaction rate,<sup>25</sup> or use of different boronic acid analogues such as diazonium salts along with activated catalysts.<sup>26</sup> Both of these approaches run into the issue that catalyst cost can make up a significant proportion of overall reaction cost, and very low catalyst loadings of extremely active catalysts are subject to deactivation under reaction conditions much more readily than standard Pd(0) catalysts.

We seek to develop a third method to increase yields in troublesome Suzuki reactions prone to protodeboronation reactions, namely polyfluorinated and heteroaromatic boronic acids. Based on the results showing increased performance of the standard Suzuki reaction using the iodide leaving group and caesium phosphate monohydrate base, we seek to deduce whether addition of this relatively unstudied base would improve rates and therefore yields in this class of reactions.

#### **4.2.1 Initial screening reaction**

To assess the possibility of increased reaction performance using caesium bases in this reaction, we must first assess whether an existing literature Suzuki cross coupling utilising a heteroaromatic boronic acid could be improved by addition of synthesised caesium phosphate monohydrate base. We elected to adapt a literature procedure from Fu *et al.*<sup>27</sup> The optimised base found in the literature was potassium phosphate, which achieved 88% conversion in 18 h under an argon atmosphere of a coupling reaction between the heteroaromatic 3-pyridineboronic acid and 2-chloroanisole.



**Scheme 47:** Adaptation of literature procedures to investigate caesium phosphate monohydrate in heteroaromatic Suzuki reactions

The reaction time was lowered from 18 hours to 17 to keep in line with the previous work on the benzene boronic acid haloanisole substrates. We were able to achieve 85% yield which was deemed an adequate reproduction of the literature reaction as the reaction was run under nitrogen instead of argon. When screening the reaction against the potassium and caesium weak bases however we found the overall yield could be increased to 96% by utilising caesium phosphate monohydrate in this reaction.

**Table 15:** Base performance under 3-pyridine Suzuki conditions

Base	$\text{Cs}_3\text{PO}_4 \cdot \text{H}_2\text{O}$	$\text{K}_3\text{PO}_4$	$\text{Cs}_2\text{CO}_3$	$\text{K}_2\text{CO}_3$
Conversion (%) (NMR)	96	85	80	88

The increased performance of potassium carbonate over caesium carbonate is may be due to the base milling effect.<sup>28</sup> Caesium carbonate is generally only available in coarse powder forms, whereas potassium carbonate is usually supplied pre-milled to a fine powder. The increased surface area of the potassium carbonate base allows for increased solubility and reactivity which in this case allows slightly higher conversions. We would expect the caesium carbonate base to have increased performance if the base was milled prior to use to reduce particle size.

Due to the improved performance of heteroaromatic Suzuki couplings facilitated by caesium phosphate monohydrate base, further analysis was required to deduce reactions in which this increase in yield would occur, and the mechanistic reasons behind the increased yield. Based on the existing methods to improve troublesome Suzuki couplings we would expect either the caesium phosphate to increase the reaction rate by stabilising a rate determining transition state involving the palladium

catalyst or by slowing the rate of hydrolysis of the C-B bond causing protodeboronation.

#### **4.2.2 Choice of substrates to probe scope of caesium phosphate monohydrate acceleration**

To directly compare caesium phosphate monohydrate base to existing reactions heteroaromatic and fluorinated boronic acids were carefully chosen to reflect a wide range of protodeboronation rates with half-lives measured under basic conditions at elevated temperatures from 5 minutes to 1 week.<sup>22</sup> This would enable elucidation of any method of action where caesium cation can improve performance in these reactions. If the 'caesium effect' was more apparent using boronic acids which were more unstable, the results would suggest a stabilization of the C-B bond during the protodeboronation mechanism enabling [boronic acid] to be relatively higher throughout the reaction than when using other alkali metal bases. If the effect was present in all reactions it is more likely that the caesium cation is directly affecting the catalyst species by slowing oxidation and keeping [catalyst] high or allowing for a lower energy barrier which would give faster turnover frequency.

Initially, four boronic acids were chosen to reflect a wide range of half-lives, coordinating and non-coordinating solvents and leaving groups taken from literature to directly compare synthesised caesium phosphate monohydrate base to published results. This allows the results to be benchmarked against existing data, ensuring the reaction results using common bases were in line with existing reactions in published data *vide infra*. In addition, we elected to sample each reaction to deduce the relative rates of product formation, as this would provide evidence of the mechanistic pathway and any increase in reaction performance. If the base was stabilising the boronic acid and slowing the rate of protodeboronation, we would expect the reaction to continue turning over further into the reaction time than a non-stabilised example. Conversely if the base was able to interact with the catalyst and speed up the rate determining step, we would expect the initial rate to be higher but the turnover to slow and halt at the same time point in the reaction due to boronic acid protodeboronation.

We selected 3-pyridylboronic acid which had a relatively long half-life of 7 days as an example of a heteroaromatic boronic acid that is unlikely to undergo a significant

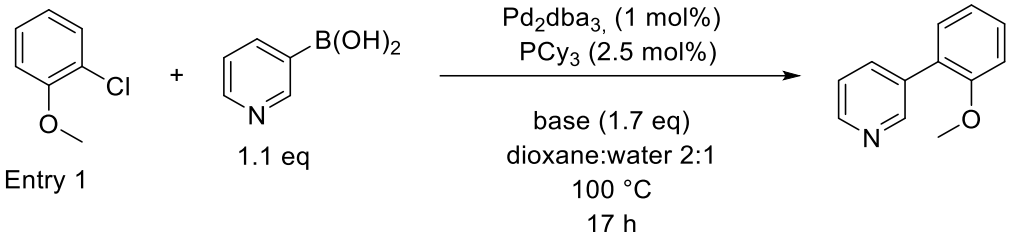
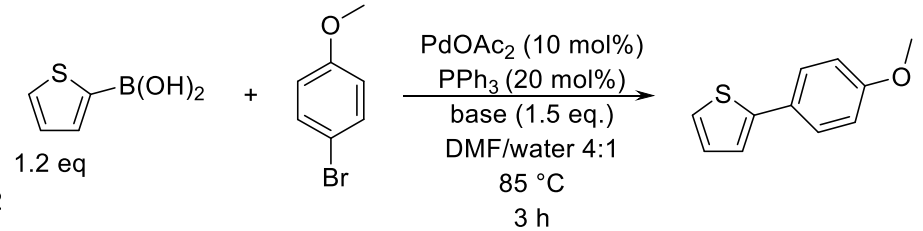
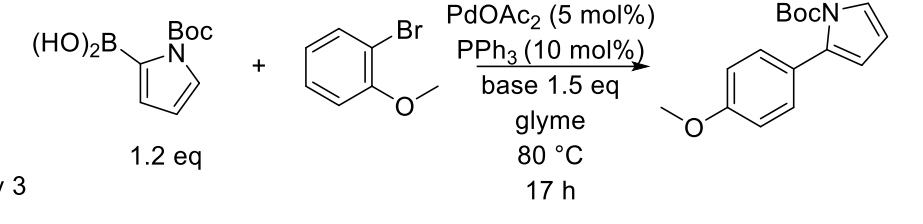
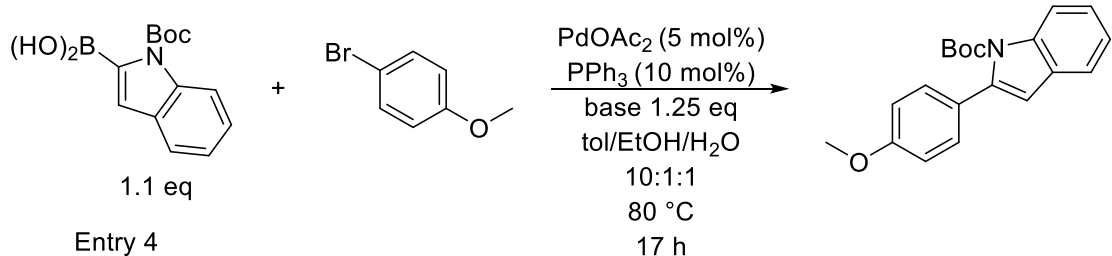
amount of protodeboronation under the reaction conditions. Any stabilisation of the C-B bond would be unnecessary in this class of boronic acids, so would provide evidence that catalyst stabilisation is the likely mechanism of action. 2-thiophene boronic acid was chosen as an example which would benefit from stabilisation of the boronic acid, with a measured half-life of 2 hours. Boronic acids with an intermediate half-life of between 30 minutes and 6 hours are useful to monitor, as increased catalytic activity and boronic acid stabilisation will both provide increased yields for the reaction end point. *N*-Boc pyrrole and indolylboronic acids were chosen as examples of boronic acids with short half-lives, as unless stabilisation of the boronic acid occurs, the half-lives of 5-30 minutes would slow reaction turnover after between 10 minutes and 1 hour, as there will be less than 10% boronic acid remaining in solution after 4 reaction half-lives.

All reactions were chosen to incorporate a methoxy tag on the aryl halide for facile determination of NMR conversion at reaction end point, to corroborate evidence supplied *via* calibrated GC (Table 16). Ether groups are electron-donating, which results in a deactivation of the aryl halide when present on the *ortho* or *para* position of the benzene ring. Despite this, acceptable yields were achieved in the literature and therefore these reactions were allowed to proceed for base screening.

A multitude of solvents and temperatures were used, from 80 °C to 100 °C, but each system had either a proportion of water in the solvent mixture, or used hydrous wet solvent which led to water deprotonation and the traditional Suzuki mechanism of hydroxyl attack on either the boronic acid or palladium centre.

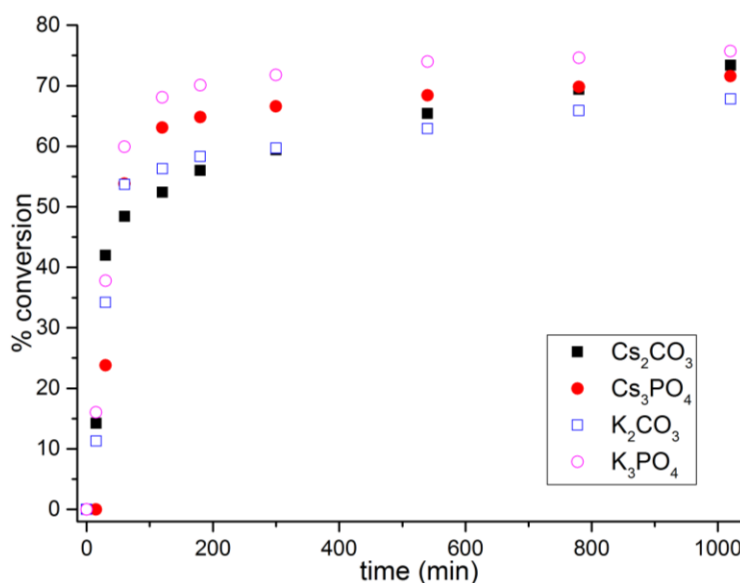
The reaction utilising 3-pyridylboronic acid used Pd(0) precatalyst Pd<sub>2</sub>(dba)<sub>3</sub>, whereas the remaining reactions were conducted with Pd(II) precatalyst Pd(OAc)<sub>2</sub>. The effect of this change with respect to the reactivity of the substrates was that the Pd(II) reactions required stirring of the catalyst mixture with boronic acid prior to reaction commencement to ensure reduction of the palladium to active Pd(0) labile to the oxidative addition of the aryl halide, while the Pd(0) reactions could be conducted in a 'one-pot' fashion *via* addition of all solid reagents followed by injection of the liquid aryl halide and then solvent, showing no induction period indicating the active precatalyst had not formed.

**Table 16:** Initial choices of literature reactions to conduct base screen

Reaction	Literature boronic acid $t_{1/2}$	Literature ideal base
<p>Entry 1</p>  <p> <math>\text{Pd}_2\text{dba}_3</math> (1 mol%)  <math>\text{PCy}_3</math> (2.5 mol%)            base (1.7 eq)            dioxane:water 2:1            100 °C            17 h         </p>	7 days	$\text{K}_3\text{PO}_4$ <sup>27</sup> 88% conversion
<p>Entry 2</p>  <p> <math>\text{PdOAc}_2</math> (10 mol%)  <math>\text{PPh}_3</math> (20 mol%)            base (1.5 eq.)            DMF/water 4:1            85 °C            3 h         </p>	2 hours	$\text{K}_2\text{CO}_3$ <sup>29, 30</sup> 76% conversion
<p>Entry 3</p>  <p> <math>\text{PdOAc}_2</math> (5 mol%)  <math>\text{PPh}_3</math> (10 mol%)            base 1.5 eq            glyme            80 °C            17 h         </p>	5 minutes	$\text{Cs}_2\text{CO}_3$ <sup>31</sup> 41% conversion
<p>Entry 4</p>  <p> <math>\text{PdOAc}_2</math> (5 mol%)  <math>\text{PPh}_3</math> (10 mol%)            base 1.25 eq            tol/EtOH/<math>\text{H}_2\text{O}</math>            10:1:1            80 °C            17 h         </p>	N/A	N/A <sup>32</sup>

Each of these reactions was screened using an automated reaction sampling robot known as an 'AmigoChem' workstation. This consisted of 4 reaction wells which were heated and stirred individually on an 'Integrity 10' platform along with a sampling robot programmed to take 10 samples into quenched GC or HPLC vials over the reaction timescale. The advantage of this platform is higher throughput due to the ability to run four reactions in parallel rather than two on a standard Schlenk line. The reactions all use a common solvent which is injected prior to reaction start which neutralises any differences in the levels of oxygen in the system, and samples can be taken regularly throughout the night, allowing observation at reaction kinetics closer to the end point. The result of using this reaction monitoring equipment gave results which led to hypotheses about the mechanism of action of the cation and anion in Suzuki couplings.

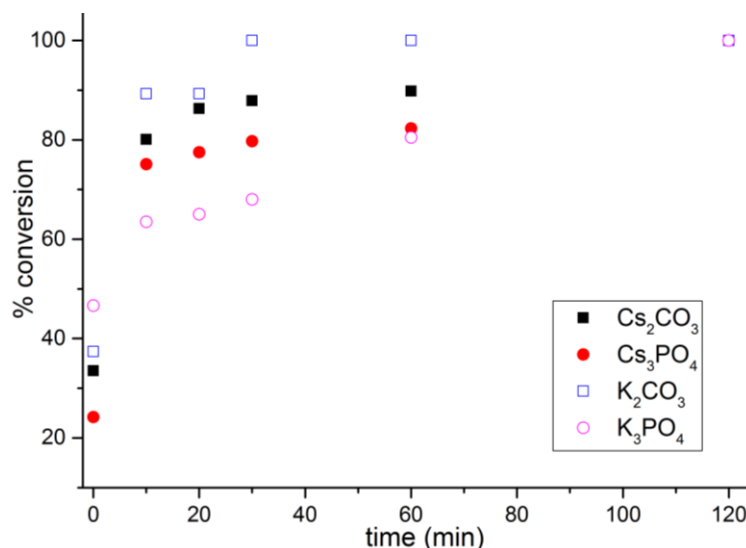
**Figure 66:** AmigoChem reaction of 3-pyridylboronic acid with 2-chloroanisole (Entry 1, Table 16)



In the reactions involving 3-pyridylboronic acid, which has a much longer half-life than the reaction time (Table 16), we see a strong initial rate from all bases with potassium phosphate appearing to be fastest at 60% conversion after 90 minutes, 6% higher than caesium phosphate monohydrate and potassium carbonate. This relatively similar performance between all studied weak bases indicates that with chloride leaving groups there does not appear to be significant acceleration in the reaction using either potassium or caesium cations. The slightly lower conversions gained on the AmigoChem relative to Schlenk line techniques (Table 15) indicates that the automated

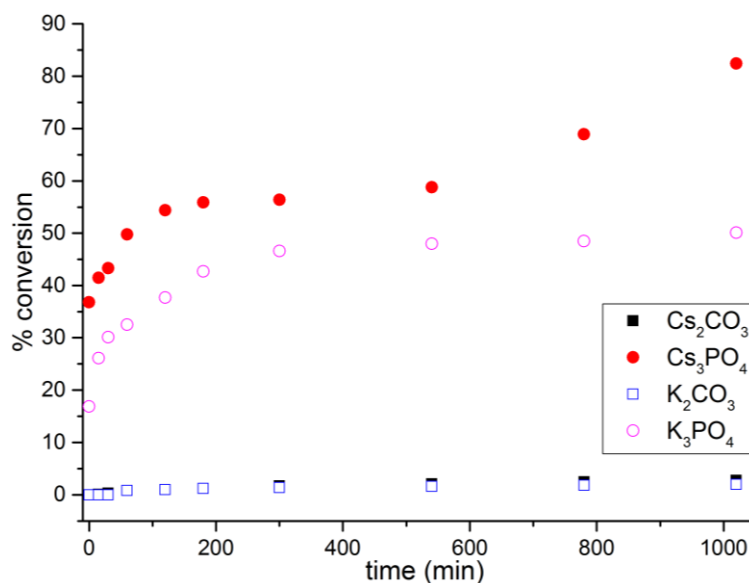
system does suffer from a small but detectable amount of air ingress, reducing the reaction yields slightly compared to a system sealed under inert gas.

**Figure 67:** AmigoChem reaction of 2-thiophene boronic acid and 4-bromoanisole  
(Entry 2, Table 16)



When changing the boronic acid to the more unstable 2-thiopheneboronic acid possessing a half-life of 2 hours, we can observe an inflection point at around 10 minutes, which could indicate catalyst decomposition. At 15 minutes all reactions undergo an inflection point reducing the high initial rate to a slow turnover. This is presumably due to a decomposition pathway of the palladium catalyst to inactive palladium nanoparticles or palladium black (Scheme 43).<sup>17</sup> This can be observed by the change in colour of the solution from orange to dark brown from approximately 10 minutes. The results gained on the AmigoChem agree with the literature ideal base of potassium carbonate, but there does not appear to be a clear trend with respect to the cations, as potassium was the better carbonate, and caesium the better phosphate base.

**Figure 68:** AmigoChem reaction of *N*Boc-2pyrroleboronic acid with 2-bromoanisole  
(Entry 3, Table 16)

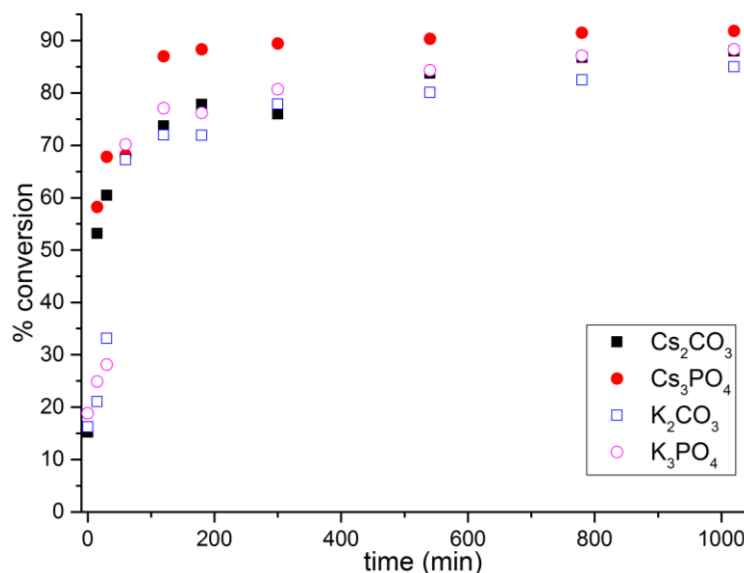


When changing to the even more unstable *N*-Boc pyrroleboronic acid, possessing a half-life of only 5 minutes under conditions of pH 12 using sodium hydroxide as a base,<sup>22</sup> we clearly see that the phosphate bases are much more effective than the carbonate bases, with both carbonate anions failing to convert more than 5% of product. The reaction in the literature achieved 41% conversion using caesium carbonate via heating to reflux under inert gas, however sampling is not uniform or reliable at reflux so the reaction was adapted to run at 5 °C below boiling. This resulted in much lower conversions of the starting material while the concentration of boronic acid was high, leading to very low conversions using the carbonate bases.

When using the phosphate bases, the observation of any conversion after several boronic acid half-lives indicates there is significant stabilisation of the C-B bond occurring. The much higher initial rate of caesium phosphate monohydrate relative to potassium phosphate also indicates there may be a further interaction between the base cation and the catalyst. The reaction using caesium can achieve over 40% more conversion than the next best base potassium phosphate, but a significant proportion of this occurs after the reaction appears to stop turning over between 300 and 540 minutes. This can be rationalised as glyme can be effectively used as a ligand in coupling reactions, particularly those involving nickel(II) catalysts.<sup>33, 34</sup> The glyme may be behaving as a ligand displacing the active triphenylphosphine, thereby deactivating the

catalyst to further turnovers. The caesium cation, behaving as caesium hydroxide, can then decompose this inactive catalyst intermediate into active palladium nanoparticles which can begin to turnover the reaction after the induction period.

**Figure 69:** AmigoChem reaction *N*-Boc-2-indoleboronic acid with 4-bromoanisole (Entry 4, Table 16)

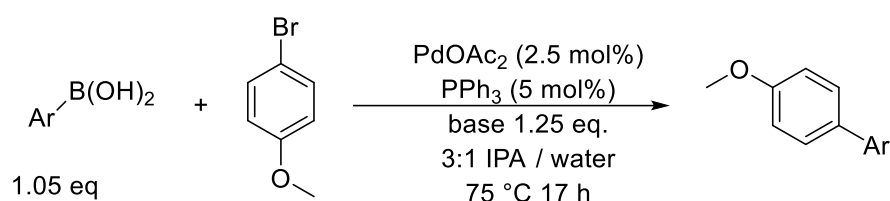


The *N*-Boc-2-indoleboronic acid behaves similarly to the 3-pyridineboronic acid in that all bases appear to have acceptable initial rates without any obvious induction period. Notably both caesium bases have much higher initial rates than the potassium equivalents which suggests a change in transmetallation mechanism by involvement of the caesium cation itself. Caesium phosphate monohydrate is superior to potassium phosphate, and caesium carbonate is superior to potassium carbonate in this reaction, suggesting that the cation plays a factor in stabilising the catalyst. The boronic acid half-life had not been evaluated in the literature, but our experiments found it to be around 30 min *vide infra*, which puts it in the same class as 2-thiopheneboronic acid.

Observing the kinetic plots and comparing to the literature data (Table 16) we can deduce that for the longer half-life boronic acids of 2 hours or over, the best performing base is identical to the base selected in the literature. When the half-life is reduced, caesium phosphate monohydrate has both better initial rate over the literature base and higher overall conversion. These results agree with the theory that the phosphate bases are able to decrease the rate of protodeboronation through stabilisation of the C-B bond, keeping [boronic acid] high for longer than achievable using carbonate bases.

It is clear that while utilising literature procedures to benchmark reaction performance and ensuring robustness of data is useful, the different mechanistic pathways the reaction can undergo, along with equilibrium and solvent effects, paint a complicated picture of base acceleration. The ideal method to better understand any base effect in these complicated reaction systems would be to remove as many variables as possible to gain a better picture of how the bases were changing reaction performance.

The system chosen for the standard conditions represents a relatively mild, non-toxic and inexpensive example of Suzuki-Miyaura cross couplings.



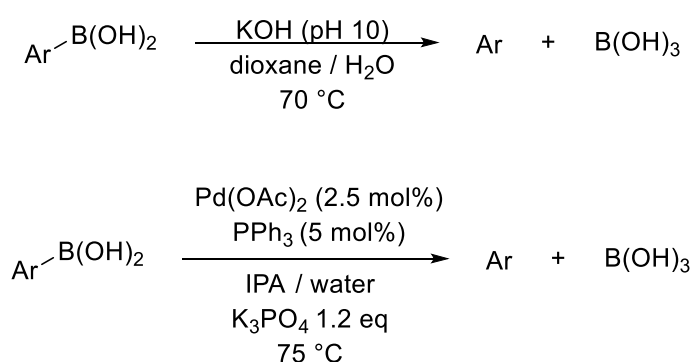
**Scheme 48:** Standard Suzuki conditions selected for catalyst screening of troublesome boronic acids

The aryl halide 4-bromoanisole was chosen due to ease of  $^1\text{H}$  NMR analysis in conjunction with being applicable to industrial reactions which do not regularly use iodide leaving groups. The bromide is likely to provide high enough conversions and rates to detect a differential between the bases, while not being too high to measure changes via GC kinetic sampling. The boronic acid loading and base loading were reduced to 1.05 and 1.25 equivalents respectively to maximise any difference in boronic acid protodeboronation. The catalyst loading was also reduced to 2.5 mol% to highlight any effect on deactivation or stabilisation. IPA /water was used as a green solvent mixture viable for industrial use, and the reaction was run at 75 °C, slightly below the boiling point of the water/IPA azeotrope to ensure uniform sampling.

Before conducting the reactions using the standardised conditions, we must first investigate whether the half-lives in the literature do agree experimentally with values taken under true reaction conditions.

### 4.2.3 Validation of boronic acid half-life

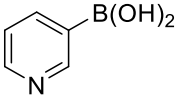
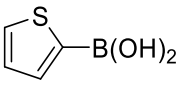
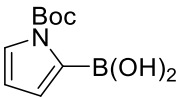
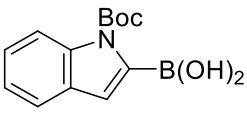
All protodeboronation rate measurements conducted by Lloyd-Jones and co-workers had been conducted in a 1:1 water / dioxane mixture at 70 °C.<sup>22, 35</sup> The protodeboronation rate is likely to be affected heavily by solvent and temperature, as well as actual components of the coupling reaction. New data on protodeboronation rate in reactions which include the catalyst, ligand as well as the base and solvent was gained using the homologated conditions without the aryl bromide to ensure no boronic acid was lost to the coupling reaction.



**Figure 70:** Comparison between GLJ (top) and BNN protodeboronation (bottom) reaction conditions

Incorporating the catalyst complex into the protodeboronation reactions to deduce the rate of decomposition under reaction conditions allows the model to be more applicable to Suzuki coupling reactions and give a more direct estimate on how long the reaction is expected to last under standard conditions. In addition, using a weak base and appropriate equivalence means the pH is very similar to that in the full reaction conditions incorporating the aryl bromide itself.

**Table 17:** Validation of  $t_{1/2}$  using coupling reaction conditions

Boronic acid	$t_{1/2}$ under standardised conditions	$t_{1/2}$ under GLJ conditions (pH 12)
	>17 hr	2 days
	1 hr	1.5 hr
	>5 min	5 min
	30 min	N/A

The authors chose to analyse run their reactions using online  $^{11}\text{B}$  or  $^1\text{H}$  NMR to gain their half-life measurements,<sup>22</sup> however we chose to neutralise the reaction by sampling 50  $\mu\text{L}$  into 2 mL acetonitrile, at room temperature thereby reducing concentration by 40 times and temperature from 75  $^\circ\text{C}$  to ambient, followed by immediate run on off-line GC to ensure no further protodeboronation had taken place.

The numbers for these reactions are all within a factor of two compared to the literature conditions, which would suggest that the literature figures are robust enough to use as a guideline for rates of protodeboronation under standard reaction conditions, and classifying into categories of which boronic acids are likely to benefit from stabilisation of the C-B boronate bond via the base anion or cation.

#### **4.2.4 Classification of boronic acids**

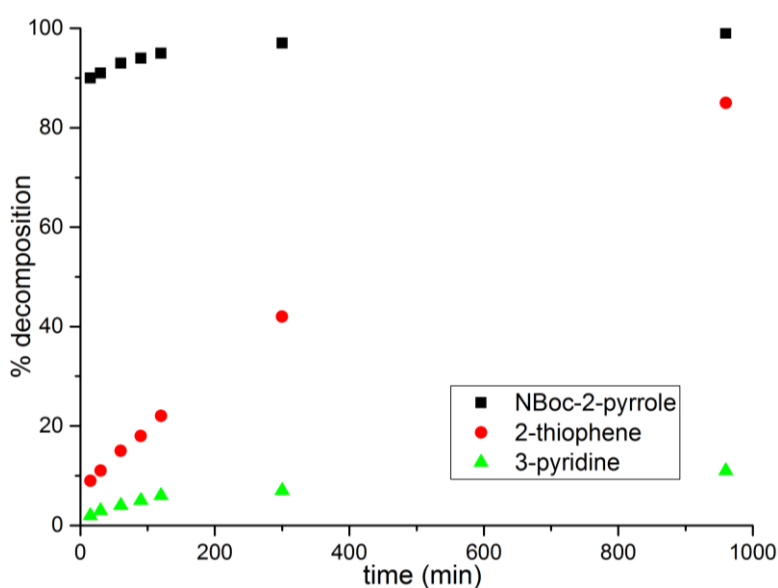
We elected to separate the boronic acids into three classes, the first of which being boronic acids which were broadly resistant to protodeboronation over the reaction timescale (17 h). These boronic acids had literature  $t_{1/2}$  of over 6 h, so would generally still be able to reach high conversions under normal reaction protocol as by the end of the reaction only some of the unreacted boronic acid would have undergone protodeboronation. These class 1 boronic acids are not discussed in depth herein, as

the standard protocol using conventional catalyst and base was satisfactory to gain reasonable to good yields of product.

Class 2 boronic acids were those with a  $t_{1/2}$  between 0.5 h to 6 h. These boronic acids generally exhibit high concentrations of active boronic acid at the start of the reaction, where decomposition occurs throughout the reaction, with the vast majority of the unreacted boronic acid undergoing decomposition to the parent aryl by the end of the 17 h reaction. These boronic acids decay at a sufficiently slow rate that they can be mediated by use of more active catalyst systems, and stabilisation of the boronic acid will increase conversion later into the reaction over unstabilised examples.

Class 3 boronic acids are those which undergo rapid protodeboronation, whose  $t_{1/2}$  is below 0.5 h, with some possessing literature  $t_{1/2}$  as low as 2.6 ms in a water dioxane mixture at high pH of over 12.<sup>35</sup> These boronic acids are particularly susceptible to protodeboronation and will decompose rapidly unless remedial action is taken in the form of protection of the boronic acid or another method to increase rates or stabilise this protodeboronation. We elected to investigate caesium phosphate monohydrate as an additional method to increase reaction conversions instead of boronic acid protection or catalyst activation in these troublesome examples.

**Figure 71:** Representative protodeboronation rates for Class 1-3 boronic acids (Figure 70, Table 17)



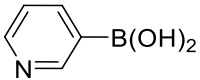
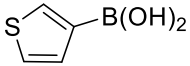
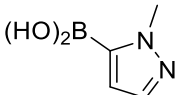
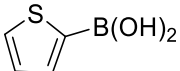
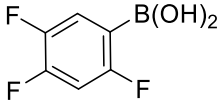
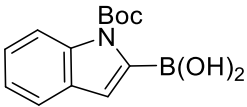
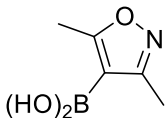
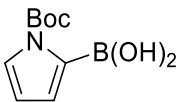
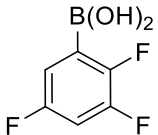
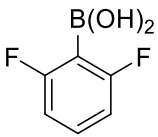
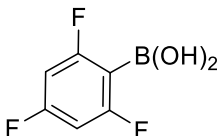
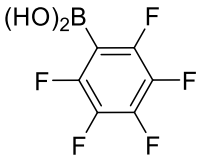
As observed even at the reaction end point, over 85% of the boronic acid concentration remains when using class 1 boronic acids, whereas when using class 2 boronic acids

there was only 15% of the boronic acid concentration left by reaction end point, meaning that a significant proportion of the boronic acid is liable to decompose unless the reaction is fast or the boronic acid can be stabilised. In the class 3 example even at the first sample point of 15 minutes over 90% of the boronic acid had decomposed into parent aryl and boric acid. To gain even modest yields using these boronic acids the reaction needs to be very fast, facilitated by increased activity of the palladium catalyst, or stabilisation of the boronic acid to increase  $t_{1/2}$ .

#### **4.2.5 Boronic acid selection for screening**

The low equivalencies of the base and boronic acid increase any difference between potential bases, keeping boronic acid excess down also reduces reaction cost as minimal reagents are lost in the reaction. A total of 7 heteroaromatic boronic acids, and 5 polyfluorinated boronic acids were chosen which included 2 class 1, 4 class 2 and 6 class 3 boronic acids in total.

**Table 18:** Boronic acids chosen for kinetic run to probe base effect (Scheme 48)

Entry	Boronic acid	$t_{1/2}$ literature	Classification
1		2 days (>17 hr expt, Table 17)	Class 1
2		10 hr	Class 1
3		90 min	Class 2
4		60 min (60 min expt, Table 17)	Class 2
5		60 min	Class 2
6		N/A (30 min expt, Table 17)	Class 2
7		15 min	Class 3
8		5 min (<5 min expt, Table 17)	Class 3
9		10 min	Class 3
10		5 sec	Class 3
11		1 sec	Class 3
12		2.6 ms	Class 3

Each of these boronic acids has been investigated under the standard conditions against caesium and potassium phosphates and carbonates (Scheme 48). There are two main possibilities of direct base interaction with the reaction substrates allowing access to higher yields in these Suzuki couplings. We would expect differences based on anion change due to different  $pK_a$ 's of the anion effecting solution pH and therefore protodeboronation rate,<sup>35</sup> but this is not a direct involvement of the cation or anion and merely involves changing the rate at which the  $\text{OH}^-$  anion is formed, along with changing the equilibria of hydroxide anion formation based on  $pK_a$  (Figure 58).

Interaction between the base cation and the catalyst could cause a change to a different mechanism or acceleration of the rate determining step based on stabilisation of catalytic intermediates, which would then present as an increase in initial rate and overall conversions. Because of the relative rates of protodeboronation and coupling reaction this would most likely have the largest effect in class 1 and 2 boronic acids, as class 3 examples may undergo the protodeboronation reaction at a faster rate than the active catalyst can perform the coupling reaction. In reactions where the boronic acid did not decompose fast, we would expect a similar rate increase in all examples studied regardless of  $t_{1/2}$  as the catalytic intermediate will be the same. A Cs-Pd species has been found by XRD studies in a C-H carboxylation reaction,<sup>36</sup> so a similar species may be present here to improve reaction rates in Suzuki reactions with boronic acids prone to protodeboronation reactions.

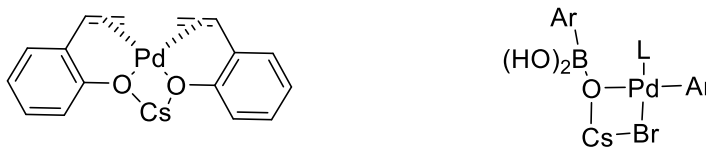


**Figure 72:** Illustration of catalytically active Pd-Cs species in literature (left),<sup>36</sup> and proposed Pd-Cs species observable in  $^{31}\text{P}$  NMR (right), (Scheme 42)

From the  $^{31}\text{P}$  and  $^{133}\text{Cs}$  NMR studies (Figure 64), any Pd-Cs species would likely involve stabilising the boronate addition of the boronate pathway (Figure 58) which would then be able to speed up reaction rates due to reducing the activation barrier to the rate determining transmetallation step.

If the base was able to interact with the boronic acid in solution and stabilize the C-B bond, slowing the relative rate of protodeboronation we would expect an increase in

overall yield due to increased [boronic acid] over the reaction timescale. We would not however expect the initial rate to increase if this were the method of interaction, as the maximum rate would be at  $t=0$ , with all boronic acid in solution before decomposition. If this were the method of activation we would expect class 3 boronic acids to have the largest increase in conversion when the stabilisation occurred, and much less in less sensitive examples.

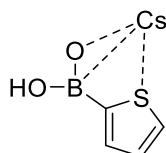


**Figure 73:** Example of possible Cs-B species reducing protodeboronation rate in troublesome Suzuki cross coupling reactions

As the caesium cation can interact with the boronic acid, it may be able to withdraw electron density from the C-B bond, thereby reducing protodeboronation rate. Previous literature reports had found that caesium clusters increase rates in catalytic reactions by reducing the transition state energy due to stabilisation of rate limiting transition states,<sup>37, 38</sup> though no caesium boronic acid species has previously been reported. Based on the work adapting literature procedures (Table 16), caesium C-B bond stabilisation appears less likely than phosphate anion stabilisation, but more work will be needed to validate this theory.

If we separate examples based on class, we can gain insight as how the bases can affect the reaction performance, and if there is a clear trend based on the class, we can make inferences as to which method of action is the dominant one.

#### 4.2.6 Class 1 boronic acids

**Figure 74:** Base screen of class 1 3-pyridylboronic acid using standardised conditions (Scheme 48, Table 18, Entry 1)

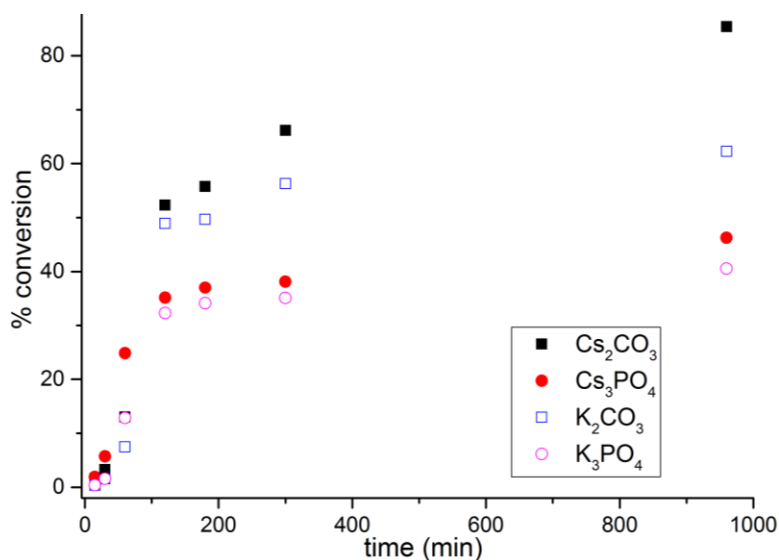
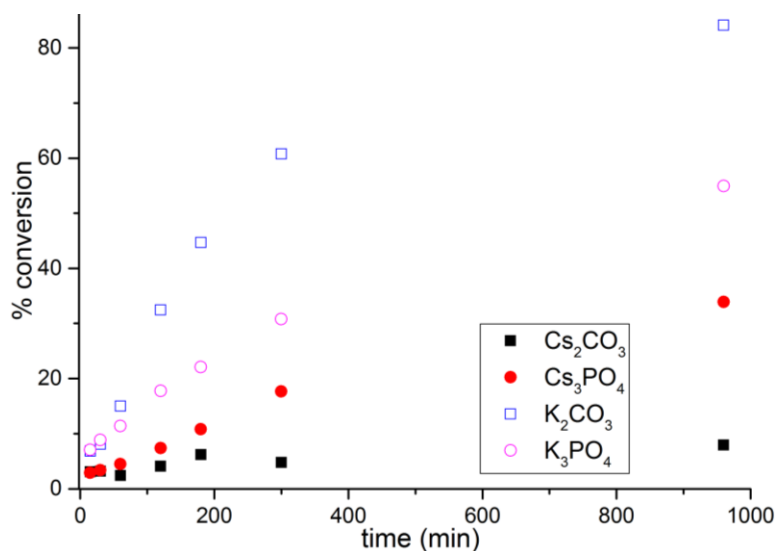


**Figure 75:** Base screen of class 1 3-thiopheneboronic acid using standardised conditions (Scheme 48, Table 18, Entry 2)



Both of the boronic acids under the standard reaction conditions would not fully undergo protodeboronation to the parent aryl. We can observe that caesium carbonate is the best base for the 3-pyridyl reaction and potassium carbonate the best base for the 3-thiophene reaction system. This lack of trend suggests that there is unlikely to be major stabilisation of the C-B bond or catalyst interaction via the cation

which is common to both reactions. These results suggest that the lower  $pK_a$  of the carbonate bases result in a lower reaction pH and therefore slower protodeboronation rate. This aligns with results found in the literature which suggests that for these boronic acid the rate of protodeboronation is highly dependent on the pH of the solution.<sup>22</sup> In both of these examples the boronic acid is in the 3-position to the heteroatom in the ring. This means the boronic acid carbon is electron deficient compared to the 2-position. We can observe that as a general trend carbonate bases are more effective in these electron deficient boronic acid examples, and further work must be conducted to elucidate whether the reverse is true for phosphates in electron rich boronic acids.

#### 4.2.7 Class 2 boronic acids

**Figure 76:** Base screen of class 2 *N*-Methyl-pyrazole-2-boronic acid using standardised conditions (Scheme 48, Table 18, Entry 3)

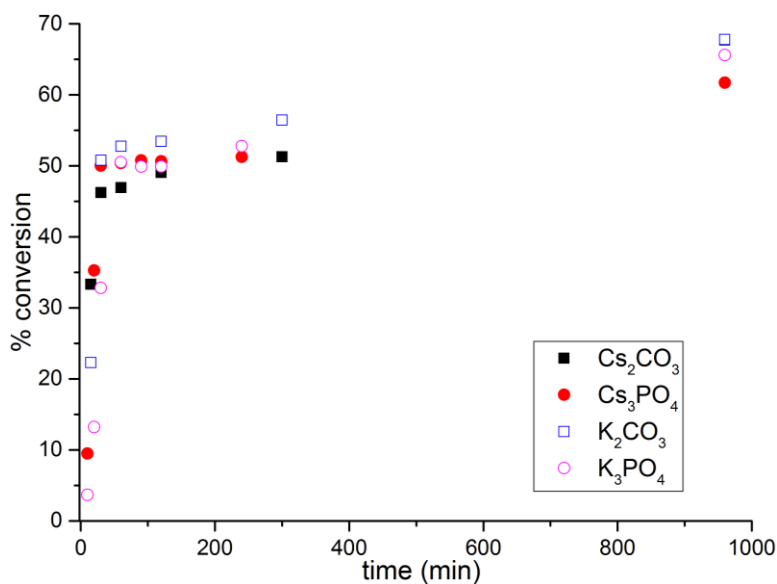


**Figure 77:** Base screen of class 2 2-thiopheneboronic acid using standardised conditions (Scheme 48, Table 18, Entry 4)

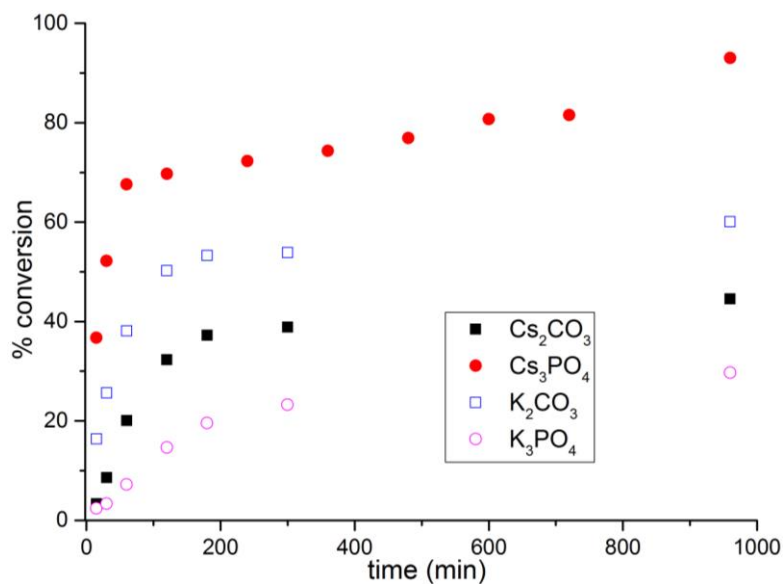


**Figure 78:** Base screen of class 2, 2,4,5-trifluorophenyl boronic acid using standardised conditions (Scheme 48, Table 18, Entry 5)

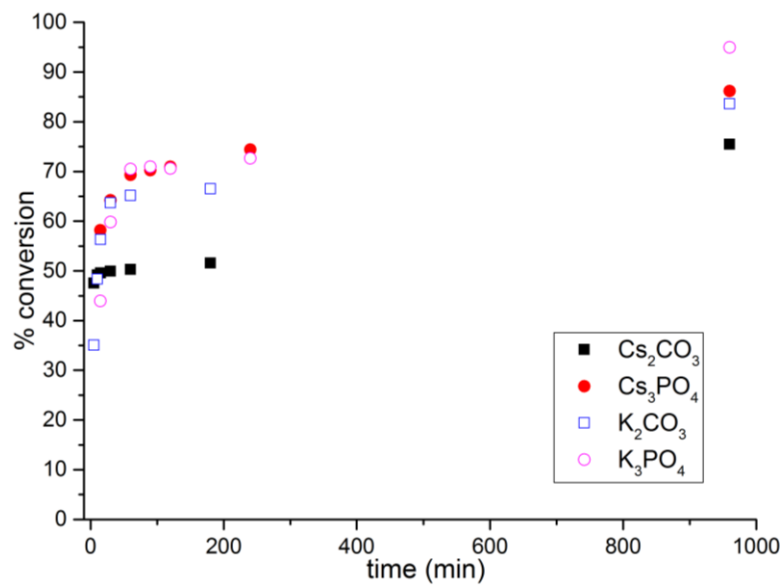
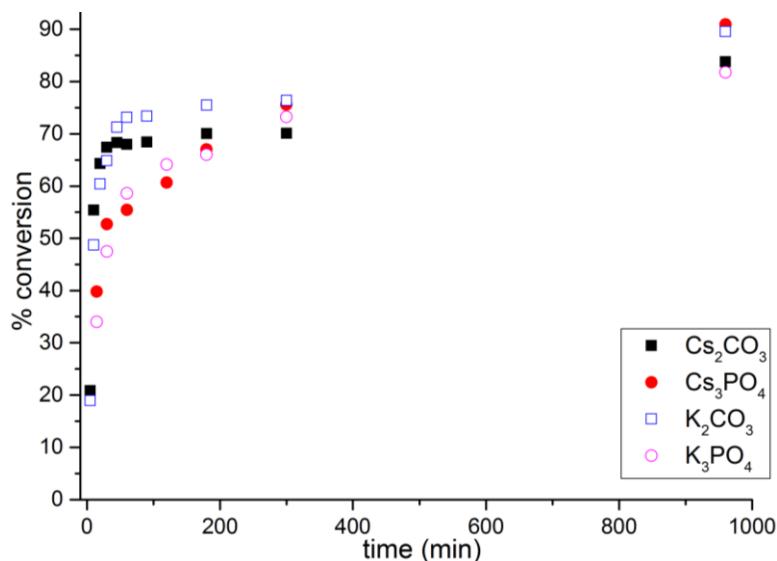


**Figure 79:** Base screen of class 2 *N*-Boc-indole-2-boronic acid using standardised conditions (Scheme 48, Table 18, Entry 6)



We can observe in these plots that the half-life of the boronic acid is not the only factor when assessing base effects in these systems. In the 2-thiophene example caesium phosphate monohydrate is clearly the superior base, gaining over 30% more conversion than the second best base of potassium carbonate, and possessing a much higher initial rate than all other studied bases. When using *N*-methylpyrazole and indole boronic acids however, the differences in the base become much more subtle, and while the initial rate appears to be fastest using caesium phosphate monohydrate and the pyrazole boronic acid, the difference is relatively small. Using these substrates the initial rate is also very high, therefore reducing reaction temperature may lead to a larger difference between bases if there is a significant change, due to a reduction in overall reaction rate as well as the protodeboronation rate.

When observing the indoleboronic acid, the carbonate base reactions have a fast initial rate, gaining 65% conversion by 20 minutes, but the phosphate bases, while initially slower, appear to continue turning over throughout the reaction. The inflection point at 60 minutes when using carbonate bases is not present using the phosphates, which suggests that the bases are able to stabilise the boronic acid so the conversion can increase even after the expected concentration of boronic acid is very low. Interestingly, in this example of the 2-indole boronic acid, the C-B bond is electron rich when the phosphate bases appear to stabilise the reaction. This agrees with data using class 1 examples. We would expect that if stabilisation of the boronic acid were the

primary factor in changing reaction performance, there would be an even larger effect when using unstable class 3 boronic acid substrates.

#### **4.2.8 Class 3 boronic acids**

**Figure 80:** Base screen of class 3 2,5-dimethylisoxazoleboronic acid using standardised conditions (Scheme 48, Table 18, Entry 7)

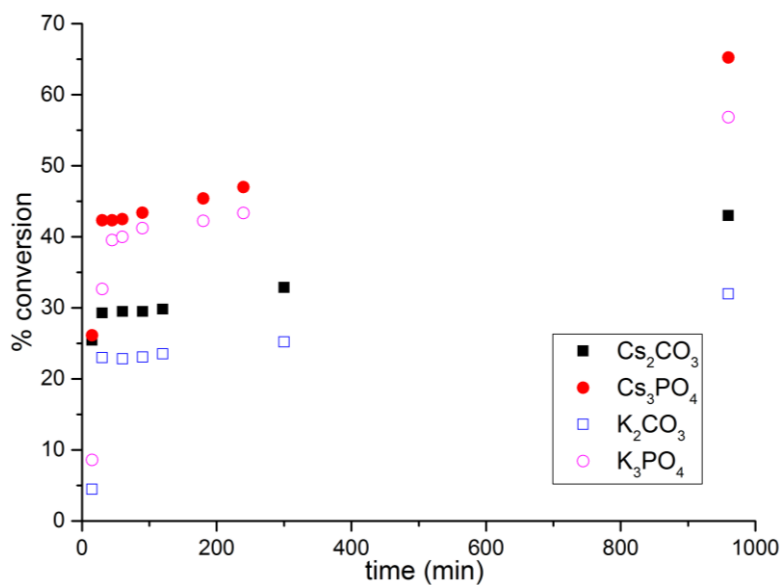


**Figure 81:** Base screen of class 3 *N*-Boc-2-pyrroleboronic acid using standardised conditions (Scheme 48, Table 18, Entry 8)

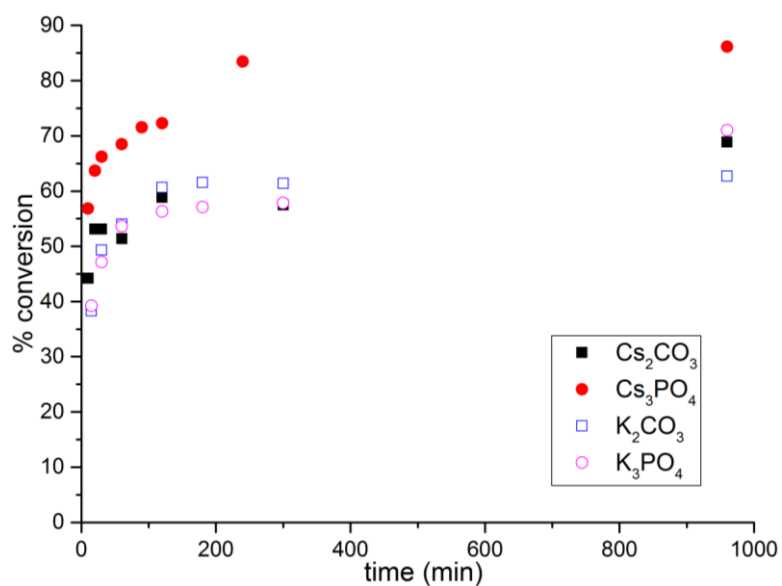


**Figure 82:** Base screen of class 3 2,3,5-trifluorophenylboronic acid using standardised conditions (Scheme 48, Table 18, Entry 9)

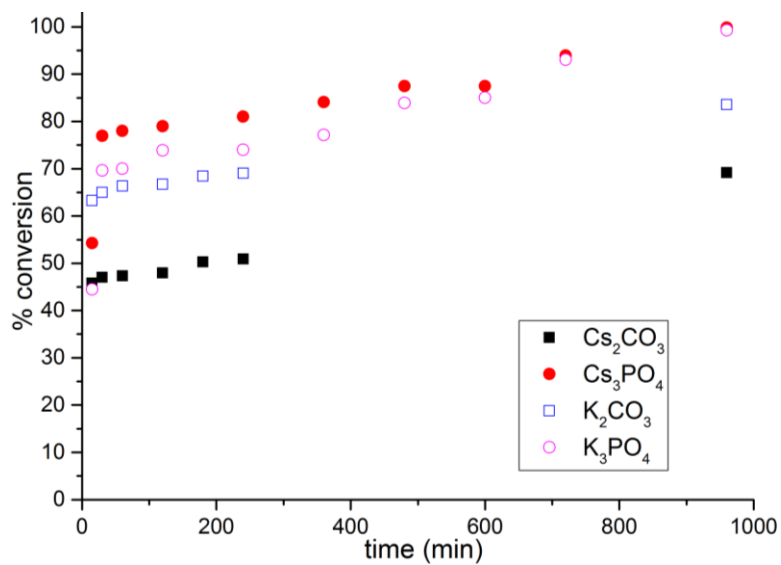


**Figure 83:** Base screen of class 3 2,6-difluorophenylboronic acid using standardised conditions (Scheme 48, Table 18, Entry 10)

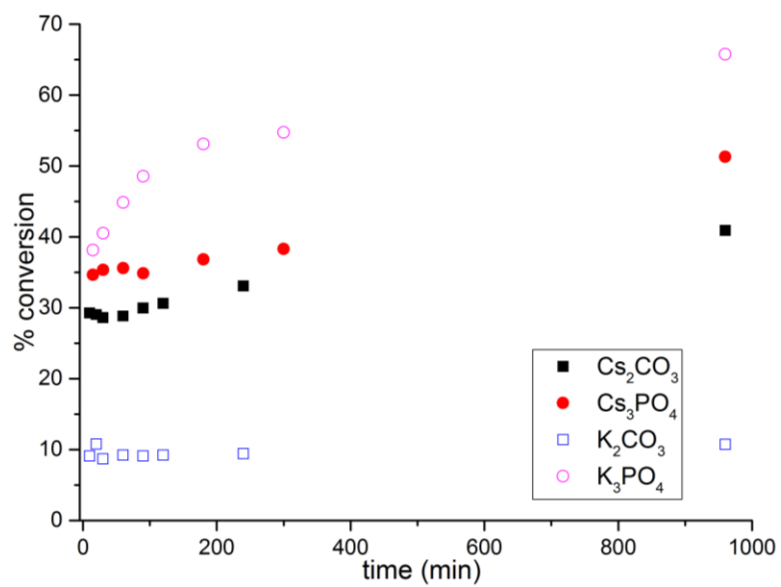
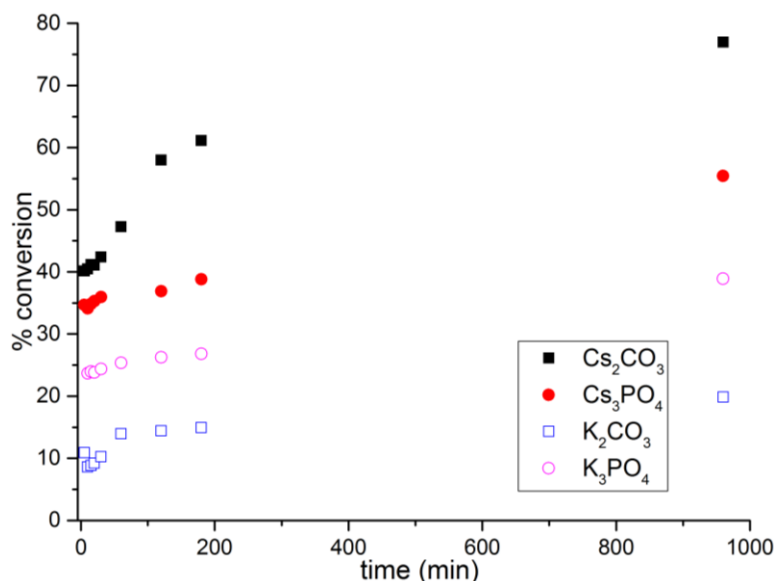


**Figure 84:** Base screen of class 3 2,4,6-trifluorophenylboronic acid using standardised conditions (Scheme 48, Table 18, Entry 11)



We can immediately see that in the non-fluorinated class 3 boronic acids the caesium phosphate monohydrate base reacts to give higher initial rates and conversions than all other bases, particularly in the pyrrole example. Notable in both of these non-fluorinated substrates is the ability for phosphate bases to keep the rate higher for a longer period, indicating as with the indole that there is a higher concentration of boronic acid until later into the reaction caused by C-B bond stabilization. We can infer from this data that the cation has a significant effect on initial rate of reaction in these examples but the stabilisation of the boronic acid is likely to be influenced more by the anion than the cation as when we observe inflection points in the kinetic data, the trend points to a phosphate effect rather than a caesium effect.

Interestingly, when using fluorinated phenylboronic acids, despite being class 3 there did not appear to be any acceleration at 75 °C using caesium phosphate. We do not see initial rates increased by use of the caesium or potassium cation as a general trend, nor do we observe significant stabilisation differences relative to the anion. When observing these boronic acids with short half-lives, clearly stabilisation does occur. Even though 2,6-difluorophenyl boronic acid possesses a listed literature half-life of only 5 seconds, the potassium phosphate reaction is able to continue at a significant rate until over 90 minutes.

The largest effect of increased reaction performance using caesium phosphate monohydrate appears to occur when the boronic acid position is electron rich. We see relatively poor performance of caesium phosphate monohydrate base in highly electron deficient fluorinated boronic acids, but good performance in 2-thiophene and *N*-Boc-2-pyrroleboronic acids where the C-B bond has increased electron density.

One factor present in several of the non-fluorinated boronic acid charts is the inflection point where the reactions transition from a higher rate to a lower rate. This does not appear to be affected by the base and therefore is likely to relate directly to the catalyst. This type of change in rate is indicative of a change in catalytic species from the ligated phosphine palladium species to palladium nanoparticles. This also corresponds to a colour change from orange to dark brown at a similar time in the reactions where this occurs.

Reactions were also run with pentafluorobenzeneboronic acid, however due to the incredibly short  $t_{1/2}$  of 2.6 ms, we were unable to gain any more conversion than 5% under any conditions tested, therefore the catalyst activation route may be the only way to ensure high conversions using this very unstable substrate. Carrow *et al.* has utilised cationic palladium precatalysts to successfully couple pentafluorophenyl boronic acid, though this had the downside of being highly air sensitive and requiring several steps to form the active 'on cycle' catalyst.<sup>25</sup>

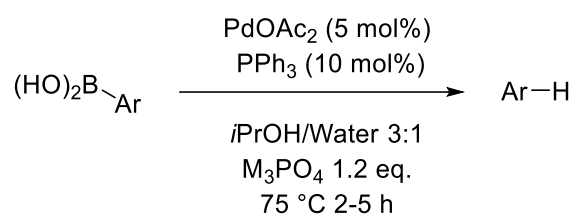
Based on these findings we hypothesise that any increase in performance gained by caesium phosphate base is likely due to two main factors. The caesium cation may be able to interact with the palladium catalyst, increasing reaction rates, and the phosphate anion may be able to reduce protodeboronation rates below those of carbonate anions in the examples shown.

#### **4.2.9 Cation influence on protodeboronation reactions**

To discover whether protodeboronation rate was changed by the cation or anion we conducted several reactions assessing the rate at which the boronic acid would undergo this hydrolysis using caesium and potassium phosphate. If the cation did influence the rate of protodeboronation we would expect a significant difference between the two studied bases, however if it was the phosphate anion which led to a

change in protodeboronation rate we would expect similar results using both bases. The change in anion leads to a change in reaction pH, so based on results from Lloyd-Jones *et al.* we would not expect a large rate differential based on cation change alone.

We selected 3 boronic acids (Table 18, Entries 3, 4 and 7) to deduce if any effect was made from the cation on protodeboronation rate. Each had increased performance using caesium phosphate monohydrate as a base, and appeared to have the protodeboronation rate slowed using phosphate bases only judging from the inflection point in the kinetic data. These substrates were selected for kinetic analysis, to deduce cation influence on boronic acid half-life, in contrast to previous work to deduce literature half-life robustness (Table 17).



**Scheme 49:** Conditions to assess extent of cation influence on protodeboronation rate

The relatively fast protodeboronation rates of 15-90 min in the literature negated the need for running reactions overnight, as the vast majority of the boronic acid was expected to decompose over the reaction time of ca. 4 half-lives.

**Figure 85:** Cation influence of protodeboronation rate on class 2 *N*-methylpyrazoleboronic acid

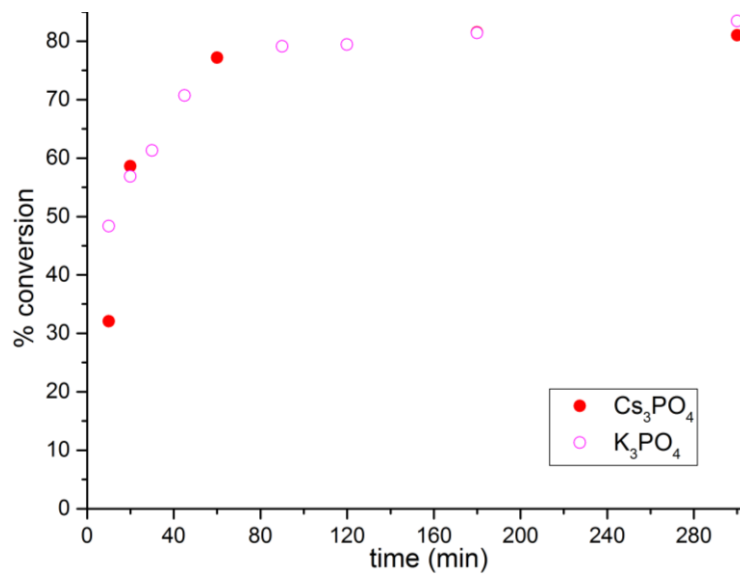


**Figure 86:** Cation influence of protodeboronation rate on class 2 2-thiopheneboronic acid

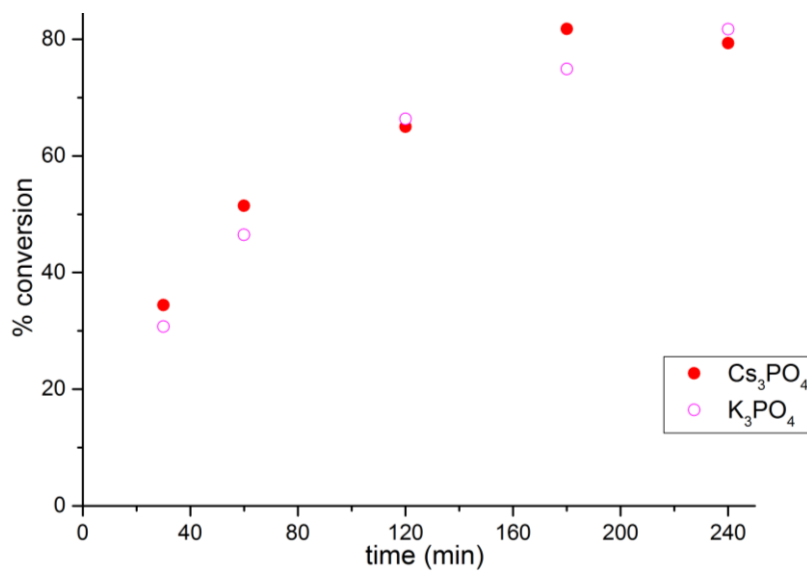
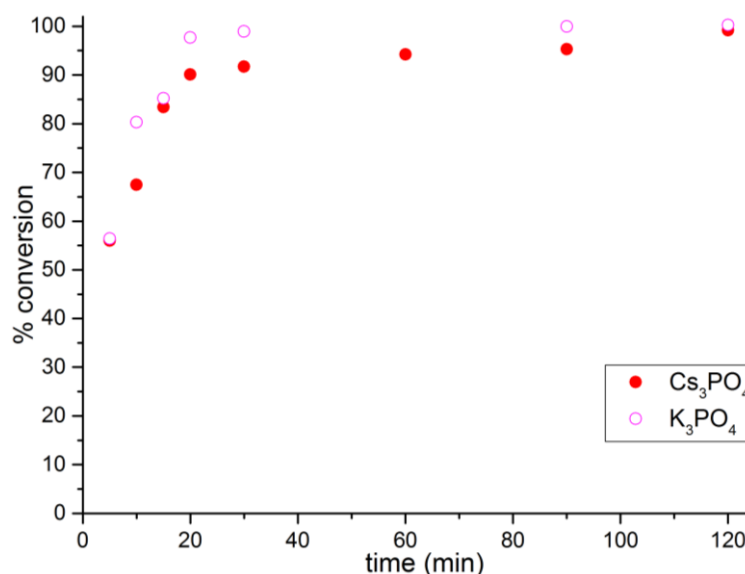


**Figure 87:** Cation influence of protodeboronation rate on class 3 3,5-dimethylisoxazoleboronic acid



Observing the initial rates of protodeboronation between the two bases, there appears to be very little change or obvious trend in the protodeboronation rate when changing the cation between potassium and caesium. This agrees with the literature where pH of solution was found to be the primary differentiating factor of protodeboronation rate.<sup>22</sup> This then indicates that the catalyst activation pathway is the primary influence of increased rate when changing cation, and the anion is able to change the rate of protodeboronation as the solution pH will change depending on base pK<sub>a</sub>.

To investigate the effect of the cation on the rate of the overall coupling reaction, and elucidate any decrease in energy barrier possible due to change in base cation, a number of boronic acids were selected for investigation at reduced temperatures of 15 to 20 °C to reduce overall rates of the coupling reaction. The lower temperature reactions cause a higher energy barrier for the reaction to overcome, leading to lower rates and increasing any difference between bases not seen at higher T.

#### 4.2.10 Lower temperature runs of coupling reaction

**Figure 88:** Lower temperature base screen of class 2 *N*-methylpyrazoleboronic acid

(Scheme 48, Table 18, Entry 3)

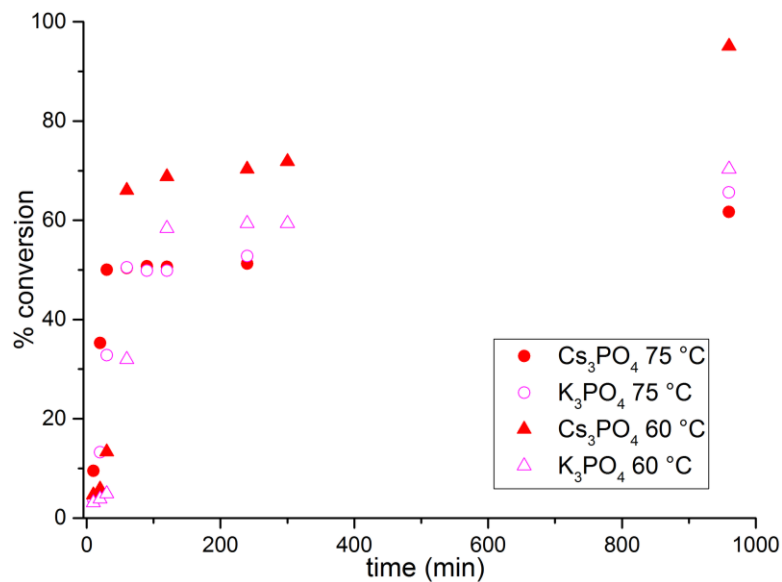


**Figure 89:** Lower temperature base screen of class 3 2,3,5-trifluorophenylboronic acid

(Scheme 48, Table 18, Entry 9)

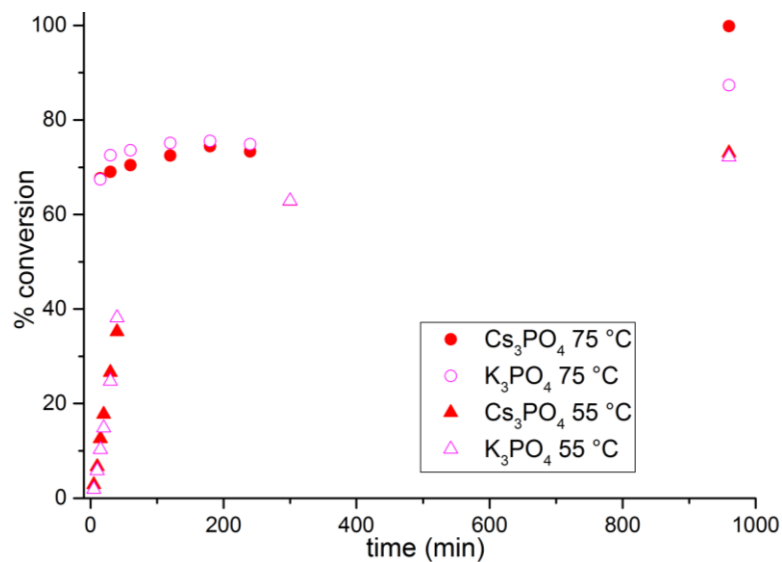
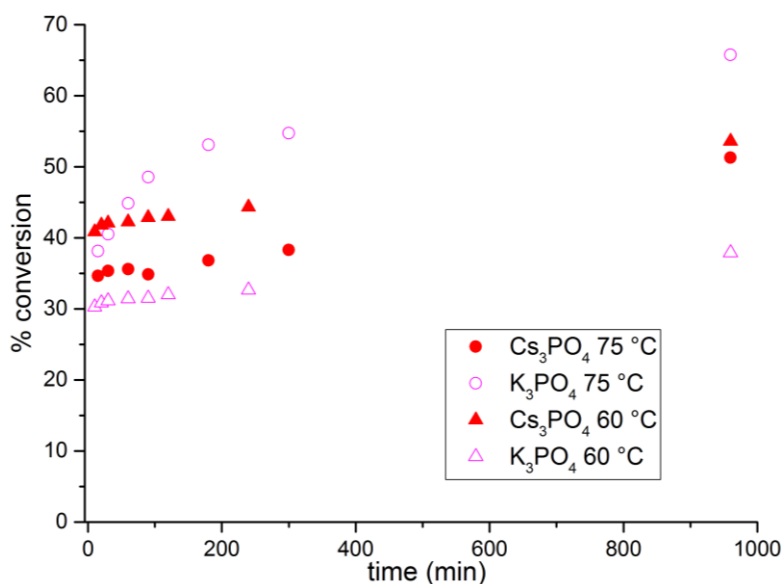


**Figure 90:** Lower temperature base screen of class 3 2,6-difluorophenylboronic acid  
(Scheme 48, Table 18, Entry 10)



In these examples of class 2 and 3 boronic acids where the caesium phosphate monohydrate base reactions could not achieve the same reaction performance as potassium phosphate under standard conditions at high temperature, the lowered temperature caused a large difference in overall conversion between the caesium and potassium bases, and in the case of *N*-methylpyrazoleboronic acid, the lower temperature actually increased overall conversion to the desired product. This increase in conversion at lower temperatures indicates that the rate of protodeboronation can be reduced by lowering reaction temperature, as well as the rate of the coupling reaction itself. The improvement of caesium phosphate monohydrate in this reaction over potassium phosphate indicates some subtle catalyst interaction that is not visible at the higher temperatures due to the low boronic acid half-life. The low initial rate, presumably due to some catalyst formation or ligation, leads to a much higher rate at 20 minutes into the reaction, after the reagents reach steady state.

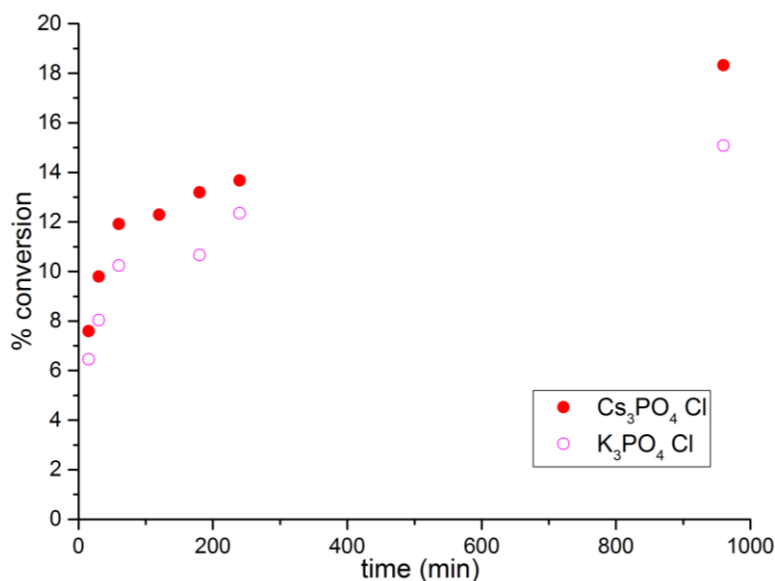
In addition to increasing the overall yield above that obtained under the standard conditions using *N*-methylpyrazoleboronic acid, the decrease in temperature increased the overall conversion for both phosphate bases. The caesium phosphate monohydrate initial rate at 60 °C was above all other bases regardless of temperature, with 5% higher conversion using caesium base at  $t=15$  min than the best base of potassium phosphate

at 75 °C. This further indicates that there is an observable 'caesium effect' where the initial rate is increased using caesium cation because of catalyst interaction.

#### **4.2.11 Chloride investigation**

Reducing temperatures with the goal of reducing the overall rate of the coupling reaction is one way to increase the differential in base performance in these reaction classes. An alternative method would be to decrease the rate of catalytic turnover by switching to a more challenging leaving group. The reaction of class 3 heteroaromatic 3,5-dimethylisoxazoleboronic acid had a small increase in initial rate imparted by caesium phosphate using the standard bromide conditions, so changing to a more challenging chloride leaving group could elucidate any underlying differences between the potassium and caesium cations.

**Figure 91:** 3,5-dimethylisoxazoleboronic acid chloride experiments using phosphate bases



Despite much lower conversions using the less active 4-chloroanisole, we can still observe caesium phosphate base providing faster initial rate and higher overall conversion by 5% in this reaction. The change in aryl halide suggests that any caesium effect in this reaction is not related to the aryl halide itself which rules out salt formation, and suggests that direct catalyst involvement is the primary factor influencing initial rate of reaction.

#### **4.2.12 Reaction Scale-up**

The knowledge gained by reducing the reaction temperature, changing boronic acid half-life and changing the leaving group allows us to infer certain methods of action of increased performance of base cations or anions in these troublesome Suzuki cross coupling reactions. What changing the substrates does not achieve however, is how the organic solubility and mass transfer between phases can influence reaction performance.

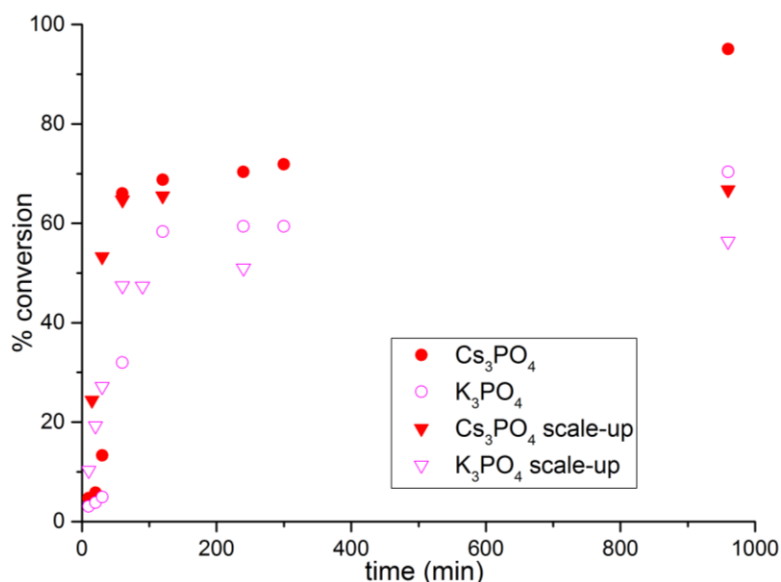
Generally when conducting reactions on a larger scale, mass transfer limitations have to be taken into account. Baffles can be used in larger reactors to increase stirring efficiency, provide better heat exchange and promote reaction mixing due to vortex formation. In smaller reactors, different mixing strategies such as overhead stirrers or cross bladed magnetic followers can be used to enhance mass transfer, but if all factors were kept the same the heat and mass transfer as well as mixing would be reduced at scale compared to smaller scale reactions.

We chose to scale up the Suzuki coupling reaction involving *N*-Methylpyrazoleboronic acid and 4-bromoanisole, using caesium and potassium phosphate bases. As the reaction vessel was changed from a Schlenk flask to a round bottom flask and the scale was increased by 4, the mass transfer of the reaction will be reduced, therefore organic solvent solubility of the bases will become a larger factor in overall reaction conversion. The larger scale of the reaction means the split solvent layers will have less surface area relative to the reaction vessel size, and so will reduce reaction rates if the base is present in the rate determining step and has lower organic solubility.

We could increase the mass transfer of the reaction by increasing the stir rate or using an overhead stirrer, but keeping these external mixing factors the same between runs we can gain a picture of how organic phase base solubility can influence the reaction. We would infer if there is a large differential between the cations at a larger scale when there was not in the original small scale reaction, that this solubility effect is a major factor in all reactions in this class. Conversely if the scale-ups show little difference between the cations compared to the smaller scale reactions, organic solubility is not the cause of increased reaction performance and therefore the soft-hard cation and

anion interactions are nullified, so the change in reactivity must be due to the catalyst or boronic acid itself.

**Figure 92:** Effect of scale-up on mass transfer of Suzuki reactions of *N*-methylpyrazoleboronic acid from 1 mmol to 4 mmol (Scheme 48, Table 18, Entry 3)



We can observe that when the reaction is run on larger scale using the same mixing methodology the overall conversion decreases for both caesium and potassium bases. While the bases appear to have similar initial rates after scale-up to their counterparts on smaller scale, the reactions stop turning over at 2 hours. This would indicate that the boronic acid is less able to be stabilised when mixing is less effective. This is then in agreement with the observation that protodeboronation is facilitated by hydroxyl attack, which occurs in the aqueous phase. Due to lower organic phase solubility and lower probability of base deprotonation in the organic phase, the pH of the organic phase is higher, which means the boronic half-life reduced relative to standard conditions. This observation agrees with the existing literature dictating reaction pH as a major factor into protodeboronation rate. While we see lower conversions using both bases when the reactions are scaled-up, there doesn't appear to be a large differential between the cations, indicating that there is not a large difference in organic phase solubility when changing cation which affects the overall reaction conversion. Clearly we can observe that mixing is highly important to the reaction with regards to mass

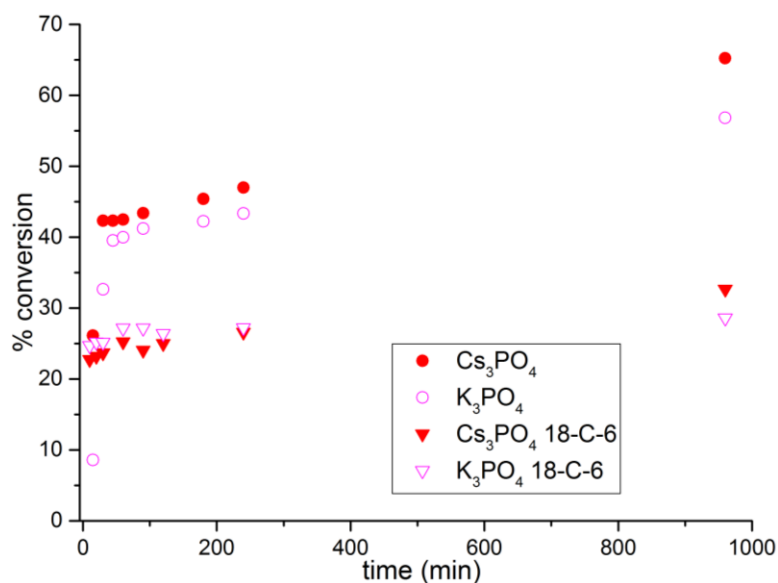
transfer, but as both bases are affected similarly this may be due to the mass transfer of the boronic acid into the organic layer for transmetalation rather than the base itself.

#### **4.2.13 Investigation into increased solubility imparted by crown ethers**

Increasing reaction volume relative to surface area and mixing has the effect of decreasing organic to aqueous phase transfer. This is due to reduced contact area of the phase boundary. Theoretically if the organic phase solubility of the base can be increased, the reaction rate will increase if the base cation or anion are involved in the rate determining step. One method to increase organic phase solubility is via complexing the cation with the crown ether ring. This then allows the anion to react readily in solution and is known as the 'naked anion effect'.<sup>39-41</sup>

Both caesium and potassium phosphate were investigated, with 3,5-dimethylisoxazoleboronic acid selected as an example where caesium cation bases can access higher yields than potassium bases. We would expect the reaction performance to be increased if the increased organic phase solubility imparted by the crown ether complexation was a major factor influencing the reaction, conversely if the caesium or potassium cation was interacting directly with the palladium catalyst, the complexation with crown ether may actually reduce this effect and thereby reduce the rate of the reaction.

**Figure 93:** Effect of crown ether complexation on coupling reaction of 3,5-dimethylisoxazoleboronic acid with 4-bromoanisole using standard conditions (Scheme 48)



The inclusion of crown ether complexes clearly reduces the overall conversion of the reaction in this case which indicates that complexation of the cation negatively impacts the rate of reaction using both potassium and caesium bases. The increased initial rate imparted by the caesium cation also appears to be negated by this complexation, which provides evidence that the cation needs to be in solution to interact with the catalyst. These results would also suggest that the cation is very important to reaction rate, and possibly that both caesium and potassium can interact with the palladium catalyst, but the caesium interaction is larger in some cases allowing for an increase in conversion at the end of the reaction. Similar results have been found by DFT by Musaev *et al.* who found that incorporation of a caesium cation in DFT calculations of a C-H activation reaction sped up the reaction by 3 fold, whereas incorporation of a potassium cation did speed up the reaction, but by only 10% over the non-cation accelerated example.<sup>42</sup> When this cationic interaction is minimized similarly to the crown ether effect, for example with an organic phosphate base, we would expect a similar non-stabilised conversion to the crown ether reactions.

#### 4.2.14 Improvement of API procedure

Based on promising evidence of caesium phosphate monohydrate utility in heteroaromatic Suzuki cross couplings, the decision was made to implement caesium phosphate in an active project API synthesis involving a late stage Suzuki reaction with heteroaromatic boronic acid. AZD3293, or lanabecestat, is a BACE-1 inhibitor which recently underwent phase III clinical trials in the fight against Alzheimer's disease.<sup>43-45</sup> The existing procedure had utilized potassium phosphate as the base and achieved good yields, but could not overcome a 30 minute induction period at the start of the reaction. If we could remove this induction period using caesium phosphate monohydrate as a base, the reaction would proceed faster and more cleanly, removing hydrolysis side products occurring as the reaction progresses.

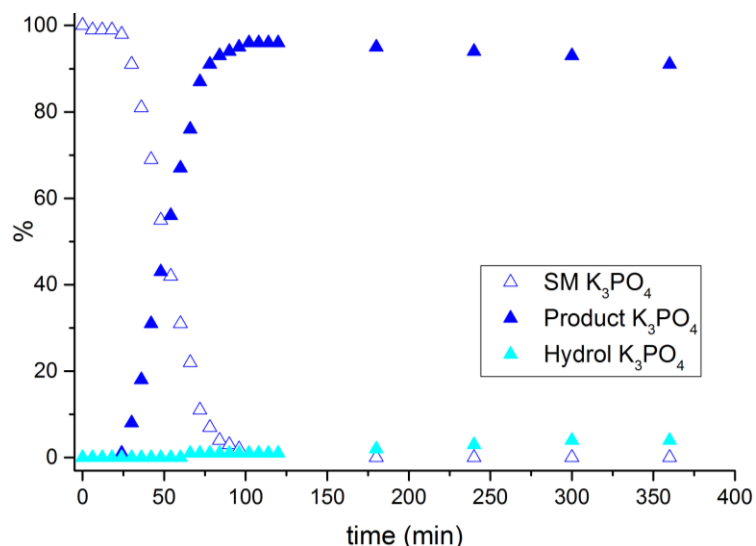
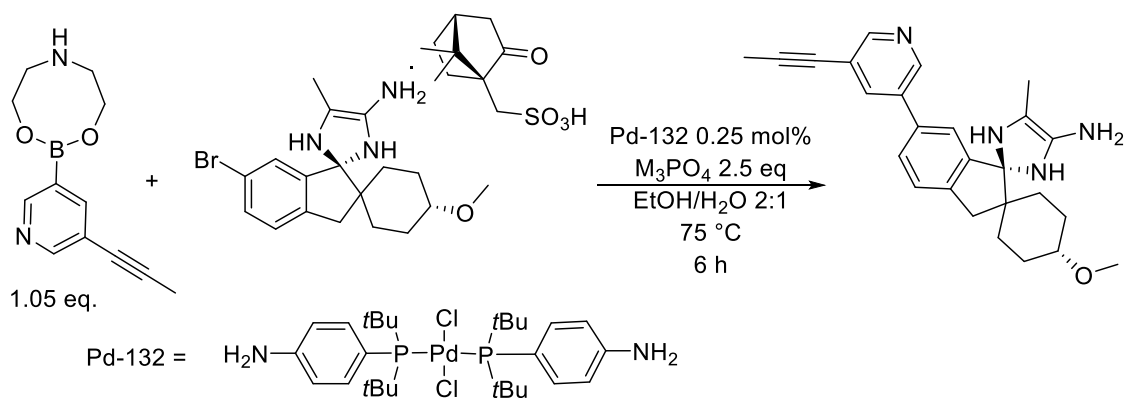
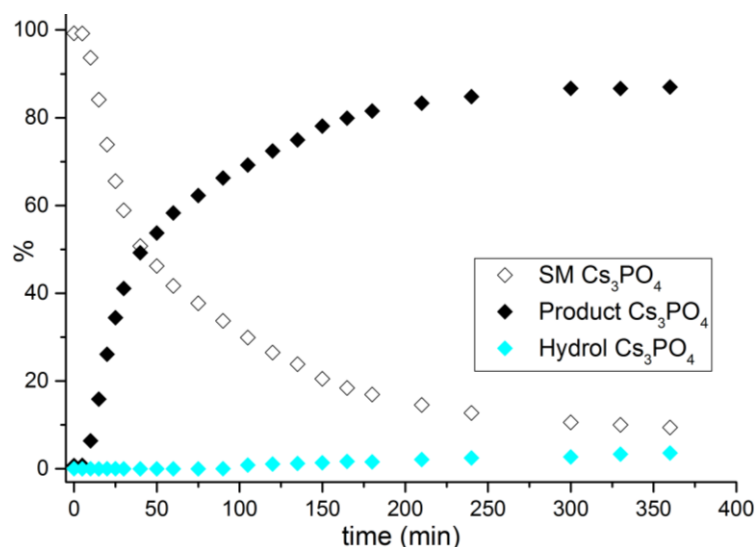


**Figure 94:** AZD3293 final step reaction screening existing procedure and kinetics using K<sub>3</sub>PO<sub>4</sub> base

Following the existing procedure the maximum conversion occurs at 100 minutes, giving 96% conversion. However at process scale the decision to run the reaction for 6 hr was taken to ensure complete conversion of the starting material. This results in a 5% drop in conversion to 91% at reaction completion, with 4% of the hydrolysis product present. We can observe the 30 minute induction period at the start of the reaction which we hope to reduce using caesium phosphate monohydrate base (Figure 95).

**Figure 95:** Caesium phosphate monohydrate effect on induction period of AZD3293



The use of caesium phosphate in this reaction successfully reduced the induction period from 30 minutes to 5. While overall conversion was slightly lower than potassium phosphate at 87%, the hydrolysis product was also lower, at 3%. At the end of the 6 hr reaction there was 10% starting material remaining, indicating that maximum conversion could be as high as 97%. This suggests that if optimisation to increase the conversion of caesium phosphate was made the reaction yields could be increased above the existing literature procedure.

The reason for the shorter induction period is likely to depend on the caesium cation accelerating the pre-catalyst activation, producing the active oxopalladium species which can then undergo oxidative addition to the boronic acid. DFT calculations had previously been conducted in the Grisorio group to suggest that decreased orbital overlap of M-OH could increase the rate of precatalyst activation due to decreased stabilisation of the intermediate after OH<sup>-</sup> attack on the palladium, and due to caesium's large cationic radius the activation pathway is faster, decreasing the induction period.<sup>12</sup>

### **4.3 Conclusions & future work**

The transmetallation step in Suzuki-Miyaura cross couplings has previously shown to be rate limiting in computational and mechanistic studies.<sup>6, 8, 10</sup> This step can be relatively complex with multiple possible pathways, the relative rates of which can alter dependant on electronic effects of the reagents (Figure 58).<sup>12</sup> We elected to run a base screen of a reaction forming 4-methoxybiphenyl with caesium and potassium phosphates and carbonates to further understand the rate limiting transmetallation step, and in particular the effects of base cation and anion on reaction rate and overall yield (Scheme 38).

When the aryl iodide was used, the reaction involving caesium phosphate monohydrate was found to be the fastest, with an initial rate 1.7 times that of the next fastest base caesium carbonate, and 2.1 times that of potassium phosphate base. Both caesium base reactions were faster than their potassium equivalents which indicates that there is a direct cation interaction of the caesium with the rate limiting transmetallation step. Previous work had indicated metal cation acceleration of oxo-palladium species (Scheme 39) was possible,<sup>12</sup> so it is likely that the base can stabilise the transition state forming the palladium hydroxide species before boronic acid addition. There was also a significant anion effect in these reactions, where phosphates performed significantly better than carbonates. This is likely due to the higher  $pK_b$  of the phosphates in aqueous media, providing 100x the concentration of  $HO^-$ , resulting in a faster transmetallation rate forming the active oxo-palladium complex.

The aryl chloride was too challenging to gain reasonable conversions with all bases, giving less than 10% conversion under the reaction conditions. When the aryl bromide was utilised however, a carbonate anion effect was found, with the cation not appearing to alter the reaction rate or yield significantly. The higher concentration of hydroxide gained by use of more basic phosphate bases may actually be altering the equilibrium of boronic acid to boronate (Figure 61). The presence of the boronate disallows the oxo-palladium pathway, so the boronate must undergo addition to the palladium resulting in removal of the bromide as the rate limiting step. When using the phosphate bases an induction period was observed, which was monitored by  $^{31}P$  NMR (Figure 63), and observed to be slow formation of the oxo-palladium boronate species due to the nucleophilic character of the phosphate anion (Figure 62).

A base screen was conducted on Suzuki reactions involving boronic acids which were prone to protodeboronation under catalytic reaction conditions. Due to the increased initial rate of the screening reaction using caesium phosphate monohydrate (Figure 59), reactions were investigated to assess if this base could avoid the need for catalyst activation or boronic acid protection as primary methods to gain acceptable yields in reactions with these troublesome boronic acids.

Caesium phosphate monohydrate was found to be the optimal base in a reaction involving 3-pyridyl boronic acid, gaining higher yields than the optimised procedure in the literature (Scheme 47),<sup>27</sup> so further investigations were warranted to deduce in which examples the synthesised caesium base was more effective than conventional bases. When conducting reactions replicating literature bases which had undergone a base screen, caesium phosphate monohydrate was found to be the optimal base using both *N*-Boc-2-pyrrole and *N*-Boc-2-indole boronic acids, gaining over 40% more conversion than the optimal base in the literature in the case of *N*-Boc-2-pyrroleboronic acid (Figure 68).<sup>31</sup> Based on the observed trends versus the literature reactions (Table 16) we hypothesise that the rate of protodeboronation is likely base anion dependant, whereas the rate of the coupling reaction and therefore initial rate is likely base cation dependant.

A total of 12 boronic acids were classified into 3 classes based on propensity for protodeboronation and run according to standardised conditions with the 4 studied bases (Table 18). Results using class 1 boronic acids which were not prone to decomposition, indicated that carbonate bases were superior when the C-B boronic acid bond was electron poor. Use of the class 2 boronic acids, particularly *N*-Boc-indole-2-boronic acid (Figure 79), indicated that the reaction would turnover for an extended period when the boronic acid C-B bond was electron rich, indicating a phosphate stabilisation effect.

When utilising class 3 boronic acids, which undergo protodeboronation at a significant rate ( $t_{1/2} < 30$  min), caesium phosphate monohydrate base was found to be the most effective in electron rich boronic acid substrates, whereas the electron poor fluorophenyl boronic acids did not appear to show an obvious trend in either base anion or cation.

Caesium phosphate monohydrate was utilised in a key step Suzuki cross coupling in the formation of Alzheimer's drug candidate Lanabecestat. The existing procedure was subject to a significant 30 minute induction period using potassium phosphate (Figure 94), however when caesium phosphate monohydrate was used in the reaction this induction period was lowered to approximately 5 minutes (Figure 95). This change is likely based on a stabilisation of the precatalyst activation to the active oxo-palladium species by the soft caesium cation.

Caesium phosphate monohydrate was shown to be an effective base in Suzuki-Miyaura cross coupling reactions involving an aryl halide coupling partner. The increased initial rate gives this base a useful role when using boronic acids which are prone to protodeboronation. When conducting reactions using electron rich boronic acids, the use of phosphate anion can allow extension of the half-life of the boronic acid, and the caesium cation can allow for increased rates, which is thought to be due to direct interaction with the catalyst. This information may allow researchers to utilise caesium phosphate base in reactions as a facile method to gain high yielding reactions using unstable boronic acids, and represents an alternative pathway to avoid precatalyst activation or boronic acid protection.

Further work on the transmetalation step in Suzuki-Miyaura reactions would benefit from the use of additional base cations and anions in addition to the four bases studied. The acceleration in rate caused by caesium bases in the reaction involving 4-iodoanisole (Figure 59), would benefit from use of both sodium and rubidium cations to better understand the full trend of cation mediated rate acceleration.

When using the 4-bromoanisole substrate (Figure 60), the proposed boronic acid  $\leftrightarrow$  boronate equilibrium hypothesis could be probed by using anions of differing  $pK_a$ 's, particularly hydroxides and fluorides, to gain a better understanding of whether reaction pH would cause the observed initial rate slowdown. In addition to this, when using either aryl halide, only a single palladium precursor and ligand were used, so changing to a more activated catalyst to alter the electronics at the palladium centre, and therefore gain more data on how the metal hydroxide mediated oxo-palladium formation can occur would benefit the project.

Future work would benefit from additional NMR studies, particularly on new style Bruker Avance spectrometers capable of heteroatom-heteroatom correlation experiments. This would enable experiments to be conducted to gain conclusive evidence of a Pd-Cs species by observing a  $^{31}\text{P}$  -  $^{133}\text{Cs}$  correlation in the palladium region of the phosphorus NMR. Alternatively, experimental evidence of a Pd-Cs bimetallic intermediate could be gained by XRD measurements of a crystal formed by a stoichiometric reaction of the caesium base with the palladium precatalyst, after oxidative addition.

The rate of protodeboronation of boronic acids was thought to be anion dependant, however when investigating the protodeboronation reactions only the base cation was changed, showing little difference between the two cations studied (Scheme 49). Using multiple different base anions with different  $\text{pK}_a$ 's would highlight if there were any interactions stabilising the C-B bond, or if protodeboronation rate was entirely reaction pH dependant.

Suzuki couplings using boronic acids prone to protodeboronation have previously been shown to have access to increased yields by using a boronic ester or similar reagents. These reagents proceed to the coupling reaction *via* slow hydrolysis to the boronic acid which then can undergo the coupling reaction or decompose via protodeboronation (Scheme 46). The project would benefit from elucidating whether there was a similar cation or anion effect in these reactions when boronic acid concentration was low due to the use of a boronic acid protecting group analogue.

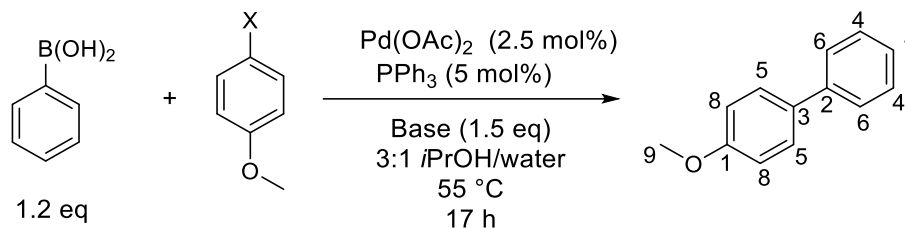
The phase splitting of all reactions in this chapter using the *iso*-propanol / water solvent system require consideration of mass transfer between the aqueous and organic phases. Cross bladed stirrer bars were used to increase this mass transfer, but if reactions could be run below the phase split point at lower concentration, the mass transfer would become much less important because the solvents would be completely miscible. This data could then be used to deduce whether aqueous and organic phase relative solubility, and therefore transfer between the two phases is important to gaining significant yields in these reactions.

#### **4.4 Experimental procedures**

Unless otherwise noted, all materials were obtained from commercial suppliers and used as received.  $\text{Cs}_2\text{CO}_3$ ,  $\text{K}_2\text{CO}_3$  and  $\text{K}_3\text{PO}_4$  were oven dried at 100 °C overnight before use.  $\text{Pd}(\text{OAc})_2$  was purchased from Fluorochem and Pd-132 was purchased from Sigma Aldrich. Unless otherwise noted, all reactions were performed under an atmosphere of  $\text{N}_2$  gas using standard vacuum-line techniques. All work-up and purification procedures were carried out with reagent-grade solvents in air. Column chromatography was carried out on prepacked flash columns on a Biotage purification unit.  $^1\text{H}$  NMR spectra were recorded in  $\text{CDCl}_3$  (TMS, no IS integration) at 300 or 500 MHz on Bruker Avance spectrometers. All chemical shift values are reported in ppm ( $\delta$ ).  $^1\text{H}$  and  $^{13}\text{C}$  NMR assignments were aided by COSY, DEPT and HMBC NMR. NMR assignments were made in order of decreasing chemical shift relative to  $^{13}\text{C}$  peaks (number) and  $^{19}\text{F}$  peaks (letter). Gas chromatography was conducted on Hewlett Packard HP 6890 Gas Chromatography apparatus, equipped with HP-5 chromatography columns (mobile phase:  $\text{H}_2$ , column length 30 m, film thickness 0.25  $\mu\text{m}$ , injection volume 1.0  $\mu\text{L}$ , split ratio 100:1, split flow 71.5 ml/min.) For kinetic experiments unless otherwise stated 50  $\mu\text{L}$  sample taken via syringe after inerting and quenched into 1 mL acetonitrile at room temperature.

#### **Standard sampling protocol**

The reaction stirring was stopped for ~5 seconds to encourage solids to settle at the bottom of the Schlenk flask. An oven dried needle attached to a luer lock syringe was purged by drawing up 1 mL of nitrogen atmosphere from the reaction and dispensing it to atmosphere and repeating 5 times. 100  $\mu\text{L}$  of reaction mixture was drawn into the syringe and diluted in 1 mL acetonitrile in a GC vial. The vial was left open to atmosphere to ensure to additional conversion would take place and the vial ran on GC without further purification.

**General procedure for formation of 4-methoxybiphenyl<sup>6, 46</sup>**

Base =  $\text{K}_3\text{PO}_4$ ,  $\text{Cs}_2\text{CO}_3$ ,  $\text{K}_2\text{CO}_3$ ,  $\text{Cs}_3\text{PO}_4 \cdot \text{H}_2\text{O}$

An oven dried Schlenk tube was charged with 4-haloanisole (0.5 mmol, 1.0 equivalents), benzene boronic acid (73 mg, 0.6 mmol, 1.2 equivalents), base (0.75 mmol, 1.5 equivalents), palladium acetate (6.0 mg, 0.025 mmol, 2.5 mol%) and triphenylphosphine (13.1 mg, 0.05 mmol, 5 mol%). The vessel was evacuated and backfilled with nitrogen 3 times to purge air from the system. Degassed *isopropanol*/water (3:1 ratio, 5 mL), spiked with *p*-xylene (0.05 M) was then added. The mixture was placed in a preheated oil bath with stirring at 55 °C for 17 hours and sampling according to the general sampling method. The mixture was allowed to cool to room temperature and the crude extracted in DCM (3 x 20 mL) before filtering through silica to give crude 4-methoxybiphenyl, This was purified with a Biotage purification system (10-25% DCM / petroleum ether) to give the pure product as colourless needles (77 mg, 84% yield). The conversions were determined by <sup>1</sup>H NMR ( $\text{CDCl}_3$ ) and calibrated GC. <sup>1</sup>H NMR (500 MHz,  $\text{CDCl}_3$ )  $\delta$  7.53 (m, 2H, H-5), 7.51 (m, 2H, H-6), 7.41 (t,  $J_{3,2} = J_{3,4} = 7.8$  Hz, 2H, H-4), 7.30 (t,  $J_{4,3} = 7.4$  Hz, 1H, H-7), 6.98 (d,  $J_{5,1} = 8.7$  Hz, 2H, H-8), 3.85 (s, 3H H-9); <sup>13</sup>C NMR (125 MHz,  $\text{CDCl}_3$ )  $\delta$  159.1 (C-1), 140.8 (C-2), 133.8 (C-3), 128.7 (C-4), 128.5 (C-5), 126.8 (C-6), 126.7 (C-7), 114.2 (C-8), 55.4 (C-9); m.p. 81 – 83 °C; GCMS ( $\text{EI}^+$ ) ( $m/z$ ):  $[\text{M} + \text{H}]^+$  calcd. For  $[\text{C}_{13}\text{H}_{12}\text{O}]$  184.5; found 184.5.

Literature data<sup>6, 46</sup>: <sup>1</sup>H NMR (300 MHz,  $\text{CDCl}_3$ )  $\delta$  7.55-7.28 (m, 7H), 6.96 (d,  $J = 9.1$  Hz, 2H), 3.81 (s, 3H); <sup>13</sup>C NMR (100 MHz,  $\text{CDCl}_3$ )  $\delta$  159.0, 140.7, 133.7, 128.6, 128.0, 126.6, 126.5, 114.1, 55.3;  $\text{ESI}^+$  MS ( $\text{ESI}^+$ ) ( $m/z$ ):  $[\text{M} + \text{H}]^+$  184.4.

**NMR study reactions forming 4-methoxybiphenyl**

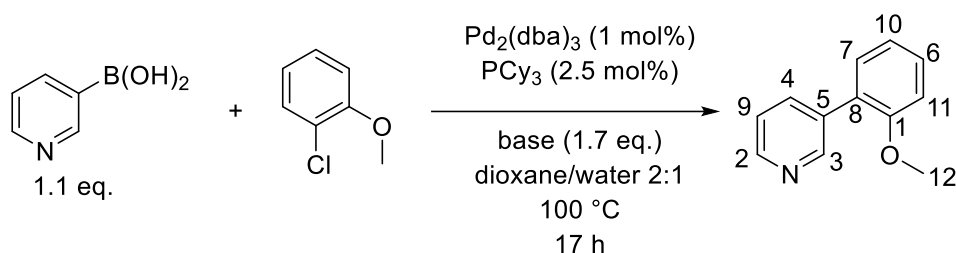
The reaction was conducted according to the general method to form 4-methoxybiphenyl, with *d*<sub>8</sub>-*isopropanol* and  $\text{D}_2\text{O}$  replacing protic solvents. The reaction was stirred at 55 °C for 5 minutes before an aliquot (0.4 mL) was taken and transferred

to an NMR tube under inert gas, which was then immediately run on a pre-shimmed NMR spectrometer at 55 °C. spectra were taken in the order  $^1\text{H}$ ,  $^{31}\text{P}$ ,  $^{133}\text{Cs}$  with each nuclei running every 15 minutes, for 7 hr. Reaction was not purified.

### **Reactions investigating phase split point of dual solvent Suzuki couplings**

An oven dried round bottom flask was charged with *isopropanol*/water mixture (3:1 ratio, 10 mL). The mixture was placed in a preheated oil bath at 50 – 75 °C. Potassium phosphate was added in portions of 50 mg followed by stirring for 5 min. The stirring was stopped and the reaction observed for phase splitting visually. This process was repeated until a phase split was visible in the solvent, and the reaction repeated 3 times to ensure reliability of results. Phase split point: 0.05 mM potassium phosphate at 50 °C, 0.06 mM potassium phosphate at 75 °C.

### **General Procedure to form 3-(2-methoxyphenyl)pyridine<sup>47</sup>**



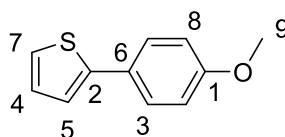
An oven dried Schlenk tube was charged with  $\text{Pd}_2(\text{dba})_3$  (9.2 mg, 0.01 mmol, 1 mol%),  $\text{PCy}_3$  (7.0 mg, 0.025 mmol, 2.5 mol%), base (1.7 mmol, 1.7 equivalents) and 3-pyridineboronic acid (135 mg, 1.1 mmol, 1.1 equivalents). The vessel was evacuated and refilled with inert gas, followed by addition of 2-chloroanisole (92  $\mu\text{L}$ , 1.0 mmol, 1.0 equivalent) and degassed water/dioxane (1:2 ratio, 4 mL). The vessel was sealed and heated to 100 °C with stirring for 17 h before being cooled to room temperature and the solution filtered through silica before evaporation to give crude 3-(2-Methoxyphenyl)pyridine as a light yellow oil. Representative 96% conversion using tricaesium phosphate as base by NMR (166 mg yield).  $^1\text{H}$  NMR (500 MHz,  $\text{CDCl}_3$ )  $\delta$  8.77 (d,  $J_{3,4} = 2.0$  Hz, 1H H-3), 8.55 (dd,  $J_{2,9} = 5.0$  Hz,  $J_{2,4} = 1.4$  Hz, 1H, H-2), 7.85 (td,  $J_{9,2,4} = 8.0$  Hz,  $J_{9,3} = 1.8$  Hz 1H, H-9), 7.39-7.36 (m, 1H, H-4), 7.33-7.31 (m, 2H, H-7,10), 7.06 (t,  $J_{6,10,11} = 7.4$  Hz, 1H, H-6), 7.01 (d,  $J_{11,6} = 8.2$  Hz, 1H, H-11), 3.90 (s, 3H, H-12);  $^{13}\text{C}$  NMR (125 MHz,  $\text{CDCl}_3$ )  $\delta$  156.6 (C-1), 150.5 (C-2), 148.1 (C-3), 136.9 (C-4), 134.3 (C-5), 130.8 (C-6), 129.6 (C-7), 127.2 (C-8), 122.9 (C-9), 121.2 (C-10), 111.4 (C-11), 55.7 (C-12); MS (ESI<sup>+</sup>): 186.34 (M+H).

Literature data:  $^1\text{H}$  NMR (500 MHz,  $\text{CDCl}_3$ )  $\delta$  8.76 (d,  $J = 2.4$  Hz, 1H), 8.54 (dd,  $J = 4.9$ , 1.8 Hz, 1H), 7.85 (dt,  $J = 7.9$ , 2.0 Hz, 1H), 7.37 (ddd,  $J = 8.7$ , 7.0, 1.2 Hz, 1H), 7.33-7.30 (m, 2H), 7.05 (td,  $J = 7.5$ , 1.0 Hz, 1H), 7.00 (d,  $J = 8.2$  Hz, 1H), 3.91 (s, 3H);  $^{13}\text{C}$  NMR (125 MHz,  $\text{CDCl}_3$ )  $\delta$  156.3, 150.1, 147.7, 136.5, 133.9, 130.4, 129.3, 126.7, 122.6, 120.8, 111.0, 55.2.

### **General Method A for AmigoChem reactions**

4 EasyMax tubes were flushed with nitrogen gas for 1 min and charged with Palladium precursor, phosphine ligand, boronic acid, and base. The tubes sealed into the EasyMax apparatus and flushed for a further 10 minutes with inert gas. Haloanisole (5 mmol, 5.0 equivalent) and p-xylene internal standard (617  $\mu\text{L}$ , 0.05 M) was added to 50 mL solvent and degassed for 30 min, before attaching to AmigoChem apparatus and charging to the tubes via sampling robot (10 mL, 1.0 equivalents haloanisole). The reactions were heated and then sampled via the robot at regular intervals every 15 minutes to quenched GC vials for analysis. The reactions were allowed to cool to room temperature and the crude extracted in DCM (3 x 20 mL) before filtering through silica to give crude product which was eluted on a biotage purification system to give purified product. Conversions determined by  $^1\text{H}$  NMR ( $\text{CDCl}_3$ ) and calibrated GC.

### **2-(4-Methoxyphenyl)thiophene<sup>48</sup>**

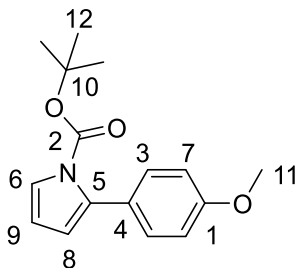


The title compound was synthesised using general method A using 2-thiophenyl boronic acid (1.2 mmol, 134 mg, 1.2 equivalents), palladium acetate (22.4 mg, 0.1 mmol, 10 mol%), triphenylphosphine (52 mg, 0.2 mmol, 20 mol%), base (1.5 mmol, 1.5 equivalents), 4-bromoanisole (124  $\mu\text{L}$ , 1.0 mmol) and DMF/water (4:1, 10 mL). The reaction was heated to 85  $^{\circ}\text{C}$  for 3 hours with regular sampling. The crude product was purified via biotage (hexane/ethyl acetate 0%-10% gradient) to give the title compound as an off-white solid (170 mg, 89% yield).  $^1\text{H}$  NMR (500 MHz,  $\text{CDCl}_3$ )  $\delta$  7.53 (d,  $J_{3,8} = 8.9$  Hz, 2H, H-3), 7.22-7.19 (m, 2H, H-5,7), 7.05 (dd,  $J_{4,5} = 5.2$  Hz,  $J_{4,7} = 3.4$  Hz, 1H H-4), 6.91 (d,  $J_{8,3} = 8.9$  Hz, 2H, H-8), 3.83 (s, 3H, H-9);  $^{13}\text{C}$  NMR (125 MHz,  $\text{CDCl}_3$ )  $\delta$  159.2 (C-1),

144.4 (C-2), 127.9 (2C, C-3), 127.3 (2C, C-4,5), 123.8 (C-6), 122.1 (C-7), 114.3 (2 C, C-8), 55.4 (C-9).

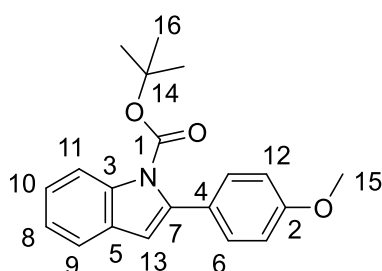
Literature data:  $^1\text{H}$  NMR (500 MHz,  $\text{CDCl}_3$ )  $\delta$  7.55 (d,  $J = 8.8$ , 2 H), 7.21 (m, 2 H), 7.05 (dd,  $J = 5.0, 3.5$ , 1 H), 6.92 (d,  $J = 8.8$ , 2 H), 3.84 (s, 3 H);  $^{13}\text{C}$  NMR (125 MHz,  $\text{CDCl}_3$ )  $\delta$  159.1, 144.3, 127.9, 127.2, 127.1, 123.8, 122.0, 114.2, 55.2.

*tert*-Butyl 2-(4-methoxyphenyl)pyrrole-1-carboxylate<sup>48</sup>



The title compound was synthesised using general method A using N-Boc-pyrrole-2-boronic acid (232 mg, 1.2 mmol, 1.2 equivalents), 2-bromoanisole (188  $\mu\text{L}$ , 1.0 mmol), palladium acetate (12.0 mg, 0.05 mmol, 5 mol%), triphenylphosphine (26.2 mg, 0.1 mmol, 10 mol%), base (1.5 equivalents), in glyme (10 mL) solvent. The reaction was heated to 80  $^\circ\text{C}$  for 17 hr with regular sampling. The crude product was purified via biotage (hexane/ dichloromethane 5%-35% gradient) to give the title compound as an off-white powder (154 mg, 86% yield).  $^1\text{H}$  NMR (500 MHz,  $\text{CDCl}_3$ )  $\delta$  7.32 (dd,  $J_{6,9} = 3.3\text{Hz}$ ,  $J_{6,8} = 1.6$  Hz, 1H, H-6), 7.27 (d,  $J_{3,7} = 8.8$  Hz, 2H H-3), 6.89 (d,  $J_{7,3} = 8.5$  Hz, 2H, H-7), 6.20 (dd,  $J_{9,6} = 3.2$  Hz,  $J_{9,8} = 3.2$  Hz, 1H, H-9), 6.13 (dd,  $J_{8,9} = 3.1$  Hz,  $J_{8,6} = 1.8$  Hz, 1H, H-8), 3.83 (s, 3H H-11), 1.38 (s, 9H, H-12);  $^{13}\text{C}$  NMR (125 MHz,  $\text{CDCl}_3$ )  $\delta$  158.9 (C-1), 149.4 (C-2), 134.9 (C-3), 130.4 (C-4, 2 C), 126.9 (C-5), 122.2 (C-6), 114.0 (C-7), 113.0 (C-8, 2 C), 110.4 (C-9), 83.4 (C-10), 55.3 (C-11), 27.7 (C-12, 3 C).

Literature data:  $^1\text{H}$  NMR (500 MHz,  $\text{CDCl}_3$ )  $\delta$  7.32 (dd,  $J = 3.3, 1.8$ , 1 H), 7.27 (d,  $J = 8.8$ , 2 H), 6.89 (d,  $J = 8.6$ , 2 H), 6.21 (t,  $J = 3.3$ , 1 H), 6.13 (dd,  $J = 3.2, 1.7$ , 1 H), 3.83 (s, 3 H), 1.387 (s, 9 H)  $^{13}\text{C}$  NMR (125 MHz,  $\text{CDCl}_3$ )  $\delta$  158.8, 149.3, 134.5, 130.3, 126.8, 122.1, 113.9, 113.0, 110.4, 83.3, 55.2, 27.6.

tert-Butyl 2-(4-methoxyphenyl)indole-1-carboxylate<sup>48</sup>

The title compound was synthesised using general method A using N-Boc-indole-2-boronic acid (289 mg, 1.1 mmol, 1.1 equivalents), 4-bromoanisole (126  $\mu$ L, 1.0 mmol), palladium acetate (11.2 mg, 0.05 mmol, 5 mol%), triphenylphosphine (26.2 mg, 0.1 mmol, 10 mol%), base (1.25 equivalents) in toluene/ethanol/water solvent mixture (10 / 1 / 1 ratio, 10 mL). The reaction was heated to 80 °C for 17 hr with regular sampling. The crude product was purified via biotage (hexane/ethyl acetate 0%-15% gradient) to give the title compound as an off-white solid (251 mg, 77% yield). <sup>1</sup>H NMR (500 MHz, CDCl<sub>3</sub>)  $\delta$  8.18 (d,  $J_{11,10}$  = 8.3 Hz, 1H, H-11), 7.53 (d,  $J_{9,8}$  = 7.5 Hz, 1H, H-9), 7.35-7.29 (m, 4H, H-6,8,10), 6.94 (d,  $J_{12,6}$  = 8.6Hz, 2H, H-12), 6.50 (s, 1H, H-13), 3.85 (s, 3H, H-15), 1.36 (s, 9H, H-16); <sup>13</sup>C NMR (125 MHz, CDCl<sub>3</sub>)  $\delta$  159.3 (C-1), 150.3 (C-2), 140.4 (C-3), 137.3 (C-4), 129.9 (2 C, C-6), 129.3 (C-5), 127.4 (C-7), 124.0 (C-8), 122.8 (C-9), 120.3 (C-10), 115.2 (C-11), 113.3 (C-12, 2 C), 109.5 (C-13), 83.3 (C-14), 55.4 (C-15), 27.7 (C-16, 3 C); MS (ESI<sup>+</sup>) ( $m/z$ ): [M + H]<sup>+</sup> calcd for [C<sub>20</sub>H<sub>21</sub>NO<sub>3</sub> H]<sup>+</sup> 323.1594; found 323.1592; m.p. 84.2 °C – 87.1 °C.

Literature data: <sup>1</sup>H NMR (500 MHz, CDCl<sub>3</sub>)  $\delta$  8.18 (d,  $J$  = 8.3, 1 H), 7.54 (d,  $J$  = 7.1, 1 H), 7.35 (d,  $J$  = 8.8, 2 H), 7.31 (t,  $J$  = 8.5, 1 H), 7.24 (t,  $J$  = 7.5, 1 H), 6.94 (d,  $J$  = 8.8, 2 H), 6.51 (s, 1 H), 3.86 (s, 3 H), 1.36 (s, 9 H); <sup>13</sup>C NMR (125 MHz, CDCl<sub>3</sub>)  $\delta$  159.2, 150.2, 140.3, 137.2, 129.8, 129.2, 127.3, 124.0, 122.8, 120.2, 115.1, 113.2, 109.4, 83.2, 55.2, 27.5.

**General procedure B for Protodeboronation experiments**

Palladium acetate (13.0 mg, 0.05 mol, 5 mol%), triphenyl phosphine (26.2 mg, 0.1 mol, 10 mol%) and phosphate base (1.2 mmole, 1.2 eq) were added to a Schlenk flask and the flask purged with nitrogen via vacuum and backfilling three times, followed by addition of degassed isopropanol / water (3:1 ratio, 10 mL), spiked with mesitylene internal standard (50 mM). The flask was heated to 60 °C or 75 °C with stirring and left to equilibrate for 15 min. The solution then turned orange indicating the precatalyst

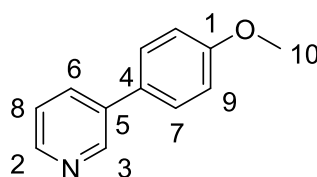
had formed. Boronic acid (1.0 mmole, 1 eq), was added under a strong nitrogen flow and the reaction was sealed and sampled for 17 h according to the general sampling method. The protodeboronation products were not purified, all products were analysed by calibrated GC or  $^1\text{H}$  NMR.

### **General procedure C for Suzuki reactions with aryl bromide**

An oven dried Schlenk tube was charged with  $\text{Pd}(\text{OAc})_2$  (6.0 mg, 0.025 mmole, 2.5 mol%), triphenylphosphine (13.1 mg, 0.05 mmole, 5 mol%) and an inorganic base (1.25 mmole, 1.25 equivalents). The vessel was evacuated and backfilled with nitrogen 3 times to purge air from the system and the haloanisole (1.0 mmole, 1.0 equivalent) was added under a strong nitrogen flow. This was followed by addition of degassed isopropanol/water (3:1 ratio, 10 mL) spiked with *p*-xylene (0.05 M). The reaction was heated to 75 °C or 60 °C and left to equilibrate for 15 min before the addition of the boronic acid (1.05 mmole, 1.05 equivalents) under strong nitrogen flow. The Schlenk tube was sealed and heated to 75 °C for 17 hours. The reaction mixture was allowed to cool to room temperature and extracted with  $\text{CH}_2\text{Cl}_2$  (3 x 20 mL) before filtering through silica (~5 g in a fritted funnel) to give the crude product. This was purified with a Biotage purification system and to give the pure product. The conversions were determined by  $^1\text{H}$  NMR ( $\text{CDCl}_3$ ) and calibrated GC.

### **Characterisation of synthesized compounds using general method C**

#### **3-(4-Methoxyphenyl)pyridine<sup>49</sup>**

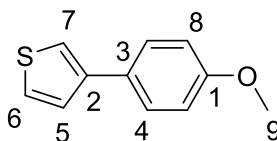


3-(4-Methoxyphenyl)pyridine was synthesised using general method C using 3-pyridyl boronic acid (1.05 eq, 129 mg). The crude product was purified by flash chromatography (hexane/ethyl acetate 10%-80% gradient) to give 3-(4-methoxyphenyl)pyridine as a white solid. (152mg, 81% yield).  $^1\text{H}$  NMR (500 MHz,  $\text{CDCl}_3$ )  $\delta$  8.83 (s, 1H, H-3), 8.55 (m, 1H, H-2), 7.83 (ddd,  $J_{6,8} = 7.9$  Hz,  $J_{6,2} = 1.7$  Hz,  $J_{6,3} = 1.7$  Hz, 1H, H-6), 7.52 (td,  $J_{7,9} = 8.7$  Hz,  $J_{7,3} = 3.0$  Hz,  $J_{7,6} = 3.0$  Hz, 2H, H-7), 7.34 (dd,  $J_{8,6} = 7.6$  Hz,  $J_{8,2} = 4.9$  Hz, 1H, H-8), 7.01 (dt,  $J_{9,7} = 8.7$  Hz,  $J_{9,9} = 2.0$  Hz, 2H, H-9), 3.86 (s, 3H, H-10).  $^{13}\text{C}$  NMR (125 MHz,  $\text{CDCl}_3$ ):  $\delta$  159.8 (C-1), 148.0 (C-2), 147.8 (C-3), 136.3 (C-4), 133.8 (C-5),

130.3 (C-6), 128.2 (C-7), 123.5 (C-8), 114.6 (C-9), 55.4 (C-10). LCMS (ESI<sup>+</sup>) (*m/z*): [M + H]<sup>+</sup> calcd. for [C<sub>12</sub>H<sub>11</sub>NO H] 186.24; found 186.34.

Literature data:<sup>49</sup> <sup>1</sup>H NMR (600 MHz, CDCl<sub>3</sub>) δ 8.81-8.80 (m, 1H), 8.53 (dd, *J*<sub>1</sub> = 4.8 Hz, *J*<sub>2</sub> = 1.6 Hz, 1H), 7.84-7.80 (m, 1H), 7.52 (d, *J* = 8.8 Hz, 2H), 7.34-7.30 (m, 1H), 7.01 (d, *J* = 8.8 Hz, 2H), 3.85 (s, 3H); <sup>13</sup>C NMR (CDCl<sub>3</sub>, 151 MHz) δ 159.7, 148.0, 147.9, 136.3, 133.8, 130.3, 128.2, 123.5, 114.6, 55.4.

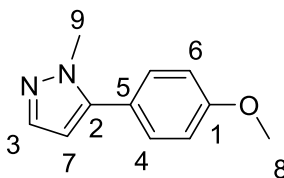
### 3-(4-Methoxyphenyl)thiophene<sup>50</sup>



3-(4-Methoxyphenyl)thiophene was synthesised using general method C using 3-thiophenyl boronic acid (1.05 eq, 134 mg). The crude product was purified via biotage (hexane/ethyl acetate 0%-15% gradient) to give 3-(4-methoxyphenyl)thiophene as an off-white solid. (127 mg, 67% yield) <sup>1</sup>H NMR (500 MHz, CDCl<sub>3</sub>) δ 7.53 (d, *J*<sub>4,8</sub> = 8.9 Hz, 2H, H-4), 7.37-7.33 (m, 3H, H-5,6,7), 6.94 (d, *J*<sub>8,4</sub> = 8.9 Hz, 2H, H-8), 3.84 (s, 3H, H-9); <sup>13</sup>C NMR (125 MHz, CDCl<sub>3</sub>) δ 158.9 (C-1), 142.0 (C-2), 128.8 (C-3), 127.6 (2 C, C-4), 126.3 (C-5), 126.1 (C-6), 118.9 (C-7), 114.2 (2 C, C-8), 55.3 (C-9).

Literature data:<sup>50</sup> <sup>1</sup>H NMR (500 MHz, CDCl<sub>3</sub>) δ 7.54 (d, *J* = 7.9 Hz, 2H), 7.36 (d, *J* = 6.3 Hz, 3H), 6.95 (d, *J* = 7.9 Hz, 2H), 3.85 (s, 3H); <sup>13</sup>C NMR (125.8 MHz, CDCl<sub>3</sub>) δ 158.9, 142.1, 128.8, 127.6, 126.3, 126.1, 119.0, 114.3, 55.4.

### 5-(4-Methoxyphenyl)-1-methylpyrazole<sup>51</sup>

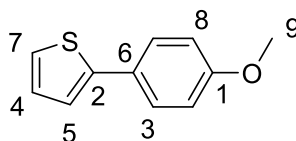


5-(4-Methoxyphenyl)-1-methylpyrazole was synthesised using general method C using 1-methyl pyrazole-5-boronic acid (1.05 eq, 132 mg). The crude product was purified via biotage (hexane / ethyl acetate 10%-25% gradient) to give 5-(4-methoxyphenyl)-1-methylpyrazole as a yellow oil (128 mg, 68% yield). <sup>1</sup>H NMR (500 MHz, CDCl<sub>3</sub>) δ 7.49 (d, *J*<sub>3,7</sub> = 1.9 Hz, 1H, H-3), 7.34 (d, *J*<sub>4,6</sub> = 8.8 Hz, 2H, H-4), 6.98 (d, *J*<sub>6,4</sub> = 8.8 Hz, 2H H-6), 6.25

(d,  $J_{7,3} = 1.8$  Hz, 1H, H-7), 3.87 (s, 3H, H-8), 3.86 (s, 3H, H-9);  $^{13}\text{C}$  NMR (125 MHz,  $\text{CDCl}_3$ )  $\delta$  160.0 (C-1), 143.7 (C-2), 138.8 (C-3), 130.3 (2 C, C-4), 123.5 (C-5), 114.4 (2 C, C-6), 106.0 (C-7), 55.7 (C-8), 37.7 (C-9).

Literature data:<sup>51</sup>  $^1\text{H}$  NMR (200 MHz,  $\text{CDCl}_3$ )  $\delta$  7.48 (d,  $J = 1.9$  Hz, 1 H), 7.32 (m, 2 H), 6.97 (m, 2 H), 6.24 (d,  $J = 1.9$  Hz, 1 H), 3.85 (s, 3 H), 3.83 (s, 3H);  $^{13}\text{C}$  NMR (50.3 MHz,  $\text{CDCl}_3$ )  $\delta$  159.1, 138.3, 133.0, 129.5 (2 C), 127.1, 121.8, 113.9 (2 C), 55.1, 32.1

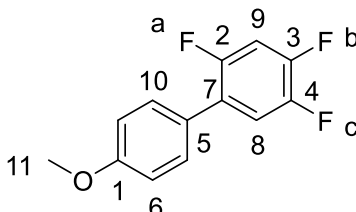
### 2-(4-Methoxyphenyl)thiophene<sup>48</sup>



2-(4-Methoxyphenyl)thiophene was synthesised using general method C using 2-thiophenyl boronic acid (1.05 eq, 134 mg). The crude product was purified via biotage (hexane/ethyl acetate 0%-10% gradient) to give 2-(4-methoxyphenyl)thiophene as an off-white solid (125 mg, 66% yield).  $^1\text{H}$  NMR (500 MHz,  $\text{CDCl}_3$ )  $\delta$  7.53 (d,  $J_{3,8} = 8.9$  Hz, 2H, H-3), 7.22-7.19 (m, 2H, H-5,7), 7.05 (dd,  $J_{4,5} = 5.2$  Hz,  $J_{4,7} = 3.4$  Hz, 1H, H-4), 6.91 (d,  $J_{8,3} = 8.9$  Hz, 2H, H-8), 3.83 (s, 3H, H-9);  $^{13}\text{C}$  NMR (125 MHz,  $\text{CDCl}_3$ )  $\delta$  159.2 (C-1), 144.4 (C-2), 127.9 (2C, C-3), 127.3 (2C, C-4,5), 123.8 (C-6), 122.1 (C-7), 114.3 (2 C, C-8), 55.4 (C-9).

Literature data:<sup>48</sup>  $^1\text{H}$  NMR (500 MHz,  $\text{CDCl}_3$ )  $\delta$  7.55 (d,  $J = 8.8$  Hz, 2 H), 7.21 (m, 2 H), 7.05 (dd,  $J = 5.0, 3.5$  Hz, 1 H), 6.92 (d,  $J = 8.8$  Hz, 2 H), 3.84 (s, 3 H);  $^{13}\text{C}$  NMR (125 MHz,  $\text{CDCl}_3$ )  $\delta$  159.1, 144.3, 127.9, 127.2, 127.2, 123.8, 122.0, 114.2, 55.2.

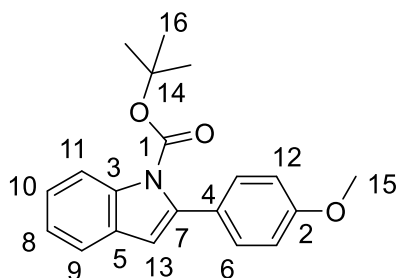
### 2,4,5-Trifluoro-4'-methoxybiphenyl



2,4,5-Trifluoro-4'-methoxybiphenyl was synthesised using general method C using 2,4,5-trifluorophenyl boronic acid (1.05 eq, 185 mg). The crude product was purified via biotage (hexane / ethyl acetate 10%-60% gradient) to give 2,4,5-trifluoro-4'-

methoxybiphenyl as an off white solid (189 mg, 81% yield). This compound is novel.  $^1\text{H}$  NMR (500 MHz,  $\text{CDCl}_3$ )  $\delta$  7.41 (d,  $J_{6,9} = 8.8$  Hz, 2H, H-6), 7.25-7.17 (m, 1H, H-8), 7.02-6.96 (m, 3H, H-9,10), 3.84 (s, 3H, H-11);  $^{13}\text{C}$  NMR (125 MHz,  $\text{CDCl}_3$ )  $\delta$  159.6 (C-1), 154.6 (ddd,  $J_{2,a} = 246$  Hz,  $J_{2,b} = 9$  Hz,  $J_{2,c} = 2$  Hz, C-2), 150.1 (ddd,  $J_{3,b} = 250$  Hz,  $J_{3,c} = 13$  Hz,  $J_{3,a} = 13$  Hz C-3), 146.9 (ddd,  $J_{4,c} = 243$  Hz,  $J_{4,b} = 13$  Hz,  $J_{4,a} = 3$  Hz, C-4), 132.2 (C-5), 130.0 (d,  $J_{6,a} = 3$  Hz, 2C, C-6), 126.3 (C-7), 125.2 (ddd,  $J_{8,c} = 16$  Hz,  $J_{8,b} = 5$  Hz,  $J_{8,a} = 5$  Hz, C-8), 115.8 (C-9), 106.0 (dd,  $J_{10,a} = 30$  Hz,  $J_{10,b} = 21$  Hz, 2C, C-10), 55.4 (C-11);  $^{19}\text{F}$  NMR (376 MHz,  $\text{CDCl}_3$ )  $\delta$  -119.7 (F-a), -136.0 (dd,  $J_{b,c} = 21$  Hz,  $J_{b,a} = 10$  Hz, F-b), -143.1 (m, F-c); MS (ESI $^+$ ) ( $m/z$ ):  $[\text{M} + \text{H}]^+$ , [cald for  $\text{C}_{13}\text{H}_{10}\text{F}_3\text{O}$  H] $^+$  239.0678, found 239.0675; m.p. 66.5  $^\circ\text{C}$  - 69.8  $^\circ\text{C}$ .

*tert*-Butyl 2-(4-methoxyphenyl)indole-1-carboxylate<sup>48</sup>

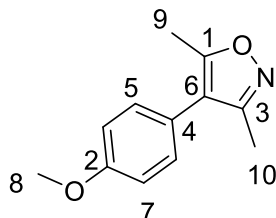


*tert*-Butyl 2-(4-methoxyphenyl)indole-1-carboxylate was synthesised using general method C using *N*-Boc-indole-2-boronic acid (1.05 eq, 274 mg). The crude product was purified via biotage (hexane/ethyl acetate 0%-15% gradient) to give *tert*-butyl 2-(4-methoxyphenyl)indole-1-carboxylate as an off-white solid (228 mg, 71% yield).  $^1\text{H}$  NMR (500 MHz,  $\text{CDCl}_3$ )  $\delta$  8.18 (d,  $J_{11,10} = 8.3$  Hz, 1H, H-11), 7.53 (d,  $J_{9,8} = 7.5$  Hz, 1H, H-9), 7.35-7.29 (m, 4H, H-6,8,10), 6.94 (d,  $J_{12,6} = 8.6$  Hz, 2H, H-12), 6.50 (s, 1H, H-13), 3.85 (s, 3H, H-15), 1.36 (s, 9H, H-16);  $^{13}\text{C}$  NMR (125 MHz,  $\text{CDCl}_3$ )  $\delta$  159.3 (C-1), 150.3 (C-2), 140.4 (C-3), 137.3 (C-4), 129.9 (2 C, C-6), 129.3 (C-5), 127.4 (C-7), 124.0 (C-8), 122.8 (C-9), 120.3 (C-10), 115.2 (C-11), 113.3 (C-12, 2 C), 109.5 (C-13), 83.3 (C-14), 55.4 (C-15), 27.7 (C-16, 3 C); MS (ESI $^+$ ) ( $m/z$ ):  $[\text{M} + \text{H}]^+$  calcd for  $[\text{C}_{20}\text{H}_{21}\text{NO}_3 \text{H}]^+$  323.1594; found 323.1592; m.p. 84.2  $^\circ\text{C}$  - 87.1  $^\circ\text{C}$ .

Literature data:<sup>48</sup>  $^1\text{H}$  NMR: (500 MHz,  $\text{CDCl}_3$ )  $\delta$  8.18 (d,  $J = 8.3$  Hz, 1 H), 7.54 (d,  $J = 7.1$  Hz, 1 H), 7.35 (d,  $J = 8.8$  Hz, 2 H), 7.31 (t,  $J = 8.5$  Hz, 1 H), 7.24 (t,  $J = 7.5$  Hz, 1 H), 6.94 (d,  $J = 8.8$  Hz, 2 H), 6.51 (s, 1 H), 3.86 (s, 3 H), 1.36 (s, 9 H);  $^{13}\text{C}$  NMR (125 MHz,  $\text{CDCl}_3$ )  $\delta$

159.2, 150.2, 140.3, 137.2, 129.8, 129.2, 127.3, 124.0, 122.8, 120.2, 115.1, 113.2, 109.4, 83.2, 55.2, 27.5.

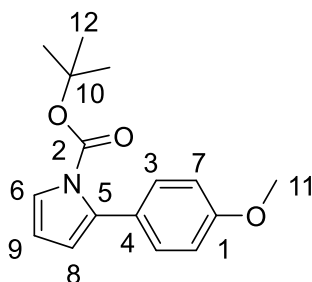
4-(4-Methoxyphenyl)-3,5-dimethylisoxazole<sup>52</sup>



4-(4-Methoxyphenyl)-3,5-dimethylisoxazole was synthesised using general method C using 3,5-dimethylisoxazol-4-yl-4-boronic acid (1.05 eq, 148 mg). The crude product was purified via a Biotage purification system (hexane/ethyl acetate 0%-25% gradient) to give 4-(4-methoxyphenyl)-3,5-dimethylisoxazole as an off white solid. <sup>1</sup>H NMR (500 MHz, CDCl<sub>3</sub>) δ 7.17 (d, *J*<sub>5,7</sub> = 8.8 Hz, 2H, H-5), 6.97 (d, *J*<sub>7,5</sub> = 8.9 Hz, 2H, H-7), 3.85 (s, 3H, H-8), 2.38 (s, 3H, H-9), 2.25 (s, 3H, H-10); <sup>13</sup>C NMR (125 MHz, CDCl<sub>3</sub>) δ 164.8 (C-1), 159.0 (C-2), 158.8 (C-3), 130.3 (C-4), 122.6 (2 C, C-5), 116.3 (C-6), 114.3 (2 C, C-7), 55.3 (C-8), 11.5 (C-9), 10.8 (C-10).

Literature data:<sup>52</sup> <sup>1</sup>H NMR (400 MHz, CDCl<sub>3</sub>) δ 7.17 (d, 2H, *J* = 8.4 Hz), 6.97 (d, 2H, *J* = 8.4 Hz), 3.85 (s, 3H), 2.38 (s, 3H), 2.25 (s, 3H); <sup>13</sup>C NMR (100 MHz, CDCl<sub>3</sub>) δ 164.6, 158.8, 158.5, 130.0, 122.4, 116.0, 114.1, 55.0, 11.2, 10.5.

*tert*-Butyl 2-(4-methoxyphenyl)pyrrole-1-carboxylate<sup>48</sup>

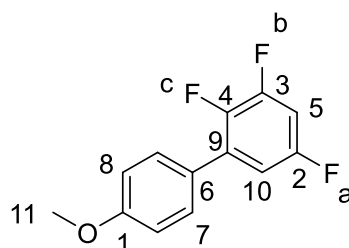


*tert*-Butyl 2-(4-methoxyphenyl)pyrrole-1-carboxylate was synthesised using general method C using *N*-Boc-pyrrole-2-boronic acid (1.05 eq, 222 mg). The crude product was purified via biotage (hexane/ dichloromethane 5%-35% gradient) to give *tert*-Butyl 2-(4-methoxyphenyl)pyrrole-1-carboxylate as an off-white powder (160 mg, 92% yield). <sup>1</sup>H NMR (500 MHz, CDCl<sub>3</sub>) δ 7.32 (dd, *J*<sub>6,9</sub> = 3.3Hz, *J*<sub>6,8</sub> = 1.6 Hz, 1H, H-6), 7.27 (d, *J*<sub>3,7</sub> = 8.8 Hz, 2H H-3), 6.89 (d, *J*<sub>7,3</sub> = 8.5 Hz, 2H, H-7), 6.20 (dd, *J*<sub>9,6</sub> = 3.2 Hz, *J*<sub>9,8</sub> = 3.2 Hz, 1H, H-

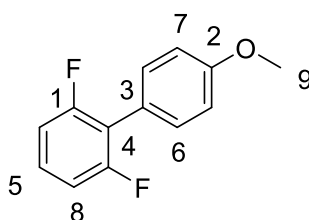
9), 6.13 (dd,  $J_{8,9} = 3.1$  Hz,  $J_{8,6} = 1.8$  Hz, 1H, H-8), 3.83 (s, 3H H-11), 1.38 (s, 9H, H-12);  $^{13}\text{C}$  NMR (125 MHz,  $\text{CDCl}_3$ )  $\delta$  158.9 (C-1), 149.4 (C-2), 134.9 (C-3), 130.4 (C-4, 2 C), 126.9 (C-5), 122.2 (C-6), 114.0 (C-7), 113.0 (C-8, 2 C), 110.4 (C-9), 83.4 (C-10), 55.3 (C-11), 27.7 (C-12, 3 C); LCMS (ESI<sup>+</sup>) ( $m/z$ ):  $[\text{M} + \text{H}]^+$ , 174.36.

Literature data:<sup>48</sup>  $^1\text{H}$  NMR (500 MHz,  $\text{CDCl}_3$ )  $\delta$  7.32 (dd,  $J = 3.3, 1.8$  Hz, 1 H), 7.27 (d,  $J = 8.8$  Hz, 2 H), 6.89 (d,  $J = 8.6$  Hz, 2 H), 6.21 (t,  $J = 3.3$  Hz, 1 H), 6.13 (dd,  $J = 3.2, 1.7$  Hz, 1 H), 3.83 (s, 3 H), 1.387 (s, 9 H);  $^{13}\text{C}$  NMR (125 MHz,  $\text{CDCl}_3$ )  $\delta$  158.87, 149.39, 134.85, 130.38, 126.85, 122.14, 113.97, 113.00, 110.44, 83.39, 55.23, 27.65.

### 2,3,5-Trifluoro-4'-methoxybiphenyl

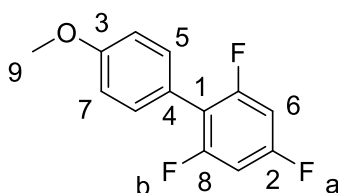


2,3,5-Trifluoro-4'-methoxybiphenyl was synthesised using general method C using 2,3,5-trifluorophenyl boronic acid (1.05 eq, 185 mg). The crude product was purified via biotage (hexane / ethyl acetate 10%-60% gradient) to give 2,3,5-trifluoro-4'-methoxybiphenyl as an off white solid. This compound is novel.  $^1\text{H}$  NMR (500 MHz,  $\text{CDCl}_3$ )  $\delta$  7.47 (dd,  $J_{7,8} = 8.9$  Hz,  $J_{7,10} = 1.2$  Hz, 2H, H-7), 6.99 (d,  $J_{8,7} = 8.7$  Hz, 2H, H-8), 6.93-6.83 (m, 2H, H-5,10), 3.86 (s, 3H, H-11);  $^{13}\text{C}$  NMR (125 MHz,  $\text{CDCl}_3$ )  $\delta$  160.0 (C-1), 157.7 (ddd,  $J_{2,a} = 242$  Hz,  $J_{2,b} = 11$  Hz,  $J_{2,c} = 3$  Hz, C-2), 151.0 (ddd,  $J_{3,b} = 251$  Hz,  $J_{3,c} = 15$  Hz,  $J_{3,a} = 15$  Hz C-3), 144.5 (ddd,  $J_{4,c} = 242$  Hz,  $J_{4,b} = 13$  Hz,  $J_{4,a} = 4$  Hz C-4), 131.4 (dd,  $J_{5,b} = 11$  Hz,  $J_{5,a} = 11$  Hz, C-5), 130.1 (d,  $J_{6,c} = 3$  Hz, C-6), 126.2 (2 C, C-7), 114.2 (2 C, C-8), 111.3 (d,  $J_{9,c} = 25$  Hz, C-9), 103.6 (dd,  $J_{10,a} = 27$  Hz,  $J_{10,c} = 21$  Hz, C-10), 55.4 (C-11);  $^{19}\text{F}$  NMR (376 MHz,  $\text{CDCl}_3$ )  $\delta$  -115.9 (m, F-a), -133.4 (dd  $J_{b,c} = 21$  Hz,  $J_{b,a} = 9$  Hz, F-b), -148.9 (m, F-c); MS (ESI<sup>+</sup>) ( $m/z$ ):  $[\text{M} + \text{H}]^+$ , [cald for  $\text{C}_{13}\text{H}_9\text{F}_3\text{O}$  H]<sup>+</sup> 239.0678, found 239.0676; m.p. 79.3 °C – 81.0 °C.

2,6-Difluoro-4'-methoxybiphenyl<sup>53</sup>

2,6-Difluoro-4'-methoxybiphenyl was synthesised using general method C using 2,6-difluorophenyl boronic acid (1.05 eq, 166 mg). The crude product was purified via biotage (hexane / ethyl acetate 5%-20% gradient) followed by heating to 130 °C *in vacuo* to give 2,6-difluoro-4'-methoxybiphenyl as an off white solid (207 mg, 87% yield). <sup>1</sup>H NMR (500 MHz, CDCl<sub>3</sub>) δ 7.41 (d,  $J_{6,7} = 8.7$  Hz, 2H, H-6), 7.24-7.20 (m, 1H, H-5), 7.00-6.95 (m, 4H, H-7,8), 3.86 (s, 3H, H-9); <sup>13</sup>C NMR (125 MHz, CDCl<sub>3</sub>) δ 160.1 (dd,  $J = 248$  Hz,  $J = 7.8$  Hz, C-1), 159.5 (C-2), 131.5 (C-3), 128.3 (t,  $J = 10.5$  Hz, C-4), 121.3 (C-5), 118.2 (C-6), 113.8 (C-7), 111.6 (dd,  $J = 19.4$  Hz,  $J = 7.5$  Hz, C-8), 55.3 (C-9); <sup>19</sup>F NMR (376 MHz, CDCl<sub>3</sub>) δ -114.8 (t,  $J = 6.8$  Hz, 2F); MS (ESI<sup>+</sup>) ( $m/z$ ): [M + H + H<sub>2</sub>O]<sup>+</sup>, [cald for C<sub>13</sub>H<sub>11</sub>F<sub>2</sub>O<sub>2</sub>]<sup>+</sup>, 237.078 found 237.090.

Literature data:<sup>53</sup> <sup>1</sup>H NMR (400 MHz, CDCl<sub>3</sub>) δ 3.82 (s, 3H), 6.89-6.98 (m, 4H), 7.17-7.24 (m, 1H), 7.36-7.39 (m, 2H); <sup>13</sup>C NMR (100MHz, CDCl<sub>3</sub>) δ 55.2, 111.5 (dd,  $J_F = 7.3, 19.2$  Hz), 113.8, 118.2 (t,  $J_F = 18.5$  Hz), 121.2, 128.3 (t,  $J_F = 10.3$  Hz), 131.5, 159.5, 160.2 (dd,  $J_F = 7.1, 246.3$  Hz); <sup>19</sup>F NMR (377MHz, CDCl<sub>3</sub>) δ -114.8 (s, 2F).

2,4,6-Trifluoro-4'-methoxybiphenyl<sup>53</sup>

2,4,6-Trifluoro-4'-methoxybiphenyl was synthesised using general method C using 2,4,6-trifluorophenylboronic acid (1.05 eq, 185 mg). The crude product was purified via biotage (hexane / ethyl acetate 0%-15% gradient) to give 2,4,6-trifluoro-4'-methoxybiphenyl as a colourless solid (200 mg, 84% yield). <sup>1</sup>H NMR (500 MHz, CDCl<sub>3</sub>) δ 7.36 (d,  $J_{5,7} = 8.3$  Hz, 2H, H-5), 6.99 (d,  $J_{7,5} = 8.6$  Hz, 2H, H-7), 6.74 (t,  $J_{6,b} = 8.1$  Hz, 2H, H-6), 3.86 (s, 3H, H-9); <sup>13</sup>C NMR (125 MHz, CDCl<sub>3</sub>) δ 161.1 (dd,  $J = 12.1$  Hz,  $J = 12.1$  Hz, C-

1), 162.1-158.7 (m, C-2), 159.6 (C-3), 131.4 (C-4), 120.4 (2C, C-5), 115.7-114.5 (m, 2C, C-6) 113.9 (C-7), 100.6-100.2 (m, 2C, C-8), 55.3 (C-9);  $^{19}\text{F}$  NMR (376 MHz,  $\text{CDCl}_3$ ),  $\delta$  -109.8 (F-a), -111.5 (F-b); MS (ESI<sup>+</sup>) ( $m/z$ ): [M + H], [cald for  $\text{C}_{13}\text{H}_{19}\text{F}_3\text{O}$  H]<sup>+</sup>, 239.0678 found 239.0674.

Literature data:<sup>53</sup>  $^1\text{H}$  NMR (400 MHz,  $\text{CDCl}_3$ )  $\delta$  3.85 (s, 3H), 6.74 (t,  $J$  = 8.4 Hz, 2H), 6.98 (d,  $J$  = 8.8 Hz, 2H), 7.35 (d,  $J$  = 8.8 Hz, 2H);  $^{13}\text{C}$  NMR (100MHz,  $\text{CDCl}_3$ )  $\delta$  55.3, 100.1-100.6 (m), 113.9, 114.7 (td,  $J_{\text{F}}$  = 4.8, 19.2 Hz), 120.4, 131.4, 159.6, 160.3 (ddd,  $J_{\text{F}}$  = 10.0, 14.8, 247.5 Hz), 161.4 (dt,  $J_{\text{F}}$  = 15.7, 247.0 Hz);  $^{19}\text{F}$  NMR (377MHz,  $\text{CDCl}_3$ )  $\delta$  -111.6 (d,  $J_{\text{F}}$  = 5.6 Hz, 2F), -109.9 (t,  $J_{\text{F}}$  = 5.6 Hz, 1F).

### **Scale-up Synthesis of 5-(4-methoxyphenyl)-1-methylpyrazole**

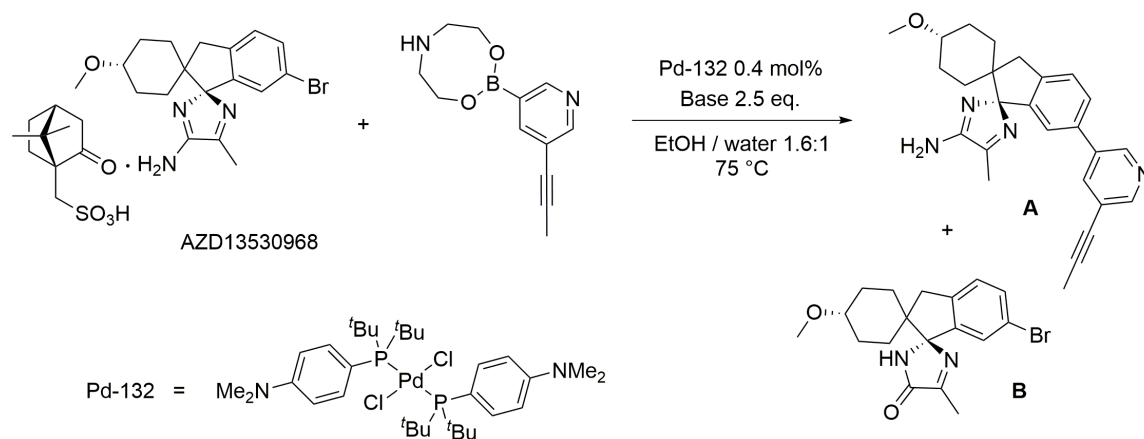
A three necked round bottom flask equipped with a nitrogen inlet and condenser, along with stirrer bar was submerged in a paraffin oil bath at room temperature. The vessel was charged with  $\text{Pd}(\text{OAc})_2$  (96.0 mg, 0.4 mmole, 2.5 mol%), triphenylphosphine (210 mg, 0.8 mmole, 5 mol%) and  $\text{Cs}_3\text{PO}_4 \cdot \text{H}_2\text{O}$  (10.22 g, 20 mmole, 1.25 eq.). The flask was purged with nitrogen *via* vacuum and backfilling three times, followed by addition of degassed isopropanol / water, spiked with *p*-xylene internal standard (50 mM), *via* a cannula (3:1 ratio, 160 mL). The mixture was then heated to 60 °C with stirring and left to equilibrate for 1 h. Its colour changed to orange indicating the formation of the precatalyst. 4-Bromoanisole (2.00 mL, 16 mmole, 1.0 eq) was then added to the reaction mixture, followed by stirring for 15 min. 1-Methylpyrazole-5-boronic acid (2.12 g, 16.8 mmol, 1.05 eq) was then added as a solid, and the reaction was sealed for 17 h. The vessel was cooled to room temperature and the crude product extracted with ethyl acetate (3 x 200 mL), before washing through silica (50 g in a fritted funnel). The crude product was then purified using a Biotage column (hexane/ethyl acetate 10 – 25% gradient) to give the product as a yellow oil in 63% isolated yield (1.89 g).

### **General method D for reactions involving 18-crown-6**

An oven dried Schlenk tube was charged with  $\text{Pd}(\text{OAc})_2$  (4.5 mg, 0.02 mmole, 4 mol%) and triphenylphosphine (10.5 mg, 0.04 mmole, 8 mol%). The vessel was evacuated and backfilled with nitrogen 3 times to purge air from the system. Degassed isopropanol/water (3:1 ratio, 5 mL) spike with *p*-xylene (0.05 M) was added and the mixture stirred and heated at 55 °C for 30 min to ensure precatalyst formation. The mixture turned orange to confirm binding of the ligand. A second oven dried Schlenk

tube was charged with boronic acid (0.6 mmole, 1.2 equivalents), 4-haloanisole (0.5 mmole, 1.0 equivalent), phosphate base (0.75 mmole, 1.5 equivalents) and 18-crown-6 (198 mg, 0.75 mmole, 1.5 equivalents). The vessel was evacuated and backfilled with nitrogen 3 times to purge air from the system. The catalyst solution was added to the reagent vessel and heated for 17 hours with regular sampling. The reaction mixture was allowed to cool to room temperature and extracted with  $\text{CH}_2\text{Cl}_2$  (3 x 20 mL) before filtering through silica (~5 g in a fritted funnel) to give the crude product. This was purified with a Biotage purification system and to give the pure product. The conversions were determined by  $^1\text{H}$  NMR ( $\text{CDCl}_3$ ) and calibrated GC.

### Synthesis of AZD3293



$\text{Cs}_3\text{PO}_4 \cdot \text{H}_2\text{O}$  (4.93 g, 10 mmole, 2.5 equivalents) was added to water (7.5 mL) and degassed by bubbling it with nitrogen. AZD13530968 (aryl bromide, 4.0 mmole, 1.0 equivalent), AZD13886149 (boronic ester, 4.2 mmole, 1.05 equivalents) and diphenyl ether (internal standard, 200 mg, 1.2 mmole) were added to an oven dried round bottom flask under nitrogen. Degassed ethanol (10 mL), and the caesium phosphate solution (7.5 mL) were then added to the flask and the mixture was stirred for 15 min. The reaction was then heated to 75 °C and stirred for a further 15 minutes before addition of Pd-132 (11.4 mg, 0.016 mmole, 0.4 mol%) in ethanol (2 mL). The reaction was stirred and sampled for 6 hr using an EasySampler robot at regular intervals every 5 minutes to quenched HPLC vials for analysis. The mixture was allowed to cool to room temperature and the crude product crashed out as an off white solid which was filtered under reduced pressure and washed with ice cold water. Conversions were determined by calibrated HPLC.

$^1\text{H}$  NMR (400 MHz, DMSO- $d_6$ )  $\delta$  8.65 (d,  $J$  = 2.3 Hz, 1H), 8.50 (d,  $J$  = 1.9 Hz, 1H), 7.88 (dd,  $J$  = 2.3, 1.9 Hz, 1H), 7.52 (dd,  $J$  = 7.8, 1.7 Hz, 1H), 7.39 (d,  $J$  = 7.8 Hz, 1H), 6.82 (d,  $J$  = 1.7 Hz, 1H), 6.52 (s, 2H), 3.19 (s, 3H), 3.08 (d,  $J$  = 15.5 Hz, 1H), 2.99 (d,  $J$  = 15.5 Hz, 1H), 2.99–2.90 (m, 1H), 2.17 (s, 3H), 2.08 (s, 3H), 1.87–1.77 (m, 2H), 1.51–1.36 (m, 3H), 1.30–1.11 (m, 2H), 1.02–0.92 (m, 1H);  $^{13}\text{C}$  NMR (100 MHz, DMSO- $d_6$ )  $\delta$  161.5, 160.5, 149.9, 146.1, 145.0, 143.1, 135.8, 135.5, 134.1, 126.4, 125.9, 120.5, 120.2, 109.0, 90.3, 78.7, 76.5, 54.8, 52.2, 39.7, 30.0, 29.0, 28.5, 28.3, 14.2, 4.0.

#### **4.5 References**

1. J. Zhang, J. Chen, M. Liu, X. Zheng, J. Ding and H. Wu, *Green Chem.*, 2012, **14**, 912-916.
2. Q. Xu, W.-L. Duan, Z.-Y. Lei, Z.-B. Zhu and M. Shi, *Tetrahedron*, 2005, **61**, 11225-11229.
3. X. Bei, H. W. Turner, W. H. Weinberg, A. S. Guram and J. L. Petersen, *J. Org. Chem.*, 1999, **64**, 6797-6803.
4. A. Suzuki, *Chem. Commun.*, 2005, 4759-4763.
5. D. G. Brown and J. Boström, *J. Med. Chem.*, 2016, **59**, 4443-4458.
6. I. Hoffmann, B. Blumenroder, S. Onodi nee Thumann, S. Dommer and J. Schatz, *Green Chem.*, 2015, **17**, 3844-3857.
7. C. Torborg and M. Beller, *Adv. Synth. Catal.*, 2009, **351**, 3027-3043.
8. A. A. C. Braga, N. H. Morgon, G. Ujaque and F. Maseras, *J. Am. Chem. Soc.*, 2005, **127**, 9298-9307.
9. C. F. R. A. C. Lima, A. S. M. C. Rodrigues, V. L. M. Silva, A. M. S. Silva and L. M. N. B. F. Santos, *ChemCatChem*, 2014, **6**, 1291-1302.
10. L. A. J. J. and L.-J. G. C., *Isr. J. Chem.*, 2010, **50**, 664-674.
11. A. J. J. Lennox and G. C. Lloyd-Jones, *Chem. Soc. Rev.*, 2014, **43**, 412-443.
12. R. Grisorio and G. P. Suranna, *ACS Macro Letters*, 2017, **6**, 1251-1256.
13. A. J. Amali and R. K. Rana, *Green Chem.*, 2009, **11**, 1781-1786.
14. A. Nasar, *J. Serb. Chem. Soc.*, 2013, **78**, 241-253.
15. W. D. Kumler and J. J. Eiler, *J. Am. Chem. Soc.*, 1943, **65**, 2355-2361.
16. W. J. DeWitte, R. C. Schoening and A. I. Popov, *Inorg. Nucl. Chem. Lett.*, 1976, **12**, 251-253.
17. C. Amatore, A. Jutand and G. Le Duc, *Chem. – Eur. J.*, 2012, **18**, 6616-6625.

18. C. M. Goff, M. A. Matchette, N. Shabestary and S. Khazaeli, *Polyhedron*, 1996, **15**, 3897-3903.
19. J. R. Vyvyan, E. A. Peterson and M. L. Stephan, *Tetrahedron Lett.*, 1999, **40**, 4947-4949.
20. A. Pérez, J. T. Nieto, A. L. Rodríguez, *Eur. Pat.* EP2607371A1, 2013.
21. X. Bian, L. Wang, J. Liu and C. Wang, *J. Chem. Res.*, 2016, **40**, 289-292.
22. P. A. Cox, A. G. Leach, A. D. Campbell and G. C. Lloyd-Jones, *J. Am. Chem. Soc.*, 2016, **138**, 9145-9157.
23. J. H. Kirchhoff, M. R. Netherton, I. D. Hills and G. C. Fu, *J. Am. Chem. Soc.*, 2002, **124**, 13662-13663.
24. W. Tang, S. Keshipeddy, Y. Zhang, X. Wei, J. Savoie, N. D. Patel, N. K. Yee and C. H. Senanayake, *Org. Lett.*, 2011, **13**, 1366-1369.
25. L. Chen, H. Francis and B. P. Carrow, *ACS Catalysis*, 2018, **8**, 2989-2994.
26. L. Chen, D. R. Sanchez, B. Zhang and B. P. Carrow, *J. Am. Chem. Soc.*, 2017, **139**, 12418-12421.
27. N. Kudo, M. Perseghini and G. C. Fu, *Angew. Chem. Int. Ed.*, 2006, **45**, 1282-1284.
28. C. Meyers, B. U. W. Maes, K. T. J. Loones, G. Bal, G. L. F. Lemièrè and R. A. Dommissie, *J. Org. Chem.*, 2004, **69**, 6010-6017.
29. S. Vásquez-Céspedes, A. Ferry, L. Candish and F. Glorius, *Angew. Chem. Int. Ed.*, 2015, **54**, 5772-5776.
30. V. P. Reddy, R. Qiu, T. Iwasaki and N. Kambe, *Org. Lett.*, 2013, **15**, 1290-1293.
31. M. Alešković, N. Basarić and K. Mlinarić-Majerski, *J. Heterocycl. Chem.*, 2011, **48**, 1329-1335.
32. M. T. Hovey, C. T. Check, A. F. Sipher and K. A. Scheidt, *Angew. Chem. Int. Ed.*, 2014, **53**, 9603-9607.
33. S. W. Smith and G. C. Fu, *J. Am. Chem. Soc.*, 2008, **130**, 12645-12647.
34. J. Mao, J. Zhang, S. Zhang and P. J. Walsh, *Dalton Trans.*, 2018, **47**, 8690-8696.
35. P. A. Cox, M. Reid, A. G. Leach, A. D. Campbell, E. J. King and G. C. Lloyd-Jones, *J. Am. Chem. Soc.*, 2017, **139**, 13156-13165.
36. K. Sasano, J. Takaya and N. Iwasawa, *J. Am. Chem. Soc.*, 2013, **135**, 10954-10957.
37. D. G. Musaev, T. M. Figg and A. L. Kaledin, *Chem. Soc. Rev.*, 2014, **43**, 5009-5031.

38. T. M. Figg, M. Wasa, J.-Q. Yu and D. G. Musaev, *J. Am. Chem. Soc.*, 2013, **135**, 14206-14214.
39. R. N. Salvatore, A. S. Nagle and K. W. Jung, *J. Org. Chem.*, 2002, **67**, 674-683.
40. S.-I. Kim, F. Chu, E. E. Dueno and K. W. Jung, *J. Org. Chem.*, 1999, **64**, 4578-4579.
41. E. E. Dueno, F. Chu, S.-I. Kim and K. W. Jung, *Tetrahedron Lett.*, 1999, **40**, 1843-1846.
42. H. Xu, K. Muto, J. Yamaguchi, C. Zhao, K. Itami and D. G. Musaev, *J. Am. Chem. Soc.*, 2014, **136**, 14834-14844.
43. M. Ciordia, L. Pérez-Benito, F. Delgado, A. A. Trabanco and G. Tresadern, *J. Chem. Inf. Model.*, 2016, **56**, 1856-1871.
44. G. Cebers, R. C. Alexander, S. B. Haeberlein, D. Han, R. Goldwater, L. Ereshefsky, T. Olsson, N. Ye, L. Rosen, M. Russell, J. Maltby, S. Eketjaell, A. R. Kugler and M. P. Murphy, *J. Alzheimer's Dis.*, 2017, **55**, 1039-1053.
45. B. Taylor, C. Fernandez Barrat, R. L. Woodward and P. A. Inglesby, *Org. Process Res. Dev.*, 2017, **21**, 1404-1412.
46. M. Trivedi, Bhaskaran, G. Singh, A. Kumar and N. P. Rath, *Inorg. Chim. Acta*, 2016, **449**, 1-8.
47. K. Billingsley and S. L. Buchwald, *J. Am. Chem. Soc.*, 2007, **129**, 3358-3366.
48. S. E. Denmark and J. D. Baird, *Org. Lett.*, 2006, **8**, 793-795.
49. A. Gavryushin, C. Kofink, G. Manolikakes and P. Knochel, *Org. Lett.*, 2005, **7**, 4871-4874.
50. G. A. Molander, S. L. J. Trice and S. D. Dreher, *J. Am. Chem. Soc.*, 2010, **132**, 17701-17703.
51. B. Fabio, L. Marco and M. Chiara, *Eur. J. Org. Chem.*, 2013, **2013**, 5621-5630.
52. A.-H. Zhou, Q. He, C. Shu, Y.-F. Yu, S. Liu, T. Zhao, W. Zhang, X. Lu and L.-W. Ye, *Chem. Sci.*, 2015, **6**, 1265-1271.
53. S. Rui, F. Yao, W. Yan, X. Qing, Y. Hai-Zhu and L. Lei, *Angew. Chem. Int. Ed.*, 2009, **48**, 9350-9354.